

# Design and testing of Adepantins - functional artificial antibiotics

---

Ilić, Nada

Doctoral thesis / Disertacija

2013

*Degree Grantor / Ustanova koja je dodijelila akademski / stručni stupanj:* **University of Split, Faculty of Science / Sveučilište u Splitu, Prirodoslovno-matematički fakultet**

*Permanent link / Trajna poveznica:* <https://um.nsk.hr/um:nbn:hr:166:154296>

*Rights / Prava:* [In copyright](#)/[Zaštićeno autorskim pravom.](#)

*Download date / Datum preuzimanja:* **2024-11-25**

*Repository / Repozitorij:*

[Repository of Faculty of Science](#)



University of Split  
Faculty of Science  
PhD Study of Biophysics

Doctoral thesis

**Design and testing of Adepantins – functional  
artificial antibiotics**

Nada Ilić

Split, 2013



**DIZAJN I TESTIRANJE ADEPANTINA – NOVIH PEPTIDNIH ANTIBIOTIKA**

Nada Ilić

Rad je izrađen na:

Prirodoslovno – matematičkom fakultetu Sveučilišta u Splitu  
i na Odjelu za znanost o životu Sveučilišta u Trstu

Sažetak

Kao važan dio urođenog imunološkog sustava svih živih bića, antimikrobni peptidi, smatraju se možebitnim rješenjem u brobi protiv bakterija otpornih na standardne antibiotike. Važna osobina dobrog kandidata za budući lijek njegova je selektivnost, koja se određuje kao omjer koncentracije pri kojoj se opaža 50%-tna hemolitična aktivnost prema eritrocitima i minimalne inhibitorne koncentracije pri kojoj se opaža 100%-tna inhibicija rasta bakterije *Escherichije coli*. Algoritmom „Designer“ dizajnirani su adeptantini – veoma selektivni umjetni peptidi u konformaciji  $\alpha$  uzvojnice, bogati glicinom i lizinom, a sličnost njihovih sekvenci s poznatim antimikrobnim peptidima manja je od 50%. Algoritam je koristio našu bazu podataka antimikrobnih peptida iz anura s poznatim indeksom selektivnosti.

Eksperimentalnim i računalnim metodama istražene su strukture i aktivnosti monomera, dimera i fluorescentno označenih oblika adeptantina. Eksperimentalna istraživanja provedena na različitim sojevima bakterija pokazala su visoku selektivnost adeptantina prema Gram-negativnim bakterijama (MIC = 0.5 - 4  $\mu$ M), naročito prema *E. coli*. U mjerenju propusnosti membrana rabljeni su različiti modeli membrana, a pokazalo se da adeptantini vrlo brzo povećavaju propusnost obje membrane *E. coli*. Time je dobiven uvid u mehanizme djelovanja adeptantina. Svi monomeri adeptantina imaju izrazito malu hemolitičnost prema eritrocitima, dok su dimeri pokazali određenu toksičnost prema ljudskim stanicama. Dokazano je da se adeptantini vežu na staničnu površinu ljudskih stanica bez popratnog oštećenja membrane. Prikupljeni rezultati potvrdili su adeptantine kao jako selektivne umjetne peptidne antibiotike.

Broj stranica: 145

Broj slika: 36

Broj tablica: 20

Broj literaturnih navoda: 97 + 15

Broj priloga: 8

Jezik izvornika: Engleski

Rad je pohranjen u: Nacionalnoj sveučilišnoj knjižnici u Zagrebu, Sveučilišnoj knjižnici u Splitu, Knjižnici Prirodoslovno – matematičkog fakulteta (PMF) Sveučilišta u Splitu.

Ključne riječi: antimikrobni peptidi, računalni dizajn, indeks selektivnosti, adeptantini, peptidi u strukturi  $\alpha$  uzvojnice, *Escherichia coli*, permeabilizacija membrane, niska toksičnost, anura.

Mentori: prof.dr.sc. Davor Juretić, redoviti profesor, PMF, Sveučilište u Splitu  
prof.dr.sc. Alessandro Tossi, izvanredni profesor, University of Trieste

Ocjenjivači: prof.dr.sc. Jasna Puizina, izvanredni profesor, PMF, Sveučilište u Splitu  
dr.sc. Bono Lučić, viši znanstveni suradnik, Institut Ruđer Bošković, Zagreb  
dr.sc. Stjepan Orhanović, docent, PMF, Sveučilište u Splitu

Rad prihvaćen: 12. 06. 2013.



**DESIGN AND TESTING OF ADEPANTINS – FUNCTIONAL ARTIFICIAL ANTIBIOTICS**

Nada Ilić

Thesis performed at:  
Faculty of Science, University of Split  
Department of life sciences, University of Trieste

**Abstract**

As an important part of the innate immune system of all organisms, antimicrobial peptides, are considered as a possible solution for fighting bacteria resistant to standard antibiotics. Crucial characteristic of peptide antibiotic, as drug candidate is its high selectivity, parameterized as the ratio of concentration causing 50% haemolysis (HC<sub>50</sub>) against erythrocytes and the minimal inhibitory concentration (MIC) against the reference bacterium *Escherichia coli*. Using the “Designer” algorithm adeptantins were designed - highly selective artificial glycine and lysine rich peptides in predominant  $\alpha$  helical conformation, having less than 50% homology of primary sequence to any known sequence of antimicrobial peptides. The algorithm used our database of anuran antimicrobial peptides with known selectivity index.

Structure and activity of adeptantins were experimentally and computationally tested in their monomeric, dimeric and fluorescently labelled form. Experimental investigations performed on different bacteria strains showed high selectivity of adeptantins for Gram-negative bacteria (MIC = 0.5 - 4  $\mu$ M), especially *E. coli*. In membrane permeabilization measurements, different membrane models were used and adeptantins showed rapid permeabilization of both membranes of *E. coli*. These tests provided insight in their mode of action. All monomeric adeptantins have exceptionally low haemolytic activity, while dimers expressed certain toxicity against host cells. It is proven that adeptantins bind efficiently to the cell surface of the host cell membranes without subsequent membrane damage. Gathered results confirmed that adeptantins are indeed highly selective artificial peptide antibiotics.

Number of pages: 145

Number of figures: 36

Number of tables: 20

Number of references: 97 + 15

Number of appendices: 8

Original in: English

Thesis deposited at The National and University Library in Zagreb, Croatia, University Library in Split, Croatia, Library of Faculty of Science of the University of Split, Croatia.

Keywords: antimicrobial peptides, computational design, selectivity index, adeptantins, helical peptides, *Escherichia coli*, membrane permeabilization, low toxicity, anuran

Supervisors: Prof.Dr. Davor Juretić, full profesor, Faculty of Science, University of Split, Croatia  
Prof.Dr. Alessandro Tossi, associate professor, University of Trieste, Italy

Reviewers: Prof.Dr. Jasna Puizina, associate professor, Faculty of Science, University of Split, Croatia  
Dr. Bono Lučić, higher research associate, Ruđer Bošković Institute, Zagreb, Croatia  
Doc.Dr. Stjepan Orhanović, assistant profesor, Faculty of Science, University of Split, Croatia

Thesis accepted: 12. 06. 2013.



Sveučilište u Splitu, Prirodoslovno-matematički fakultet

Odjel za fiziku, Poslijediplomski sveučilišni doktorski studij Biofizika

“Dizajn i testiranje adepantina – novih peptidnih antibiotika”

Doktorski rad autorice Nade Ilić kao dio obaveza potrebnih da se dobije doktorat znanosti  
\_\_\_\_\_ godine.

Dobiveni akademski naziv i stupanj: doktorica prirodnih znanosti iz polja kemije.

Povjerenstvo u sastavu:

1. prof.dr.sc Jasna Puizina, predsjednik
2. prof.dr.sc. Davor Juretić, mentor
3. prof.dr.sc. Alessandro Tossi, komentor
4. dr.sc. Bono Lučić, član
5. doc.dr.sc. Stjepan Orhanović, član

prihvatilo je izrađeni doktorski rad dana \_\_\_\_\_.

Obrana disertacije održati će se \_\_\_\_\_.

Predsjednik povjerenstva:

\_\_\_\_\_

prof.dr.sc Jasna Puizina

Voditelj studija:

\_\_\_\_\_

prof.dr.sc. Davor Juretić

Predsjednik vijeća studija:

\_\_\_\_\_

prof.dr.sc. Vlasta Bonačić-Koutecky





Sveučilište u Splitu, Prirodoslovno-matematički fakultet

Odjel za fiziku, Poslijediplomski sveučilišni doktorski studij Biofizika

Povjerenstvo za obranu doktorskog rada u sastavu:

1. prof.dr.sc Jasna Puizina, predsjednik \_\_\_\_\_
2. prof.dr.sc. Davor juretić, mentor \_\_\_\_\_
3. prof.dr.sc. Alessandro Tossi, komentor \_\_\_\_\_
4. dr.sc. Bono Lučić, član \_\_\_\_\_
5. doc.dr.sc. Stjepan Orhanović, član \_\_\_\_\_

Potvrđuje da je disertacija obranjena dana 12. srpnja 2013. godine.

Dekan

\_\_\_\_\_

prof.dr.sc Marko Rosić



## Table of Contents

Table of Contents .....	I
List of Figures.....	III
List of Tables.....	VII
List of appendices.....	IX
List of abbreviations .....	X
List of bacteria used .....	XI
1. Introduction.....	1
1.1. Antimicrobial peptides – basic information .....	1
1.1.1. Hydrophobicity and hydrophobic moment .....	3
1.1.2. AMP mode of action.....	4
1.2. New approaches in AMP research – databases and algorithms construction.....	6
1.3. About the thesis .....	8
1.4. Hypothesis and goals of the thesis.....	8
2. Materials and methods .....	11
2.1. Construction of an AMP activity database (AMPad) and relevant algorithms .....	11
2.1.1. The AMPad database.....	11
2.1.2. Sets of peptides from the AMPad database.....	11
2.1.3. „PredictorSelector“ algorithm.....	12
2.1.4. „Designer“ algorithm.....	14
2.2. SPPS (solid phase peptide synthesis) of designed peptides.....	15
2.2.1. Selection of peptides for synthesis.....	15
2.2.2. Synthesis difficulty prediction .....	16
2.2.3. Solid phase synthesis.....	16
2.2.4. Cleavage and workup .....	18
2.3. Peptide characterization and purification.....	19
2.3.1. ESI-MS (electro spray ionization mass spectrometry).....	20
2.3.2. RP - HPLC .....	22
2.3.3. Peptide modification (acetamidation, dimerization, bodipylation).....	22
2.3.3.1. Blocking of cysteine by iodoacetamidation.....	22
2.3.3.2. Covalent dimerization .....	24
2.3.3.3. Bodipylation - Fluorescent labelling with BODIPY maleimide.....	25
2.3.4. Quantification.....	27

2.4.	Structure analysis .....	29
2.4.1.	CD spectroscopy in different solvents.....	30
2.4.2.	Preparation and use of liposomes.....	31
2.5.	Antimicrobial activity assays .....	33
2.5.1.	MIC assays .....	33
2.5.2.	MBC assays .....	35
2.5.3.	Effect of AMPs on bacterial growth kinetics and IC <sub>50</sub> .....	36
2.5.4.	Barrier effect of outer membrane – permeabilization kinetics .....	37
2.6.	Bacterial membrane permeabilization assays.....	38
2.6.1.	Spectroscopic analysis of permeabilization to chromogenic substrates .....	39
2.6.2.	Flow cytometric analysis of permeabilization to PI.....	40
2.7.	Interaction of peptides with host cells.....	41
2.7.1.	Haemolysis assay.....	41
2.7.2.	Flow cytometric analysis of cellular AMP uptake.....	43
3.	Results .....	45
3.1.	Peptide sets derived from the AMPad database.....	45
3.2.	From designed to synthesized peptides.....	54
3.3.	High yields and purity of the adeptantins and modified analogues.....	57
3.4.	Confirmed secondary structure.....	62
3.5.	Effects of adeptantins on bacterial cells.....	67
3.6.	Effects of adeptantins on host cells.....	75
4.	Discussion .....	81
5.	Conclusion .....	85
6.	References (alphabetical order) .....	87
6.1.	Web link references (in order of appearance) .....	95
	CV and list of publications .....	97
	Abstracts .....	99
	Acknowledgements .....	101
	Appendices .....	103

## List of Figures

Figure 1.	Helical AMP interaction with biological membranes; in bulk solution peptides are random coil, while in the presence of membrane they structure as amphipathic $\alpha$ helices; the peptides' subsequent insertion into the membrane is then more likely to result in toroidal pore formation than in a classical barrel-stave pore. ....	5
Figure 2.	Example preparative HPLC chromatogram for ADP2(AM) peak showing fractions expected to contain pure targeted peptide, in this case fractions 5 - 7; X axes – time in minutes, Y axes – absorbance in <i>mAU</i> (milli absorbance units). ....	21
Figure 3.	Adeparantins 2 and 3 in amidated form; cysteine on C-terminus is blocked. AA coloured in red represent difference from the ADP1 sequence. Note that by amidating the C-terminus, a negative charge is removed, so that the overall charge increases by +1. ....	23
Figure 4.	Adeparantins 2 and 3 in dimerised form, connections achieved with disulphide bridge between cysteines on C-terminus. AA coloured in red represent difference from the ADP1 sequence.....	25
Figure 5.	Adeparantins 2 and 3 labelled with BODIPY maleimide on cysteines at the C-terminus. AA coloured in red represent difference from the ADP1 sequence.....	26
Figure 6.	BODIPY molecule and its reaction with SH group in the Cysteine side chain. ....	27
Figure 7.	Scheme for vesicles in different sizes; MLV = multi lamellar vesicles are large “onion-like” structures, SUV = small unilamellar vesicle, 15-30 <i>nm</i> in diameter, unstable and tending to fuse spontaneously at temperatures below phase transition temperature; LUV = large unilamellar vesicles, 100-200 <i>nm</i> or larger in diameter, stable on storage. ....	31
Figure 8.	Scheme of mini-extruder (Avanti Polar Lipids, Alabaster, AL) (as in Web link [13]) .....	33
Figure 9.	Lipopolysaccharide (LPS) structure in <i>E. coli</i> with genes involved in its synthesis; * predicted activity of the <i>waaP</i> gene product (as in Yethon and Whitfield, 2001).....	38
Figure 10.	Propidium iodide (IP) molecule (as in Web link [14]).....	40
Figure 11.	Relationship between peptide length and number of peptide entries in the whole AMPad database, “training” and “testing” sets and “set of the best peptides” (SBP). ....	47
Figure 12.	Distribution of the peptides in the AMPad database divided in three sets considering peptide length by number of AA and experimental TI value; SBP („set of the best peptides“) constructed from peptides included in both sets that have TI greater than 20.....	48
Figure 13.	Example of the results given by Virginia university helical wheel application (Web link [1]) and HydroMCalc tool (Web link [8]); Aschapin1 was used for experimental testing, as very selective antimicrobial peptide. Separation between hydrophilic and hydrophobic AA is clearly visible.....	52

Figure 14.	Sequence moments for adeptantins 1, 2 and 3; small arrows are calculated by using amino acids index scales (Appendix 2, Appendix 3, Appendix 4), red for Janin's (Janin 1979) scale and blue for Guy's (Guy 1985) scale; sum of the small vectors result in sequence moments presented by the large vectors; angle between sequence moments is used to calculate D-descriptor as the cosine of that angle.....	53
Figure 15.	Cladogram tree from Clustal W tool showing sequence alignment of 7 resulting peptides from the „Designer“ algorithm; Seq4 was later called adeptantin 2 and is most similar to adeptantin 1; Seq1 later called adeptantin 3 and is most different from adeptantin 1.....	55
Figure 16.	Prediction of the synthesis difficulty for ADP1 by Peptide companion tool. Most AA are between upper two lines indicating difficult synthesis.....	56
Figure 17.	ESI-MS analysis of adeptantins, A) ADP2, B) ADP3.....	58
Figure 18.	ESI-MS molecular weight analysis of A) ADP2(AM) and B) ADP3(AM) .....	59
Figure 19.	ESI-MS molecular weight analysis of A) [ADP2] <sub>2</sub> and B) [ADP3] <sub>2</sub> .....	60
Figure 20.	ESI-MS molecular weight analysis of A) ADP2(BY) and B) ADP3(BY). Graphs contain two peaks where lower peak represents correct one for bodipy-labeled peptide while higher one is a “shadow peak” that can often be noticed during MS analysis of fluorescently labeled peptides possibly due to loss of one fluorine under ESI conditions.....	61
Figure 21.	CD spectra of ADPs (20 $\mu$ M of peptide) measured in A) H <sub>2</sub> O and B) sodium phosphate buffered (SPB, 10 mM); ADP1(—); ADP2(AM) (---); [ADP2] <sub>2</sub> (----); ADP2(BY) (-----); ADP3(AM) (- - -); [ADP3] <sub>2</sub> (-·-·-·); ADP3(BY) (·····).....	63
Figure 22.	CD spectra of ADPs (20 $\mu$ M of peptide chain) measured in A) phosphate buffered saline (PBS, pH7.4), B) 50% trifluoroethanol (TFE) and C) 50% isopropanol (iPrOH); ADP1(—); ADP2(AM) (---); [ADP2] <sub>2</sub> (----); ADP3(AM) (- - -); [ADP3] <sub>2</sub> (-·-·-·).....	63
Figure 23.	Helix % with increasing TFE; ADP1 —●—; ADP2(AM) —■—; [ADP2] <sub>2</sub> —□—; ADP3(AM) —▲—; [ADP3] <sub>2</sub> —△—. .....	65
Figure 24.	CD spectra of ADPs (20 $\mu$ M of peptide chain) measured in A) 1:1 phosphatidylglycerol/ diphosphatidylglycerol LUVs in PBS (PG/dPG) and B) 2:2:1 phosphatidylcholine/ sphingomyelin/cholesterol LUVs in PBS (PC/SM/Ch); ADP1(—); ADP2(AM) (---); [ADP2] <sub>2</sub> (----); ADP3(AM) (- - -); [ADP3] <sub>2</sub> (-·-·-·).....	67
Figure 25.	Example of MIC results for <i>E. coli</i> all ADPs; rows: ADP1, ADP2(AM), [ADP2] <sub>2</sub> , ADP2(BY), ADP3(AM), [ADP3] <sub>2</sub> , ADP3(BY), empty; columns: 1 <sup>st</sup> – 11 <sup>th</sup> peptide + bacteria + MH starting with concentration 128 $\mu$ M and decreasing by two-fold dilution method, 12 <sup>th</sup> negative control = bacteria + MH; white dots on the bottom of the well is grown bacteria.....	68
Figure 26.	Example of MIC results for <i>S. aureus</i> all ADPs; rows: ADP1, ADP2(AM), [ADP2] <sub>2</sub> , ADP2(BY), ADP3(AM), [ADP3] <sub>2</sub> , ADP3(BY), empty; columns: 1 <sup>st</sup> – 11 <sup>th</sup> peptide +	

	bacteria + MH starting with concentration 128 $\mu M$ and decreasing by two-fold dilution method, 12 <sup>th</sup> negative control = bacteria + MH; white dots on the bottom of the well is grown bacteria.....	69
Figure 27.	A) Curves from data collected after growth kinetics for <i>E. coli</i> monomers at concentration 1 $\sim M$ and dimers at concentration 0.5 $\sim M$ ; B) inhibition percentage at 210 min extracted from growth curves; Bacteria control (.....); adepantins ADP1 (—, —●—); ADP2(AM) (- - -, —■—); ADP3(AM) (- - -, —▲—); [ADP2] <sub>2</sub> (—□—); [ADP3] <sub>2</sub> (—△—).....	70
Figure 28.	Effect of A) ADP2(AM) and B) [ADP2] <sub>2</sub> on growth kinetics of <i>E. coli</i> (1), <i>P. aeruginosa</i> (2), <i>K. pneumoniae</i> (3) and <i>S. typhimurium</i> (4), experiments were done three times in triplicates. ....	71
Figure 29.	Effect of ASC1, PSEU2 and ADP1 on growth kinetics of <i>E. coli</i> ; PSEU2 ≡◆≡ ; ASC1 ≡◆≡ ; ADP1 —●— ; mean of two experiments performed in triplicates (Juretić et al., 2009).....	72
Figure 30.	Growth kinetics of A) <i>E. coli</i> BW 25113 strain and B) <i>E. coli</i> BW 25113 $\Delta waaP$ strain affected by adepantins (ADP1 —●— ; ADP2(AM) —■— ; [ADP2] <sub>2</sub> —□— ; ADP3(AM) —▲— ; [ADP3] <sub>2</sub> —△—).....	73
Figure 31.	Permeabilization of the inner and outer membrane of <i>E. coli</i> ML-35 pYC by ADPs determined by following the hydrolysis of the impermeant chromogenic substrate A) Gal-ONp by a cytoplasmic $\beta$ -galactosidase and B) CENTA <sup>®</sup> by the periplasmic enzyme $\beta$ -lactamase respectively (no peptide —○— ; ADP1 —●— ; ADP2(AM) —■— ; [ADP2] <sub>2</sub> —□— ; ADP3(AM) —▲— ; [ADP3] <sub>2</sub> —△—).....	74
Figure 32.	Permeabilization of <i>E. coli</i> ATCC 25922 ( $10^6$ cells/ml) inner membrane caused by ADPs (0.25 $\sim M$ ) and determined by % of PI-positive bacterial cells by flow cytometric analyses; (ADP1 —●— ; ADP2(AM) —■— ; [ADP2] <sub>2</sub> —□— ; ADP2(BY) —◇— ; ADP3(AM) —▲— ; [ADP3] <sub>2</sub> —△— ; ADP3(BY) —▽—).....	75
Figure 33.	Adepanatin-induced haemolysis on 0.5% RBC; ADP1 —●— ; ADP2(AM) —■— ; [ADP2] <sub>2</sub> —□— ; ADP3(AM) —▲— ; [ADP3] <sub>2</sub> —△— ; Results are from four experiments carried out in triplicate.....	76
Figure 34.	Pseudin and ascaphin-induced haemolysis on 0.5% RBC; PSEU2 ≡◆≡ ; PSEU2 A9 ≡●≡ ; ASC1 ≡◆≡ ; ASC1 I2 ≡●≡ ; Results are from two experiments carried out in triplicate.....	78
Figure 35.	ADPs interaction with U937 cells, as measured by flow cytometry, presented on monoparametric histograms; A) ADP2(BY) and B) ADP3(BY) demonstrates the effect after 5 minutes where the black line is control, the green line is peptide at concentration 0.1 $\sim M$ and the red line is peptide at concentration 1 $\sim M$ ; C) ADP2(BY) and D) ADP3(BY) where empty curve is for U937 cells in the absence and filled curve in presence of ADPs (1 $\sim M$ ) while dashed line represents U937 cells with ADPs and the impermeant, extracellular quencher Trypan blue added.....	79
Figure 36.	Fluorescence dot plots expressing results of monitoring fluorescence at 525 nm (BODIPY) and 610 nm (PI) on the flow cytometer for human leukemic monocytes	



(U937,  $10^6$  cells/ml) treated with peptides ( $1 \sim M$ ) A) ADP2(BY) or B) ADP3(BY) and PI for 30 min at room temperature before treating cells with Trypan blue. ....80

## List of Tables

Table 1.	Resulting sequences (seq) of the „Designer“ algorithm with original restrictions; sequences are ordered as „Designer“ algorithm offered; adeptantin 1 (ADP1), adeptantin 2 (ADP2), adeptantin 3 (ADP3); red letters represent amino acid (AA) residues that are different considering adeptantin 1; the complete result with calculated parameters is presented in Table 9, on page 53.....	7
Table 2.	Peptides and their variations used to test an early version of the „Mutator“ algorithm as well as to be referent peptides to the study of adeptantins.....	8
Table 3.	Cleavage mixtures for different types of peptides (Web link [11]).....	17
Table 4.	Calculation for the volume of TFE to be added to the peptide in order to calculate percentage of $\alpha$ helix. ....	31
Table 5.	Example of microtiter plate preparation for MIC assay; a) 100 $\mu$ l MH – x $\mu$ l of peptide; b) 50 $\mu$ l of MH where peptide was later added; c) 50 $\mu$ l of MH without peptide that serves as a bacterial growth control; concentrations in B row represents final peptide concentration in those wells achieved by serial two-fold dilution. ....	35
Table 6.	Example of microtiter plate preparation for bacterial growth kinetic; First column is negative control containing bacteria with medium without peptide; each peptide has 3-5 concentrations in triplicates; well 12H contains only 200 $\mu$ l 100 % MH as a blank to avoid any possible background noise.....	37
Table 7.	“Set of the best peptides” (SBP) where the first 15 peptides are from the “testing” set and the last 11 peptides from the “training” set, in both cases ordered by descending value of TI. ....	46
Table 8.	Three descriptors with the highest correlation found by „PredictorSelector“. Although D-descriptor (in the second row) has slightly lower correlation than the first one, it was chosen because it is much simpler than the first one. For codes of the used scales see Appendix 5. Correlation is among descriptor values and experimentally determined TI values for peptides in the “training” set. ....	50
Table 9.	Output adeptantin sequences from the „Designer“ algorithm. ....	54
Table 10.	Theoretical and measured yields of ADP2 and ADP3 with and without resin. ....	57
Table 11.	Theoretical and measured MW and yields of ADP1, unmodified ADP2 and ADP3, ASC1 and ASC1 I2, PSEU2 and Pseu2 A9. ....	58
Table 12.	ADP2 and ADP3 modifications with its theoretical versus measured MW and their yields; for ADP2(AM) and [ADP2] <sub>2</sub> modification reaction was performed twice, therefore, the yields are higher. ....	59
Table 13.	Mass concentration of peptides tested in the first set of tests. ....	62
Table 14.	Results of methods used for determining concentration of adeptantins. ....	62
Table 15.	% helicity of ADPs in different environments according to the method of Reed and Reed 1997. Peptides were 20 $\mu$ M in H <sub>2</sub> O, 50% trifluoroethanol (TFE), anionic	

LUV (PG/dPG = phosphatidylglycerol/diphosphatidylglycerol; 95:5) and neutral LUV (PC/SM/Ch = phosphatidylcholine/sphingomyelin/cholesterol; 2:2:1) in PBS buffer. Dimerization was taken into account by normalising ellipticity per residue. <sup>(1)</sup>No corrections for the presence of the BODIPY chromophore were made (% helicity shown in parentheses). .....66

Table 16. MIC values for adeptantins, pseudins and ascaphins; <sup>(1)</sup>assays were carried out in 100% (v/v) MH broth using  $5 \times 10^5$  cells/ml bacteria in the logarithmic phase; each value is the mean of at least 3 independent determinations carried out in duplicate. ....68

Table 17. MBC (minimal bactericidal concentration), <sup>(1)</sup> Concentration resulting in no bacterial growth, 2 independent determinations carried out in duplicate. ....70

Table 18. IC<sub>50</sub> value of peptides; <sup>(1)</sup> Concentration resulting in 50% growth inhibition of bacteria, calculated from data in figure (Figure 27). ....71

Table 19. IC<sub>50</sub> value of ADP2(AM) and [ADP2]<sub>2</sub> measured for the following bacteria: *E. coli*, *P. aeruginosa*, *K. pneumoniae* and *S. typhimurium*; <sup>(1)</sup> Concentration resulting in a 50% growth inhibition of bacteria, calculated from data in figure (Figure 28). ....72

Table 20. Haemolytic, MIC and TI values for tested peptides; Haemolytic activity tested for peptides, expressed as HC<sub>50</sub> value; <sup>(1)</sup> determined from Figure 33 and Figure 34; MIC values from Table 16; TI value calculated from experimental data (TI calculated) and predicted one (TI predicted); <sup>(2)</sup> For ADP1, the first value is from second set of tests together with other ADPs, while the second value is from the first set of tests when only ADP1 was tested along with PSEU2 and ASC1. <sup>(3)</sup> Values are for original peptide sequence not iodoacetamidated one. ....77

## List of appendices

Appendix 1. "Set of AMPad peptides" (SAP) that forms AMPad database.....	105
Appendix 2. Contribution to the sequent moment of each AA for Janin and Guy scale - ADP1.....	107
Appendix 3. Contribution to the sequent moment of each AA for Janin and Guy scale - ADP2.....	108
Appendix 4. Contribution to the sequent moment of each AA for Janin and Guy scale - ADP3.....	109
Appendix 5. Table of amino acid scales from Split 3.5 algorithm [7] used for finding D-descriptor .....	110
Appendix 6. Preparative RP-HPLC spectra for ADP2(AC) (both synthesis), [ADP2] <sub>2</sub> (both synthesis), ADP2(BY), ADP3(AC), [ADP3] <sub>2</sub> , ADP3(BY) .....	115
Appendix 7. Analytical RP-HPLC for ADP1 (first testing name was DESC1) ADP2(AC), [ADP2] <sub>2</sub> , ADP2(BY), ADP3(AC), [ADP3] <sub>2</sub> , ADP3(BY), all graphs overlapped for comparison. ....	123
Appendix 8. ESI - MS and Analytical RP-HPLC for ADP1 (first testing name was DESC1), PSEU2 (first testing name was PSEU2B), PSEU2 A9 (first testing name was PSEU2A), ASC1 (first testing name was ASC1B), ASC1 I2 (first testing name was ASC1A).....	131

## List of abbreviations

AA(s) – amino acid(s)

ADP(s) – adepantin(s)

AMP(s) – antimicrobial peptide(s)

Cfu – colony forming units / ml

Conc. or c. - concentration

HC<sub>50</sub> – concentration that causes 50% haemolysis of RBC

MilliQ H<sub>2</sub>O - ultrapure laboratory grade water

HPD(s) – host defence peptide(s)

IC<sub>50</sub> – half maximal inhibitory concentration (for bacterial growth)

LPS - Lipopolysaccharides

MLV - multi lamellar vesicles, large “onion-like” structures

LUV - large, unilamellar vesicles

M – Mol (*mM* – milli mol; *μM* – micro mol)

MIC – minimal inhibitory concentration

MW – molecular weight

OD – optical density

PG/dPG – Phosphatidylglycerol/Diphosphatidylglycerol

PC/SM/Ch – Phosphatidylcholine/Sphingomyelin/Cholesterol

Pbf – 2,2,4,6,7-pentamethyldihydrobenzofuran-5-sulfonyl

RBC – red blood cells, erythrocytes

SPPS - solid phase peptide synthesis

SUV - small, unilamellar vesicles or sonicated, unilamellar vesicles

TI - therapeutic index

## List of bacteria used

### *Escherichia coli*

- ATCC25922
- BW2553
- UWaap-BW2553
- ML-35pYC

### *Staphylococcus aureus*

- ATCC25923

### *Pseudomonas aeruginosa*

- ATCC27853

### *Salmonella typhimurium*

- ATCC14082

### *Klebsiella pneumoniae*

- clinical isolate



## 1. Introduction

In the never ending battle against microbes, only recently has the ancient weapon been rediscovered. Antimicrobial peptides (AMPs) have existed in nature for millions of years and are still very functional in defending their producers against bacteria, fungi and viruses (Bullett et al., 2004; Yeaman and Yount, 2007). Natural antimicrobials are produced by unicellular and multicellular organisms to act directly on microbes or to profoundly modulate innate immune system response. In the case of direct action, the suggested term for this agents is “antimicrobial peptide”, while in the case of modulating or enhancing the host immune response to infectious agents, the term “host defence peptide” has been suggested (Fjell et al., 2012). Antibiotics in current use present a negative side effect: the explosion of the resistant bacteria that do not respond to any kind of antimicrobial treatment (Taubes, 2008; McKenna, 2011). Therefore, a new kind of antibiotics is desired. Antimicrobial peptides present one of the possible solutions showing promising results. Natural AMPs are however not sufficiently selective for direct use on humans. To improve this, most AMP alterations have been made according to experts’ experience or just plain guessing. Even so, the increase in antibacterial activity, measured as a reduction in MIC (minimal inhibitory concentration), has in most instances increased toxicity as well measured as an increase in  $HC_{50}$  (peptide concentration that causes 50% haemolysis of erythrocytes). This effect has discouraged the pharmaceutical industry, where the requirement for good drugs with low side effects and toxicity is of the utmost importance.

AMPs are interesting research material due to low probability for bacteria to gain resistance to them; they tend to be fairly selective in killing bacteria cells. They maintain this ability also against pathogens, multidrug resistant to conventional antibiotics, having a predominantly nonstereospecific mechanism of action against bacterial membranes (Hancock and Lehrer 1998; Glukhov et al., 2005; Marr et al., 2006). Due to these advantages of AMPs, many laboratories have engaged in AMP research over the past decades (Hancock and Sahl 2006; Bommarius and Kalman 2009; Zhang and Falla 2010). The growing amount of data available on several interesting characteristics of AMPs, has led to the necessity for constructing databases and computational tools for predicting novel and improving existing AMPs (Juretić et al., 2009; Juretić et al., 2011; Aoki et al., 2012; Hammami and Fliss 2010; Novković et al., 2012).

### 1.1. Antimicrobial peptides – basic information

Our body uses several ways to defend itself against pathogens that are constantly attacking its integrity. An interesting and very efficient way of the body to protect itself is by using AMPs (antimicrobial peptides) and HDPs (host defence peptides). Both have extraordinary molecular diversity, differing in length from 12 to hundreds of AA residues and belonging to several structural classes.

HDPs are natural and endogenous, gene-encoded polypeptides and are widely distributed among all known kingdoms: animal, plant and bacteria. The fact that they are gene encoded connects their evolution with that of their microbial targets. This, and the fact that they are evolutionary very ancient components of the innate immune system of many species (Zasloff, 2002), has resulted in such molecular diversity. Some HDPs are active against eukaryotic micro- and macro-predators as well.



Unlike HDP notation, which is reserved for endogenous molecules of host defence, the term AMP is used to describe both natural and synthetic peptides showing antimicrobial activity. They therefore have even greater variety in their structure (Yeaman and Yount, 2003) but generally tend to be shorter in length than HDPs, consisting of 10 to approximately 46 AA. HDPs and natural ADPs not only differ widely in their primary structure within and among the different producer organism, but there is also a great diversity in their secondary structure. Those found so far are forming  $\alpha$  helices,  $\beta$  sheets,  $\beta$  hairpins, random coil or combine more than one of the mentioned structures. The most abundant and widespread in nature are probably those with a linear  $\alpha$  helical structure that appears to be particularly successful in defending their producing organism. These AMPs are invariably positively charged (+2 to +9), with the possibility to spatially organise cationic and hydrophobic amino acids (AA) on the opposite faces of the helix, a hydrophobic side and a polar side. This effect is nicely visible in an Edmundson or “helical wheel” projection (Schiffer and Edmundson 1967) (Web link [1]). This results in a transversal amphipathicity, and enables peptides to interact with both water and biological membranes. Change in the amphipathicity influences change in antimicrobial activity, but can increase toxicity towards mammalian cells with neutral membranes (Dathe and Wieprecht 1999). All those characteristics have placed  $\alpha$  helical AMPs amongst the most studied antimicrobial peptides.

Possible modes of action AMPs use to defend the host organism are:

- Disruption of the microbial membranes, which are negatively charged and selectively attract positively charged AMPs (primary antimicrobial mechanism).
- Interaction with secondary targets in the cells by interrupting vital metabolic processes, when translocated in the cell.
- Interference with external molecular targets on the microbial envelope and causing severe damage. Targets can be lipids involved in cell-wall synthesis and autolytic enzymes required for cellular division.
- Creating pores in the cytoplasmic membrane without disrupting it, but provoking a decrease in the membrane potential, electrical field and proton-motive force, which in turn blocks the ATP synthesis.

Outside the membrane, in aqueous bulk solution, many AMPs are in random coil or extended conformation (Figure 1), while in the presence of phospholipid membrane or membrane mimetic solvent they tend to assume more regular structures. As AMPs are active when folded in their final secondary structure (Tam et al., 2001; Unger et al., 2001), the mode of action is also defined by the membrane that peptides interact with. Cells, depending on which organism they belong to, have differences in their membrane composition, but peptides interact with all of them on the basis of electrostatic interactions. AMPs selectivity is based on the difference between bacterial and mammalian cell membranes (Aoki et al., 2012). Bacterial cells have anionic character, depending on membrane components, and therefore attract cationic AMPs (Glukhov et al., 2005; Umeyama et al., 2006). Along with membrane phospholipids, in Gram-negative bacteria, important negative components of the surface are phosphate groups of membrane

lipopolysaccharides in the outer membrane, while in Gram-positive bacteria negative charges are contributed by lipoteichoic acids of the peptidoglycan. In mammalian cells negative charge of the membrane is not strongly expressed, and the membrane is additionally stabilized with an abundance of cholesterol reducing its susceptibility to AMPs (Matsuzaki et al., 1995). Negatively charged phospholipids are much more abundant at the external side of cytoplasmic membrane in bacteria than in human cells. This is one of the main reasons why peptides act differently on various membranes, and is also the fact researchers are trying to use in adjusting peptides for medical use.

The membrane electrochemical gradient is the result of unequal distribution of ions inside and outside the cell membrane. Unequal ion distribution creates transmembrane potential. Potential measured in bacterial cells is  $-130$  to  $-150$  mV, while in mammalian cells it is  $-90$  to  $-110$  mV. This more highly negative transmembrane potential of bacterial membrane can drive cationic peptide in the cell through the membrane, reducing their concentration on the surface. The difference in membrane electrochemistry can contribute to selective toxicity of AMPs targeting microbial and avoiding human cells, which would be the perfect case. Considering differences of the membranes, it can be noticed that AMPs can be selective for bacterial with respect to eukaryotic cells, as well as selective for Gram-negative with respect to Gram-positive bacteria. Those variations can make AMPs potential drugs with specific targets in possible future medical use.

### 1.1.1. Hydrophobicity and hydrophobic moment

Beside conformation and charge, other functionally important AMP properties are hydrophobicity and hydrophobic moment.

Hydrophobicity (H) is the numerical value quantifying a dislike for water for each amino acid side-chain. There are more than 100 hydrophobicity scales in the literature differing in these values. Examples of the scales are Eisenberg consensus scale (Eisenberg et al. 1984), Tossi CCS scale (Tossi et al. 2002), Janin (Janin 1979) and Guy (Guy 1985) scale. The mean hydrophobicity (H) of the peptide is defined as the sum of hydrophobicity values of each AA averaged over the total length of the peptide. Percentage of hydrophobic AA in the peptide can also be defined as peptide hydrophobicity. For most AMPs approximately 50% are hydrophobic AA that makes them moderately hydrophobic but quite amphipathic and optimized against the membranes of the microbes (Yeaman and Yount 2003). A change in the percentage of hydrophobicity can lead to a change in their specificity, as well as a change in membrane permeabilization. The effect was tested on magainin2 and its analogues with slight changes in hydrophobicity (Wieprecht et al., 1997).

Hydrophobic moment ( $\mu$ H) is a quantitative measure of amphipathicity (Eisenberg 1984). It is defined for each AA residue as a vector, starting from the symmetry axis of the helix and pointing towards  $\alpha$ C atom of the given AA residue, with the value of scalar hydrophobicity parameter of the same residue. Mean hydrophobic moment of the peptide is, then, the vectorial sum of the individual AA hydrophobicities, averaged over the helix length. In some cases, it can be normalized to an ideal, perfectly amphipathic  $\alpha$  helix.

### 1.1.2. AMP mode of action

Helical AMPs are likely to be membrane active if: they have about 50% hydrophobic AA residues in the primary structure, if they have a net positive charge deriving from at least 20% of charged AA in the sequence, and if they are amphipathic. Those characteristics enable peptides to come into initial contact with the targeted membrane. Once bound to the membrane, different AMPs have different modes of actions, but all are based on membrane permeabilization and passage through the membrane. To activate any of the processes, peptides need to reach threshold concentrations of the peptide, accumulated on the outer leaflet of the membrane that enables peptides to damage the membrane itself, following a conformational transition, and/or peptide aggregation. Peptide aggregation can lead to formation of the pores in the membrane, enabling molecular transfer in the damaged cell. Many AMPs act in this manner, as described by the Shai-Matsuzaki-Huang (SHM) model (Zaslouff 2002).

In the pores, the hydrophobic part of the peptide faces and inserts itself into the membrane. The hydrophilic part initially faces the extracellular medium. After the pore is formed, it faces the centre of the pore. There are many models of peptide permeabilization through the membrane. This is the result of peptide diversity which leads to diversity in their mode of action (Epanand and Vogel 1999). Until now there is no consensus on the exact mechanism, although three of them are most commonly used (Yeaman and Yount 2003, Shai 1999, Brogden 2005): barrel-stave, toroidal pore and carpet mechanism (Figure 1, carpet mechanism is not shown). The name of each mechanism is derived from the shape of the pore or type of lesion formed in the membrane.

Barrel-stave is formed when peptides (Oren and Shai 1998),  $\alpha$  helical or  $\beta$  sheet, with threshold concentration, bridge the membrane perpendicularly in the form of the barrel like ring, while they are parallel among themselves. Toroidal pore or wormhole mechanism is the most accepted one. Peptides are interlaced with phospholipids in the form of a toroid through the whole pore (Figure 1), while the pores are slightly bigger than those of barrel-stave. In the carpet mechanism, peptides act as detergents while “carpeting” the outer membrane (Shai 1999, Epanand and Vogel 1999, Brogden 2005). A particularity of this model is that peptides cover the membrane like a carpet, whether locally by self-association or by covering the whole membrane with monomers. Permeabilization starts with the threshold concentration of the peptide reached, disrupting membrane to peptide covered micelles.

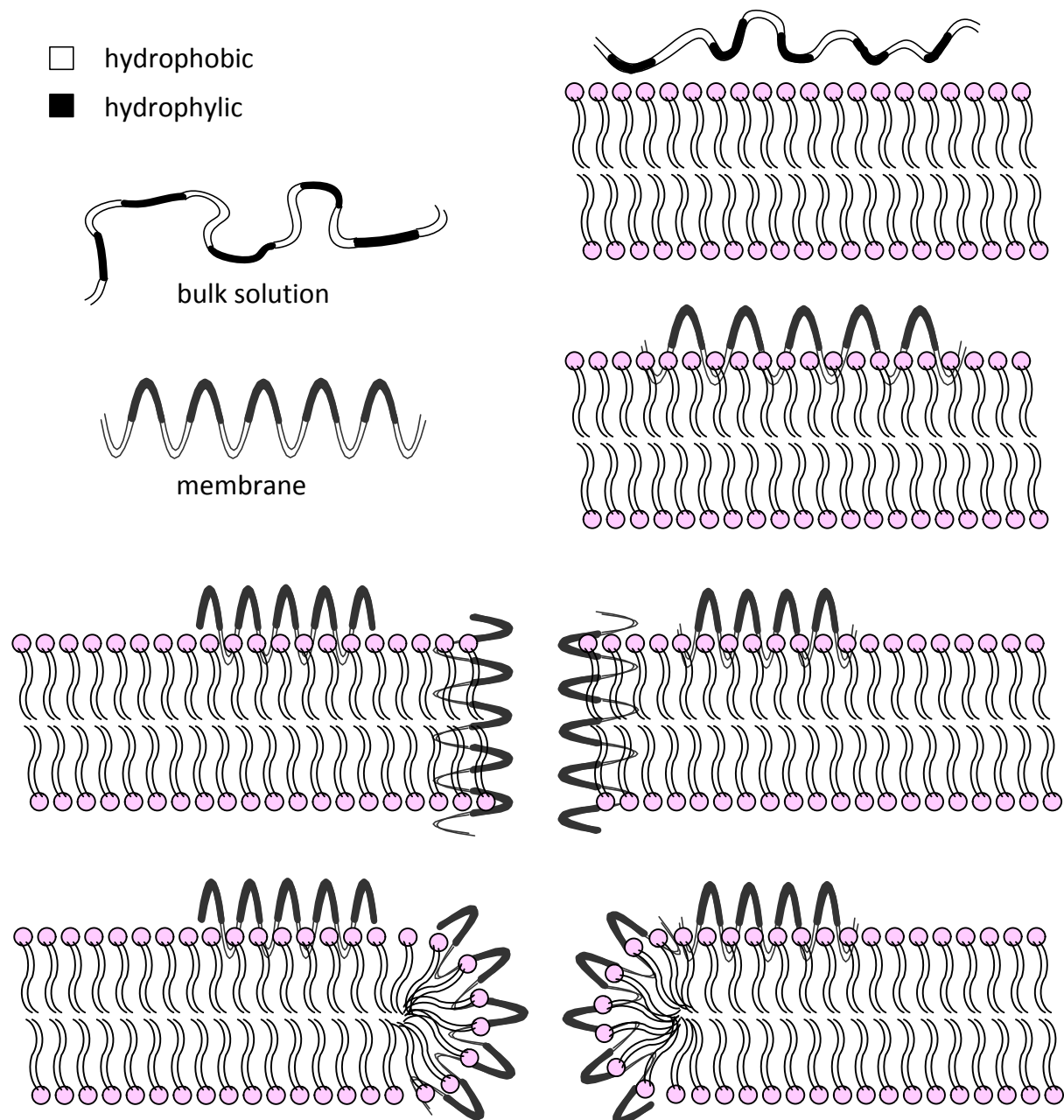


Figure 1. Helical AMP interaction with biological membranes; in bulk solution peptides are random coil, while in the presence of membrane they structure as amphipathic  $\alpha$  helices; the peptides' subsequent insertion into the membrane is then more likely to result in toroidal pore formation than in a classical barrel-stave pore.

Membrane penetration is not the only way AMPs can affect bacteria. There are several other mechanisms. One of the mechanisms is targeting intercellular components, similar to some classical antibiotics. Most of those mechanisms are based on inhibition, such as inhibition of: enzymatic activity, cell wall synthesis, nucleic acids or protein synthesis, but they also affect protein folding, key cellular processes, metabolic turnover (Nguyen et al., 2011).

## 1.2. New approaches in AMP research – databases and algorithms construction

The field studying AMPs is relatively new and constantly developing. In order to render peptide research easier and reduce the cost of further laboratory work it is convenient to develop databases and computational tools as knowledge-based methods. As every tool development in bioinformatics and data-mining, research starts with an extensive data collection. In fact, several databases have been created collecting thousands of AMP sequences, listed along with their characteristics (Hammami and Fliss 2010). Each database has a different number of peptides depending on what it was collected for. AMPad database (Juretić et al., 2009), has 73 AMPs of amphibian origin, with  $\alpha$  helical structure, while DADP database (Web link [2]) created later has 2571 amphibian AMPs (Novković et al. 2012). On the other hand, AMSDb database (Web link [3]) has 895 eukaryotic antimicrobial peptides (Tossi and Sandri 2002). There are several other databases such as: CAMP (Thomas et al., 2010), APD (Wang et al., 2009) (Web link [4]), AMPer (Fjell et al., 2007), that all cover diverse origin AMP sequences. Most sequences represent common biophysical parameters such as molecular size, cationicity and amphipathicity, which can be essential for AMPs activities (Hammami and Fliss 2010). Those databases are later used for all types of research, including creation of computational tools for AMP design, prediction or predicting certain parameters relevant for peptides activity, like TI. So far, several algorithms have been developed from the AMPad database: “PredictorSelector”, „Designer“ (Juretić et al. 2009) and „Mutator“ (Kamech et al., 2012).

Peptides, which are the main subject of this thesis, are artificial AMPs proposed by „Designer“ algorithm, named adepantins (ADPs) from **A**utomatically **D**esigned **P**eptide **A**ntibiotic **N**umber 1, 2 and 3. The algorithm was created using a collected set of 73 peptides (described in 2.1 and 3.1) effective against *Escherichia coli*, extracted from anurans (mainly frogs) and that have preference for  $\alpha$  helix conformation in hydrophobic environment. The constructed database was named AMPad (Juretić et al., 2009) and it lists peptide name, sequence, MIC and  $HC_{50}$  value expressed in  $\mu M$ , and therapeutic index (TI) value for each peptide. The TI is a ratio of  $HC_{50}$  and MIC, and it represents the measure of selectivity of the peptide.

$$TI = HC_{50}/MIC \quad (1)$$

where TI is therapeutic index representing selectivity,  $HC_{50}$  is peptide concentration causing 50% of haemolysis of red blood cells, and MIC is minimal inhibitory concentration.

From the AMPad database, three sets were formed: the „training“ set, the „testing“ set and the „set of the best peptides“ (SBP) (described in 2.1 and 3.1). The „training“ set consists of 36 non-homologous peptides with less than 70% pairwise identity, „testing“ set consists of the remaining 37 peptides, while SBP contains all peptides from AMPad database with  $TI > 20$ . Non-homologous peptides were chosen for the „training“ set with the intention of using data-mining procedures for extracting general rules for highly selective AMPs with measured TI. The concept of sequence moments (constructed by Prof. Davor Juretić) facilitated the data-mining-procedure and the selection of optimal parameters for TI prediction by using the „PredictorSelector“ algorithm (constructed by Prof. Damir Vukičević).

Sequence moments were presented as vector summation of chosen set of amino acid attributes for a peptide sequence bent into right angle arc of 90° (Juretić et al., 2009.). The cosine of the angle between sequence moments is called D-descriptor and it leads to the predicted TI value by using linear one-parameter model expressed with the equation  $TI = 50.126 - 44.803D$ . Hydrophobicity values used to calculate sequence moments are associated with the scales of Guy (Guy 1985) and Janin (Janin 1979) (see Figure 14, str. 53, Appendix 2, Appendix 3, Appendix 4). The maximal predicted TI value in this model is 95, while the measured value for the same peptide can be significantly higher. When constructed, the „Designer“ algorithm contained certain restrictions. By selecting a certain range of mean physicochemical parameters, a peptide length of 23 AA, net positive charge of 4 or 5 and  $TI > 85$ , such restrictions were enforced to reduce the number of proposed peptides. The algorithm then proposed 7 peptides (Table 1) (see in 2.1.4, 3.2).

Table 1. Resulting sequences (seq) of the „Designer“ algorithm with original restrictions; sequences are ordered as „Designer“ algorithm offered; adeptantin 1 (ADP1), adeptantin 2 (ADP2), adeptantin 3 (ADP3); red letters represent amino acid (AA) residues that are different considering adeptantin 1; the complete result with calculated parameters is presented in Table 9, on page 54.

Abbreviation of peptide name	Sequence
ADP3 (seq1)	GLKGLLGKALKG <b>IGKHIGKAQGC</b>
seq2	GLKGLLGKALGEAKGLLGKHKGC
seq3	GITQGVKLGIGKHVKGALKGIGC
ADP2 (seq4)	GIGKHVKGALKGLKGLLKL <b>GEC</b>
seq5	GIGKHVKGALKGVKGLLKL <b>GEC</b>
seq6	GIGKHVKGALGELKGLLKL <b>GKGC</b>
ADP1	GIGKHVKGALKGLKGLLKL <b>GES</b>

Adeptantin 1 was the first AMP from this group of 7 to be tested (see 2.2.1 and 3.1). It is the only AMP from the proposed group that ends with S (Serine) at the C-terminus. All others end with C (Cysteine) AA which has a reactive sulphhydryl group. That reactivity, in the following experimental tests, was used to label the peptides with fluorescent label and to construct adeptantin dimers. In the case of adeptantin monomers with C-terminal Cys the cysteine was blocked by iodoacetamidation. From the same series of ADPs two additional peptides, the most similar one (ADP2) and one with highest molecular diversity to ADP 1 (ADP3), were chosen to undergo further testing.

The „Mutator“ algorithm is a bioinformatical tool, designed by prof. Damir Vukičević with the help of Prof. Davor Juretić, to improve AMPs by suggesting possible point mutations one by one, with constant increase of the peptides' TI value. Recently, it was improved and tested (Kamech et al., 2012). Its construction began in the same time as development of the „Designer“ and the „Predictor“ algorithm. Preliminary laboratory experiments on two peptides were done to prove the results in the early stage of the algorithm development. Since this algorithm was still under construction, the chosen peptides were not only supposed to test early „Mutator“ algorithm but, more importantly, to serve as referent peptides in the adeptantin testing study. In the end, one good and one mediocre antimicrobial peptide, considering their TI values, were selected. They were synthesized along with their versions with one point mutations proposed by the preliminary version of the „Mutator“ algorithm (Table 2).

Table 2. Peptides and their variations used to test an early version of the „Mutator“ algorithm as well as to be referent peptides to the study of adeptantins.

Peptide name	abbreviation	sequence
Ascaphin 1	ASC1	GFRDVLKGAAKAFVKTVAGHIAN
Ascaphin 1 I2	ASC1 I2	GIRDVLKGAAKAFVKTVAGHIAN
Pseudin 2	PSEU2	GLNALKKVFQGIHEAIKLINNHVQ
Pseudin 2 A9	PSEU2 A9	GLNALKKVAQGIHEAIKLINNHVQ

The results gathered in the first tests of the „Mutator“ algorithm confirmed improvements in peptides TI. However, improvements were not significant enough to exclude human error while performing tests. Therefore, „Mutator“ algorithm was left for further development. The results were recently published in (Kamech et al., 2012), and the algorithm can be tested at corresponding Web address (Web link [5]). Ascaphin 1 and pseudin 2 were left as referent peptides in the first sets of experiments on adeptantins, more precisely, by testing of adeptantin 1 (Juretić et al., 2009).

### 1.3. About the thesis

In the methods and results of the thesis the whole process will be described, from data gathering to the collecting of the results after adeptantins are tested. The description will follow all steps of the process, although some parts of it were not done by me. Firstly, the database construction will be described, which is the part I participated in. The next step is its division into desired sets of peptides adapted for further managing (also mainly my part of the work), and will be described as the next step of the work. This will be followed by the algorithms construction process, which was the part of the work performed by Prof. Davor Juretić and Prof. Damir Vukičević, and will be described as the relevant part of the process on how adeptantins were constructed. In the following paragraph, there will be a presentation of why we chose adeptantin 1, 2 and 3 for the testing, as well as what peptides we took as referent ones and why. At this point, I must point out that laboratory testing of the peptides were performed in two set of assays, one where ADP1 and referent peptides were used, and the second where ADP1 was the referent peptide while ADP2 and 3 were under testing. In subsequent paragraphs, all laboratory experiments carried out by me during this process will follow a logical order, starting from synthesis, purification, modification and characterization, through quantification and structural analysis. Antimicrobial activity and bacterial membrane permeabilization assays will show how ADPs react when in contact with bacterial strains of interest. To be able to determine selectivity of ADPs, their interaction with host cells was tested. In the discussion part of the thesis results will be discussed and some future prospective will be given. Thesis will end with the conclusion.

### 1.4. Hypothesis and goals of the thesis

The lack of sophisticated methods capable of improving natural and known AMPs initiated the idea for constructing algorithms that could assist laboratory work by performing in-silico peptide design. One of the algorithms constructed was named „Designer“, a software created by prof. Damir Vukičević with the sequence moment concept at its core, which suggests the primary structures of novel AMPs. „Designer“ algorithm proposed AMPs



named adeptantins (ADP) (Automatically Designed Peptide Antibiotic Number 1, 2 and 3). Their subsequent experimental testing was the main objective of this thesis.

The main hypothesis of the thesis was that adeptantins should be highly selective for Gram-negative bacteria and have very low haemolytic activity. This was substantially proved, except for modifications (dimerization) that resulted in an interesting increase in toxicity (a sort of exception that proves the rule).

In order to confirm this hypothesis several more specific factors were addressed:

- ADPs are predicted to be alpha helical peptides (proved).
- ADPs were designed to have high selectivity against *Escherichia coli*, against which „Designer“ parameters are trained, but not necessarily against other Gram-negative bacteria or the Gram-positive *Staphylococcus aureus* (proved).
- ADPs are expected to have high HC<sub>50</sub> values (50% haemolysis of erythrocytes), resulting in low haemolytic activity (proved).
- ADPs should permeabilize both the inner and outer membrane of *E. coli* (proved).
- Dimerization might improve ADPs antimicrobial activity due to double alpha helix and therefore improve selectivity (proved to be true for antimicrobial activity but not for selectivity).
- Fluorescently labelled ADPs should help reveal the mode of action (partly proved).

To confirm the hypothesis made, two kinds of methods were used. The first set was mainly theoretical, required in constructing the algorithm, while the second set of methods represents the major part of the thesis, and was mainly experimental.

The goals of the work described in the thesis were thus:

- Construction of a new database consisting of antimicrobial peptides with certain characteristics addressing data collected for AMPs against *E. coli* (participating in the process of collecting, verifying and sorting data).
- Dividing the gathered database in „training“ and „testing“ sets, and an additional “set of the best peptides” (SBP), consisting of the peptides with TI > 20 from both sets.
- Prediction of at least one peptide with the required characteristics that was later called adeptantin 1 (ADP1) (participating in the process).
- Testing hypothesis about ADPs presented above.
- Collected data that can later be included into another database for possible construction of additional bioinformatical tools.

The accomplishment of the first and the second goal enabled the construction of three new bioinformatical tools named “PredictorSelector”, „Designer” and “Predictor”. The



main contribution in creating these tools came from Prof. Dr. Davor Juretić and Prof. Dr. Damir Vukičević. The tools were later used to accomplish the third and the fourth goal.

## 2. Materials and methods

### 2.1. Construction of an AMP activity database (AMPad) and relevant algorithms

#### 2.1.1. The AMPad database

To be able to create any software for AMP construction, the crucial step was to create a proper and representative database of natural AMPs with the data we considered useful at that time. The data were values for the minimal inhibitory concentration (MIC) and for 50% haemolysis of human red blood cells (HC<sub>50</sub>). The values have been chosen as those which represent AMP selectivity through the Therapeutic index (TI). In a recent article (Ilić et al., 2013), the TI index was renamed selectivity index (SI) as the same group of scientists suggested in their earlier works (Juretić et al., 2009; Juretić et al., 2011). The TI index is given by expression (1).

The search for required data throughout the literature consisted mostly of scanning the PubMed application (Web link [6]) using their search tool. The keywords applied to the search tool were: antimicrobial, peptides, AMP, peptide antibiotics, MIC, HC50, selectivity, amphibian, anuran, frog, TI or therapeutic index,  $\alpha$  helix, helical, and different combinations of these. At that time, the PubMed search tool proposed a limited number of articles containing required data. Research results on AMPs, although abundant, were not published with the type and amount of data we required for forming a big AMP database with data of interest. Later, our group constructed a large database named DADP: the database of anuran defence peptides (Novković et al., 2012).

Peptides considered for the entry into the AMPad database were of amphibian origin and had propensity to form  $\alpha$  helix in membrane mimetic solvent (predicted and/or experimentally verified propensity). Furthermore, only data representing MIC and HC50 values, expressed in  $\mu M$ , measured by performing the same type of assay with the same concentrations of the target cells, were extracted and listed in the database. MIC values used had to be determined by the serial dilution method. Furthermore, if values for several *E. coli* strains were present, the value for the most sensitive strain was selected. A criterium for selecting HC<sub>50</sub> values was that they had to be measured with fresh human blood from healthy donors. Also, articles not containing all the required data for the same peptide were omitted, as well as articles containing data for peptides for which the same data were measured later. Artificial peptides or peptides with more than two point mutations were also excluded from the database.

#### 2.1.2. Sets of peptides from the AMPad database

To be able to construct any kind of bioinformatical tool we needed a minimum of two sets of peptides with certain characteristics. AMPad database is a relatively small database with only 73 AMPs, which was divided into „training“ and „testing“ sets. For that purpose, bioinformatical multiple alignment tool Clustal V (version used in 2008) was used. Database was divided by the rule that the „training“ set must consist of nonhomologous peptides with less than 70% pairwise identity. This was a necessary criterium for extracting rules as general as possible. All other peptides formed the „testing“ set. The „training“ set than was

subjected to various analyses in order to extract rules and logic needed for software construction. (Appendix 1; Juretić et al., 2009).

An additional set of peptides was required for algorithm construction. In order to construct an algorithm able to offer good and selective antibiotics, a set of the best AMPs from the AMPad database needed to be extracted. For that purpose, all peptides in the AMPad database were sorted by decreasing TI value, and then all peptides with TI values greater than 20 were extracted to form a set called the „set of best peptides“ (SPB). TI value 20 was chosen to be the threshold, because in literature AMPs with  $TI \geq 20$  are still considered to be good antibiotics as well as selective ones (Juretić et al., 2009).

AMPs not listed as  $\alpha$  helical in the original article were examined by using SPLIT algorithm version 3.5 (Juretić et al., 1998) (Web link [7]). For all peptides also the distribution of the polar/hydrophilic and nonpolar/hydrophobic amino acids (AA) was observed either by using the Virginia university helical wheel application (Web link [1]) or HydromCalc tool (Web link [8]).

### 2.1.3. „PredictorSelector“ algorithm

Peptides, in the primary structure, are represented as a sequence of AA. Each of those AA has certain characteristics expressed as position-dependent attributes, presented mostly as smoothed values. All AA attributes are presented as two-dimensional plots for sequence profiles. Such a profile is for example the Kyte-Doolittle hydrophobicity profile (Kyte and Doolittle 1982). For the „Designer“ algorithm construction, the whole sequence profile for the chosen set of AA attributes is converted into one vector with two components, named sequence moment. That was possible by summation of all vectors representing AA attributes in chosen sequence, when the sequence was bent into right angle arc. The „PredictorSelector“ found the best descriptors when sequence was bent in the first quadrant of coordinate system. N-terminal of the peptide is located then at the positive y-axes, while the C-terminal is located on positive x-axes (Figure 14, page 53). AA attributes vectors are defined in length and orientation by direct or smoothed attribute value. The results showed that smoothed attribute values with omitted attribute of a central residue in a sliding window (used for smoothing) produced the best descriptors. In this case too, the criterion for choosing descriptors was the correlation with measured TI values of the „training“ data set peptides. The inclination of resulting vector, named the sequence moment vector, is given with respect to the x-axis. The sequence moment vector is therefore an indicator of the lengthwise asymmetry of the peptide for the chosen attribute profile, and is not associated with secondary structure of the peptide. Lengthwise asymmetry is different from sidewise asymmetry or amphipathicity. Sidewise asymmetry is associated with secondary structure of the peptide, and measured by Eissenberg's hydrophobic moment (Eissenberg et al., 1982). Lengthwise asymmetry of the peptides is additionally emphasized with the observation that AAs closer to the N-terminus are more relevant for AMP activity (Tossi et al., 1997; Tossi et al., 2000), and that is included in calculation of the sequence moments as optimized weighting factor (Juretić et al. 2009). To be more specific, for the job of converting sequence profiles of AA attributes into sequence moments the following was necessary:

- 144 different scales of AA attributes obtained from studies describing protein folding and integral membrane proteins (Juretić et al. 1998 (b), Gromiha 2005, Yuan et al., 2006)
- Finding sequence profiles from AA attributes by considering three simple methods: direct usage, smoothing with central AA in a sliding window (mean values), smoothing with central AA in sliding window but not taking into account the attribute for the central AA itself (sequence environment values).
- Determining peptide bending angle between 15 possible ones from  $\pi/15$ ,  $\pi/14$ ... to  $\pi$ .
- Determining weighting values among 0, 1, 1/2, 1/3, 1/4.

These characteristics were applied at the „training“ set of 36 nonhomologous peptides, to obtain sequence moments, for all pairs of sequence profiles corresponding to the same angle and weighting value. In practice, this means that „PredictorSelector“ algorithm examined all pairs of AA attributes (all pairs of AA scales), all weighting values, all bending angles and each of the three methods for creating sequence profiles to find the best descriptors.

Finding frequent motives of the best peptide antibiotic was also of great interest. For this purpose, the „set of the best peptides“ (SBP) extracted from AMPad database was used and two indices were introduced: AA selectivity index and motif regularity index. Incorporation of the motives, found in the peptides of SBP, in new designed peptides is estimated by means of a motif regularity index (Juretić et al., 2009; Juretić et al., 2011). The lower the motif regularity index value is, the greater regularity associated with the new peptide is. The statistical analysis behind motif regularity index combines:

- definition of the AA selectivity index scale,
- definition of the succeeding AA for each AA residue extracted from the SBP set in a manner that it is one of the five most common successors of required AA,
- definition of the AA placed in the  $i + 4$  position with respect to any AA, which is the AA spatially close in an  $\alpha$  helical conformation, also extracted from the SBP set in the manner that it is one of the five most common successors in that position.

AA selectivity index selects AA with high frequency among most effective frog-derived antibiotics (Juretić et al., 2009; Juretić et al., 2011). It must be noticed that selectivity index scale reflects selectivity but not necessarily the antimicrobial potency. Fifth possible most common successor in both groups was chosen among glutamic acid (E), aspartic acid (D), glutamine (Q) and histidine (H), in that way additionally favouring AA most significant for selective frog-like peptide antibiotics.

A hydrophobicity index scale CCS was used for global hydrophobicity and amphipathicity calculation for each synthesized peptide sequence (Tossi et al., 2000; Tossi et al. 2002). Hydrophobicity index scale was derived from the normalized and filtered

consensus of 163 published scales with values that arbitrarily ranges between +10 for phenylalanine (F) and -10 for arginine (R). Hydrophobicity of the peptide was calculated as the mean value by dividing sum of hydrophobicity indices for AA in the given peptide, with length of the peptide, while mean hydrophobic moment was calculated as described in Eisenberg et al., 1982. A perfectly amphipathic, 18 residue peptide, consists of only two AA, most hydrophilic Arg and most hydrophobic Phe, with maximum hydrophobic moment of 6.4 when CCS scale is used as the reference scale. For each predicted peptide relative amphipathicity was determined with respect to already mentioned perfect amphipathic peptide.

#### 2.1.4. „Designer“ algorithm

All the above mentioned characteristics of the peptides were used in the „PredictorSelector“ algorithm that led to choosing the D-descriptor, as the simplest descriptor extracted from position dependent physicochemical properties. The D-descriptor is defined as a cosine of the angle between sequence moments vectors (see Section 3.1, page 45, for the D-descriptor definition too). A linear one-descriptor fit for predicted TI was then obtained:  $TI = 50.126 - 44.803D$ , such that correlation between predicted and measured TI was  $r^2 = 0.83$ . The second goal of this process was the creation of the “Designer” algorithm. D-descriptor was a good base but it has its limitations, for example the range of predicted TI is limited to  $5 < TI < 95$ , while that of measured ones ranges from less than 0.5 to well over 100. The intent was to create an algorithm that distinguishes between good and mediocre peptides when considering TI, but not to predict the exact TI itself. Furthermore, for designing peptides an algorithm has to be taken into account, apart from the high predicted TI value:

- appropriate net positive charge
- hydrophobic moment
- hydrophobicity
- the peptide length

all of which are relevant to its antimicrobial potency.

If these characteristics were applied to a peptide with approximately 20 AA, the algorithm could not work, because the number of possibilities needed to be checked would be extremely large. Therefore additional physicochemical and rational data mining derived restrictions were applied along with a recursive algorithm, all based on the structural and chemical characteristics of the peptides from the SBP set. The peptide length chosen for the initial peptide design was 23 AA. The following restrictions were applied following the most frequently found characteristics in natural AMPs, especially in SBP (Juretić et al., 2009):

1.  $TI > 85$  predicted (for D-descriptor model maximal  $TI = 95$ ),
2. 4 or 5 for net positive charge, counting Lys and Arg as +1, Glu and Asp as -1, His as neutral and not taking the N- or C-termini into account,

3. 0.0 to – 1.2 for mean hydrophobicity using CCS scale (Tossi et al., 2002),
4. separation of polar (E, D, Q, N, G, K, R) from nonpolar (A, L, M, V, I, F, W) AA residues in helical wheel projection (design was limited to helix-forming amphipathic peptides, where Gly residues are part of polar helix face, and Hys are not),
5. limits to two neighbouring identical AA,
6. three C-terminal AA residues as in at least one good natural peptide antibiotic,
7. Gly for the first AA residue,
8. Leu or Ile on the second position,
9. minimum of nine residues E, D, Q, H, G, having high AA selectivity index, must be present in a designed paptide,
10. motif regularity index lower than 2.5 (Juretić et al., 2011).

These precise rules for peptide design were such to result in an algorithm executable in reasonable time and a workable load of suggested AMPs expected to have high TI value as well as good antimicrobial activity against *Escherichia coli*. Recursive algorithm eliminated partial peptide sequences as soon as they violated one of the proposed restrictions.

All files connected to „Designer“ algorithm including AMPad database, are available at (Web link [9]). TI values can be calculated for any query sequence using the tool “Predictor” available at Web link [10], with full name “Therapeutic index estimator for frog-derived helical antimicrobial peptides”. The “Predictor” is incorporated in the “Designer” algorithm.

## 2.2. SPPS (solid phase peptide synthesis) of designed peptides

An easy and rapid way to produce peptides needed for testing is solid phase synthesis. Adepantins were synthesised on the CEM Liberty synthesizer.

### 2.2.1. Selection of peptides for synthesis

Restrictions implemented in the algorithm were strict enough to predict a small number of peptides, only 7 of them. Among them, the only peptide in the group ending with S (Ser; Serine) at the C terminus was chosen to be tested first. It was called adeptantin 1 (ADP1). The remaining peptides from the group end with C (Cys; Cysteine). For additional testing, two more peptides from the same group were selected: having the most and the least similar primary sequence to adeptantin 1, later called adeptantin 2 (ADP2) and adeptantin 3 (ADP3) respectively. Sequences were aligned and compared using bioinformatical tool Clustal V (version used in 2008). As the Cys at the C terminus has a reactive sulphhydryl group, its reactivity was exploited in for experimental testing, such as for labelling the peptides with a fluorescent molecule, constructing dimers, or just blocking the Cys by iodoacetamidation. Another two peptides of natural origin were used as reference peptides in the first sets of

experiments: ascaphin 1 (ASC1) (Conlon et al., 2004) and pseudin 2 (PSEU2) (Olson et al., 2001). These had also been used for the first tests of the „Mutator“ algorithm, ASC1 as an example of a “good” antimicrobial peptide, with high TI, and PSEU2 as a mediocre one.

### 2.2.2. Synthesis difficulty prediction

The first step in the laboratory testing was preparing for the synthesis, using a software connected to the Liberty peptide synthesizer to calculate AA weights as well as those for other necessary reagents, solvent volumes etc. The Liberty PepDriver software controls all aspects of the synthesis automatically. A separate software, PeptideCompanion from CoshiSoft can be used to predict difficult coupling sequences in the peptide and help decide whether it is necessary to apply longer coupling cycles, double coupling and/or increased deprotection cycles. For adeptantins, most of the couplings were predicted to be difficult so double-coupling reactions were carried out at most positions.

### 2.2.3. Solid phase synthesis

There are two techniques for synthesizing peptides in the laboratory. The classical approach is the liquid phase peptide synthesis which is mostly replaced by widely accepted solid phase peptide synthesis (SPPS) (Merrifield, 1963; Kent, 1988). The liquid phase peptide synthesis is a classical method still used for industrial purposes in large scale production. SPPS was pioneered by Merrifield, and is used for producing peptides:

- that are natural but cannot be obtained recombinantly from bacteria,
- that have unnatural AA,
- that have altered backbone characteristics,
- for synthesizing peptides and proteins from D-amino acids (D-AA).

The solid support must be treated with a linker to allow “hosting” the growing peptide chain during its construction, so that the peptide is not washed away when other reagents are removed during washing in synthesis cycles. Using SPPS result in good yields at each coupling cycle, and consequently also of the final product. For this purpose, each incoming AA is added in a large excess (at least 4x), and in combination with appropriate activating agents. While ribosomic peptide synthesis starts from the N-terminus and proceeds towards the C-terminus, SPPS creates peptide from C to N- terminus. There are widely used chemistries, Fmoc and Boc. The t-Boc (tert-butyloxycarbonyl) chemistry was the originally proposed version by Merrifield, in 1963, where t-Boc is the  $\alpha$ -amino protecting group and it is removed from the growing peptide using neat trifluoroacetic acid (TFA), while side chain protecting groups and cleavage from the resin at the end of synthesis requires hydrofluoric acid, and is dangerous. In Fmoc (9-Fluorenylmethoxycarbonyl) SPPS, basic conditions are required to remove the  $\alpha$ -amino protecting group (20% piperidine in DMF), while side chain deprotection and resin cleavage require TFA. For adeptantins synthesis we used the Fmoc group.

Two groups of compounds are normally used for activations: triazoles and carbodiimides (very reactive with high probability for causing AA racemisation). Triazoles most commonly used are:

- HOBt (1-hydroxy-benzotriazole), an organic compound used both as coupling reagent and racemisation suppressor, that can improve peptide yields in synthesis,
- PyBOP (Benzotriazol-1-yl-oxytripyrrolidinophosphonium hexafluorophosphate), another coupling reagent used as a substitute for the originally used but carcinogenic BOP,
- HCTU (2-(6-Chloro-1H-benzotriazole-1-yl)-1,1,3,3-tetramethylammonium hexafluoro phosphate) activating group that speeds up reaction.

There are several types of resins and linkers used in SPPS. One of those is commonly used because of its characteristic of not swelling too much in DCM (Dichloromethane), a solid gel type support called Polyoxyethylene glycol polystyrene based resin in combination with Polyamide linker (PAL). The PEG hybrid polystyrene resin is used in synthesis of long and difficult peptides and ADPs were predicted to have difficult synthesis by synthesis software. During the synthesis, the side chains in the growing peptide must be protected. For this purpose Fmoc-AA are commercially available with appropriate protecting groups. The link of the peptide with the resin, as well as its side chain protection, remains unaltered throughout synthesis. Only when the peptide is completed, is it cleaved using Trifluoroacetic acid (TFA) scavenger mixture. Scavengers are used along with TFA to prevent reattaching the cleaved side-chain protecting groups. DMF is removed from peptide with the resin by washing with Dichloromethane (DCM) in order to prevent TFA acidolysis inhibition. The TFA – scavenger cleavage mix depends on the variety of AA side chain protecting groups, for instance those in Table 3:

Table 3. Cleavage mixtures for different types of peptides (Web link [11])

Peptides	Cleavage mix (v/v)
Any peptide	TFA/thioanisole/water/phenol/EDT (82.5/5/5/5/2.5)
Any except Arg(Pbf) or unprotected Trp	TFA/TIS/water/EDT (94/1/2.5/2.5)
Any except Arg(Pbf), Cys(Trt), Met, or unprotected Trp	TFA/TIS/water (95/2.5/2.5)

The SPPS is based on repeated cycles of reactions consisting of coupling, deprotection and washing in-between those two steps. Peptide is built from its C-terminus that is attached to resin, leaving the N-terminus of the last AA in the peptide chain free to react. Each AA N-terminus needs to be deprotected before each coupling by using 20% Piperidine in Dimethylformamide (DMF). Washing with DMF is performed after both coupling and deprotection in order to remove excess reagents.

When the synthesis is performed, it is desirable to have peptides with high yields and low racemisation. Microwave irradiation (MWR) helps in coupling acceleration and prevents peptide aggregation. In order to catalyze AA coupling, activation reagents are used, as well as an increase in reaction temperature the alternating electromagnetic radiation. The



disadvantage of this kind of synthesis is a possible racemisation when a Cys or His coupling occurs.

All peptides synthesized in the thesis were amidated at the C-terminal. This peptide version is easier to synthesize as the amide is already present in the linker and the C-terminal AA can be coupled directly as in a normal cycle.

After the test AMPs were chosen, all peptides were synthesized in solid phase as C-terminal amides on CEM Liberty automated microwave peptide synthesizer (CEM corporation, Matthews, NC) using Fmoc-PAL-PEG-PS resin (substitution 0.34 mmol/g) (Juretić et al., 2009; Ilić et al., 2013). Couplings were carried out with PyBop as activator, at 75°C in DMF, with a fourfold excess of AA. During the first C-terminal coupling, preactivated Fmoc-Cys(-Trt)OPfp was used at 45°C to reduce racemisation of the cysteine.

The scale for peptide amount that can be synthesized on CEM Liberty microwave assisted automated synthesizer is from 0.1 to 1.0 *mmol*. For ADPs 0.1 or 0.5 *mmol* was used. Masses and volumes of all reagents needed were calculated using PepDriver program. All amounts of AA were dissolved in calculated volumes of NMP (N-Methyl-2-pyrrolidone). Further, for ADP2 and ADP3 synthesis:

- 13.5 g of HOBt was dissolved in 80 ml DMF,
- 15 g PyBOP in 115 ml NMP,
- 2 x 0.15 g of resin in 5 ml DCM each,
- 12.2 ml of DIPEA (N,N-diisopropylthylamine) in 57.8 ml NMP,
- 0.5 ml of Collidine in 9.5 ml NMP.

Prepared HOBt in DMF was mixed with 720 ml of additional DMF and 200 ml Piperidine (20%). All reagents were added to the machine to perform synthesis.

When reference peptides were synthesized, synthesis was performed until points where wild type peptide differed from mutated one. Then, the resin was removed from the synthesizer, washed, dried and weighed. This amount was split into two halves, swelled again, replaced in the synthesizer to finish the synthesis. In this manner, the common parts of the peptides were synthesised together, while the variant parts were synthesised separately.

#### 2.2.4. Cleavage and workup

Peptide synthesizer delivers synthesized peptides attached to resin. To separate peptide from the resin, it was necessary to use one of the cleavage methods. For all peptides, cleavage was done using trifluoroacetic acid (TFA) – scavenger mixture consisting of TFA with thioanisole (TA), phenol (PhOH), water (H<sub>2</sub>O), 3,6-dioxo-1,8-octanedithiol (DoDt) and triisopropylsilane (TIPS). Ratio of the chemicals was 83 : 3 : 2 : 2 : 8 : 2, respectively. The process is published on the Web (Web link [12]) and will be described only for one peptide.

The tubes with peptide attached to resin were taken out of the peptide synthesizer, washed with DMF (Dimethylformamide) and transferred to the weighted plastic syringes. The syringes were placed on a vacuum station where DMF was removed from the peptide-resin. DCM (Dichloromethane) was added and resin was left in DCM for few minutes to swell, and then it was pumped out. To thoroughly wash the resin in the syringe before cleavage, isopropanol was used several times and afterwards, cold Petroleum ether. Peptide-resin was dried with nitrogen in syringe protected with parafilm, to eliminate any remaining washing compound, until constant mass was achieved. Weighing peptide-resin enabled determining the exact yield and comparing it with the theoretical one.

At this point, resin was cleaved from the peptide. Syringe with dried peptide-resin was once again placed on the vacuum station and DCM was added for resin to swell for a few minutes. After DCM was pumped out, TFA-scavenger mixture was added (4 ml for each peptide), the syringe was sealed and left for 3 hours at room temperature on easy shake. The peptide dissolved in the cleaving mixture was pumped out into a new weighted test tube, while the resin remained in the syringe. Additional 1 ml of TFA-scavenger mixture was added to the resin and drained to the new test tube with peptide.

Precipitation of the peptide from the mixture was accomplished by adding tert-Butyl methyl ether (TBME) at -20°C and centrifugation at 3000 rpm for 5 minutes. TBME was decanted from the tube with peptide sediment, and another aliquot of 15 ml TBME was added. This process was repeated three times to promote peptide precipitation. The peptide was dried with nitrogen for approximately 30 minutes until its mass remained constant. This process produced peptide in the solid state allowing to measure peptide yield and compare it with theoretical one.

### 2.3. Peptide characterization and purification

After synthesis and cleavage peptides were checked on a mass spectrometer to distinguish if the peptides were synthesized correctly, and if they were pure. Since all peptides were synthesized with excellent yields the peptides were quite pure, purification by preparative RP-HPLC was not always necessary to separate fractions that contained desired peptide. Peptide purity were confirmed by ESI-MS on an Esquire 4000 mass spectrometer.

Cleaved, dried and weighted peptides were dissolved in 200 µl of solvent A (0,05% TFA in H<sub>2</sub>O), vortexed and centrifuged at 1300 rpm (round per minute) for 3 minutes. That solution is used later for mass spectrometry and analytical HPLC.

Counterions and impurities in the peptide solution after cleavage and nitrogen drying were eliminated with the mixture HCl (10 mM) and Diethyl ether (DEE) in the ratio 50 : 50. In the falcons with dried peptides 5 – 10 ml of 10 mM HCl was added and vortexed to dissolve the peptide. Then the same volume of DEE was added to extract impurities, vortexed and centrifuged at 2500 rpm for 5 minutes. The ether fraction was then removed, and the process was repeated 3 to 5 times. After the last ether elimination the peptide solution in HCl was divided into weighted eppendorf tubes and lyophilized. This is the process usually performed after preparative RP-HPLC, but since ADPs had high purity it was performed directly on the crude peptides, before analytical HPLC testing, since preparative HPLC was skipped not to lose peptide.

### 2.3.1. ESI-MS (electro spray ionization mass spectrometry)

Mass spectrometry instrument used for this experiment was a Bruker Daltonics Esquire 4000 and on it molecular weight (MW) of each peptide was tested. Later measured MW was compared with theoretically calculated one by the synthesis protocol software.

10  $\mu$ l aliquot of each peptide fraction to be tested on ESI-MS was mixed with 90  $\mu$ l of mass solvent (H<sub>2</sub>O : Acetonitrile (ACN) : formic acid, 50 : 50 : 0,1 %), injected into spectrometer and measured.

ESI-MS was also used to test purity of fractions of each peptide collected during HPLC run. Fractions expected to contain desired peptide were analysed, which are those fractions collected when the main peak was visible on the HPLC chromatogram for each peptide (Figure 2).

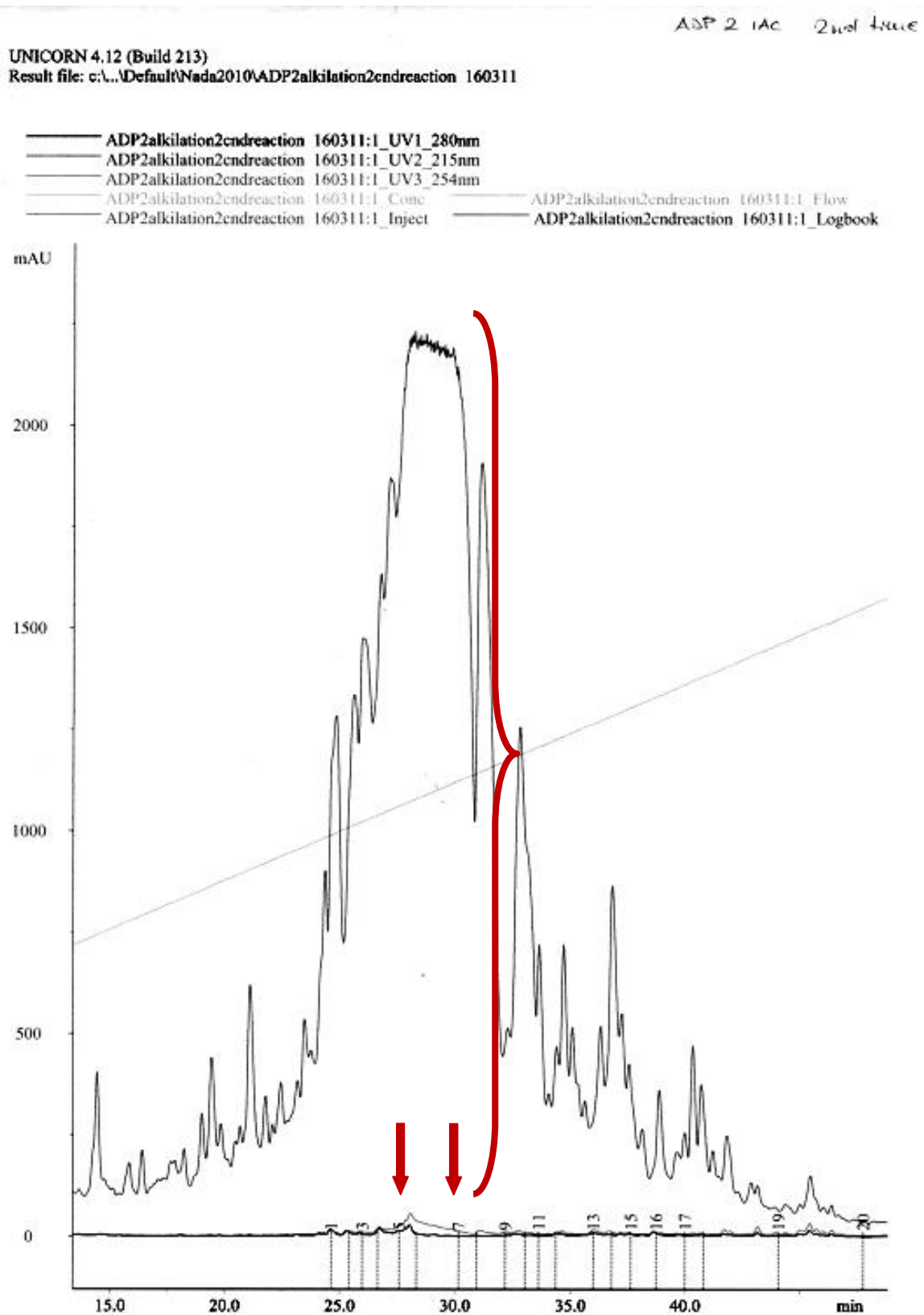


Figure 2. Example preparative HPLC chromatogram for ADP2(AM) peak showing fractions expected to contain pure targeted peptide, in this case fractions 5 - 7; X axes – time in minutes, Y axes – absorbance in *mAU* (milli absorbance units).

### 2.3.2. RP - HPLC

RP-HPLC of ADPs can be divided in two different sets: analytical HPLC and preparative HPLC purification.

Preparative HPLC for ADPs, if required, was carried out with 2 *ml/min* flux on a preparative reversed phase Waters RadialPak C18 column (21 *mm* x 150 *mm*, 5  $\mu$ *m*, 300 Å) using a 20-55% gradient of acetonitrile (solvent B) in 70 minutes. The loop used for bodipylylated peptides was 10 *ml* and for dimerised peptides 2 *ml*. Absorbance was followed at 215 *nm* where absorbance of the peptide bonds can be monitored and at 280 *nm* where absorbance of the Tryptophan (W) and Tyrosine (Y) can be observed (Aguilar, 2003). The third wavelength monitored, 254 *nm* where Phenylalanine (F) has maximum absorbance, was not important for ADPs. For the first set of HPLC runs, smaller quantities of ADP1, PSEU2 and ASC1 were purified on a semipreparative Waters column (XTerra C18, 7  $\mu$ *m*, 300 Å, 19 x 300 *mm*) using a 25 – 45% gradient of solvent B in 60 minutes with 5 *ml/min* flow.

For the second set of synthesis (ADP2 and 3), analytical RP-HPLC was carried out after cleaving, drying, weighing and dissolving peptides in 200 *ml* of solvent A. Since synthesized ADPs were exceptionally pure, preparative HPLC was skipped in order not to lose peptide but analytical RP-HPLC was performed. Preparative RP-HPLC, on the other hand, was performed after all peptides modifications such as Bodipylation, dimerization etc.

For analytical RP-HPLC, adeptantins were eluted with a flow rate of 2 *ml/min* and a gradient of 15 – 60% of solvent B in 45 to 70 minutes. Column used for analysis was Phenomenex C18 column (Jupiter size 100 x 10.00 *mm*, 5  $\mu$ *m*, 300 Å,) with 2 *ml* loop. For confirming purity another analytical RP-HPLC was performed. 50  $\mu$ *g* of each peptide (5  $\mu$ *l* peptide stock + 85  $\mu$ *l* solvent A (H<sub>2</sub>O + 0.05  $\mu$ *l* TFA)) was injected in RP-HPLC using analytical column and 100  $\mu$ *l* loop.

In both types of RP-HPLC adeptantins were expected to elute at 25-35% of solvent B. Fractions expected to contain desired peptide were collected and left aside for further testing.

### 2.3.3. Peptide modification (acetamidation, dimerization, bodipylation)

ADP2 and 3 have cysteine as the last AA on the C-terminus which is very reactive and enabled usage of this feature to create more testing possibilities of the same peptides. When ADP 2 and 3 were synthesized and lyophilised, a certain amount of the crude peptides were split into three aliquots and each aliquot was treated differently as described below. After each procedure purity and correct mass of the peptides were checked by RP-HPLC and ESI-MS followed by lyophilisation.

#### 2.3.3.1. Blocking of cysteine by iodoacetamidation

In the first aliquot of both peptides, reactive sulphhydryl group on C-terminal cysteine was blocked by iodoacetamidation (Creighton, 2002) (Figure 3) to avoid interference when peptides were used as monomers in further tests. This peptide modification was prepared

twice for ADP2 due to numerous experiments done with it. The preparation will be described only for 10 mg aliquot.

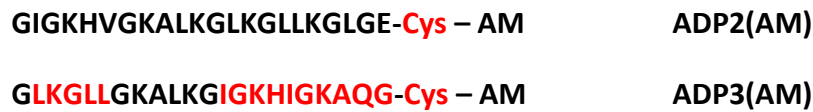


Figure 3. Adepantins 2 and 3 in amidated form; cysteine on C-terminus is blocked. AA coloured in red represent difference from the ADP1 sequence. Note that by amidating the C-terminus, a negative charge is removed, so that the overall charge increases by +1.

For reaction of iodoacetamidation following reagents had to be prepared:

- a) 0.5 M Tris8 buffer with 2 mM EDTA in 10 ml MilliQ H<sub>2</sub>O and pH 8
  - 600 mg TRIS (Tris(hydroxymethyl)aminomethane, C<sub>4</sub>H<sub>11</sub>NO<sub>3</sub>, MW = 121.14 g/mol)
  - 3.72 mg Na<sub>2</sub>-EDTA (Ethylenediaminetetraacetic acid, [CH<sub>2</sub>N(CH<sub>2</sub>COOH)CH<sub>2</sub>COONa]<sub>2</sub> · 2H<sub>2</sub>O, MW = 372.24 g/mol)
  - all dissolved in 10 ml MilliQ H<sub>2</sub>O
  - pH 10 was corrected with 37% HCl to reach 8 pH
  - purged with N<sub>2</sub> (nitrogen) for 2-5 minutes
- b) 100 mM Ascorbic acid solution in TRIS8 buffer
  - 88 mg Ascorbic acid (C<sub>6</sub>H<sub>8</sub>O<sub>6</sub>, MW = 176.1 g/mol)
  - 5 ml of Tris8 buffer
  - All done in dark, protected with aluminium foil and freshly prepared before starting reaction.
  - Used as iodine traces scavenger.

Prepared mixture was centrifuged to avoid reactants loss on the sides of falcon.
- c) Acid quench solution is 0.5 M Citric acid
  - 480 mg Citric acid (HOC(COOH)(CH<sub>2</sub>COOH)<sub>2</sub>, MW = 192.13 g/mol)
  - 5 ml of MilliQ H<sub>2</sub>O
- d) 100 mg Iodoacetamide (C<sub>2</sub>H<sub>4</sub>ION, MW = 184.86 g/mol) dissolved in 300 ~l Tris8 buffer (for adepantins in total 600 ~l was used due to their difficult dilution) under nitrogen to achieve 2.2 M solution always prepared fresh and kept in dark. To be able to dissolve Iodoacetamide, water bath on 65°C was used. (IAc MW = 56.7 g/mol)

e) 10 mg of each peptide ADP2 and ADP3 dissolved in 200  $\mu$ l of MilliQ H<sub>2</sub>O (in assay peptide can be dissolved in 100 – 300  $\mu$ l of water).

Product of the reaction is collected in 2 ml eppendorf tube. Most of the steps require dark surroundings because of the light sensitivity of some chemicals and is done under hood. The whole reaction requires time precision.

After weighing chemicals and preparing all laboratory equipment, including HPLC, the reaction can be started. All needed chemicals must be dissolved and mixed following assay steps.

The procedure starts with TRIS8 buffer preparation, see a) above. TRIS8 is then added to Iodoacetamide, see d) above, vortexed and put in water bath on 65°C until the solid is completely dissolved. 10  $\mu$ l of ascorbic acid solution, preparation see b) above, is added to the solution as iodine scavenger. The mixture is then transferred in the eppendorf with dissolved peptide, see e), and vortexed for 30-60 seconds. Adepantins needed little longer to dissolve and extra 300  $\mu$ l of TRIS8 buffer, but since they don't have Tyrosine they are not so sensitive and the time before the next step can be slightly prolonged. To stop the reaction 500  $\mu$ l of acid quench solution is added, see c) above. The final mixture is diluted with 400  $\mu$ l of the solvent A (0.05% TFA in H<sub>2</sub>O), pH is adjusted at 2-3, centrifuged and injected in RP-HPLC for purification where semipreparative column (Phenomenex C<sub>18</sub>) and 2 ml loop is used. HPLC fractions from the main peaks were examined with ESI-MS to determine purity and molecular weight on the iodoamidated modification of the peptides. Pure fractions were combined together for each peptide and lyophilized during the night. Then we add 1 ml 10 mM HCl to the tube (if there is several tubes the same solution is transferred from one to another) and then transferred to the weight eppendorf tube. Additional wash was performed by adding 0.5 ml ACN : (10mM) HCl (50:50) to tubes in which lyophilisation occurred and transferring once again everything to the marked and weight eppendorf.

This mixture was lyophilized once more for 5 - 6 hours after eppendorf tube was protected with parafilm, and cooled at -80°C for 15 minutes. Finally, the crude peptide was weighted on analytical balance so that exact yields of each peptide could be determined.

### 2.3.3.2. Covalent dimerization

In the second aliquot of both peptides covalent dimerization was performed (Figure 4). Dimerization was achieved by formation of an intermolecular disulfide bridge as described in Tam et al., 1991. The reason for creating this peptide form was to probe the effect of AMPs aggregation often noticed on the microbial surface that can also affect cytotoxicity to host cells membranes.

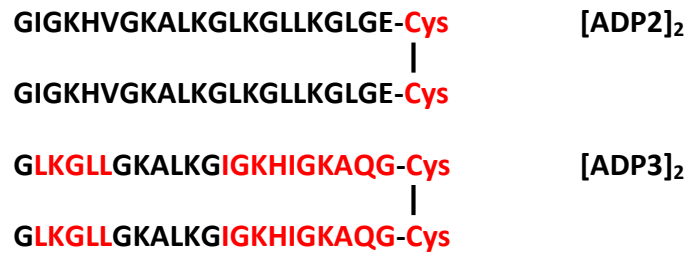


Figure 4. Adepantins 2 and 3 in dimerised form, connections achieved with disulphide bridge between cysteines on C-terminus. AA coloured in red represent difference from the ADP1 sequence.

Each of two ADPs were prepared using 20 mg of crude peptide, but ADP2 had to be prepared once more for 10 mg. Procedure will be explained for 20 mg aliquot.

Aliquots of 20 mg for each peptide was measured and dissolved in 1 ml MilliQ H<sub>2</sub>O with 20% DMSO (Dimethyl sulfoxide). As we used 1 mM DMSO the mixture was 800 ~l H<sub>2</sub>O + 200 ~l DMSO. Reaction starts the moment the mixture is combined with peptide, but to be sure of its completion it must be allowed to proceed for at least 24 hours, while adepantins were left during the weekend (~ 48 hours).

To confirm that the dimerization occurred, mixtures from both eppendorf tubes were brought to pH 6 (must be in between 6 – 6.5) using NaOH 0.5 M or HCl 10 mM and then examined on ESI-MS. After confirmation, peptides were prepared for HPLC by lowering pH to 2 – 3. This time we used Phenomenex semipreparative column with precolumn (Jupiter 5~C<sub>18</sub> 300A, size 100 x 10 mm 5 micron), loop of 2 ml, and the flux of the solvent B (0,05% TFA in ACN (acetonitrile)) was brought from 20 – 45% in 45 minutes. Fractions from the main peaks were tested for purity of the peptides and pure fractions combined together for each peptide. Combined pure fractions of both peptides were lyophilized during the night. We later added 1 ml 10 mM HCl to the tube and then transferred it to the weighted eppendorf tube. Additional wash was performed by adding 0.5 ml ACN : (10 mM) HCl (50:50) to tubes in which lyophilisation occurred and transferring once again everything to the marked and weighted eppendorf tube.

This mixture was lyophilized once more for 5 - 6 hours after eppendorf tube was protected with parafilm, and cooled at -80°C for 15 minutes. Finally, the crude peptide was weighted on analytical balance so that exact yields of each peptide can be determined.

### 2.3.3.3. Bodipylation - Fluorescent labelling with BODIPY maleimide

The third aliquot of both peptides was labelled on C-terminal cysteine (Figure 5) with fluorescent dye BODIPY-N-(2-aminoethyl)maleimide (BY) (Figure 6) as described in (Scocchi et al., 2008). BY was chosen to fluorescently label peptides because of its stability, strong fluorescence, lack of charge and relatively small dimensions. It enabled following the peptides' interaction with membranes as well as internalization into cells by monitoring fluorescence at 525 nm.



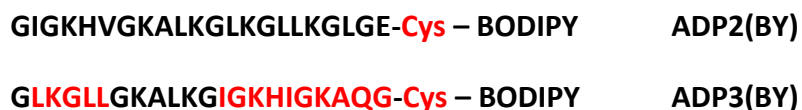


Figure 5. Adepantins 2 and 3 labelled with BODIPY maleimide on cysteines at the C-terminus. AA coloured in red represent difference from the ADP1 sequence.

The whole reaction was performed in the dark due to BODIPY's photosensitivity. For the reaction 6 mg aliquot of each crude peptide was weighted in two different eppendorf tubes (3+3 mg). Aliquot of 2 mg BODIPY (MW = 414 g/mol) was also weighted for each peptide. Reaction will be described for one peptide, but was performed for both of them separately.

BODIPY was dissolved in total 3 ml Acetonitrile (ACN, CH<sub>3</sub>CN) in the way that ACN was added to the eppendorf tube with BODIPY, vortexed until it turned yellow and then transferred in a larger falcon tube in several smaller amounts (1+1+1 ml). This way, all BODIPY residues were transferred. To this mixture 7 ml of 10 mM Sodium phosphate buffer (SPB) at pH 7.5 was gradually added, vortexed each time and saturated with N<sub>2</sub> gas by bubbling for 1 – 2 minutes. The next step was adding peptide by transferring a small amount of the resulting solution to one of the eppendorf tubes with crude weighted peptide, vortexing and transferring it back to falcon tube with the rest of the mixture and vortexing again. It was important to adjust pH to 6 – 7 because overly acidic surrounding prevents BODIPY to attach to peptide. This last step initiated the labelling reaction. Mixture was put on shake for 2 hours in the dark. After that, the second aliquot of the peptide was added following the same steps as before and again put on shake for 2 hours. The mixture is left in the fridge overnight.

The next step was to stop the reaction and block any unbound BODIPY from further interaction with the peptide. For this purpose, 10 mg of L-Cys hydrochloride monohydrate (Cys-SH, MW = 175.63 g/mol) in eppendorf tube was prepared and then transferred to the tube with peptide BODIPY-mixture and vortexed. At that point, pH was adjusted to 2-3 using 1 M HCl, 10 ml solvent A (0.05% TFA in H<sub>2</sub>O) was added and everything injected to RP-HPLC. For extracting pure peptide, Phenomenex semipreparative column (Jupiter 5- C<sub>18</sub> 300A, size 100x10.00 mm 5 micron) with precolumn was used with loop of 10 ml, and the flux of the solvent B (0,05% TFA in ACN (acetonitrile)) was brought from 15 – 50% for ADP2 and 20 – 55% for ADP3 in 60 minutes (20 – 80 min). Fractions from the main peaks were tested for purity of the peptides and pure fractions combined together for each peptide. Combined pure fractions of both peptides were lyophilized during the night. 1 ml 10 mM HCl were added to the tube and then transferred to the weighted eppendorf tube. Additional wash was performed by adding 0.5 ml ACN : (10 mM) HCl (50:50) to tubes in which lyophilisation occurred and everything was transferred once again to the marked and weighted eppendorf.

This mixture was lyophilized once more for 5 - 6 hours after eppendorf tube was protected with parafilm, and cooled at -80°C for 15 minutes. Finally, the crude peptide was weighted on analytical balance so that exact yields of each peptide could be determined.

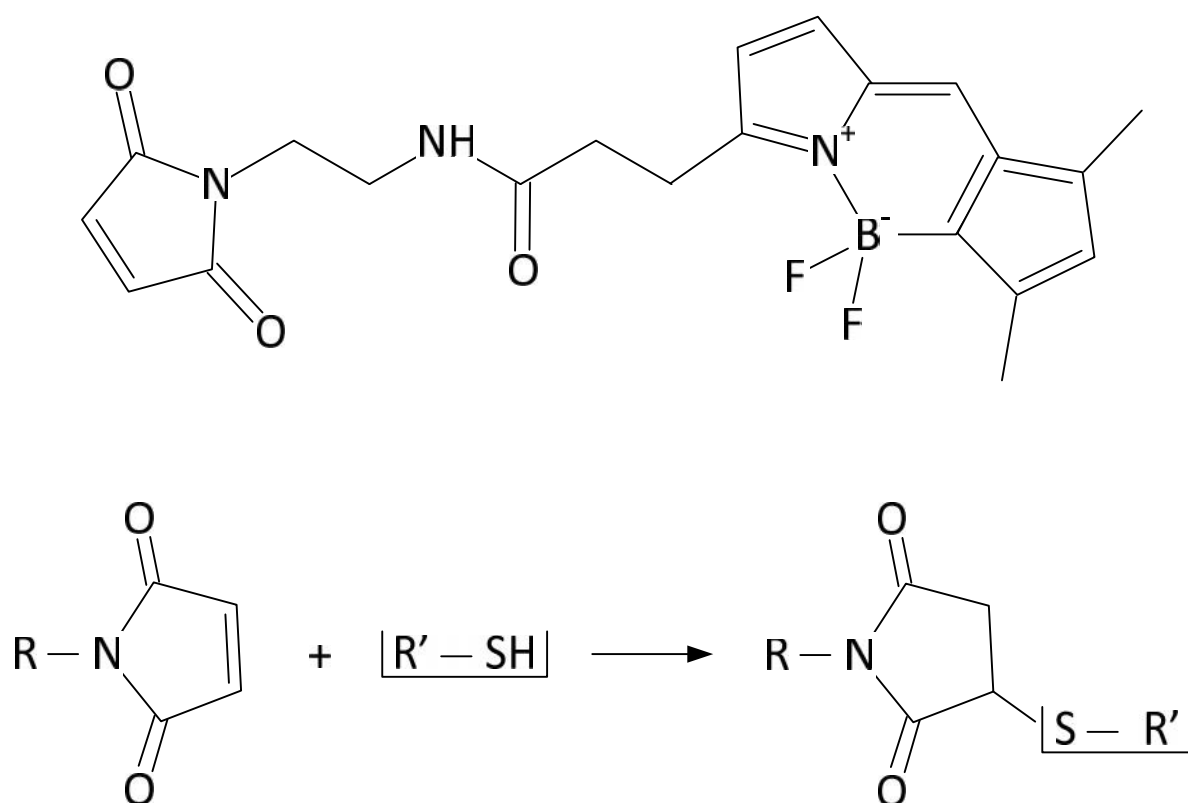


Figure 6. BODIPY molecule and its reaction with SH group in the Cysteine side chain.

### 2.3.4. Quantification

For all subsequent analysis peptide solutions were prepared from purified and lyophilized peptides dissolved in water and then quantified by at least two independent methods.

Exact concentration of each peptide was determined by using following methods:

- Mass concentration - accurately weighting peptides used to prepare solutions and dividing it with the volume of the solution,
- Waddell method (Waddell, 1956) – spectrophotometrical method,
- Quantification by molar extinction coefficient of peptide bond (Kuipres & Gruppen, 2007),
- Quantification by molar extinction coefficient of BODIPY [ $79000 M^{-1} cm^{-1}$  at  $504 nm$  in MeOH, Molecular Probes Handbook, Invitrogen, 10th Ed. p. 107],
- Kaiser test (ninhydrin test) (Kaiser et al. 1970).

Ad a) **Mass concentration** was calculated by dividing weight of the peptide with the volume of the solvent peptide was dissolved in, in adepantin case *MilliQ* H<sub>2</sub>O. Mass concentration was taken as reference concentration, later confirmed by another method. The most important step in this method was to determine exact yield of each peptide

purified and lyophilized by weighing it on analytical balance. Furthermore, on the basis of the peptide weight and its molecular weight it was decided which volume of the solvent to use. In the first set of tests there were more than enough peptides for all experiments, so it was decided to target specific concentration by dissolving calculated peptide weight in corresponding volume of water (Table 13). Targeted concentrations were 10 *mg/ml* for ADP1, PSEU2 and PSEU2 A9, while it was 5 *mg/ml* for ASC1 and ASC1 I2. To maintain a relatively high peptide concentration, in the second set of tests on adeptantins, peptides were dissolved in 500  $\mu$ l MilliQ H<sub>2</sub>O. This is the way stock solution was created.

Ad b) **Waddell method** (Waddell, 1956) is a method used to estimate peptide concentration based on the difference between spectrophotometric absorption at wavelengths 215 and 225 *nm*. To perform this method, it was necessary to have a peptide that needed quantification, a reference peptide with similar characteristics and known concentration, and a solution for testing. In the second set of tests adeptantin 1 was taken as the reference peptide, as the peptide most similar to other adeptantins. For bodipylated modifications Bac7(1-13)CysBy (3.5 *mg/ml*) was used. Measurements were performed on Ultrospec 2100 Pro (Amersham Bioscience) spectrophotometer using quartz 1 *cm* (1 *ml*) cuvette. The measuring range of the instrument is 0.05 – 0.5 *nm*. The solution used as a blank solution is the mixture of MilliQ H<sub>2</sub>O and 1/150 *N* NaOH 500  $\mu$ l each. This was also the control sample used to reduce background noise in the measurements. When the blank measurement was made in the same solution, peptide was added 3 times 2  $\mu$ l and measurement performed after each adding. The same procedure was made for reference peptide as well as for the peptide needed to be quantified. Here the absorbance values were obtained in the way that volume of the peptide added to the blank solution, 2, 4 and 6  $\mu$ l, was multiplied with appropriate dilution factor, 500, 250 and 166.6 respectively, and the results were averaged for each peptide. Concentration of the desired peptide was then extracted by using the simple method of comparing ratio of the concentration and absorbance between reference and desired peptide.

Ad c) **Quantification by molar extinction coefficient** (direct measure of a dye's ability to absorb light) (Kuipers and Gruppen, 2007) is the method that measures peptide bond contribution in the quantified peptide along with the sum of each present AA contribution at 214 *nm*. The solution used for blank probe and later as a buffer to dissolve peptide is a mixture of MilliQ H<sub>2</sub>O and AcCN in the ratio 80 : 20 with 0.1% *Trifluoroacetic acid* (TFA). Peptide concentration was calculated after measuring absorbance of the peptide, calculating its molar extinction coefficient and taking into account that cuvette used was 1 *cm* in width.

Cuvette is filled with the aliquot of 1 *ml* buffer for the blank probe and measured. After that, in the 990  $\mu$ l buffer, peptide is added to the cuvette in each step (the volume of 2.5  $\mu$ l). Concentration values are obtained by averaging the products of absorbance measured for following peptide volumes: 2.5, 5, 7.5 and 10  $\mu$ l and their belonging dilution factors 397, 199, 133 and 100 respectively.

Ad d) **Extinction coefficient of BODIPY** was used for quantifying bodipylated peptides (79000  $M^{-1} cm^{-1}$  at 504 *nm* in MeOH, Molecular Probes Handbook, Invitrogen, 10<sup>th</sup> Ed. p. 107). Once again buffer solution was prepared from the methanol, inserted in 1 *ml* cuvette and measured at 504 *nm*. Measurements were performed for buffer without peptide to exclude any background noise. Afterwards, peptide was added. Absorbance for peptide

aliquots of 2 and 4  $\mu\text{l}$  was measured and multiplied with appropriate dilution factors, 500 and 250 respectively, and then divided by cuvette width and BODIPY extinction coefficient.

Ad e) **Kaiser test (ninhydrin test)** (Kaiser et al. 1970) measures absorbance at 570  $\text{nm}$  and is usually used for determination of completeness of AA coupling at each step in SPPS. It is a fast and sensitive colour test based on reaction of ninhydrin reagents with small samples of resin + peptide.

For performing this test a kit with the already prepared solutions was used:

- Phenol,  $\sim 80\%$  in ethanol (30  $\mu\text{l}$ ),
- Potassium cyanide (KCN) in  $\text{H}_2\text{O}$  / pyridine (30  $\mu\text{l}$ ),
- Ninhydrin, 6% in ethanol (30  $\mu\text{l}$ ).

Additionally 905  $\mu\text{l}$  of 70% ethanol in *MilliQ*  $\text{H}_2\text{O}$  was used as well as 5  $\mu\text{l}$  of desired peptide dissolved in *MilliQ*  $\text{H}_2\text{O}$ . Peptide is mixed with all 3 solutions from the kit and heated to 110°C in water baths as the assay requires. Ethanol is added last and the solution is heated to 110°C for 5 minutes until it turns dark blue indicating that free primary amine is present. In the same routine the blank probe was prepared to avoid any background noise, but with 910  $\mu\text{l}$  of ethanol without peptide. The solution was then transferred into 1  $\text{ml}$  cuvette and measured in spectrophotometer. Peptide concentration was obtained using the ratio of measured absorbance at 570  $\text{nm}$  multiplied by the dilution factor 500 and extinction coefficient ( $15700 \text{ M}^{-1} \text{ cm}^{-1}$ ).

In the end, the concentrations determined by the various spectroscopic methods were used to correct the calculated mass concentration. Stock solutions of all peptides with concentration 1.28  $\mu\text{M}$  were prepared.

## 2.4. Structure analysis

Adeparins were expected to be  $\alpha$  helical peptides taking into consideration that the AMPad database was created from  $\alpha$  helical peptides. To be sure that „Designer“ algorithm is really constructing  $\alpha$  helical peptides circular dichroism (CD), spectroscopy was performed, which is a method normally used in determining secondary structure of the peptides (Kelly et al., 2005).

The same amplitudes of two components of an electrical field acting orthogonally and 90° out of phase cause circular polarization. Depending on point of view or source there are two cases of circular polarization right-handed (clockwise) and left-handed (anticlockwise). Determination of the peptides' secondary structure is based on optical activity of amino acids that absorb polarized light differently. Secondary structures of peptides such as  $\alpha$  helix and  $\beta$  sheet or hairpin are asymmetric themselves which is also the characteristic used when the structure is determined by absorbance difference ( $\Delta A = A_L - A_R$ ) measured using CD-spectropolarimeter. The measure, in this case, is molar ellipticity in degrees correlated with absorbance difference by equation:

$$\theta = 32.98 \Delta A \quad (2)$$

Wavelengths below 240 nm are used to determine peptides' secondary structure, in ADPs experiments in range 200 – 240 nm, while peptide bonds absorb at 214 nm. Specific secondary structures have characteristic CD spectra in shape and magnitude in the mentioned far UV spectral region.

Peptides are detected to be random coil in aqueous solutions in most cases, while in organic solvents or in liposome solution they tend to structure. The instrument used for these experiments was *J-715 Spectropolarimeter (Jasco, Tokyo, Japan)*.

#### 2.4.1. CD spectroscopy in different solvents

Analyses of adeptantins secondary structure was carried out with CD spectrometry at wavelengths from 200 nm to 240 nm (far-UV spectral region). For each of the tests the blank probe was measured in order to eliminate any possible background noise, and the probe was of the solvent later used for testing peptides. The volume of the blank probes was 400  $\mu$ l, and when the peptide was added the targeted peptide concentration was 20  $\mu$ M (393.75  $\mu$ l MilliQ H<sub>2</sub>O + 6.25  $\mu$ l peptide). Later, the adeptantin dimers were also measured with the concentration of 10  $\mu$ M to achieve 20  $\mu$ M with respect to the peptide chains. The cuvette used was the narrow one of 0.2 cm.

First inorganic solvents were tested:

- MilliQ H<sub>2</sub>O
- PBS 150 mM with NaCl
- SPB 10 mM

Later two organic solvents were used:

- Isopropanol in SPB 10 mM (50:50%)
- TFE in different concentrations 10-50%; with SPB 10 mM

These two organic solvent were used because they are compatible with far UV spectral region unlike ACN, DCM and chloroform. Unlike normal aqueous solvents they induce secondary structure formation in peptides and proteins. TFE in particular is known to strongly induce conformational transition of peptides and proteins to  $\alpha$ -helical structure (Hirota et al., 1997). The helical content was estimated from the molar ellipticity at 222 nm (Reed and Reed 1997). With TFE it is possible to monitor the percentage of helicity in the peptide with regard to TFE concentration increase.

Blank measurements were taken in only SPB 10 mM, 400  $\mu$ l in 0.2  $\mu$ l cuvette, for baseline noise control in order to exclude any background noise. 6.25  $\mu$ l peptide (20  $\mu$ M) was mixed with 393.75  $\mu$ l of SPB 10 mM and the CD spectrum determined, and then, in order to distinguish more precisely the amount of the organic solvent needed to induce peptide folding in the  $\alpha$  helix, TFE was gradually added as it can be seen from the Table 4.

Table 4. Calculation for the volume of TFE to be added to the peptide in order to calculate percentage of  $\alpha$  helix.

% TFE	Volume TFE needed	Volume TFE added	Dilution factor of the peptide
5	21.05	21.05	1.05
10	44.44	23.39	1.11
20	100	55.56	1.25
30	171.43	71.43	1.43
40	266.67	95.24	1.67
50	400	133.33	2

Measurements were performed after each TFE addition from 5% to 50% and for each peptide. The final volume in the cuvette was 800  $\mu$ l.

#### 2.4.2. Preparation and use of liposomes

Standard procedure most commonly used for understanding how membrane-active peptides function in living cells is by obtaining information on their structure when bound to the membrane. Artificial phospholipid bilayers are normally used in biophysical approaches in that kind of study, although efforts have been made to find a method for the same kind of studies in native biomembranes, for example solid state NMR (Koch et al., 2012). For the adeptantin study standard procedures were used with CD spectroscopic measurements.

In order to predict ADPs behaviour in membranes two types of model membranes were chosen, one mimicking bacterial cells with anionic characteristics and other mimicking host cells that are neutral. Both of the model membranes are liposomes of the large unilamellar vesicles type (LUV) (Figure 7) prepared as described by Morgera et al., (2009).

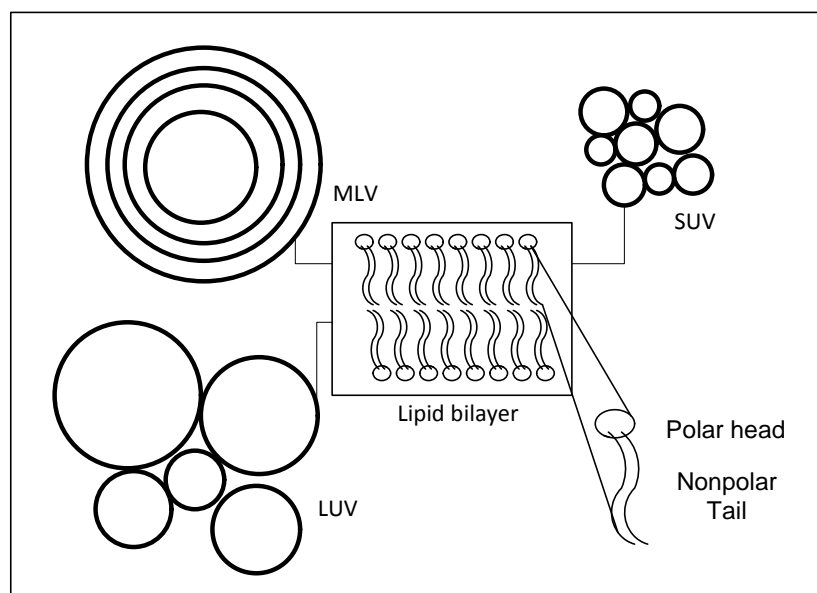


Figure 7. Scheme for vesicles in different sizes; MLV = multi lamellar vesicles are large “onion-like” structures, SUV = small unilamellar vesicle, 15-30  $nm$  in diameter, unstable and tending to fuse spontaneously at temperatures below phase transition temperature; LUV = large unilamellar vesicles, 100-200  $nm$  or larger in diameter, stable on storage.

Liposome variations used to test ADPs are:

a) Anionic liposomes:

- Phosphatidylglycerol (PG), 380  $\mu\text{l}$  = 95%
- Diphosphatidylglycerol (dPG), 20  $\mu\text{l}$  = 5%

b) Neutral liposomes:

- Phosphatidylcholine (PC), 100  $\mu\text{l}$  = 40%
- *Sphingomyelin* (SM), 100  $\mu\text{l}$  = 40%
- *Cholesterol* (Ch), 50  $\mu\text{l}$  = 20%

The procedure for the preparation of both liposome variations was the same. Concentration of the liposomes prepared was 4 mM in 1 ml and later diluted to 400  $\mu\text{M}$ . For preparation only glassware were used since *Chloroform* dissolves some plastics. All lipids were from Sigma, and all were dissolved in 2:1 *Chloroform-Methanol* ( $\text{CHCl}_3/\text{MeOH}$ ) solution to obtain concentration 10 mM for anionic and 20 mM for neutral liposomes.

Liposomes solutions were mixed in given ratios in a small round bottom flask. Later, the solvent was evaporated using dry nitrogen stream while flask was constantly rotated to avoid any clumps or uneven part in liposome film that was forming on the sides of the flask. Finally, liposomes were vacuum-dried by placing flask in a Heto vacuum centrifuge for 3 hours. 1 ml of 150 mM *Phosphate buffered saline* (PBS) was used to resuspend liposomes while rotating for 1 hour at 40°C in *Buchi R110 Rotavapor*. Achieved phospholipid concentration was 4 mM. The conversion from MLV to LUV was achieved by subjecting vesicles to several (in ADPs case 5) freeze–thaw cycles where thermal shocks were provided by placing flask alternately in 50°C water and -196°C liquid nitrogen. The final step was the sizing of the vesicles by passing them 10 times through a mini-extruder (*Avanti Polar Lipids*, Alabaster, AL) (Figure 8) using successive polycarbonate filters with 1  $\mu\text{m}$ , 0.4  $\mu\text{m}$  and 0.1  $\mu\text{m}$  pores.

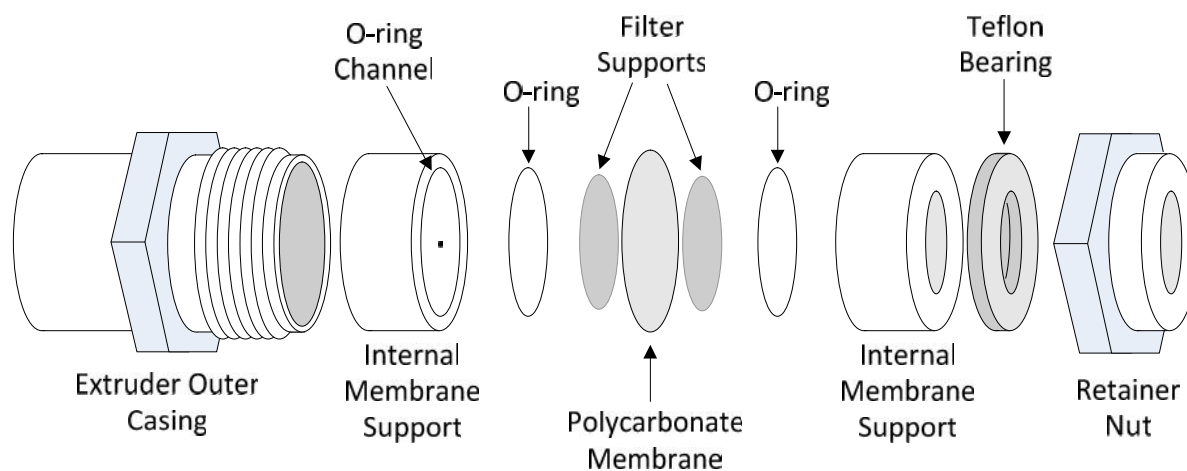


Figure 8. Scheme of mini-extruder (Avanti Polar Lipids, Alabaster, AL) (as in Web link [13])

After all the vesicles were reduced to the desired size, both variations of liposomes were diluted with 150 mM PBS to 400  $\mu$ M in 8 ml. For that purpose 800  $\mu$ l PG/dPG was dissolved in 7200  $\mu$ l 150 mM PBS and 640  $\mu$ l PC/SM/Ch in 7360  $\mu$ l 150 mM PBS. Once again CD was measured in 0.2 cm wide cuvette at wavelengths from 200 nm to 240 nm, by adding each of the peptides to achieve concentration of 20  $\mu$ M. Dimers were used at 10  $\mu$ M peptide concentration to get a better correlation with dichrographs of the monomers.

Monomers of adeptantins, ADP1, ADP2(AM), ADP2(BY), ADP3(AM), ADP3(BY) at 20  $\mu$ M had similar behaviour forming  $\alpha$  helices as in the presence of TFE while dimers were used at 10  $\mu$ M peptide concentration to get good correlation with dichrographs of the monomers.

## 2.5. Antimicrobial activity assays

To be able to confirm AMPs as antibiotics, their antimicrobial activity must be tested. Adeptantins are AMPs constructed to have high TI value with to the assumption that MIC values can be low, especially against *Escherichia coli*, Gram-negative (G-) bacteria, since processing data collected for *Escherichia coli* is used for ADPs design. In order to confirm assumption that ADPs have low MIC value three tests were performed MIC, MBC and IC<sub>50</sub> value testing.

### 2.5.1. MIC assays

MIC assay or minimum inhibitory concentration assay measures the minimum concentration of AMP needed to inhibit visible growth of microorganisms after incubation. Since the assay requires the incubation time of 18 hours it is not known whether peptides activity is bacteriostatic or bactericidal. MIC values were determined using a broth microdilution susceptibility test (Benincasa et al., 2004; Juretić et al., 2009; Ilić et al., 2013). To perform this assay it was necessary to decide on bacteria strains and mediums depending on goals wanted to be achieved and on expected sensitivity of peptides.



**a) Antimicrobial activity was tested on the reference strains:**

- *Escherichia coli* ATCC25922
- *Staphylococcus aureus* ATCC25923
- *Pseudomonas aeruginosa* ATCC27853
- *Salmonella typhimurium* ATCC14082
- *Klebsiella pneumoniae* - clinical isolate

**b) Medium used:**

- Mueller-Hinton agar (MHa) – solid (for bacterial cultivation before experiment)
- Mueller-Hinton broth (MH) – liquid (for the experiment itself)

**Preparation of bacteria:**

All bacteria strains were stored at  $-80^{\circ}\text{C}$  while not in use. When needed for testing, bacteria were routinely grown onto MHa plates and reinseeded in case of overgrowth or oldness every 20 days. One day before the experiment, two or three bacterial colonies were dispersed in 5 ml of MH for each bacteria and left overnight in a bacterial incubator at  $37^{\circ}\text{C}$ . On the day of experiment 500  $\mu\text{l}$  of overnight bacterial culture were overseeded in additional 15 ml MH and put into motion incubator for 2 hours in order to get active cells in their exponential growth phase.

For the MIC assay, the ideal number of bacterial cells is in range  $1 \times 10^5 - 5 \times 10^5$  so average is  $2.5 \times 10^5$  and that is the desired final concentration for each bacteria in each microtiter plate well. But since the bacteria and MH are added into microtiter plate well at ratio 50:50 the bacteria concentration is reduced by half so used concentration needs to be  $5 \times 10^5$ .

To achieve the exact concentration of bacteria, dilution factor is calculated on the basis of known ratio between the concentration and the absorbance measured at 600 nm. The reference ratio used for bacteria was  $A = 0.031 \text{ nm}$  to achieve  $4.6 \times 10^7$  (*E. coli*), 0.100 for  $1 \times 10^8$  (*S. aureus*), 0.039 for  $1.45 \times 10^8$  (*P. aeruginosa*), 0.038 for  $1.7 \times 10^8$  (*S. typhimurium*), and 0.148 for  $1.1 \times 10^9$  (*K. pneumoniae*). Calculation was performed as follows:

$$\alpha_{r600} : \text{cfu}_r = \alpha_{m600} : x$$

Where  $\alpha_{r600}$  represents the reference absorbance,  $\text{cfu}_r$  reference bacterial number,  $\alpha_{m600}$  measured absorbance and x number of bacteria needed. Dilution factor (df) is calculated as follows:

$$x / 5 \cdot 10^5 = \text{df}$$

$$V_f / \text{df} = V_{(\text{bacteria stock})}$$

$$V_f - V_{(\text{bacteria stock})} = V_{(\text{MH})}$$

The volume of MH needed for bacterial dilution to the final volume ( $V_f$ ) is calculated based on the number of wells used for each bacteria and increased by at least 2-3 ml for easier manipulation (7-10 ml was used).

### Preparation of the experiment:

Stock peptide concentration used to determine MIC was mostly 1.28 mM. 96-well polypropylene microtiter plate (Sarstedt, Nümbrecht, Germany) has 8 rows with 12 columns and in each well the total volume used was 100  $\mu$ l. In each well from 2 – 12, 50  $\mu$ l of MH was placed, while in the first well 100  $\mu$ l MH – x  $\mu$ l of peptide was placed. After placing x  $\mu$ l of peptide in the first well 50  $\mu$ l of MH suspension was transferred to the second and well stirred, then 50  $\mu$ l from the second well was transferred to the third, and the process was repeated until the 11<sup>th</sup> well was reached, while the 12<sup>th</sup> was the control well not treated with the peptide. This way, each step effectively dilutes the peptide two times for example 128  $\mu$ M  $\rightarrow$  64  $\mu$ M  $\rightarrow$  32  $\mu$ M  $\rightarrow$  16  $\mu$ M  $\rightarrow$  8  $\mu$ M  $\rightarrow$  4  $\mu$ M  $\rightarrow$  2  $\mu$ M  $\rightarrow$  1  $\mu$ M  $\rightarrow$  0.5  $\mu$ M  $\rightarrow$  0.25  $\mu$ M  $\rightarrow$  0.125  $\mu$ M (Table 5) and the process is called serial two-fold dilution. Lastly, in each well 50  $\mu$ l of adjusted inoculums of bacteria was added, covered with a sterile sticker and plastic cover and incubated overnight 18 hours in a bacterial incubator at 37°C.

Table 5. Example of microtiter plate preparation for MIC assay; a) 100  $\mu$ l MH – x  $\mu$ l of peptide; b) 50  $\mu$ l of MH where peptide was later added; c) 50  $\mu$ l of MH without peptide that serves as a bacterial growth control; concentrations in B row represents final peptide concentration in those wells achieved by serial two-fold dilution.

well	1	2	3	4	5	6	7	8	9	10	11	12
A												
B	128 $\mu$ M	64 $\mu$ M	32 $\mu$ M	16 $\mu$ M	8 $\mu$ M	4 $\mu$ M	2 $\mu$ M	1 $\mu$ M	0.5 $\mu$ M	0.25 $\mu$ M	0.125 $\mu$ M	0 $\mu$ M
C												
D												
E												
F												
G												
H	↓	↓					↓					↓
	a)	b)					c)					

MIC values were obtained as the mean values of at least 3 independent determinations where MIC value was taken as the lowest concentration of AMP resulting in complete inhibition of visible bacteria growth.

### 2.5.2. MBC assays

Minimal bactericidal concentration (MBC) of the peptide is defined as the minimal concentration of chosen peptide that will cause 99.9% of reduction of bacterial growth. The assay was performed as a follow up of the MIC assay to determine whether MIC value was only bacteriostatic or also bactericidal. The process will be described for only one peptide, although it was performed for all of them.

After collecting MIC values, 10  $\mu$ l aliquots of the medium with peptide and bacteria were taken from the microtiter plate wells with no visible bacterial growth (MIC value) and from the next two wells with higher concentration, 2x MIC and 4x MIC. To allow colony growth, taken aliquots were plated on MH agar plates and incubated for 24 hours. Peptide concentration causing at least a 99.9% reduction of the number of bacteria present at the beginning of MIC assay was defined as MBC value (Tossi et al., 1994). The experiment was repeated two times in duplicate.

### 2.5.3. Effect of AMPs on bacterial growth kinetics and IC<sub>50</sub>

IC<sub>50</sub> value or half maximal inhibitory concentration is the concentration of the AMP necessary to inhibit given biological process (e.g. cell growth) by 50%, and was extracted from the data gathered with bacterial growth kinetics (Mattiuzzo et al., 2007). For this assay the same bacteria and mediums as for MIC assay were used (see 2.5.1 on page 33). Results from MIC assay were taken as orientation for peptide concentrations in bacterial growth kinetics.

#### Preparation of bacteria:

Bacteria were prepared the same way as for the MIC assay when considering storing, routinely growing and overnight preparation of bacteria. The part of the procedure that differs was oversemination on the day of the experiment. The aliquot taken was 300  $\mu$ l of overnight culture instead of 500  $\mu$ l. The final concentration of bacteria in microtiter plate needs to be  $1 \times 10^6$  cfu. Therefore, for the assay each bacteria was prepared in  $2 \times 10^6$  cfu since, when put in the microtiter plate they were diluted two times. The number of bacteria was calculated in the same way as for MIC assay using same referent values.

#### Preparation of experiment:

Starting peptide concentration used for bacterial growth kinetics was 1.28 mM.

The total volume used in microtiter plate wells (Sarstedt, Nümbrecht, Germany) of 200  $\mu$ l was achieved with 100  $\mu$ l MH – x  $\mu$ l of peptide and 100  $\mu$ l of adjusted inoculums of bacteria. For each peptide there were 3 - 6 different concentrations used for each bacteria, performed in triplicates and repeated at least 3 times. The concentrations of peptides were obtained by two-fold dilution technique used also in MIC assay, but in smaller number of dilutions (Table 6). MIC values were taken as orientation and the first attempt of this assay was only for orientation and later assay was repeated with lower concentration of the peptides in order that bacterial growth was visible.

Table 6. Example of microtiter plate preparation for bacterial growth kinetic; First column is negative control containing bacteria with medium without peptide; each peptide has 3-5 concentrations in triplicates; well 12H contains only 200 ~/ $100\%$  MH as a blank to avoid any possible background noise.

well	1	2	3	4	5	6	7	8	9	10	11	12
A	MH + bacteria	ADP1 8 ~M	ADP1 4 ~M	ADP1 2 ~M	ADP1 1 ~M	ADP2(AM) 1.6 ~M	ADP2(AM) 0.8 ~M	ADP2(AM) 0.4 ~M	ADP3(AM) 8 ~M	ADP3(AM) 4 ~M	ADP3(AM) 2 ~M	ADP3(AM) 1 ~M
B	MH + bacteria	-II-	-II-	-II-	-II-	-II-	-II-	-II-	-II-	-II-	-II-	-II-
C	MH + bacteria	-II-	-II-	-II-	-II-	-II-	-II-	-II-	-II-	-II-	-II-	-II-
D	MH + bacteria	[ADP2] <sub>2</sub> 0.4 ~M	[ADP2] <sub>2</sub> 0.2 ~M	[ADP2] <sub>2</sub> 0.1 ~M	[ADP2] <sub>2</sub> 0.05 ~M	[ADP2] <sub>2</sub> 0.025 ~M	[ADP3] <sub>2</sub> 0.4 ~M	[ADP3] <sub>2</sub> 0.2 ~M	[ADP3] <sub>2</sub> 0.1 ~M	[ADP3] <sub>2</sub> 0.05 ~M	[ADP3] <sub>2</sub> 0.025 ~M	/
E	MH + bacteria	-II-	-II-	-II-	-II-	-II-	-II-	-II-	-II-	-II-	-II-	/
F	MH + bacteria	-II-	-II-	-II-	-II-	-II-	-II-	-II-	-II-	-II-	-II-	/
G	/	/	/	/	/	/	/	/	/	/	/	/
H	/	/	/	/	/	/	/	/	/	/	/	MH 100%

-II-: repeat of the well above, / : empty well. Wells A1 to F1 are positive controls (bacteria with no peptide). Well H12 is a negative control (MH broth with no bacteria or peptide), required to test for contamination.

*In vitro* monitoring of bacterial growth inhibition was performed on a microtiter plate reader (Tecan Männedorf, Switzerland) with periodic shaking at 37°C where optical density (OD) was measured at 620 nm every 10 min for 4 hours. Mean concentration of the peptide which inhibits bacterial growth by 50% at 210 min was taken as IC<sub>50</sub> value.

#### 2.5.4. Barrier effect of outer membrane – permeabilization kinetics

To test the barrier effect of the outer membrane, the *E. coli* BW 25113 (a K12 strain) was used with its deletion mutant *UwaaP* (Yethon et al., 1998) (Figure 9). The whole assay was performed as bacterial growth inhibition assay.

To achieve the exact concentration of bacteria, a dilution factor is calculated on the basis of known ratio in-between concentration and the absorbance measured at 600 nm in 1 ml cuvette in which for blank measurement was 1 ml of MH and for bacteria concentration measurement 900 ~/ $100\%$  MH + 100 ~/ $100\%$  bacteria. The reference ratio for the used bacteria was 0.031 OD at 600 nm, to achieve  $4.6 \times 10^7$ . The calculation was performed as described in equations on page 34. The microtiter plate was prepared as previously described for bacterial growth inhibition assay only with different positioning of bacteria and peptides concentrations. Bacterial growth inhibition was also performed on a microtiter plate reader (Tecan Männedorf, Switzerland) with periodic shaking at 37°C where optical density (OD) was measured at 620 nm every 10 min for 4 hours.

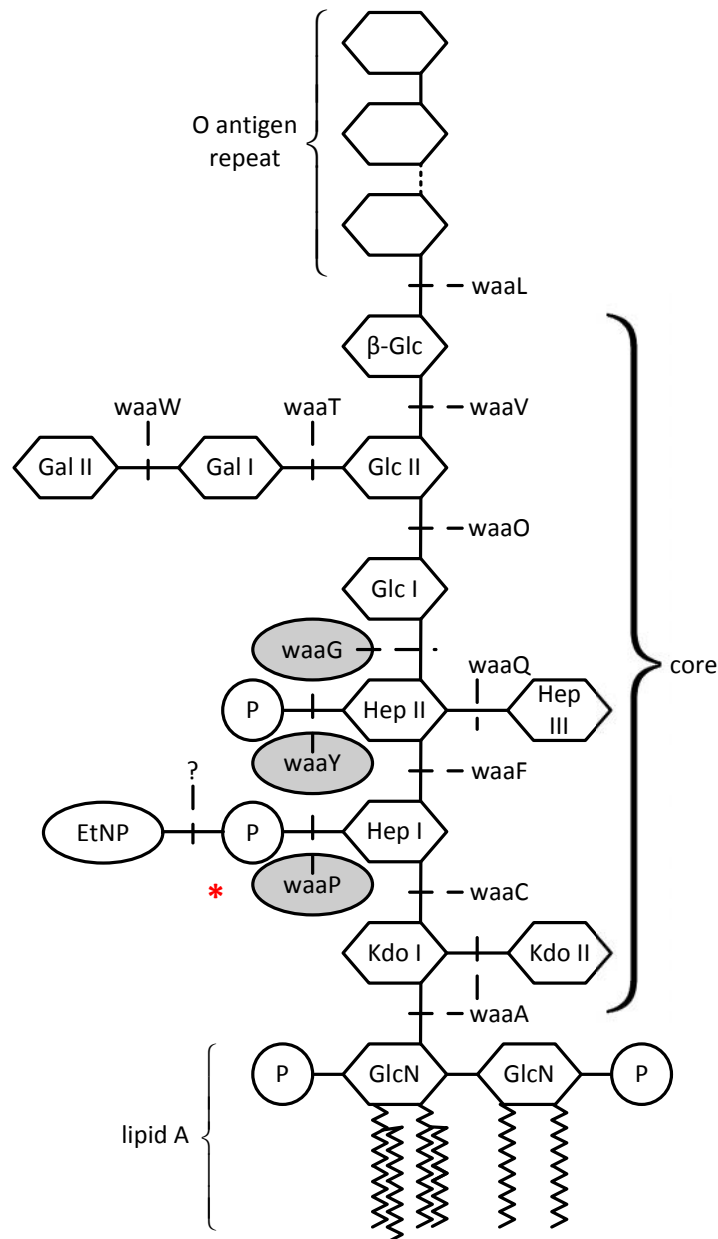


Figure 9. Lipopolysaccharide (LPS) structure in *E. coli* with genes involved in its synthesis; \* predicted activity of the *waaP* gene product (as in Yethon and Whitfield, 2001).

## 2.6. Bacterial membrane permeabilization assays

One of the crucial information on peptides mode of action was to determine whether peptides permeabilize membrane and which one was permeabilized, outer or inner membrane. The main target for testing permeabilization was *Escherichia coli* and its genetically altered strains, since adepantins design used data collected for *E. coli*. Testing the permeabilization is based on absorbance or florescence when the reagents, which normally cannot penetrate the cell, come in contact with certain molecules from the cell after membrane ruptures. Inner membrane permeabilization was determined by measuring the propidium iodide (PI) and Gal-ONp uptake by bacterial cells, while outer membrane permeabilization was determined by CENTA<sup>®</sup> uptake.

### 2.6.1. Spectroscopic analysis of permeabilization to chromogenic substrates

PI assay was also used to discover whether adeptantins permeabilize membrane and help find approximate concentration of peptides necessary for that process. To confirm permeabilization two other assays were performed, one for outer and other for inner membrane. For both assays adeptantins were prepared in concentration 0.25  $\mu$ M to be easier to handle.

The permeabilization of the outer membrane of *E. coli* by adeptantins was evaluated by following the unmasking of the periplasmic hydrolytic enzyme  $\beta$ -lactamase, using extracellular CENTA<sup>®</sup> as substrate (Jones et al., 1982), while that of the cytoplasmic membrane by unmasking cytoplasmic  $\beta$ -galactosidase activity using extracellular o-nitrophenyl- $\beta$ -D-galactopyranoside (Gal-ONp) as substrate, as described previously (Tiozzo et al., 1998; Zelezetsky et al., 2005). The  $\beta$ -galactosidase constitutive, lactose-permease deficient, ampicillin resistant *E. coli* ML-35 pYC strain was used.

#### Preparation of bacteria:

In 15 ml of MH broth with 0.05 mg/ml of ampicillin (MW = 349.41 g/mol) bacteria were sown and left overnight in bacteria incubator at 37°C. The next morning 300  $\mu$ l of bacterial suspension was added to 15 ml of fresh MH broth with 0.05 mg/ml of ampicillin and placed in the motion incubator at 37°C for 2 hours. In order to remove MH medium, the suspension was centrifuged at 3500 rpm for 10 minutes and pellet of bacteria was resuspended in PBS buffer to concentration of  $1 \times 10^8$  cfu/ml. The concentration was confirmed by measuring absorption at 600 nm on Ultrospec 2100 Pro (Amersham Bioscience) spectrophotometer. The final concentration of bacteria in microtiter plate well was  $1 \times 10^7$  cfu/ml.

#### Protocol for outer membrane:

Fresh 50 mM CENTA<sup>®</sup> (MW = 535.6 g/mol) solution in DMSO was prepared by dissolving 1.4 mg of CENTA<sup>®</sup> in 52.27  $\mu$ l of DMSO. CENTA<sup>®</sup> solution was then brought to 1.5 mM concentration by diluting it 33x in PBS. 156  $\mu$ l pure PBS was placed into each well of the microtiter plate which were then treated with 4  $\mu$ l of desired peptide, 20  $\mu$ l of prepared CENTA<sup>®</sup> solution and 20  $\mu$ l of bacteria dispersed in PBS, so total volume in the well was 200  $\mu$ l. Controls, negative as bacteria suspension without peptide and positive as well treated with SMAP-29 peptide were also placed to microtiter plate. Later adeptantin dimers were used as positive controls since they permeabilize membranes more than SMAP-29. Plate was then placed on microtiter plate reader (Tecan Männedorf, Switzerland) for measurement with periodic shaking at 37°C where optical density (OD) was measured at 405 nm every 10 min for two hours.

#### Protocol for inner membrane:

15 mM Gal-ONp (MW = 301.3 g/mol) solution in PBS was prepared. 158  $\mu$ l pure PBS was placed into each well of the microtiter plate which were then treated with 2  $\mu$ l of desired peptide, 20  $\mu$ l of prepared Gal-ONp solution and 20  $\mu$ l of bacteria dispersed in PBS,

so the total volume in the well was 200  $\mu$ l. Controls were prepared as described for CENTA<sup>®</sup>. The plate was then placed on a microtiter plate reader (Tecan Männedorf, Switzerland) for measurement with periodic shaking at 37°C where optical density (OD) was measured at 405 nm every 10 min for two hours.

### 2.6.2. Flow cytometric analysis of permeabilization to PI

The method used for examining and counting number of cells with certain feature is called flow cytometry. In the first experiment this method was used for testing propidium iodide (PI) (Figure 10) uptake by bacterial cells after addition of adeptantins. PI cannot be found in living cell due to its inability to pass through cell membrane. Once membrane is damaged, in this case with AMPs making pores in it, PI enters cell and binds to nucleic acids. When bound to the DNA, its red fluorescence increases up to 30 times. This fluorescence increase allows evaluation of the viability of the bacterial cells. Cells that fluorescence were counted as dead cells due to their membrane permeabilization. PI is cationic molecule with the molecular mass 668.3946 Da.

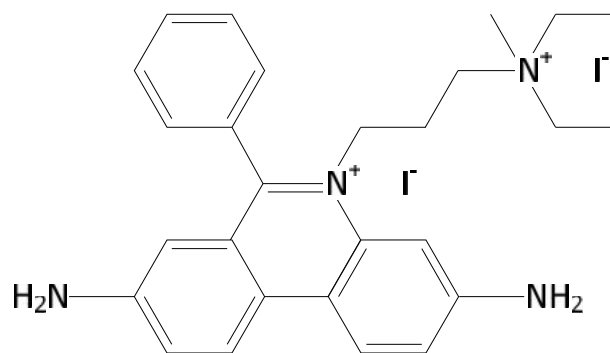


Figure 10. Propidium iodide (PI) molecule (as in Web link [14]).

The bacteria strain used for this procedure was *E. coli* ATCC25922 and was prepared in the same way as for the IC<sub>50</sub> assay. Two to three colonies of bacteria were dispersed in 5 ml of MH medium and left overnight at 37°C in bacterial incubator. From an overnight culture, a volume of 300  $\mu$ l was seminated in 15 ml MH medium and put in a motion incubator for 2 hours (exponential growth phase). The desired final concentration for bacteria was  $1 \times 10^6$  cfu to which 10  $\mu$ g/ml PI and 0.25  $\mu$ M peptides were added (starting from prepared stock solution of 25  $\mu$ M peptide). This peptide concentration is lower than that used in other assays so that a useable signal could be obtained.

PI uptake by bacterial cells was measured using flow cytometry as described in Podda et al., 2006. 10  $\mu$ l of PI was added to a glass test tube with 1 ml of bacteria, and 10  $\mu$ l of peptide. Timing started when peptide was added to the mixture. While waiting for measurement for a given period of time, the tube was placed in a thermostated water bath adjusted to 37°C. Measurements were performed in a FC500 instrument (Beckman Coulter, Lexington, MA) after the following incubation times: 15, 30, 45, 60 and 90 minutes. Data analysis was performed with the FCS Express3 software (De Novo Software, Los Angeles, CA)

and results were expressed as a percentage of PI positive cells for all peptides in each measured time period.

## 2.7. Interaction of peptides with host cells

AMPs can have good antimicrobial activity, but in order for them to be useable as antibiotics they must have a low toxicity. Not all AMPs listed in AMPad database have that kind of selectivity. Some have low MIC value and are quite toxic to erythrocytes, representative of host cells. Toxicity in this case was expressed in terms of a  $HC_{50}$  value that represents peptide concentration required to induce 50% of haemolysis of red blood cells (RBC). The  $HC_{50}$  value enters in the expression for the therapeutical index  $TI = HC_{50}/MIC(1)$  where MIC is the minimal inhibitory concentration for *E. coli*. A low  $HC_{50}$  value indicates high toxicity. If it is also associated with a high MIC (poor antimicrobial potency), this will lead to a low TI value, so that the respective peptide does not represent good and selective antimicrobial antibiotic. To test the selectivity of adeptantins, as predicted with „Predictor“ algorithm (Juretić et al., 2009) it was thus necessary to obtain haemolysis values so as to obtain their  $HC_{50}$  value.

### 2.7.1. Haemolysis assay

Haemolytic activity of the peptides was assessed on freshly isolated human erythrocytes (RBC), obtained from healthy donors, by monitoring release of haemoglobin at 405 nm.

#### Preparation required the day before the experiment:

- Scheme for peptide order on microtiter plate used for faster results collecting, taking into account that each conc. will be performed in triplet,
- Fresh buffers: 1) PBS (10 mM SPB + 139 mM NaCl, pH=7,4), 2) PBS + 1 mM EDTA, 3) 1% TritonX-100 in PBS (final conc. be 0.2%),
- PBS was added to eppendorfs at the volume required for each peptide conc. that would be added (50  $\mu$ l - x  $\mu$ l of peptide),
- PBS + Triton X was added to eppendorfs required for total lysis (positive control).

#### Content of Eppendorfs used on the day of the experiment:

- TOTAL LYSIS (Triton) - 270  $\mu$ l PBS + 80  $\mu$ l 1% Triton X + 50  $\mu$ l erythrocytes = 400  $\mu$ l (x3),
- BLANK: 50% PBS + 50% prepared erythrocytes (50:50  $\mu$ l) + 300  $\mu$ l cold PBS added later to stop reaction = 400  $\mu$ l (x3),
- PEPTIDE: 50  $\mu$ l erythrocytes + (50-x)  $\mu$ l PBS + x  $\mu$ l peptide stock + 300  $\mu$ l cold PBS added later to stop the reaction = 400  $\mu$ l (x3).



**Procedure:**

- a) Before dealing with blood the following preparations were made:
- waste bag for all waste material that comes in contact with blood,
  - container with ice,
  - balance for the centrifuge,
  - protective clothing (lab coat, gloves, cotton mask, safety glasses).
- b) Blood washing:
- If the blood was from the blood bank, all information on the bag (serial n°, blood type etc.) are recorded.
  - If the blood is extracted directly from a donor record name and sex.
  - Blood was transferred into a falcon tube with anticoagulant (heparin).
  - 5 ml of the treated blood was transferred into a test tube.
  - 15 ml of the cold (PBS + 1 mM EDTA) was added in order to deactivate the effect of Ca<sup>++</sup>.
  - The mixture was centrifuged at 1500 rpm for 15 min that depends on centrifuge and blood. The result had to be sedimentation and to achieve that it was better to put centrifugation on lower rpm and longer time period. For adeptants the optimal combination was 15 min on 1500 rpm.
  - Supernatant was eliminated with a glass Pasteur pipette and another aliquot of PBS was added at a 1:1 ratio with blood.
  - Washing was repeated 3-5 times with cold PBS and erythrocytes were then transferred to another test tube avoiding white foamy part on top.
  - Another aliquot of PBS in 1:1 ratio with RBC was added.
- c) Erythrocytes concentration:
- Different RBC dilutions were prepared from the starting test tube in eppendorfs to get for example 40x, 50x and 60x (e.g. 50x = 20 µl RBC + 980 µl PBS for a total 1ml).
  - The blank cuvette was filled only with 800 µl of PBS.
  - A test cuvette was filled with 540 µl PBS + 160 µl 1% Triton X + 100 µl erythrocytes (previously prepared dilutions) to a total of 800 µl mixture.
  - Absorbance was measured at 405 and 415 nm.

- If the measurement was near 1.3 for 405 *nm* and 1.8 for 415 *nm* the RBC concentration had the correct values, corresponding to 1% RBC, and that dilution could be used. If the measured values were not in the desired range, the dilution of RBC was adjusted to achieve them.

d) Haemolysis:

- To the previously prepared eppendorf tubes aliquots of chosen dilution of 50  $\mu$ l RBC were added (50:50  $\mu$ l).
- Peptides were added to the desired concentration (x *ml* stock) and stirred very slightly in order not to affect the lysis process.
- The eppendorf tubes were then incubated at 37°C for 30 min without motion.
- To block the reaction 300  $\mu$ l of cold PBS was added and the eppendorf tubes left for 5 minutes on an ice-bath before centrifuging at 1000 rpm for 5 minutes.
- 200  $\mu$ l from each supernatant was transferred carefully into a microtiter plate well so as not to take sediment or create bubbles that could disturb absorbance reading.
- Absorbance was measured at 405 *nm* with a microtiter plate reader (Tecan Männedorf, Switzerland).
- To extract percentage of haemolysis the following formula was used:

$$\% \text{ HAEMOLYSIS} = [(A_x - A_b) / (A_t - A_b)] \cdot 100 \quad (3)$$

where  $A_b$  is absorbance at 405 *nm* of blank wells,  $A_x$  is the absorbance at 405 *nm* of wells with peptide,  $A_t$  is the absorbance at 405 *nm* of wells with TritonX-100 (positive control corresponding to 100% haemolysis). Experiments were performed three times in triplicates for each peptide, and mean values of % haemolysis were plotted against peptide concentration so that  $HC_{50}$  values could be extrapolated for each peptide as the concentration of the peptide producing 50% haemolysis, taking standard deviation into account to estimate the error.

Adeparantins in concentrations ranging from 5-500  $\mu$ M were incubated with washed 0.5% RBC in PBS (achieved by mixing 50  $\mu$ l of 1% RBC and 50  $\mu$ l PBS with ADPs) for 30 minutes at 37°C without shaking. A parallel incubation in the presence of 0.2% Triton was carried out to determine absorbance at 100% haemolysis.  $HC_{50}$  value was taken as the mean concentration  $\pm$  SD of the peptide causing 50% haemolysis.

### 2.7.2. Flow cytometric analysis of cellular AMP uptake

Flow cytometry was also used to monitor surface binding and internalisation of BODIPY-labelled adeparantins with respect to the U937 cell line (human monocytic lymphoma) at  $10^6$  cells/*ml*. Monocytes were incubated with ADP2(BY) and ADP3(BY) at concentrations 0.1  $\mu$ M and 1  $\mu$ M and treated with PI for 5 minutes at room temperature, after which fluorescence was measured at 525 *nm* (BODIPY) for membrane interaction and at 610 *nm* (PI)

for membrane permeabilization at 5, 15, 30 minutes. At the end the, treated cells were incubated with 0.1% Trypan blue (TB) quencher, to distinguish between surface bound peptide (quenched) and internalised peptide (unquenched).

### 3. Results

#### 3.1. Peptide sets derived from the AMPad database

Construction of the AMPad database was based on a comprehensive literature survey, mostly using the PubMed-NCBI database (Web link [6]). Relevant articles were found using keywords like antimicrobial, peptides, MIC, HC<sub>50</sub>, TI,  $\alpha$  helical, amphipathic, rana, frog, etc. This literature research performed by Prof. Juretić (Juretić et al., 2009) was the basis for all subsequent work, including the already mentioned construction of the peptide database, the development of algorithms based on its contents, and the eventual laboratory testing of novel peptides suggested by these algorithms.

In the AMPad database we included all peptides that to our knowledge were available in the literature at the time, with the following characteristics:

- Amphibian origin,
- $\alpha$  helical in membrane mimetic solvent,
- Natural peptide or peptide with maximum 1 point mutation,
- Available MIC and HC<sub>50</sub> values, if possible in the same article (5 peptides do not follow this rule),
- MIC values determined using the broth microdilution susceptibility test,
- HC<sub>50</sub> values determined using freshly isolated human red blood cells from healthy donors. Many of the peptides found were tested in Conlon's laboratory, and therefore can be assumed to have been tested under the same conditions.

All of the peptides had an  $\alpha$ -helical structure, either experimentally determined or predicted. For those peptides for which published experimental data was unavailable, the helix-forming propensity was predicted by using the SPLIT algorithm version 3.5 (Juretić et al., 1998) (Web link [7]).

The AMPad database consists of a set of 73 amphibian,  $\alpha$  helical peptides. For each, the TI value was calculated from the collected MIC and HC<sub>50</sub> data. This set "set of AMPad peptides" was termed SAP (Appendix 1). SAP was then split into two sets termed the "training" and "testing" set. The requirements were that peptides in the "training" set should be non-homologous, i.e. with less than 70% pairwise identity. All the remaining peptides formed the "testing" set.

To get information on the pairwise identity, the Clustal V (version used in 2008) tool was used on the whole SAP set of peptides (Higgins et al., 1992). The resulting data were placed in a triangular matrix, consisting of peptide names and value of identity. All peptides with identities  $\geq 70\%$  were then identified and extracted to join the "testing" set while the ones remaining in the matrix formed the "training" set. An additional peptide set termed "set of the best peptides" (SBP) included 26 AMPs with TI > 20, 11 from the "training" and 15 from the "testing" set (Table 7).

Table 7. "Set of the best peptides" (SBP) where the first 15 peptides are from the "testing" set and the last 11 peptides from the "training" set, in both cases ordered by descending value of TI.

	Peptide name	Peptide sequence	HC50	MIC	TI(exp)
1	Magainin 2 analogue F5W	GIGKWLHSAKFKGAFVGEIMNS	1000,00	8,00	125,00
2	Pseudin 2 analogue K3, K10, K14	GLKALKKVFQGIHKAIKLINNHVQ	330,00	5,00	66,00
3	Magainin-analogue-12W-MG2	GIGKFLHSAKKGAFVGEIMNS	550,00	12,50	44,00
4	Pseudin 2 analogue F19	GLNALKKVFQGIHEAIKLFNNHVQ	430,00	10,00	43,00
5	Brevinin-2PRc	GLMSVLKGVLTAGKHIFKNGGSLDQA KCKISGQC	125,00	3,00	41,66
6	Temporin-1DRa-Lys-7	HFLGTLKLNLAKKIL-NH <sub>2</sub>	330,00	8,00	41,25
7	Esculentin-1ARb	GLFPKFNKKVKTGIFDIIKTVGKEAGMD VLRTGIDVIGCKIKGEC	120,00	3,00	40,00
8	Ranatuerin-2CSa	GILSSFQKGVAKGVAKGVDLAGKLLLET L KCKITGC	150,00	4,00	37,50
9	Brevinin-2TSa	GIMSLFKGVLTAGKHVAGSLVDQLKCK ITGGC	100,00	3,00	33,33
10	Brevinin-2PRd	GLMSVLKGVLTAGKHIFKNVGGSLDQ AKCKITGQC	100,00	3,00	33,33
11	Brevinin-2PRe	GILLSVLKGVLTAGKHIFKNVGGSLDQ AKCKISGQC	80,00	3,00	26,67
12	Dermaseptin-L1	GLWSKIKEAAGAAGKAALNAVTVGLVNQ GDQPS	200,00	8,00	25,00
13	Ranatuerin-2BYa	GILSTFKGLAKGVAKDLAGNLLDKFKCKI TGC	120,00	5,00	24,00
14	Ranatuerin 1 analogue K8	SMLSVLKKLGKVLGKLVACKINKQC	110,00	5,00	22,00
15	Brevinin-2PRb	GLMSLFRGVLTAGKHIFKNVGGSLDQ AKCKITGEC	65,00	3,00	21,67
1	PGLA	GMASKAGAIAGKIAKVALKAL-NH <sub>2</sub>	900,00	8,60	104,65
2	ESCULENTIN-1ARa	GIFSKINKKAKTGLFNIKTVGKEAGMD VIRAGIDTISCKIKGEC	180,00	2,00	90,00
3	ASCAPHIN 1	GFRDVLKGAAKAFVKTAVAGHIAN-NH <sub>2</sub>	200,00	3,00	66,67
4	DERMASEPTIN 3	ALWKNMLKGIGKLAGKAALGAVKLVG AES	50,00	0,80	62,50
5	RANATUERIN-2AUa	GILSSFQKGVAKGVAKNLAGKLLDELKCKI TGC	290,00	5,00	58,00
6	XPF	GWASKIGQTLGKIAKVLKELIQPK-NH <sub>2</sub>	375,40	8,80	42,66
7	ESCULENTIN-1GRA	GLFSKFAGKGIKNLIFKGVKHIGKEVGM DVIRTGIDVAGCKIKGEC	210,00	6,00	35,00
8	PEXIGANAN	GIGKFLKAKKFGKAFVKILKK	45,00	1,50	30,00
9	BREVININ-2GRb	GVLGTVKNLLIGAGKSAAQSVLKTLSCKL SNDC	180,00	6,00	30,00
10	DERMASEPTIN 1	ALWKTMLKLGTMALHAGKAALGAAA DTISQGTQ	40,00	1,50	26,67
11	MAGAININ 2	GIGKFLHSAKFKGAFVGEIMNS	1000,00	50,00	20,00

The peptides sequences selected for entry into our database varied in size from 13 to 46 residues, with a distribution as shown in Figure 11. The largest number of peptides collected and included in the database was in the 20 - 29 AA range. A peptide with a length of 20 AA can span the membrane of Gram-negative bacteria which may affect the size of

AMPs, frequently over 20 residues, although for peptides acting by the “carpet mechanism” (see section 1.1.2 page 4), that interact with the membrane in a parallel manner, the permeabilization mechanism is not necessarily dependent on peptide size.

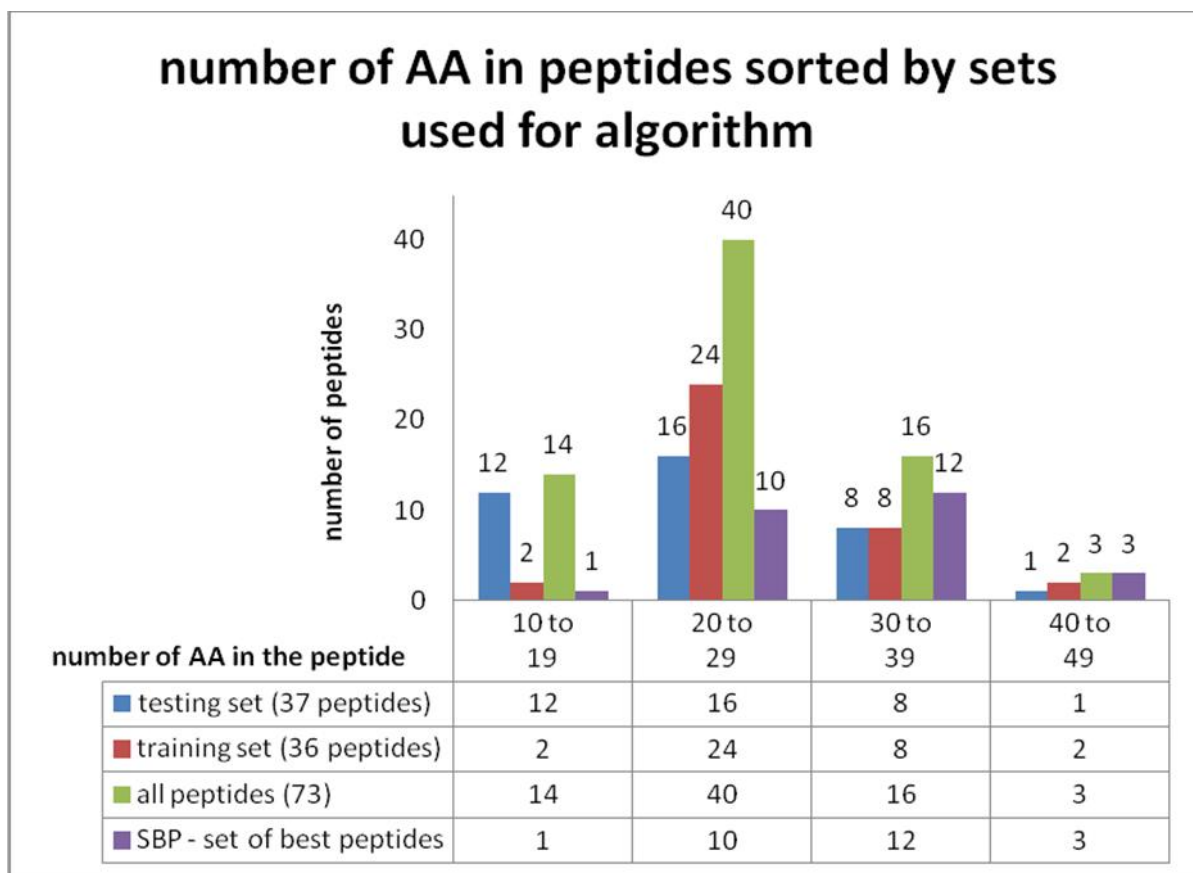


Figure 11. Relationship between peptide length and number of peptide entries in the whole AMPad database, “training” and “testing” sets and “set of the best peptides” (SBP).

This is evident when considering the distribution of the peptides’ TI values in dependence of their sequence length (Figure 12), which has a very wide length distribution (13 - 46). This is irrespective of the TI value, so that peptides with  $TI < 20$  range from 13 – 37, and those with  $TI > 20$  range from 14 – 47, although most of these peptides are  $> 20$ .

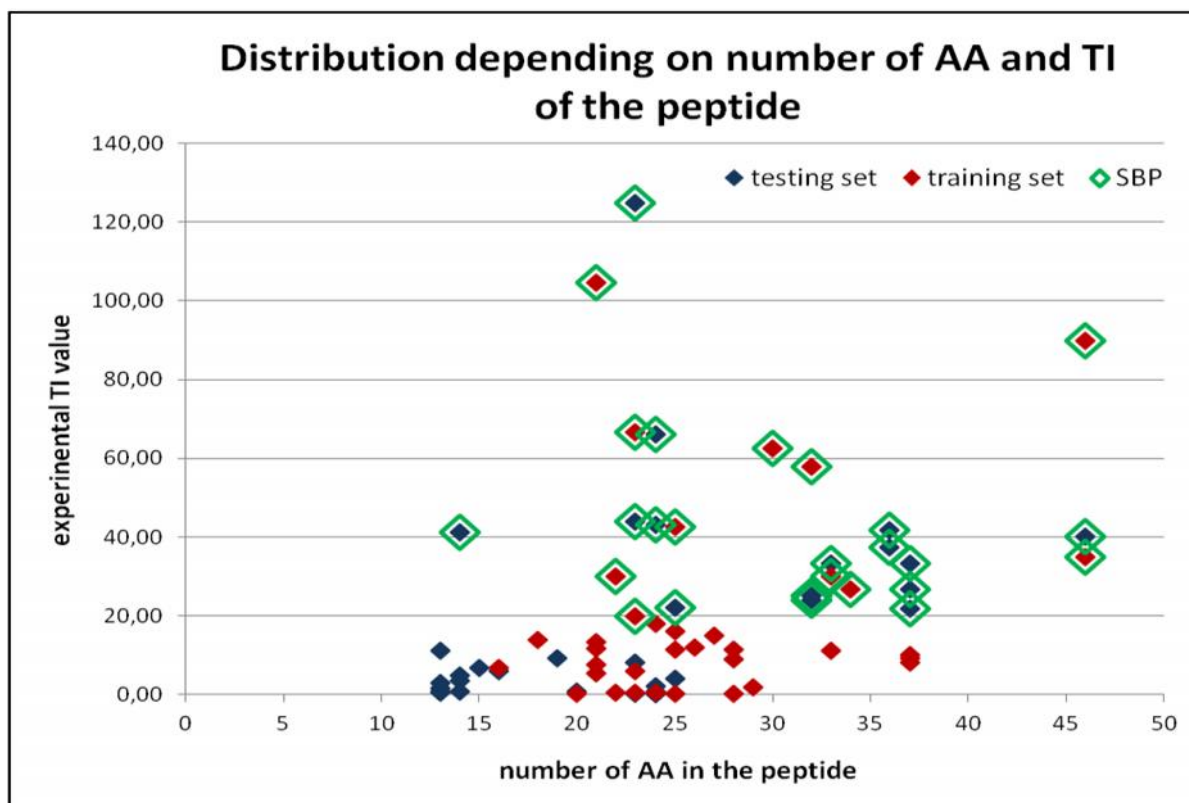


Figure 12. Distribution of the peptides in the AMPad database divided in three sets considering peptide length by number of AA and experimental TI value; SBP („set of the best peptides“) constructed from peptides included in both sets that have TI greater than 20.

The adeptantins proposed by the algorithm all have the length of 23 AA, with the idea of creating  $\alpha$  helical peptides that could span the membrane of the Gram-negative bacteria, but also corresponding to the length of peptides forming the largest cluster of peptides from AMPad database (Figure 11). From the table given in Figure 11 one can note that the “training” and the “testing” set have the largest number of peptides in the same cluster as the ADPad database consisting of peptides with 20-29 AA length.

Once the AMPad database was created, it was then possible to correlate TI to the peptides' position-dependent physicochemical properties. This made use of the concept of sequence moments as defined by Prof. Davor Juretić (2009), so that for each peptide, the sequence profiles were converted into vectors (Figure 14; Juretić et al., 2009; Juretić et al., 2011).

The next step was to create an optimal descriptor, by finding the correlation between a scalar descriptor extracted from the sequence moments and the measured TI value of each peptide in the „training“ set.

The correlation with scalar descriptors corresponding to a single scale of AA attributes was not high, with  $r^2 = 0.52$ . A better choice of attributes used a triplet consisting of two AA scales and one smoothing technique, assigning 2700 descriptors to each triplet (see 2.1.3). Out of 2700 descriptors for each triplet, the best combination, consisting of Janin and Guy scale and smoothing process that excludes the central AA in the sliding window of length 11 AA, resulted in a correlation coefficient  $r^2 \geq 0.83$  with respect to the “training” data set. The

comparable correlation was obtained for the simple descriptor found by Prof. Damir Vukičević, named D-descriptor (see Table 8), defined as the cosine of the angle between sequence moments obtained using the hydrophobicity scales of Guy (Guy 1985) and Janin (Janin 1979), with the peptide sequence set in an arc of  $\alpha = \pi/2$ , with a smoothing process that excludes the central AA in the sliding window used to sum all sequence environment vectors, and using a weighing factor  $q = 1/3$  (see Figure 14) (Juretić et al., 2009; Juretić et al., 2011). The sliding window is 11 AA long, excludes central AA and while approaching the termini of the sequence reduces number of AA symmetrically. For the first AA the value is calculated as the mean value of the second and the third AA. Similar is for the last AA where value is calculated as the mean of two previous AA. The chosen pair of AA attribute scales were both hydrophobicity scales differing in their classification of three AA residues in particular, Gly, Ala and His. In Janin scale, Gly is considered to be buried in the membrane while in the Guy scale it is considered polar. This led to the possibility of forming unusual sequences, like all Gly, Ala or His peptides that are not likely to exist in nature, but are predicted to have maximal TI value by the D-descriptor. This was one of the limitations of D-descriptor model, and for this reason, a filter was set to avoid sequences with repeated residues. Another limitation was the fact that it is trained on frog-derived peptides and is considered to be reliable only for this type of peptides. Only extended comparisons with databases of helical AMPs collected from other microorganisms (e.g. insect peptides or mammalian cathelicidins) (Tossi et al., 2000), will show if it is more universally applicable.



Table 8. Three descriptors with the highest correlation found by „PredictorSelector“. Although D-descriptor (in the second row) has slightly lower correlation than the first one, it was chosen because it is much simpler than the first one. For codes of the used scales see Appendix 5. Correlation is among descriptor values and experimentally determined TI values for peptides in the “training” set.

Angle between sequence moments: multiply by angle in radians Scales: 7, 35 Smoothing technique: sliding window of length 11 AA that excludes middle AA Bending angle: $\pi/5$ Weighting exponent: 1/2 Length of the sequent moment corresponding to scale 7: length in the nominator Length of the sequent moment corresponding to scale 35: disregard Correlation= 0.915613
Angle between sequence moments: multiply by cosine of this angle Scales: 5, 31 Smoothing technique: sliding window of length 11 AA that excludes middle AA Bending angle: $\pi/2$ Weighting exponent: 1/3 Length of the sequent moment corresponding to scale 5: disregard Length of the sequent moment corresponding to scale 31: disregard Correlation= -0.911006
Angle between sequence moments: multiply by angle in radians Scales: 29, 31 Smoothing technique: sliding window of length 11 AA that excludes middle AA Bending angle: $\pi/2$ Weighting exponent: 1/2 Length of the sequent moment corresponding to scale 29: length in the nominator Length of the sequent moment corresponding to scale 31: length in the denominator Correlation= 0.907174

The best linear fit between predicted TI value and D-descriptor value:  $TI = 50.126 - 44.803D$ , was found after the D-descriptor values were calculated for the „training“ set of peptides. From this, TI values could be predicted from the D parameter of each peptide in the „testing“ set. The correlation of the measured and predicted TI values for the “testing” set gave an acceptable indication of correlation expressed as the determination coefficient ( $R^2 = 0.64$ ). Statistical methods were not used in standard manner (Juretić et al., 2009). The Pearson r correlation is used on the nonstandard distribution of data in an attempt to predict which peptides have high TI value, which was achieved. That way D-descriptor was designed to distinguish between good and mediocre peptide antibiotics, which is indicated by the angle between sequence moments. The bigger the angle is, the better antibiotic peptide is supposed to be. Although the chosen D-descriptor was selected out of many other possible descriptors using only 11 peptides with high TI values (part of the “training” set, see Table 7), additional tests justified the choice (Juretić et al., 2009).

The “Designer” algorithm was then constructed using D-descriptor to suggest the sequence of potential AMPs with high selectivity (high TI), with some additional restrictions

to lower the number of generated peptides to a workable load. Amphipathicity is one of the characteristics of AMPs that helps them interact with membranes. The amphipathicity of a peptide can be visualised by considering a helical wheel projection, such as that of ascaphin 1 shown in Figure 13. Ascaphin 1 is known to be good peptide antibiotic. Using the Virginia University helical wheel application (Web link [1]) or HydroMCalc tool (Web link [8]), it can be seen that the AA residues are distributed so as to cluster on different sides (sectors) of the projection, and this was one of the features included in the „Designer“ algorithm.

The „Designer“ algorithm thus uses recursive algorithm with inbuilt simple restrictions to greatly reduce the number of sequences, and then the inbuilt TI-predictor, based on linear D-descriptor model, eliminated 81% of the rest of proposed peptides with length of 23 AA leaving a workable load of only 7 peptides. The sequence moment vectors for three of these peptides: adeptantin 1, 2 and 3 are shown in Figure 14, where it can be seen that there is a large angle separating the vectors determined using the Guy and Janins scales respectively.



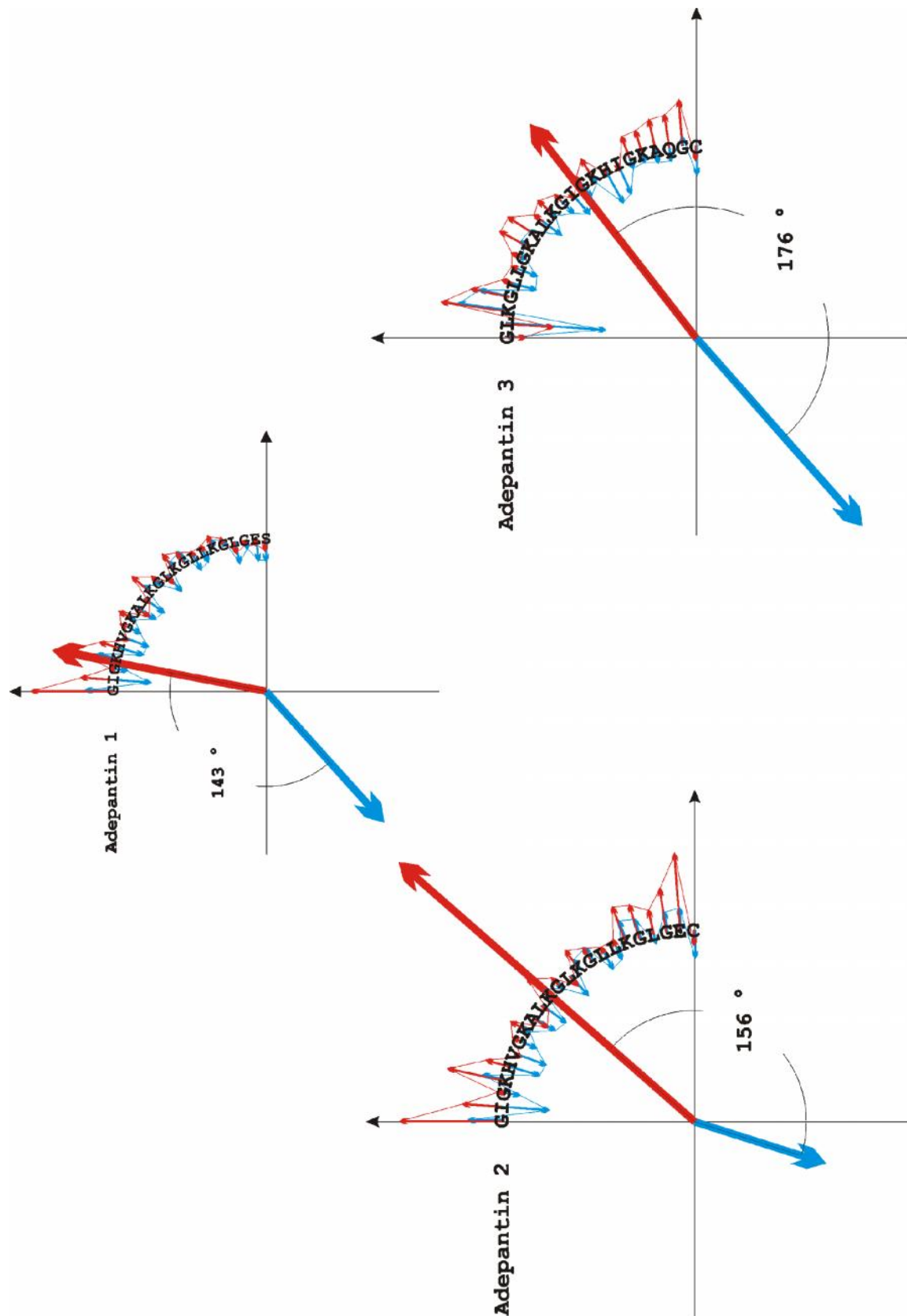


Figure 14. Sequence moments for adeptantins 1, 2 and 3; small arrows are calculated by using amino acids index scales (Appendix 2, Appendix 3, Appendix 4), red for Janin's (Janin 1979) scale and blue for Guy's (Guy 1985) scale; sum of the small vectors result in sequence moments presented by the large vectors; angle between sequence moments is used to calculate D-descriptor as the cosine of that angle.

### 3.2. From designed to synthesized peptides

Restrictions included in the „Designer“ algorithm (Juretić et al., 2009) produced a workable load of 7 peptides (Table 9). Restrictions were created in a manner to suggest peptides with high TI values and to be active against Gram-negative bacteria.

Table 9. Output adeptant sequences from the „Designer“ algorithm.

Peptide name	Peptide sequence	TI <sub>(pred)</sub>	Motif regularity index	Mean hydrophobicity index (H)	Peptide net positive charge <sup>(1)</sup>
Adeparentin 3	GLKGLL <u>GLKALGIGKHIGKAQGC</u>	94.841	2.385	-1.061,	5
-	GLKGLLGLKALGEAKLLGKHKGC	94.917	2.487	-1.074,	4
-	GITQGVKLGIGKHHVKGKALGIGC	85.143	2.436	-0.857,	4
Adeparentin 2	<u>GIGKHVKGKALGLKGLLGLGEC</u>	91.101	2.308	-0.891,	4
Adeparentin 1	<u>GIGKHVKGKALGLKGLLGLGES</u>	85.838	2.308	-0.978,	4
-	GIGKHVKGKALGVKLLKGLGEC	91.915	2.410	-1.135,	4
-	GIGKHVKGALGELKLLKGLKGC	94.905	2.410	-0.891,	4

TI<sub>(pred)</sub> is the value predicted by the D-descriptor model; mean hydrophobicity is based on CCS scale (Web link [8]); red underlined – “small” motifs in ADPs ([G,S,A]XXX[G,S,A] and GXXGXXXG) (Senes et al., 2000);. <sup>(1)</sup> Note that during the peptide design and filtering process, charge was determined assigning +1 to Lys and Arg and -1 to Glu and Asp. His was considered neutral. Both N- and C-termini were considered free and therefore cancelled each other out.

„Designer“ output proposed 6 peptides ending with Cysteine, while only one ends with Serine. Cysteine at the C-terminus of the proposed peptides may be the result of the requirement that three C-terminal AA residues should be the same as in at least one good natural peptide antibiotic. Cys is present at the C-terminus of many helical AMPs derived from frogs (Tossi et al. 2000, Simmaco et al. 1998) as it is part of the so-called “Rana-box” consisting of Cys on the last and 6<sup>th</sup> from the last position, connected with disulfide bridge. A single Cys residue in a sequence can be problematic, as it is quite reactive, so adeptant 1 (ADP1), as the only one ending with a Serine, was considered to be the most suitable first candidate for performing verification tests. With a predicted TI of 86, ADP1 was not the peptide predicted to be the most selective in the group, but was in any case expected to be very selective. The „Designer“ algorithm required a net positive charge of 4 or 5 and the mean hydrophobicity from 0.0 to -1.2 as often found for helical AMPs (Tossi et al., 2000) using the CCS scale (Tossi et al., 2002).

Three so-called “small” motifs [G,S,A]XXX[G,S,A] are present in the sequence (Table 9), a primary structural feature that indicates a high probability of membrane insertion and helix-helix interaction in the membrane (Senes et al., 2000), respectively. Furthermore, when compared to the primary structures of known  $\alpha$  helical peptides, ADP1 was less than 50% identical to any of them. As for the reference peptides from the “training” set, it was decided to test two of these, picking one mediocre peptide, pseudin 2 (PSEU2) (Olson et al., 2001), and one good peptide antibiotic with high TI, ascaphin 1 (ASC1) (Conlon et al., 2004). This would not only provide reference data for comparing the activity of ADP1, but would also confirm the experimental data for at least two of the database peptides, and the capacity of the algorithm to predict TI that correlate to the real one. These peptides were

then also used in a first evaluation of the „Mutator“ algorithm, a version of „Designer“ used to suggest point mutations to improve the selectivity of known peptides.

For the second set of tests, two additional peptides were taken from the „Designer“ set (Table 9), choosing the most and the least similar in primary structure to adeptantin 1. While adeptantin 2 (ADP2) differs from the ADP1 only in the last position (Ser → Cys), alignment using the Clustal W (version used in 2010) showed that adeptantin 3 (ADP3) differed in maximal number of positions (Figure 15). The purpose for additional testing was to test if other adeptantins are as selective as ADP1 and to use reactive sulphhydryl group of the Cys at the C-terminus for additional testing.

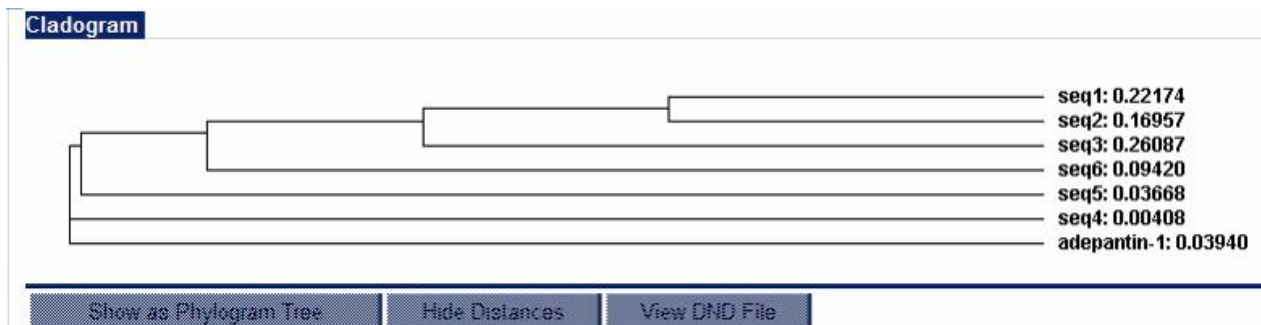


Figure 15. Cladogram tree from Clustal W tool showing sequence alignment of 7 resulting peptides from the „Designer“ algorithm; Seq4 was later called adeptantin 2 and is most similar to adeptantin 1; Seq1 later called adeptantin 3 and is most different from adeptantin 1.

In preparation for the synthesis, peptides sequences were evaluated using different software programs. Furthermore, it was decided to synthesize the peptides as C-terminal amides. This would not only increase stability and facilitate syntheses, but also increase the charge by +1, likely increasing the potency. The online ExPASy ProtParam tool provided MW as well as pI, stability indices, hydrophobicities etc. (Web link [15]) for the amidated peptides. Results for ADP1 are presented below:

## Adeptantin 1 (ADP1 or DESC1) [2259,79]

**GIGKHVKGKALKGLKGLLKGLGES-NH<sub>2</sub>**

**Number of amino acids:** 23

**Molecular weight:** 2259.7

**Theoretical pI:** 10.18

**Total number of negatively charged residues (Asp + Glu):** 1

**Total number of positively charged residues (Arg + Lys):** 5

**Instability index:**

The instability index (II) is computed to be -22.25

This classifies the protein as stable.

**Aliphatic index:** 118.70

**Grand average of hydropathicity (GRAVY):** -0.013

Next, the Peptide Companion tool (CoshiSoft) was used to predict possible difficult coupling points in the synthesis. This tool attempts to estimate the aggregation potential of the peptides and relates this to decreased coupling efficiency due to steric hindrance. Although it does not take side-chain protecting groups into consideration, it has been quite

an effective tool in the experience of the Trieste University peptide synthesis lab. The result presented is for ADP1 (Figure 16):

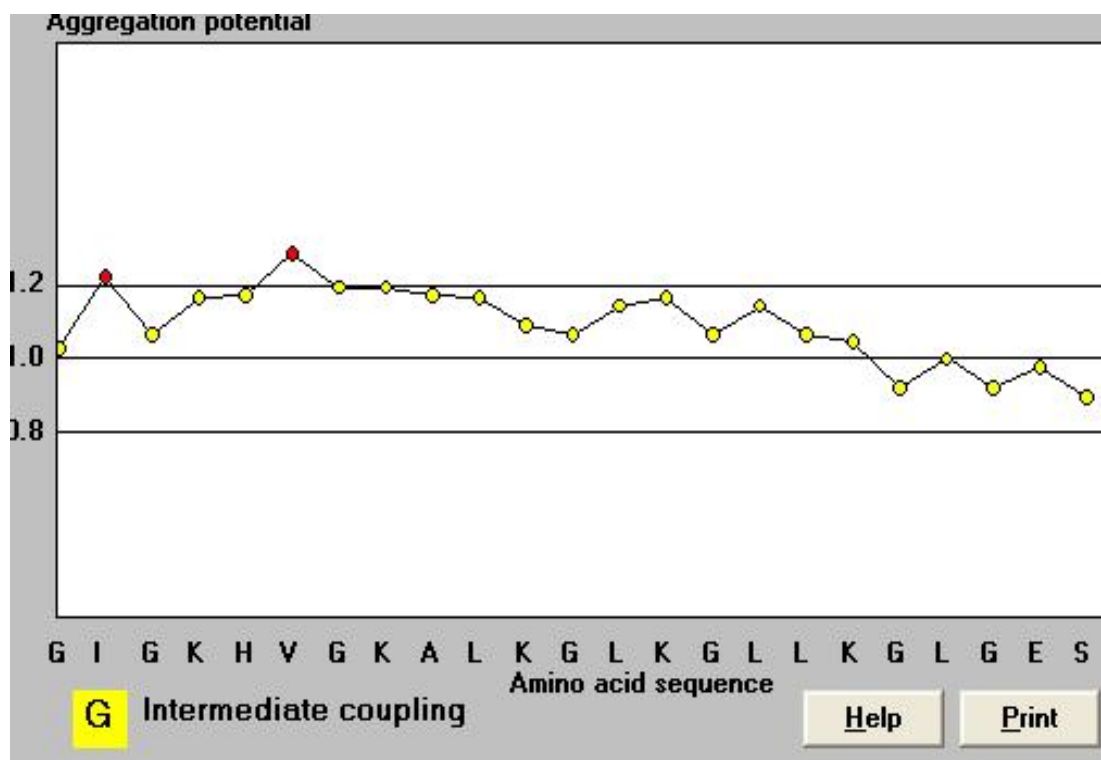


Figure 16. Prediction of the synthesis difficulty for ADP1 by Peptide companion tool. Most AA are between upper two lines indicating difficult synthesis.

As is visible from the figure the aggregation potential was high (1 - 1.2) at almost all positions from the 6<sup>th</sup> away from the C-terminus (the peptide is synthesised C-term → N-term), meaning that couplings among AA in adepantin were to be considered generally difficult. This suggested the use of double-coupling cycles throughout the synthesis. This procedure ensured that the peptides were synthesized in good yields and in quite high purity.

The PepDriver software controlling the synthesizer took double-coupling into account when calculating reagent weights and solvent volumes for chemicals to be used for each synthesis. Peptides were synthesized individually at a 0.05 mmol scale. The yield was estimated for the weight of the peptide-resin complex as well as for the weight of cleaved peptide, and taking into account probable losses during the work-up and purification process, the yields can be considered good. As an example, yields for the synthesis of adepantin 2 and 3 are shown in Table 10.

Table 10. Theoretical and measured yields of ADP2 and ADP3 with and without resin.

compound	Theoretical yield (mg)	Measured yield (mg)	% of theoretical yield
ADP2-resin	324.33	265	82
ADP3-resin	327.19	229	70
ADP2	113.8	102	90
ADP3	112.3	93	83

The theoretical yield for the peptide-resin complex was calculated by multiplying the weight of the resin by the resin substitution and MW of fully protected peptide and adding this to the initial resin mass. The resin used was Fmoc-Linker-AM-Champion in an amount of 0.15 g, resin substitution was 0.34 mmol/g and for ADP2 and ADP3, fully protected MW was 3418.3 and 3474.4 respectively. For ADP3 the lower yield is principally due to technical difficulties during synthesis. The theoretical yield for cleaved peptide was calculated by multiplying synthesis scale 0.05 and peptides MW. The yield was  $\geq 90\%$  (only ADP3 had a loss of approximately 10% due to technical difficulties), so both peptides were synthesized in excellent yields.

### 3.3. High yields and purity of the adeptantins and modified analogues

ESI-MS carried out on all peptides confirmed that molecular weights were in good correspondence with the calculated values (Table 11). The measurements confirmed not only that the correct peptide was present, but also a high level of purity as only one peak is present (Figure 17, Figure 18, Figure 19, Appendix 8). Graphs for bodipylylated peptides have two peaks where lower peak represents correct one for bodipylylated peptide while higher one is a “shadow peak” (Figure 20).



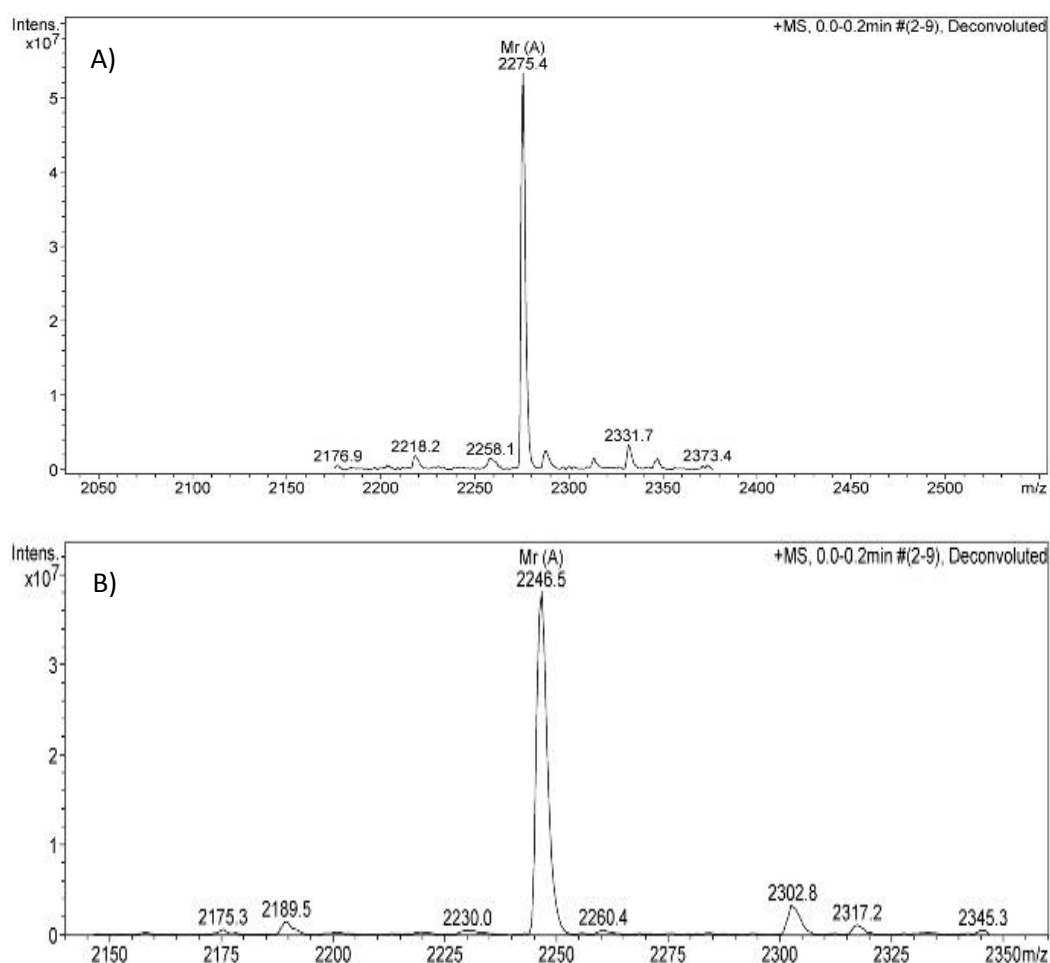


Figure 17. ESI-MS analysis of adeptins, A) ADP2, B) ADP3.

Table 11. Theoretical and measured MW and yields of ADP1, unmodified ADP2 and ADP3, ASC1 and ASC1 I2, PSEU2 and Pseu2 A9.

Peptide abbreviation	Theoretical MW	Measured MW	Yield (mg)
ADP1	2259.0	2259.7	25.8
ADP2	2275.8	2275.4	76
ADP3	2246.8	2246.5	66.2
ASC1	2369.8	2369.5	3.2
ASC1 I2	2335.8	2335.6	3.8
PSEU2	2684.2	2683	32.4
PSE2 A9	2608.1	2608	31.2

After preparative RP-HPLC purification, the purity of ADP1, PSEU2 and ASC1 increased to >99%, as confirmed by the analytical RP-HPLC (see Appendix 7 and Appendix 8). Thanks to the high purity of crude ADP2 and ADP3 these were directly used in modification reactions (iodoacetamidation, covalent dimerization or BODIPY labelling) and purified by semipreparative RP-HPLC only after modification (see Figure 2, page 21). Fractions containing the desired peptide were identified by ESI-MS (see Appendix 6), pooled and

lyophilised. In this case also, purity >99% was confirmed by RP-HPLC. All peptides were synthesized in good yields, considering the inevitable losses due to reversed phase chromatography, including the ADP2 and ADP3 modifications, which were recovered in *mg* quantities (Table 12).

Table 12. ADP2 and ADP3 modifications with its theoretical versus measured MW and their yields; for ADP2(AM) and [ADP2]<sub>2</sub> modification reaction was performed twice, therefore, the yields are higher.

Peptide abbreviation	Theoretical MW	Measured MW	Yield (mg)
ADP2(AM)	2332.87	2332,4	6.3
[ADP2] <sub>2</sub>	4549.62	4549.3	6.6
ADP2(BY)	2689.82	2689.6	2.3
ADP3(AM)	2303.83	2303.3	3.8
[ADP3] <sub>2</sub>	4491.54	4491.5	4.6
ADP3(BY)	2660.87	2660.5	3.6

The blocking of cysteine by iodoacetamidation was performed to avoid unwanted reactions due to the free sulfhydryl in the C-terminal cysteine which could interfere with structural determination and functional assays. This reaction results in a side chain with hydrophobicity characteristics similar to those of glutamine. This reaction gave excellent yields for both peptides. ESI-MS molecular weight analysis coupled with RP-HPLC confirmed structure and quality of peptides (Table 12, Figure 18, Appendix 6).

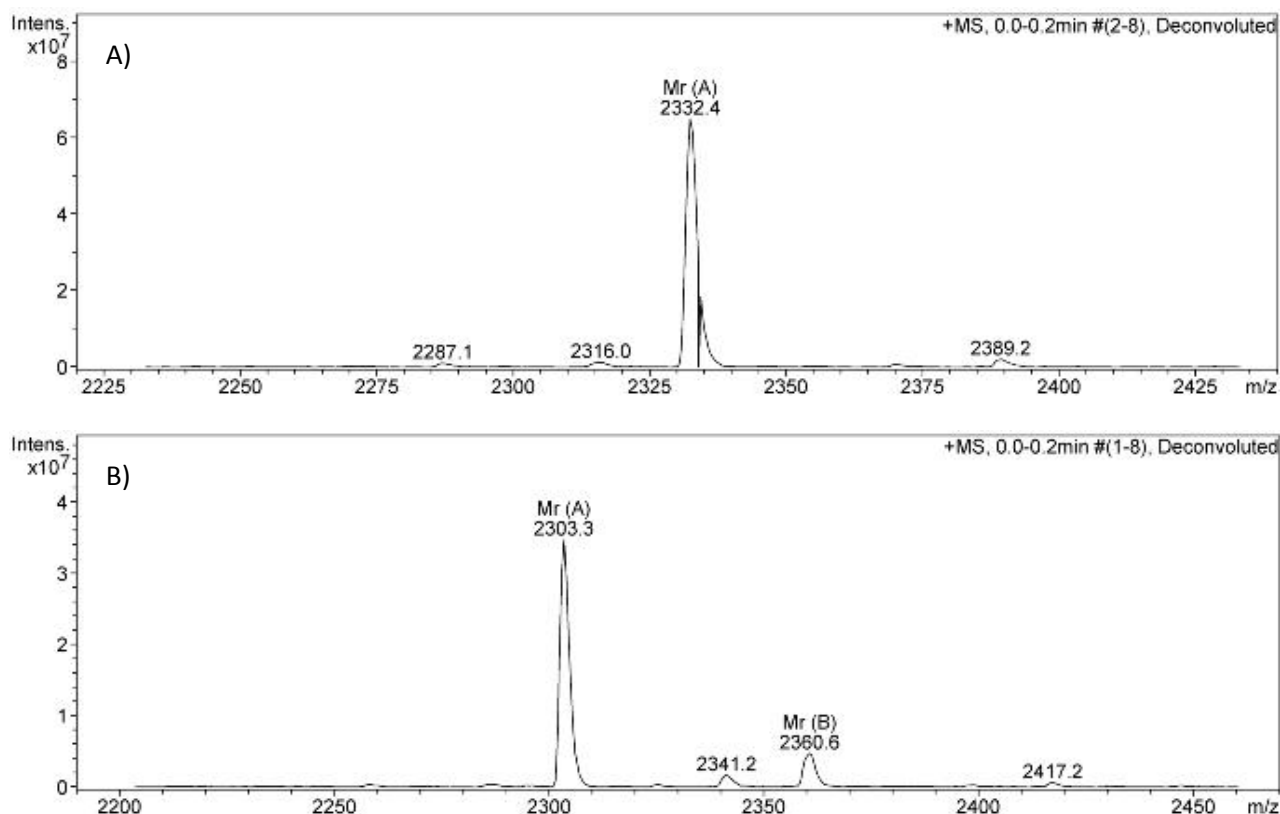


Figure 18. ESI-MS molecular weight analysis of A) ADP2(AM) and B) ADP3(AM)

The possibility of dimer synthesis by formation of an intermolecular disulphide bridge enabled us to test the effects of peptide aggregation. This may occur at the membrane surface in particular, and it is believed to have a significant effect on the mode of action and pore formation. This process can affect antimicrobial activity as well as host cell cytotoxicity as will be discussed below.

Dimerization proceeded in good yields by simply exposing a sufficient concentration of the peptide to oxidizing conditions, and monitoring continuously using analytical RP-HPLC coupled to ESI-MS (Table 12, Figure 19, Appendix 6).

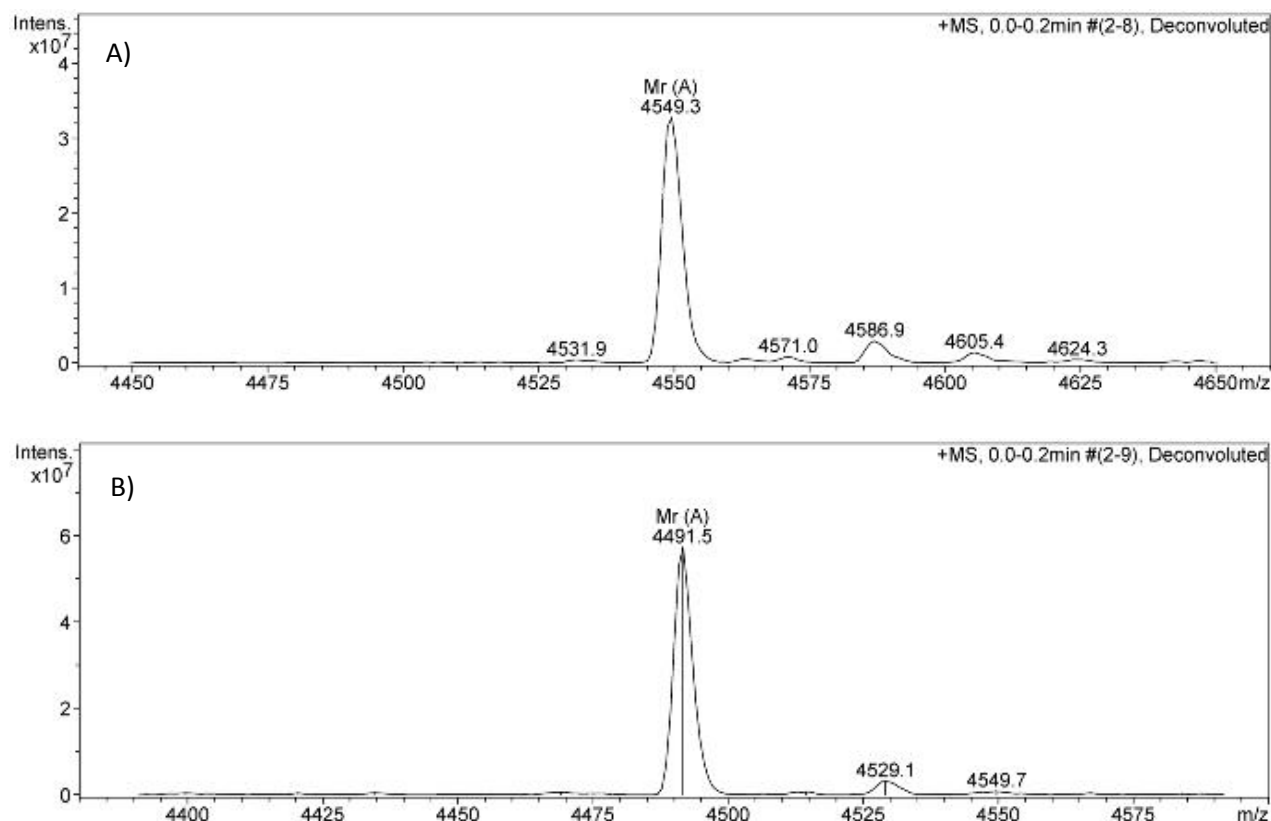


Figure 19. ESI-MS molecular weight analysis of A) [ADP2]<sub>2</sub> and B) [ADP3]<sub>2</sub>

The presence of a C-terminal Cys residue also allowed us to label these peptides with the fluorescent probe BODIPY. It was chosen for labelling peptides since it is uncharged, small, stable and strongly fluorescent. This modification was used to follow peptides' interaction with membranes, as well as to see if it internalized into cells or remained on their surface, by monitoring its fluorescence at 525 nm, as it will be discussed later.

The bodipylation reaction went well for both peptides, with good yields. ESI-MS coupled with RP-HPLC confirmed the correct structure and quality of peptides (Table 12, Figure 20, Appendix 6).

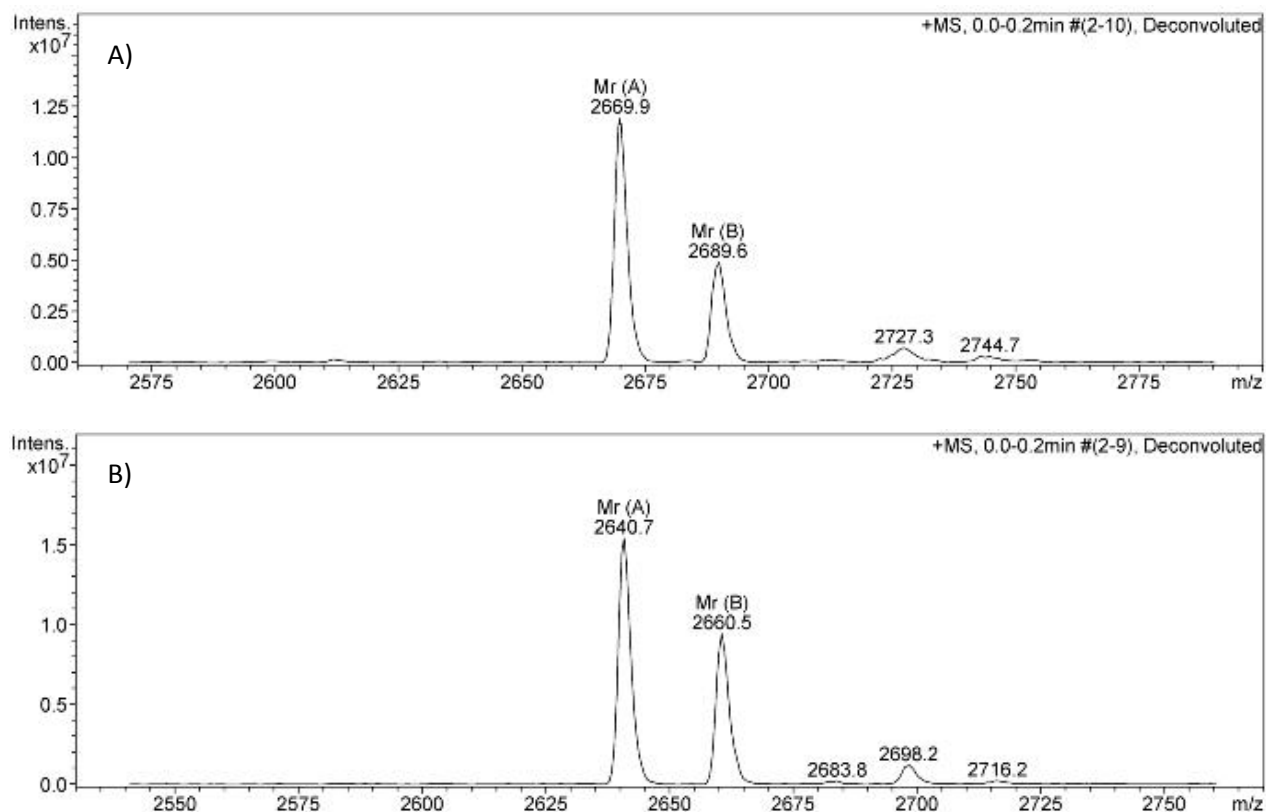


Figure 20. ESI-MS molecular weight analysis of A) ADP2(BY) and B) ADP3(BY). Graphs contain two peaks where lower peak represents correct one for bodipy-labeled peptide while higher one is a "shadow peak" that can often be noticed during MS analysis of fluorescently labeled peptides possibly due to loss of one fluorine under ESI conditions.

The exact concentration of each peptide was determined by using the following methods: mass concentration, Waddell method and quantification by molar extinction coefficient. All peptides were measured on analytical balance after lyophilisation and dissolved in *MilliQ* H<sub>2</sub>O, and concentrations are shown in Table 13. In the second set of adepantin dilutions, peptides were dissolved in exactly 500  $\mu$ l *MilliQ* H<sub>2</sub>O (Table 14) and concentrations were then double-checked with methods other two methods.

Table 13. Mass concentration of peptides tested in the first set of tests.

Peptide abbreviation	Peptide weight (mg)	Volume MilliQ H <sub>2</sub> O (ml)	Concentration	
			mg/ml	mM
ADP1	12.7	1.27	10	4.4
ASC1	3.8	0.76	5	2.7
ASC1 I2	3.2	0.64	5	3.6
PSEU2	16	1.6	10	3.7
PSEU2 A9	16.2	1.62	10	3.8

Table 14. Results of methods used for determining concentration of adeptantins.

PEPTIDE ABBREV.	WEIGHT		WADDELL		MOLAR EXTINCTION COEFFICIENT		USED VALUE	
	mg/ml	mM	mg/ml	mM	mg/ml	mM	mg/ml	mM
ADP2(AM)	7.2	3.1	6.5	2.8	5.1	2.2	6.5	2.8
	6.8	2.9	5.7	2.5	5.2	2.2	5.7	2.5
ADP3(AM)	7.6	3.3	6.7	2.9			6.7	2.9
[ADP2] <sub>2</sub>	8.8	1.9	7.9	1.8	5.9	1.3	7.9	1.8
	8.8	1.9	8.0	1.8	7.8	1.7	8.0	1.8
[ADP3] <sub>2</sub>	9.2	2.1	8.8	2.0	6.0	1.3	8.8	2.0
ADP2(BY)	4.6	1.7	4.4	1.7	4.8	1.8	4.4	1.7
ADP3(BY)	7.2	2.7	5.5	2.1	6.9	2.6	6.9	2.6
ADP1			10	4.4			10	4.4

For ADP2(AM) and [ADP2]<sub>2</sub> modification reaction was performed twice, and both measurements are presented in the table.

In general, the best agreement between mass-calculated concentrations was obtained using the extinction coefficient of labelled peptides. For unlabelled peptides concentrations were often underestimated using the extinction coefficients at 214 nm according to Kuipres and Gruppen 2007, and are generally closer to the weight-calculated ones using the Waddell method. Using the mean extinction coefficient determined by Kupres and Gruppen for the peptide bond, the molar extinction coefficient calculated for adeptantins was  $26400 \pm 1600 \text{ mol}^{-1}\text{cm}^{-1}$ . For the dimers, it was calculated in terms of helix numbers, rather than molecule numbers. In conclusion, while not exactly reflecting the mass-calculated concentrations, spectroscopic methods confirmed the general trend and led to a slight down correction of values that were generally centred around those measured using the Waddell method.

### 3.4. Confirmed secondary structure

All peptides used for creating AMPad database were  $\alpha$ -helical. The peptides predicted by the “Designer” algorithm were therefore expected to have amphipathic  $\alpha$ -helical structures as well. To confirm this hypothesis, the structure of ADPs was determined by monitoring their behaviour in different environments using CD spectrometry. Each

secondary structure (random coil,  $\alpha$  helix and  $\beta$  sheet) of ADPs results in characteristic and quite different looking spectral bands with different magnitudes.

The first CD spectra were intended to observe the behaviour of ADPs in different solutions, both aqueous and organic.

Aqueous conditions tested were:

- MilliQ H<sub>2</sub>O
- PBS (SPB + 150 mM NaCl)
- SPB (10 mM sodium phosphate buffer)

All ADPs remained unstructured in all three conditions (Figure 21, Figure 22 A)), as spectra conform to the shape and magnitude of a random coil structure. Dimers tested at concentration 20  $\mu$ M also have random coil structure (Figure 21) but with twice the magnitude. However, when normalized for number of chains rather than molecules showed spectra quite similar to the monomeric peptides (Figure 22 A)).

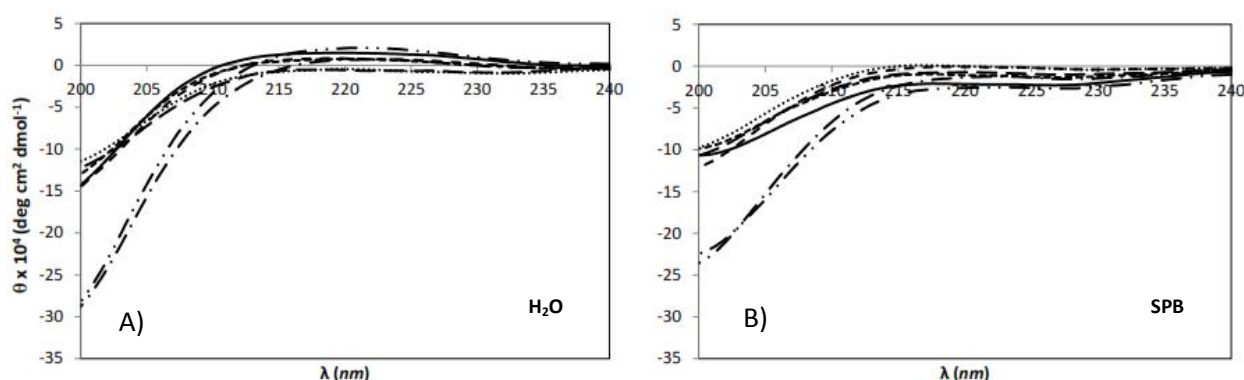


Figure 21. CD spectra of ADPs (20  $\mu$ M of peptide) measured in A) H<sub>2</sub>O and B) sodium phosphate buffered (SPB, 10 mM); ADP1(—); ADP2(AM) (---); [ADP2]<sub>2</sub> (-·-·-); ADP2(BY) (·····); ADP3(AM) (- - -); [ADP3]<sub>2</sub> (-·-·-); ADP3(BY) (·····).

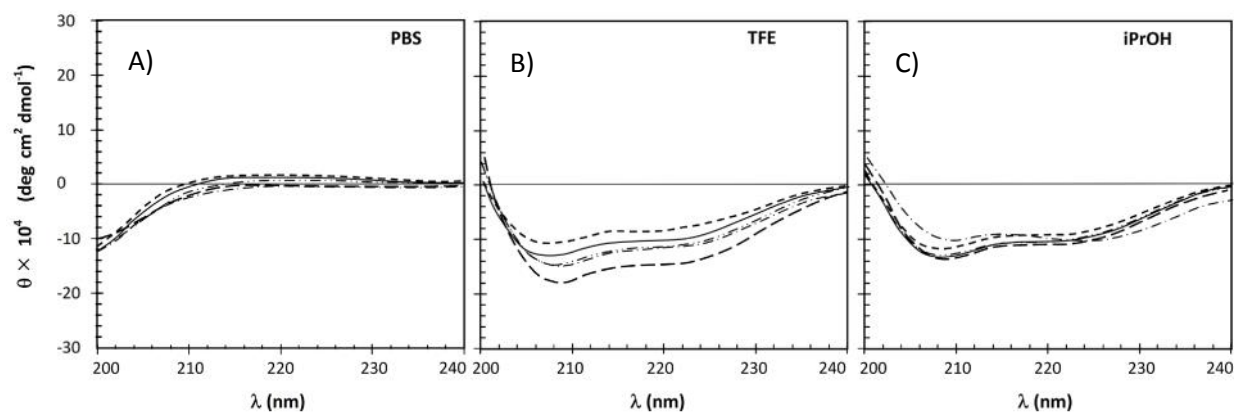


Figure 22. CD spectra of ADPs (20  $\mu$ M of peptide chain) measured in A) phosphate buffered saline (PBS, pH7.4), B) 50% trifluoroethanol (TFE) and C) 50% isopropanol (iPrOH); ADP1(—); ADP2(AM) (---); [ADP2]<sub>2</sub> (-·-·-); ADP3(AM) (- - -); [ADP3]<sub>2</sub> (-·-·-).

Two more organic conditions were also used:

- Isopropanol (iPrOH) in SPB (50:50%)
- Trifluoroethanol (TFE) at increasing concentrations v/v (10-50%), with SPB

In the presence of 50% isopropanol, ADPs clearly formed  $\alpha$  helical structure (Figure 22 C)), confirming that ADPs have a propensity for adopting an amphipathic  $\alpha$  helical conformations if an environment is provided that is compatible with the formation of a hydrophobic sector. The helical conformation of peptides and proteins can in fact be induced and stabilized with alcohols which favour intrachain H-bond formation (Hirota et al., 1997). TFE is often used for inducing such an effect as a helix-favouring solvent, and with adeptantins beginning to induce helix formation at about 10% v/v, whereas helix formation is effectively complete at 30% v/v (Figure 23). Helix formation was not particularly favoured in the covalent dimers when in contact with these helix-favouring solvent, considering that spectra in the presence of iPrOH are not markedly different in intensity or shape between monomers and dimers.

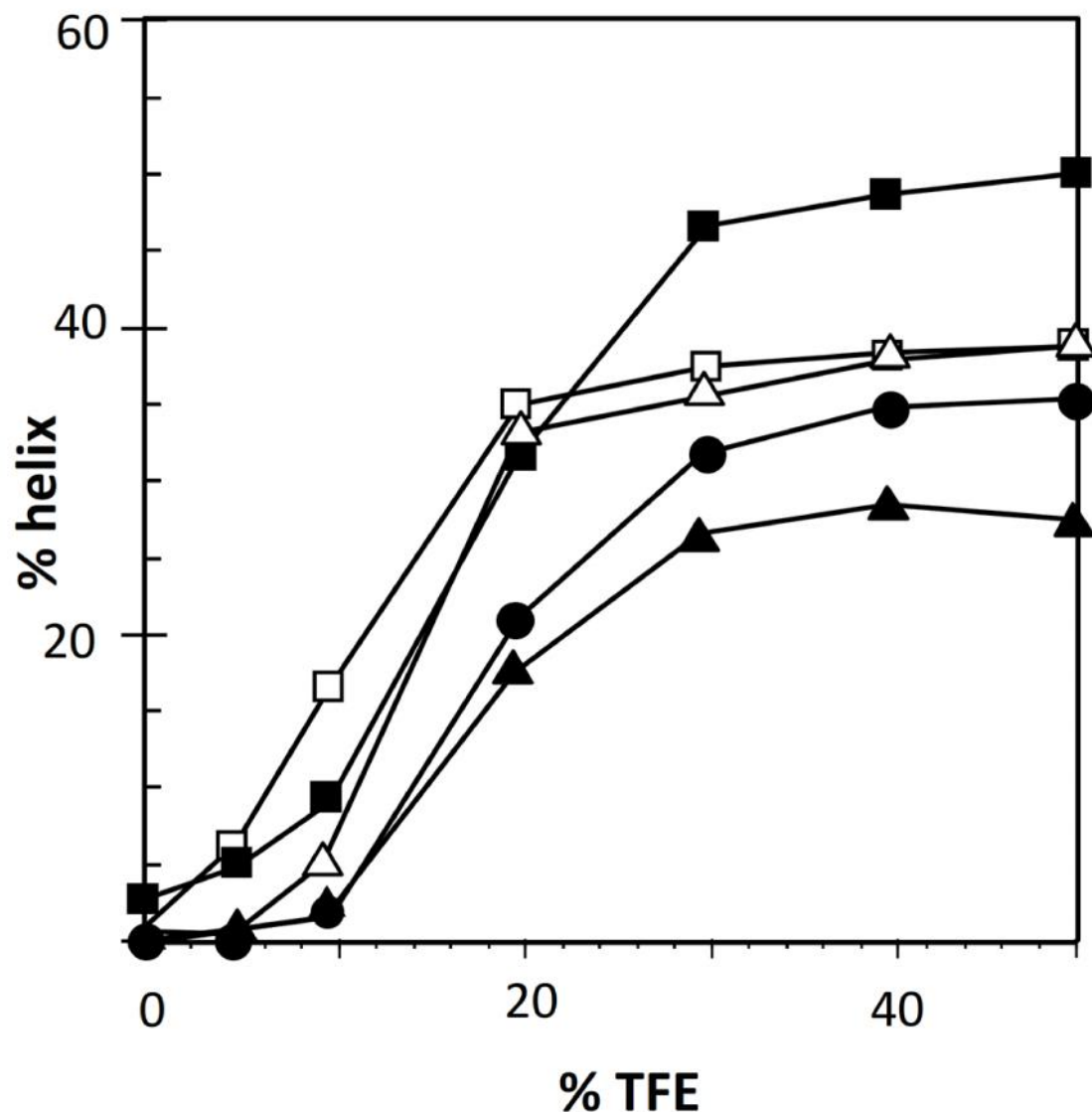


Figure 23. Helix % with increasing TFE; ADP1 —●—; ADP2(AM) —■—; [ADP2]<sub>2</sub> —□—; ADP3(AM) —▲—; [ADP3]<sub>2</sub> —△—.

The percentage helicity was determined in aqueous conditions, and in the presence of TFE and both types of liposomes suspensions (anionic or neutral), after normalizing the ellipticity per residue at 222 *nm* to take dimerization into account, using the method of Reed and Reed 1997. It was however not corrected for the presence of the BODIPY chromophore (Table 15).



Table 15. % helicity of ADPs in different environments according to the method of Reed and Reed 1997. Peptides were 20  $\mu$ M in H<sub>2</sub>O, 50% trifluoroethanol (TFE), anionic LUV (PG/dPG = phosphatidylglycerol/diphosphatidylglycerol; 95:5) and neutral LUV (PC/SM/Ch = phosphatidylcholine/sphingomyelin/cholesterol; 2:2:1) in PBS buffer. Dimerization was taken into account by normalising ellipticity per residue. <sup>(1)</sup>No corrections for the presence of the BODIPY chromophore were made (% helicity shown in parentheses).

Peptide	% helical conformation			
	H <sub>2</sub> O	TFE	LUV (PG/dPG)	LUV (PC/SM/Ch)
ADP1	<5	35	55	<10
ADP2(BY) <sup>(1)</sup>	(<5)	(40)	(50)	(<10)
ADP2(AM)	<5	45	60	<5
[ADP2]2	<5	40	50	<10
ADP3(BY) <sup>(1)</sup>	(<5)	(55)	(50)	(<5)
ADP3(AM)	<5	30	53	<10
[ADP3]2	<5	40	45	<10

Peptide structuring in contact with model membranes (LUVs) can provide insight into the mode of action. Prokaryotic cell membranes were mimicked with anionic LUVs consisting of PC/dPG liposomes, while eukaryotic cell were mimicked with neutral LUVs consisting of PC/SM/Ch liposomes. The % helix per residue of all peptides, calculated in the presence of both types of LUVs is also shown in the Table 15.

All ADPs showed helix formation when in contact with anionic LUVs (see Figure 24 A)), and the monomers behaved very similarly. The dimeric ADPs showed a distinct change in the shape of their spectra, and in particular the decrease of the  $\theta^{208}/\theta^{222}$  ratio to <1 is an indication that the helices are more aggregated when in contact with the membrane. A less marked decrease in the  $\theta^{208}/\theta^{222}$  ratio is evident also for monomeric peptides with respect to helices forming in the presence of TFE, so that covalent dimerization likely enhances this effect. These results are indication of a strong interaction with anionic membranes and are in line with the fact that ADPs can easily permeabilize bacterial membranes and likely have a membranolytic antimicrobial activity, as described later in section 3.5.

When in contact with neutral LUVs (see Figure 24 B)) all ADPs remained substantially in the random coil form, suggesting that there was no efficient insertion in this type of membrane, and that ADPs remained unstructured. This behaviour is in the line with a low capacity to lyse eukaryotic membranes, as shown by a low haemolytic activity, as described later in section 3.6. Results of haemolysis confirmed low haemolytic activity for monomers, while dimers showed unexpected increase in haemolysis.

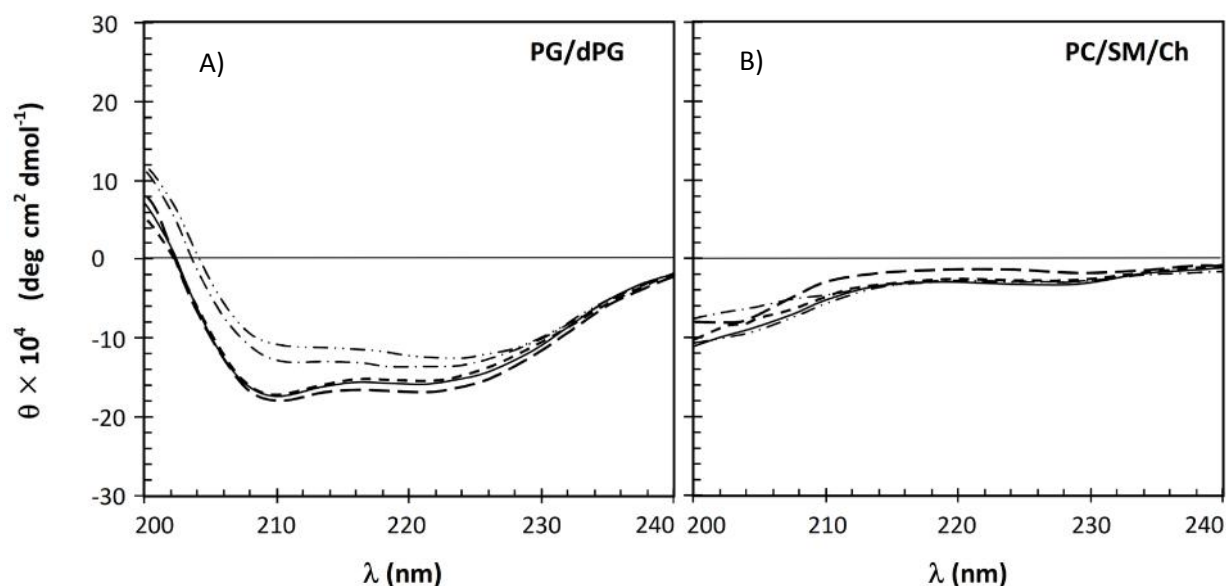


Figure 24. CD spectra of ADPs (20  $\mu$ M of peptide chain) measured in A) 1:1 phosphatidylglycerol/diphosphatidylglycerol LUVs in PBS (PG/dPG) and B) 2:2:1 phosphatidylcholine/sphingomyelin/cholesterol LUVs in PBS (PC/SM/Ch); ADP1(—); ADP2(AM) (---); [ADP2]<sub>2</sub> (-·-·-); ADP3(AM) (- - -); [ADP3]<sub>2</sub> (-·-·-·-).

### 3.5. Effects of adeptantins on bacterial cells

Assessment of antimicrobial activity of adeptantins was done by determining MIC and IC<sub>50</sub> values against both Gram-negative and Gram-positive bacteria of interest. Confirmation of the killing activity against *E. coli* was provided by performing MBC assay. From Table 16, Table 17 and Table 18 it is visible that ADPs have a good antimicrobial activity.

Results for MIC assays were determined by examining microtiter plates after 18 hours of incubation at 37°C. The MIC value was taken as the lowest concentration of the peptide resulting in the complete inhibition of visible growth. Results are mean values of at least three independent experiments carried out in duplicate, and are summarised for all peptide tested, as well as for all bacteria of interest in Table 16. MIC values are also presented for the two natural reference peptides ascaphin 1 and pseudin 2.

Adeptantins were designed peptide antibiotics using *Escherichia coli*, a Gram-negative bacterium, used as the target microorganism, in the computational approach. This selectivity was confirmed by the MIC assay (Table 16). There was however some difference in the activity between the three ADPs, and the activity was also affected by their modifications. ADP2 was more active than ADP1 and 3, bodipylation increased activity, but in particular, the dimers were significantly more active than acetamidated monomers of the same peptide against *E. coli* (Figure 25). All ADPs showed low activity against the Gram-positive bacterium *S. aeruginosa* (Figure 26) underlining that their activity was directed against Gram-negative bacteria. The reason for that lower activity may be differences in the membrane composition and/or the presence of a thicker peptidoglycan layer in the Gram-positive bacteria.

Table 16. MIC values for adeptantins, pseudins and ascaphins; <sup>(1)</sup> assays were carried out in 100% (v/v) MH broth using  $5 \times 10^5$  cells/ml bacteria in the logarithmic phase; each value is the mean of at least 3 independent determinations carried out in duplicate.

PEPTIDE	MIC ( $\sim M$ ) <sup>(1)</sup>				
	<i>E. coli</i> ATCC 25922	<i>S. aureus</i> ATCC 25923	<i>P. aeruginosa</i> ATCC 27853	<i>S. typhimurium</i> ATCC 14028	<i>K. pneumoniae</i> (c. i.)
ADP1	2-4	>128	16	-	-
ADP2(AM)	1	>128	32	16-32	64
[ADP2] <sub>2</sub>	0.5-1	128	2	1	1
ADP2(BY)	1	64	-	-	-
ADP3(AM)	4	>128	-	-	-
[ADP3] <sub>2</sub>	0.5	64-128	-	-	-
ADP3(BY)	1	>64-64	-	-	-
PSEU2	8	32	>64	-	-
PSEU2 A9	8-16	128	>128	-	-
ASC1	2	32	16	-	-
ASC1 I2	4	32-64	16-32	-	-

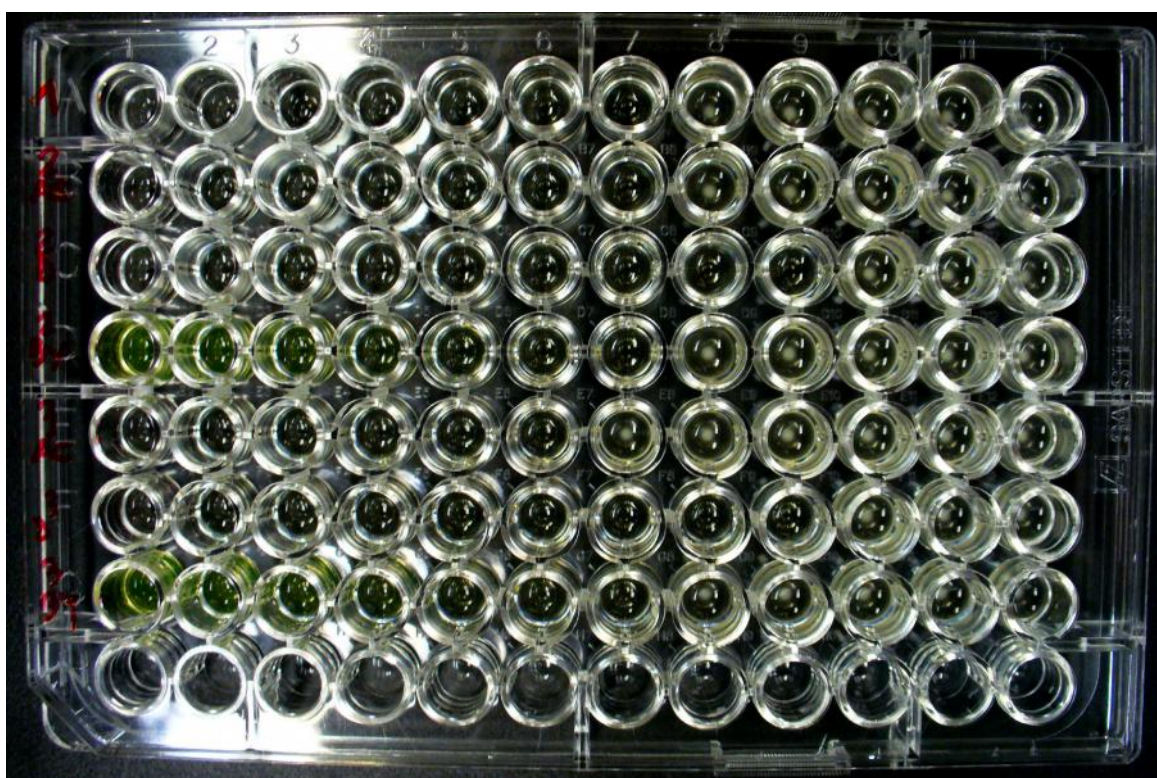


Figure 25. Example of MIC results for *E. coli* all ADPs; rows: ADP1, ADP2(AM), [ADP2]<sub>2</sub>, ADP2(BY), ADP3(AM), [ADP3]<sub>2</sub>, ADP3(BY), empty; columns: 1<sup>st</sup> – 11<sup>th</sup> peptide + bacteria + MH starting with concentration 128  $\mu M$  and decreasing by two-fold dilution method, 12<sup>th</sup> negative control = bacteria + MH; white dots on the bottom of the well is grown bacteria.



ADP2(AM) was the most active peptide and was therefore chosen to be tested on other Gram-negative bacteria along with its dimer.  $[\text{ADP2}]_2$  showed a more potent, broad-spectrum activity than ADP2(AM), that was also less active against *P. aeruginosa*, *S. typhimurium* and *K. pneumoniae* (Table 16,) than against *E. coli*.

In the first set of tests ADP1 was tested on *P. aeruginosa* and showed moderate activity as well as ASC1 and ASC1 I2, while PSEU2 and PSEU2 A9 had poor activity. For both control peptides MIC values against *E. coli* were in acceptable correlation with literature data, as ASC1 had a measured MIC = 2  $\mu\text{M}$ , against literature value of 3  $\mu\text{M}$ , while PSEU2 had measured MIC = 8  $\mu\text{M}$  against a literature value of 20  $\mu\text{M}$  (Conlon et al., 2004; Olson et al., 2001). For PSEU2 there was a larger difference that may derive from the presence of the amidated C-terminus. Peptides with amidated C-terminus have been reported to have a somewhat stronger antibacterial activity, likely due to the increased cationicity.

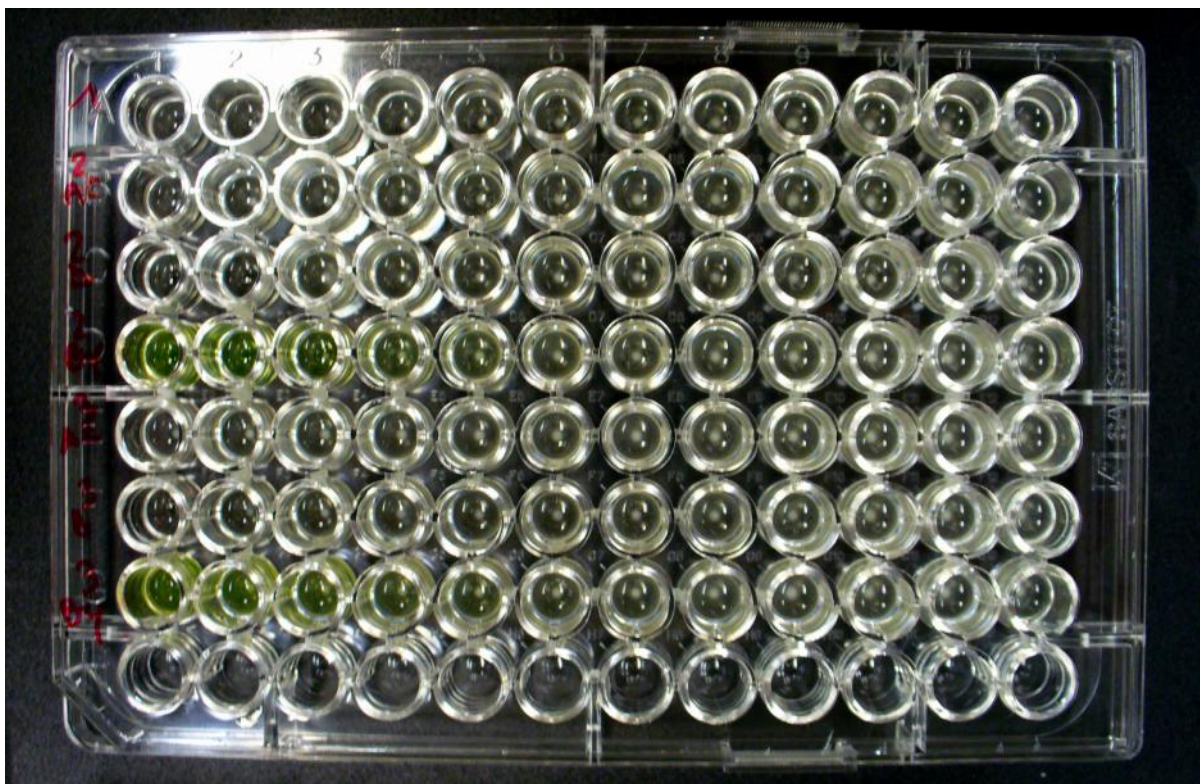


Figure 26. Example of MIC results for *S. aureus* all ADPs; rows: ADP1, ADP2(AM),  $[\text{ADP2}]_2$ , ADP2(BY), ADP3(AM),  $[\text{ADP3}]_2$ , ADP3(BY), empty; columns: 1<sup>st</sup> – 11<sup>th</sup> peptide + bacteria + MH starting with concentration 128  $\mu\text{M}$  and decreasing by two-fold dilution method, 12<sup>th</sup> negative control = bacteria + MH; white dots on the bottom of the well is grown bacteria.

Minimal bactericidal concentration (MBC) assay was performed (Table 17) following the MIC assays and revealed that the MBC values are consistently two-fold higher than the corresponding MIC values (Table 16). One can thus conclude that ADPs are bacteriostatic at subtoxic concentration and become bactericidal at a threshold concentration between 1-8  $\mu\text{M}$ , depending on the peptide. These results were also confirmed with bacterial growth inhibition assay (Table 18).

Table 17. MBC (minimal bactericidal concentration), <sup>(1)</sup> Concentration resulting in no bacterial growth, 2 independent determinations carried out in duplicate.

PEPTIDE	MBC ( $\sim M$ ) <sup>(1)</sup>
	<i>E. coli</i> ATCC 25922
ADP1	4
ADP2(AM)	2
[ADP2] <sub>2</sub>	2
ADP3(AM)	8
[ADP3] <sub>2</sub>	0.5-1

Bacterial growth kinetics assay with chosen bacteria enabled IC<sub>50</sub> value calculation as a value representing concentration of the peptide which inhibits bacterial cell growth by 50% at 210 min and was extrapolated from the given graph for each peptide (see Figure 27 B), Figure 28).

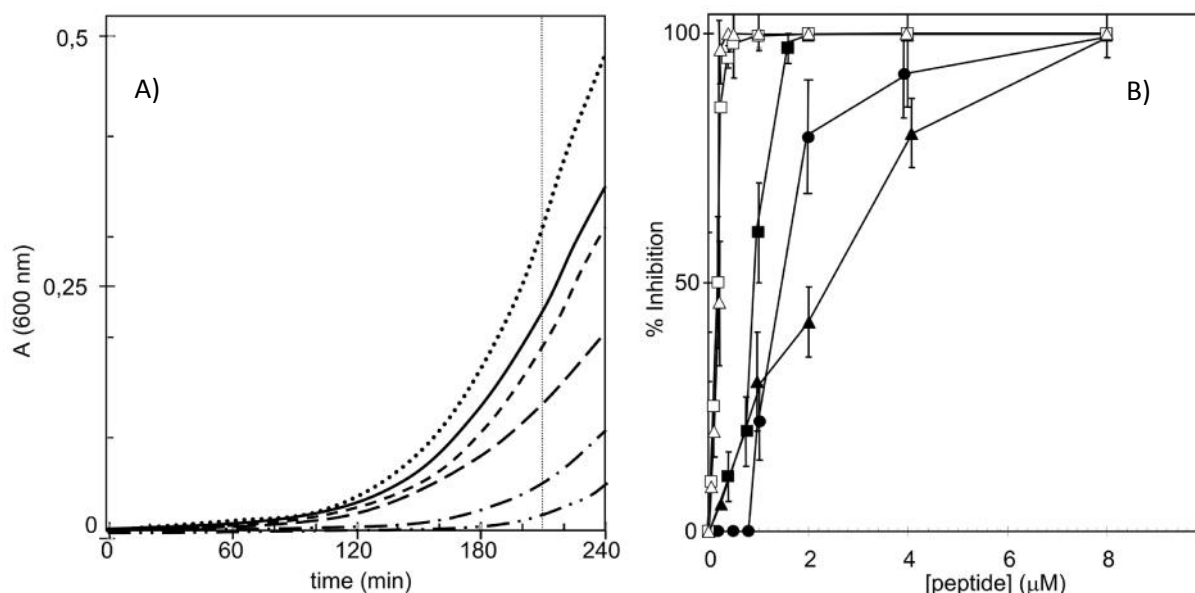


Figure 27. A) Curves from data collected after growth kinetics for *E. coli* monomers at concentration 1  $\sim M$  and dimers at concentration 0.5  $\sim M$ ; B) inhibition percentage at 210 min extracted from growth curves; Bacteria control (.....); adeptantins ADP1 (—, —●—); ADP2(AM) (- - -, —■—); ADP3(AM) (- - -, —▲—); [ADP2]<sub>2</sub> (- - - - , —□—); [ADP3]<sub>2</sub> (....., —△—).

Examining values gathered with this assay (Table 18) and comparing them with MIC values (Table 16) a similar trend is observed. Dimers of both adeptantins were very active against *E. coli* and [ADP2]<sub>2</sub> was also quite active against other types of bacteria it was tested on (see Figure 28 B) and Table 19). This behaviour may indicate that helix aggregation favours the mechanism of action of these peptides, so that covalent linking of two helices makes them therefore more active. As the monomer ADP2(AM) was the most active, it was chosen to be tested, together with its dimer on another three species of bacteria (see Figure 28 A) and Table 19). It is remarkable how a single residue modification, from Ser in ADP1 to acetamidated Cys in ADP2 (similar to glutamine) can considerably alter activity of the

peptide. In any case, for all tested peptides there was a good correlation between the % growth inhibition (see Figure 27, Figure 28 and Figure 29) with results collected from MIC assays.

Table 18. IC<sub>50</sub> value of peptides; <sup>(1)</sup> Concentration resulting in 50% growth inhibition of bacteria, calculated from data in figure (Figure 27).

PEPTIDE	IC <sub>50</sub> (~M) <sup>(1)</sup>
	<i>E. coli</i> ATCC 25922
ADP1	1.5 ± 0.3
ADP2(AM)	0.8 ± 0.1
[ADP2] <sub>2</sub>	0.2 ± 0.05
ADP3(AM)	2.3 ± 0.3
[ADP3] <sub>2</sub>	0.2 ± 0.05

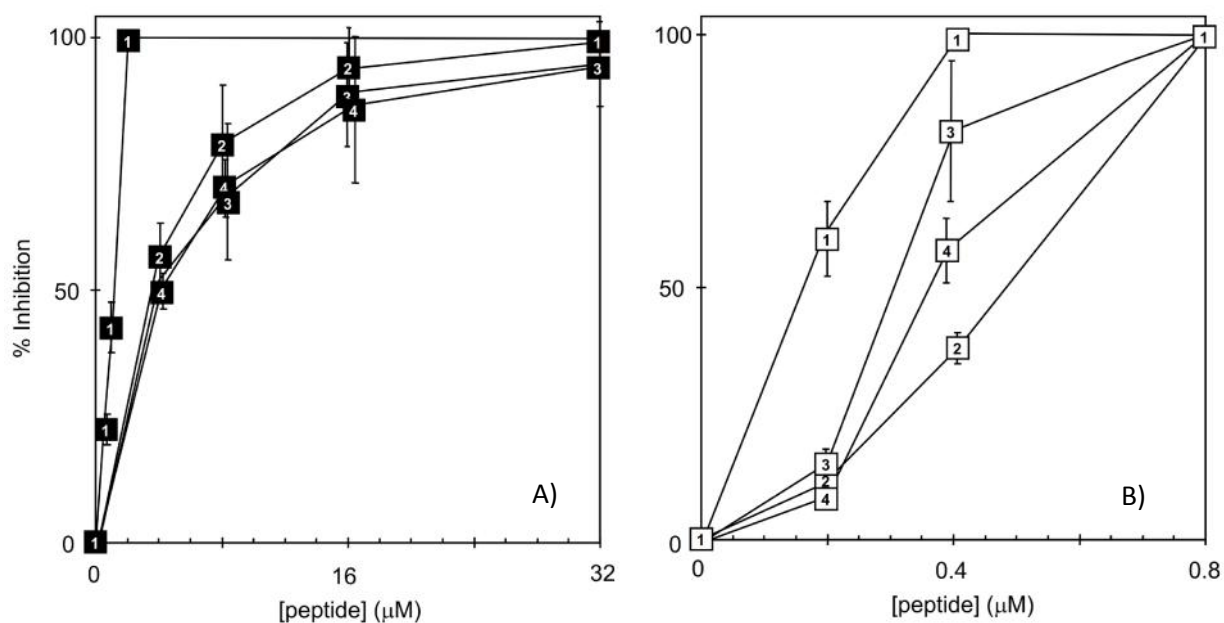


Figure 28. Effect of A) ADP2(AM) and B) [ADP2]<sub>2</sub> on growth kinetics of *E. coli* (1), *P. aeruginosa* (2), *K. pneumoniae* (3) and *S. typhimurium* (4), experiments were done three times in triplicates.

Table 19. IC<sub>50</sub> value of ADP2(AM) and [ADP2]<sub>2</sub> measured for the following bacteria: *E. coli*, *P. aeruginosa*, *K. pneumoniae* and *S. typhimurium*; <sup>(1)</sup> Concentration resulting in a 50% growth inhibition of bacteria, calculated from data in figure (Figure 28).

PEPTIDE	IC <sub>50</sub> (~M) <sup>(1)</sup>			
	<i>E. coli</i> ATCC 25922	<i>P. aeruginosa</i> ATCC 27853	<i>K. pneumoniae</i> (clinical isolate)	<i>S. typhimurium</i> ATCC 14028
ADP2(AM)	1	3.6	3.8	4
[ADP2] <sub>2</sub>	0.16	0.49	0.31	0.37

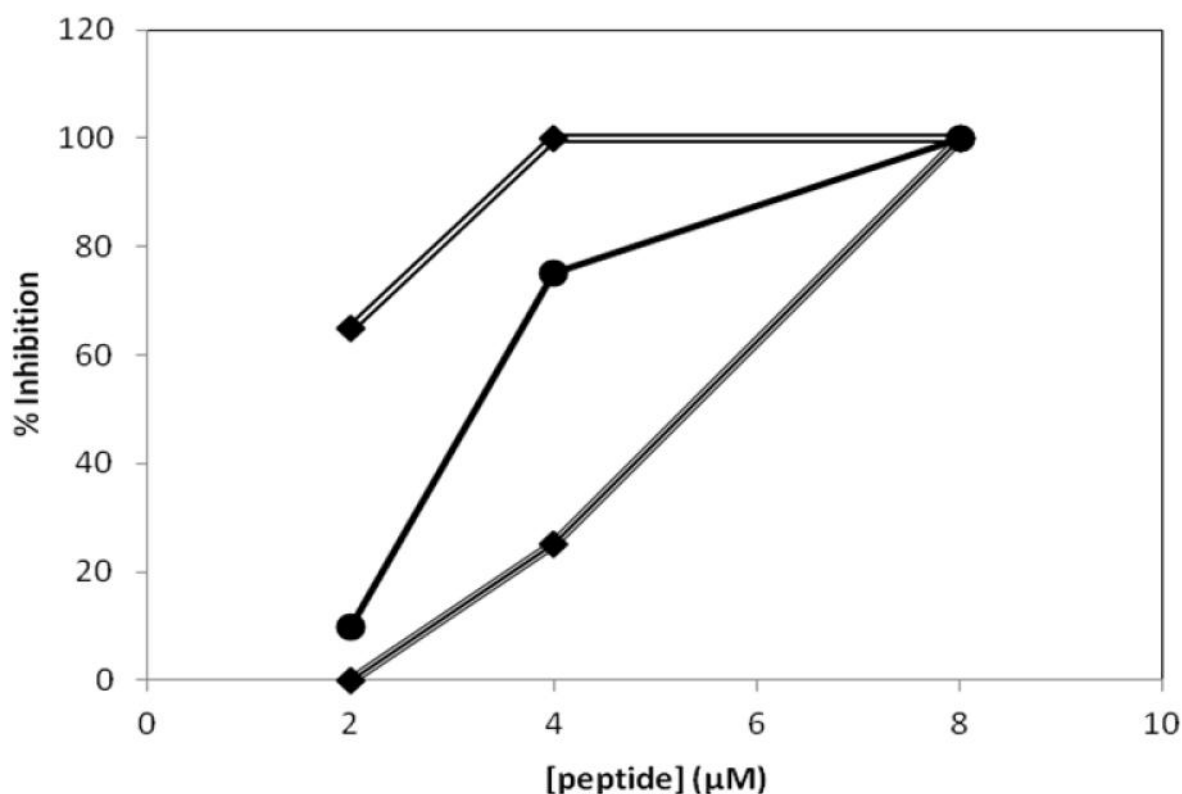


Figure 29. Effect of ASC1, PSEU2 and ADP1 on growth kinetics of *E. coli*; PSEU2  $\equiv \blacklozenge \equiv$ ; ASC1  $\equiv \blacksquare \equiv$ ; ADP1  $\equiv \bullet \equiv$ ; mean of two experiments performed in triplicates (Juretić et al., 2009).

One possible factor affecting the activity of adeptantins against *E. coli*, is the barrier effect exerted by the outer membrane. To probe this barrier effect, we compared % growth inhibition with respect to the *E. coli* BW 25113 strain (a K12 derived strain in which the LPS lacks the O-antigen polysaccharide) with that against the ATCC strain that has a fully developed O-antigen. Furthermore, this relatively rapid assay can provide much needed information by using mutant strains with specifically altered membranes, due to different modifications of the core oligosaccharide in the outer membrane lipopolysaccharides layer (LPS), as for example its anionicity due to the presence of phosphate groups, or its stability. For example, the  $\Delta waaP$  mutant of *E. coli* BW 25113 lacks a key kinase necessary for the phosphorylation of the first heptose in the core oligosaccharide and as a consequence has an incompletely formed core saccharide with destabilized outer membrane (Yethon et al., 1998). The intention was to distinguish whether the changes in outer membrane will affect

adepantins activity, and therefore indicate to what extent the need to overcome it affects the subsequent permeabilization of the cytoplasmic membrane, and to this end, the results of the bacterial growth inhibition assay in the presence of the different peptides is shown in Figure 30.

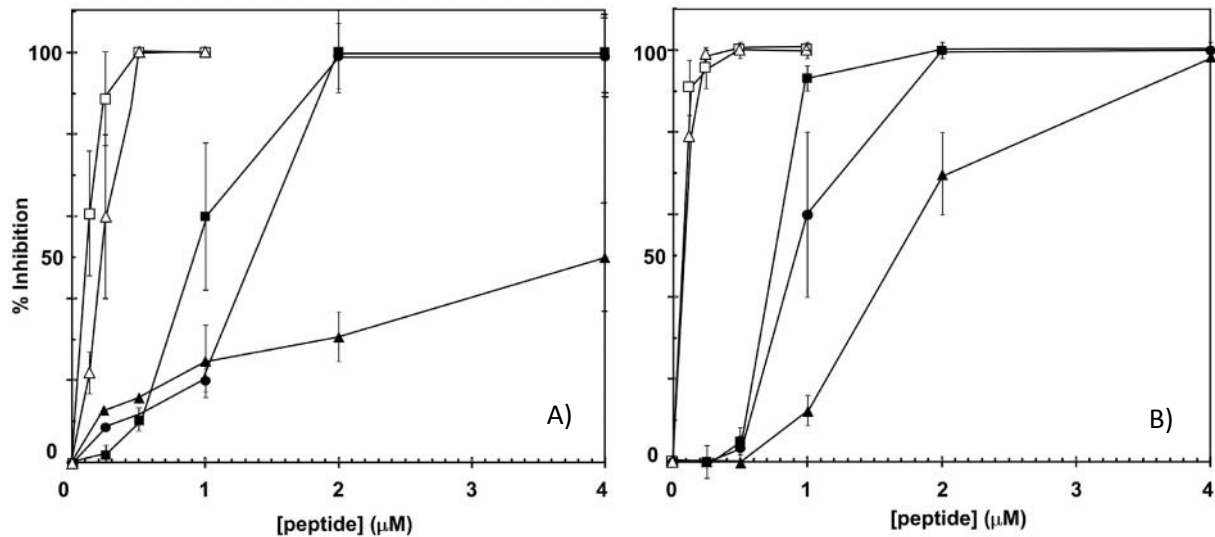


Figure 30. Growth kinetics of A) *E. coli* BW 25113 strain and B) *E. coli* BW 25113  $\Delta waaP$  strain affected by adeptantins (ADP1—●—; ADP2(AM)—■—; [ADP2]<sub>2</sub>—□—; ADP3(AM)—▲—; [ADP3]<sub>2</sub>—△—).

When results for *E. coli* BW 25113 and its mutant strain were compared to those for *E. coli* ATCC 25922, it was evident that the lack of the O-antigen did not influence the behaviour of adeptantins significantly, so that the O-antigen was not obstacle for ADP's activity. Again, dimers inhibited bacterial growth best, while for monomers ADP2(AM) was the most potent, followed by ADP1 and then by ADP3. A similar trend was noticed for the  $\Delta waaP$  mutant, indicating that destabilising LPS layer of outer membrane does not improve activity, so that this is likely not an obstacle for ADPs reaching the cytoplasmic membrane. It is a significant result for the ADP dimers in particular, as these are larger molecules that could be expected to be slowed down by the outer membrane on their trajectory to the cytoplasmic membrane.

Membrane permeabilization studies were performed on both outer and inner membranes. These served to gain more insight into the effects of membrane insertion, which CD spectroscopy indicated was particularly relevant to anionic membranes. This process could in fact lead to the membrane permeabilization as part of ADPs mode of action. Permeabilization of both membrane types was tested using the *E. coli* ML-35 pYC strain that constitutively produces both a cytoplasmic  $\beta$ -galactosidase and a periplasmic  $\beta$ -lactamase.

Gal-ONp is used as an extracellular chromogenic substrate for  $\beta$ -galactosidase, with which it can react only when a membrane-active peptide, in this case an adeptantin, permeabilizes the inner membrane. Its hydrolysis by the cytoplasmic galactosidase results in a product detected by absorption increase to 405 nm. CENTA<sup>®</sup> is used as a chromogenic substrate for the periplasmic lactamase, which it can reach only if the outer membrane is destabilized or permeabilized. Hydrolysis of the  $\beta$ -lactam ring results in a change of colour from 340 nm to 405 nm. Curves showing the variation of absorption at 405 nm with time, in



the presence of Gal-ONp or CENTA<sup>®</sup> are thus a measure of the permeabilization kinetics for the cytoplasmic and outer membranes respectively (Figure 31 A) and B)).

Monomeric adeptantins resulted in significant hydrolysis of both chromogenic substrates at a quite low peptide concentration. The dimers however hydrolysed both membranes more rapidly confirming that dimerization can be related to increasing potency, as observed in MIC and growth kinetics assays, due to more efficient membrane permeabilization. It is significant that permeabilization was even faster than with the cathelilcidin peptide SMAP-29 which is used as a reference for a high rate of outer and cytoplasmic membrane permeabilization (Skerlavaj et al., 1999). It should also be noticed that Gal-ONp hydrolysis is almost as fast as CENTA<sup>®</sup> hydrolysis, indicating that the peptides move rapidly through the outer membrane and immediately start permeabilizing the cytoplasmic membrane, in agreement with growth kinetics studies that had indicated that the outer membrane was not a formidable barrier for these peptides. Bodipylated peptides were not included in the measurements as the presence of BODIPY interferes with absorption measurements at 405 nm.

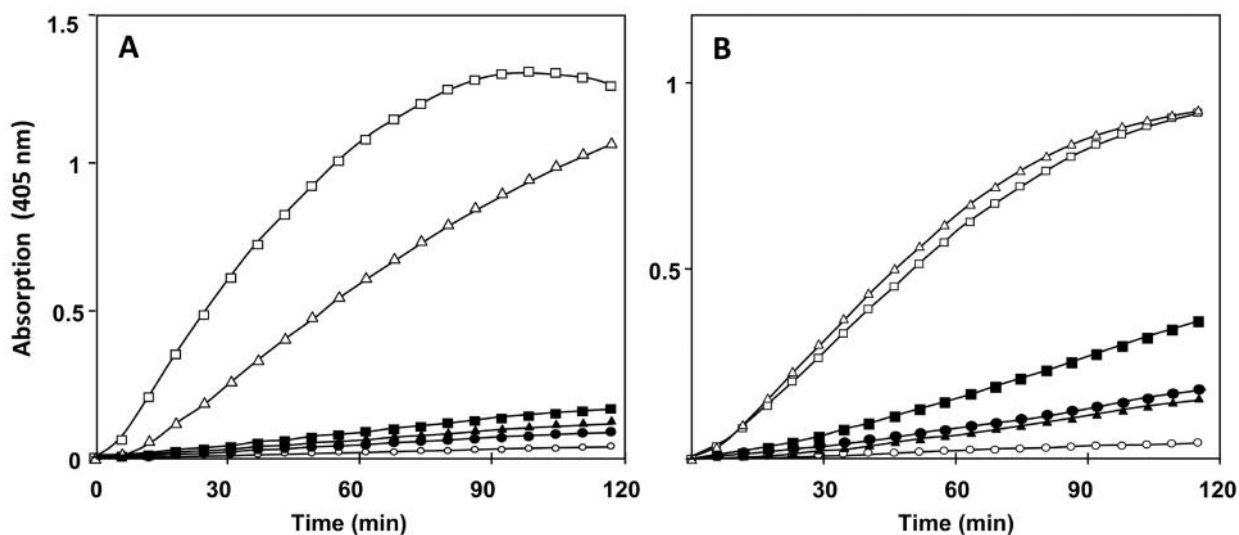


Figure 31. Permeabilization of the inner and outer membrane of *E. coli* ML-35 pYC by ADPs determined by following the hydrolysis of the impermeant chromogenic substrate A) Gal-ONp by a cytoplasmic  $\beta$ -galactosidase and B) CENTA<sup>®</sup> by the periplasmic enzyme  $\beta$ -lactamase respectively (no peptide —○— ; ADP1 —●— ; ADP2(AM) —■— ; [ADP2]<sub>2</sub> —□— ; ADP3(AM) —▲— ; [ADP3]<sub>2</sub> —△—).

Another way of probing membrane permeabilization is to monitor the internalization of propidium iodide into bacteria using flow cytometry. This assay was performed in duplicate using only 0.25  $\mu$ M peptide and the averaged results are shown in Figure 32. Adeptantins monomers at this sub-toxic concentration showed no permeabilization. On the contrary, dimers reached more than 90% permeabilization within 15 minutes. This was in agreement with their increased permeabilizing capacity as measured with Gal-ONp uptake, as well as a greater antimicrobial potency. Bodipylated peptides were also measured by this assay and have shown higher level of permeabilization than unmodified monomers which have reached their maximum within 15 - 30 minutes. What was more interesting in the time

range is that after 30 minutes, fluorescence started to drop, an effect we were not able to explain.

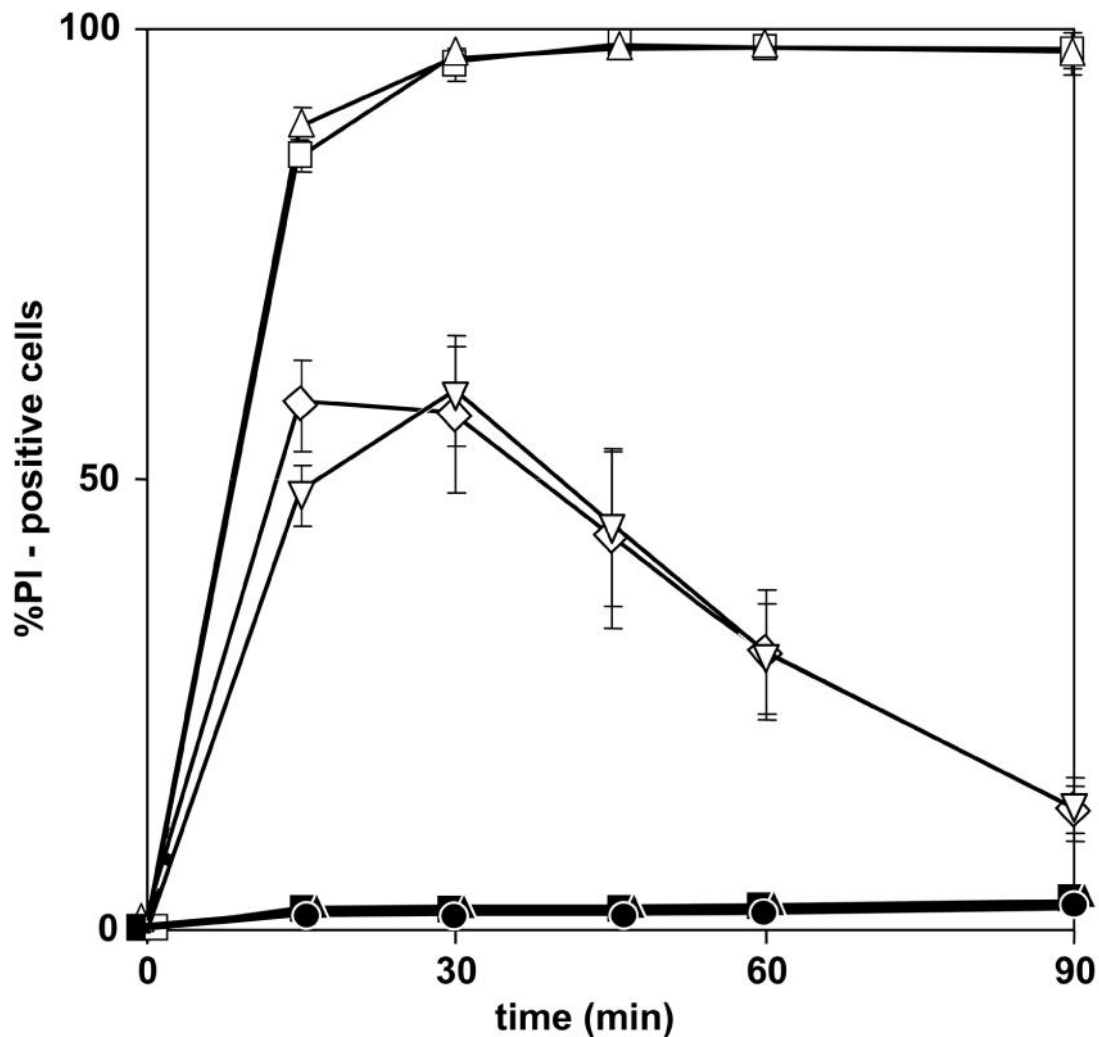


Figure 32. Permeabilization of *E. coli* ATCC 25922 ( $10^6$  cells/ml) inner membrane caused by ADPs (0.25  $\mu$ M) and determined by % of PI-positive bacterial cells by flow cytometric analyses; (ADP1 —●— ; ADP2(AM) —■— ; [ADP2]<sub>2</sub>—□— ; ADP2(BY)—◇— ; ADP3(AM)—▲— ; [ADP3]<sub>2</sub>—△— ; ADP3(BY)—▽—).

### 3.6. Effects of adeptantins on host cells

Adeptantins were created to be selective peptides. This means that they need to have a high TI, due to low MIC values against *E. coli* (and our MIC assays gave the desired low MIC values), but also due to high HC<sub>50</sub> values. To verify this, haemolysis assays were performed. These are instrumental in determining the TI, but it is necessary to obtain other evidence for a low capacity to permeabilize cellular membranes in general. For this reason the capacity of ADPs to lyse human cells was also tested by monitoring PI internalization by flow cytometric analysis.

HC<sub>50</sub> values for adeptantins were determined from the data gathered in human RBC haemolysis assays based on the activity of increasing peptide concentrations on 0.5% v/v

fresh erythrocytes. Results were collected from four different experiments carried out in triplicate and are displayed in Figure 33 as mean values for each peptide concentration, with errors based on SD.  $HC_{50}$  values were then extrapolated from the curves as peptide concentration causing 50% haemolysis.

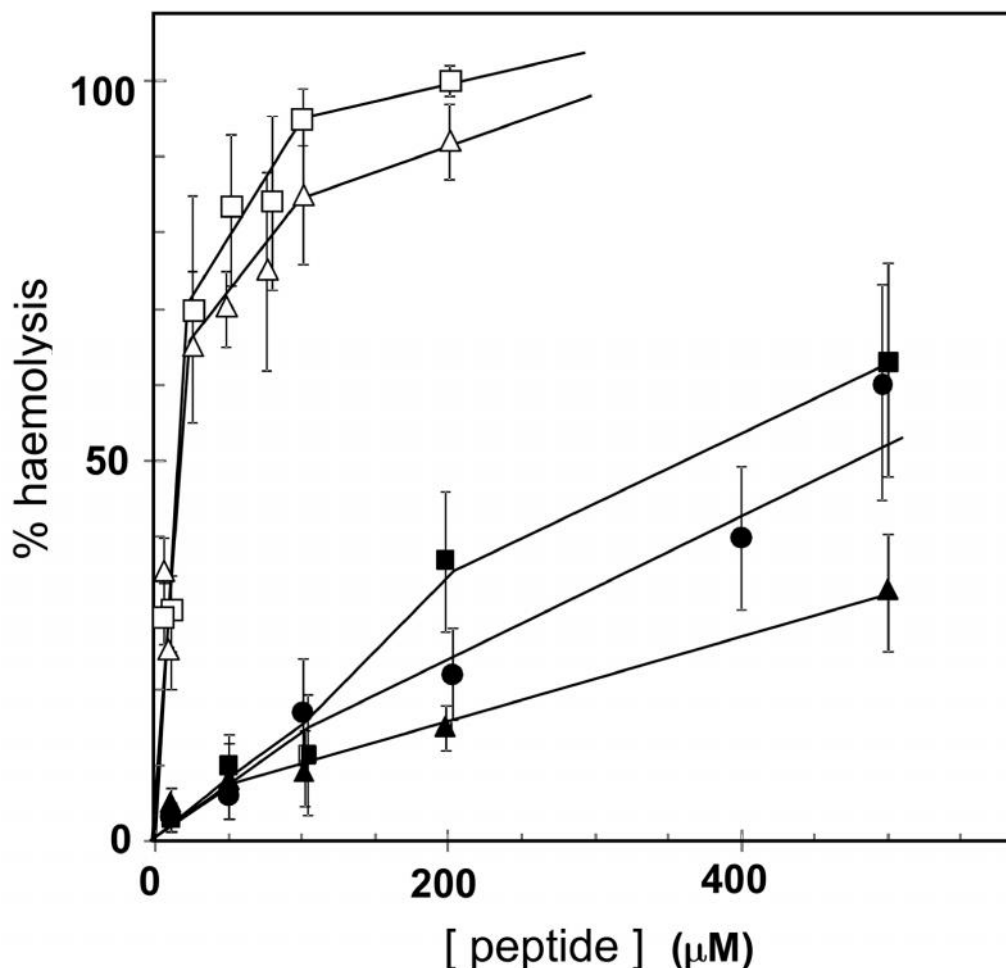


Figure 33. Adepantin-induced haemolysis on 0.5% RBC; ADP1 —●— ; ADP2(AM) —■— ; [ADP2]<sub>2</sub> —□— ; ADP3(AM) —▲— ; [ADP3]<sub>2</sub> —△— ; Results are from four experiments carried out in triplicate.

Figure 33 and Table 20 show that monomeric forms of ADPs had very low haemolytic activities, with  $HC_{50}$  values  $>400 \mu M$ . Activity decreased in the order ADP2(AM), ADP1, ADP3(AM), so that there was a certain correlation between haemolytic and antimicrobial activity, even though the antimicrobial concentrations are two orders of magnitude lower. Dimers instead showed much lower  $HC_{50}$  values than monomers indicating that their toxicity towards RBC was considerably greater, being significant already at antimicrobial concentrations. This effect was not predictable from CD in the presence of eukaryotic cell-like, neutral LUVs, as no structuring of peptides into helices was observed for either monomers or dimers (Figure 24). If dimers had a greater tendency to insert into neutral membranes, explaining their greater haemolytic activity, this would have been evident by CD. Their increased lytic activity to host cells must have an alternative explanation, one possibility is that it derives from some kind of surface type of interaction, favoured for the dimeric peptides. Another explanation could be that dimerization slightly shifts the equilibrium from a random coil to a helical form in dimeric peptides, with respect to

monomeric ones. The proportion of structured peptides, capable of inserting into the membrane, would remain too low to be observable by CD, but might be sufficient for lytic activity. In any case, dimerization, which would favour peptide aggregation, appears to favour lytic activity against eukaryotic and prokaryotic cells.

Table 20. Haemolytic, MIC and TI values for tested peptides; Haemolytic activity tested for peptides, expressed as  $HC_{50}$  value; <sup>(1)</sup> determined from Figure 33 and Figure 34; MIC values from Table 16; TI value calculated from experimental data (TI calculated) and predicted one (TI predicted); <sup>(2)</sup> For ADP1, the first value is from second set of tests together with other ADPs, while the second value is from the first set of tests when only ADP1 was tested along with PSEU2 and ASC1. <sup>(3)</sup> Values are for original peptide sequence not iodoacetamidated one.

Peptide abbreviation	$HC_{50}$ ( $\mu M$ ) <sup>(1)</sup>	MIC ( $\mu M$ )	TI (calculated)	TI (predicted)
ADP1	480 ± 60 (> 800 <sup>(2)</sup> )	2 - 4	190 ± 90	86
ADP2(AM)	400 ± 100	1	400 ± 100	91 <sup>(3)</sup>
[ADP2] <sub>2</sub>	16 ± 4	0.5 - 1	16 ± 4	-
ADP3(AM)	> 500	4	> 125	95 <sup>(3)</sup>
[ADP3] <sub>2</sub>	20 ± 4	0.5	40 ± 8	-
PSEU2	50	8	6	7
PSEU2 A9	> 200	8 – 16	> 30	90
ASC1	80	2	40	54
ASC1 I2	> 200	4	> 60	80

It should be pointed out that in the first set of assays (Juretić et al., 2009), the haemolysis curves presented in Figure 34 and Table 20 are relative to the wild type control peptides ascaphin 1 and pseudin 2 and point mutations of each, measured together with ADP1. For both control peptides the  $HC_{50}$  values were less correlated with literature data than their MIC values. For ASC1 the measured value was 80 against literature value of 200 and for PSEU2 the measured value was 50 against a literature value of 360 (Conlon et al., 2004; Olson et al., 2001). In any case, as can be seen from Table 20, the haemolytic activity was decreased for mutated peptides, confirming the ability of the D-descriptor method to guide variations to improve selectivity. The variability in haemolysis results is due to slightly different methods used in different laboratories, and also due to the fact that different RBCs from different donors are used every time. This can be appreciated when comparing the  $HC_{50}$  value measured for ADP1 in assays performed in different times.

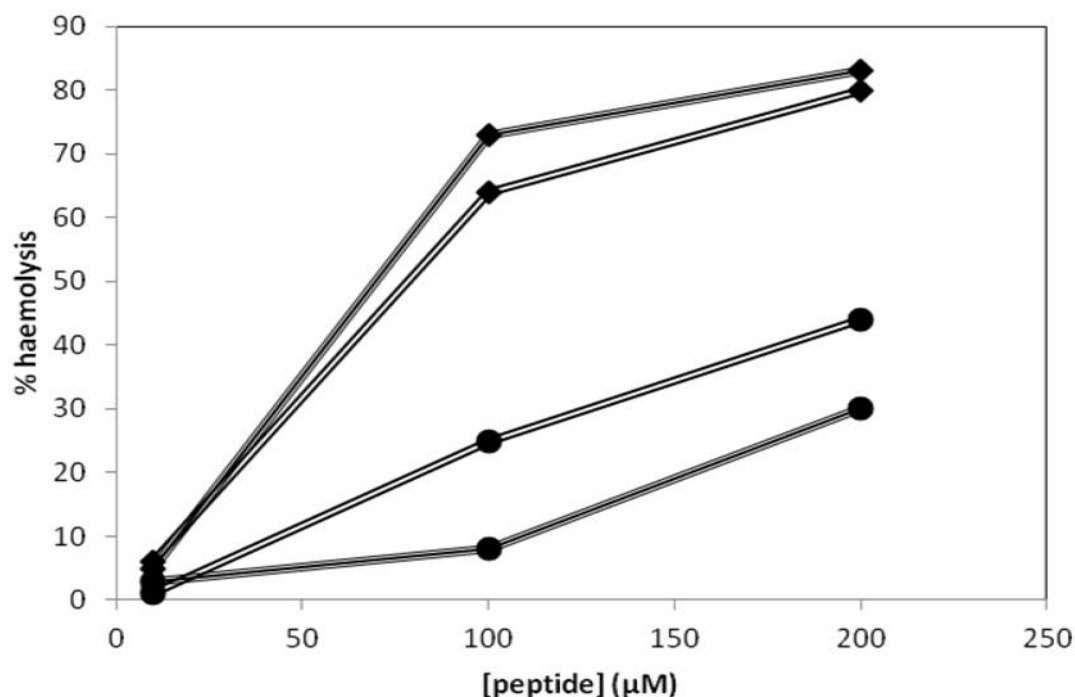


Figure 34. Pseudin and ascaphin-induced haemolysis on 0.5% RBC; PSEU2  $\blacklozenge$ ; PSEU2 A9  $\bullet$ ; ASC1  $\blacklozenge$ ; ASC1 I2  $\bullet$ ; Results are from two experiments carried out in triplicate.

The results from MIC and  $HC_{50}$  enabled TI value calculation (Table 20) for all peptides. High TI values indicate a high selectivity for all adeptantins as expected by TI prediction from the “Predictor” algorithm (Juretić et al., 2009). It should be pointed out that the predicted TI is just indicative, as is limited to a maximum value of 95 by the “Predictor” algorithm. Any predicted TI approaching this value generally corresponds to much higher measured TI (see for example ADP1, ADP2(AM) and ADP3(AM) in Table 20). The calculated TI value significantly lower than the value 95 corresponds to a low measured TI (see, for example, pseudin 2 in Table 20).

To further correlate the cytotoxicity of peptides by their capacity to interact with and permeabilize cellular membranes, a flow cytometric study was carried out. This study used bodipyated ADP2 and 3 to probe interaction with host cells membranes. By using the impermeant quencher Trypan blue, it was possible to distinguish peptides bound to the surface of U937 cells, from peptides inserted into the membrane, or that could have been translocated into the cytoplasm through a pore-mediated self-promoted uptake mechanism. To probe the capacity of peptides to permeabilize the membrane, PI was used instead, as any lesions in the membrane would allow it to internalize and bind to the DNA, becoming fluorescent. Fluorescently labelled peptides efficiently and rapidly bound to the membrane surface, as could be seen in the shift to a higher fluorescence value in gate 1 at increasing peptide concentration, after only a 5 min exposure (see in Figure 35 A) and B)). However, treatment with Trypan blue significantly decreased the fluorescence, so peptides are just surface bound (see Figure 35 C) and D)). PI treatment showed that even if peptides attach to the membrane, they do so without damaging it, as shown by the fact that there is an increase in fluorescence at 525 nm (fluorescence axis for BODIPY fluorescence in Figure 36) whereas there was little shift at 610 nm (fluorescence axis representing PI fluorescence Figure 36).

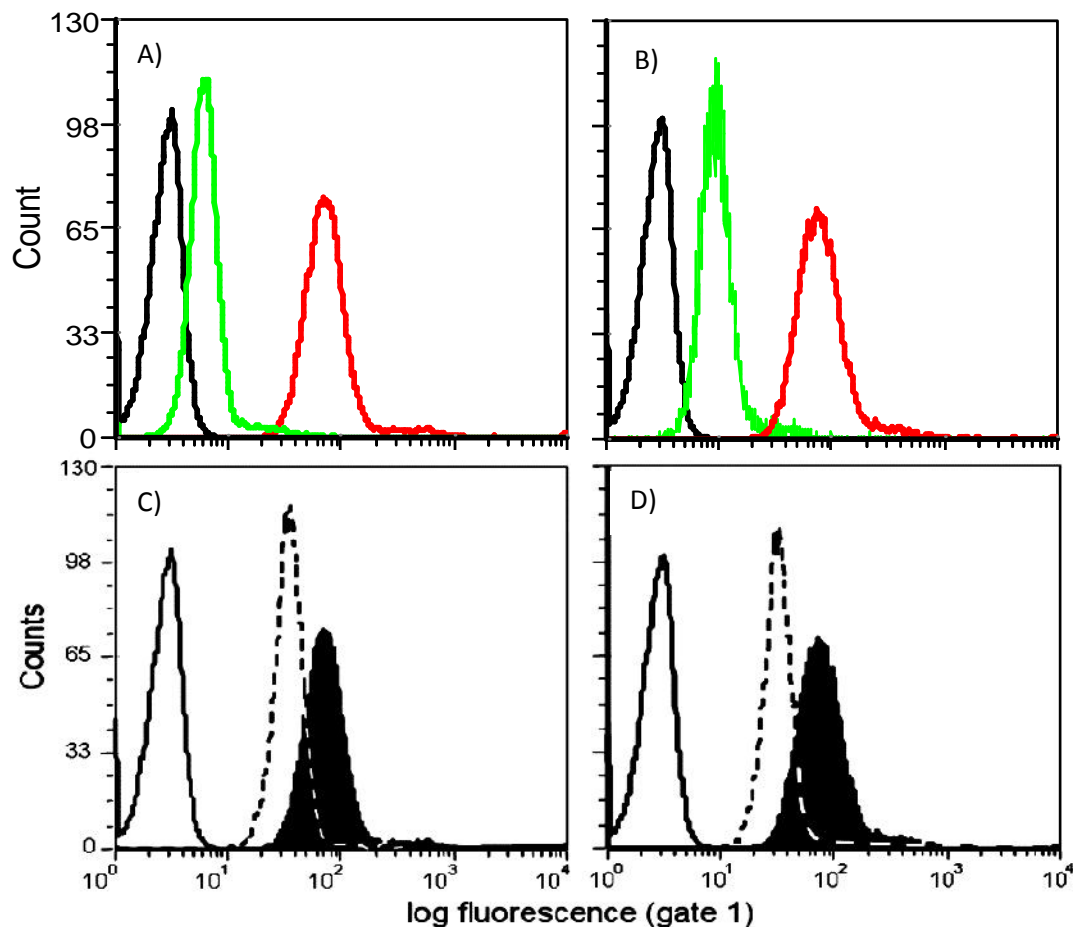


Figure 35. ADPs interaction with U937 cells, as measured by flow cytometry, presented on monoparametric histograms; A) ADP2(BY) and B) ADP3(BY) demonstrates the effect after 5 minutes where the black line is control, the green line is peptide at concentration  $0.1\text{-}M$  and the red line is peptide at concentration  $1\text{-}M$ ; C) ADP2(BY) and D) ADP3(BY) where empty curve is for U937 cells in the absence and filled curve in presence of ADPs ( $1\text{-}M$ ) while dashed line represents U937 cells with ADPs and the impermeant, extracellular quencher Trypan blue added.

Efficient binding of ADP2(BY) and ADP3(BY) to the U937 cell membrane is visible in the shift of monoparametric peak to a considerably higher position in Figure 35 C) and D). The effect was noticed within 5 minutes of interacting time and it depends on the concentration of the peptide Figure 35 A) and B). Peptide fluorescence was reduced by the trypan blue quencher revealing that ADPs remain bound to the outer side of the cell membrane.

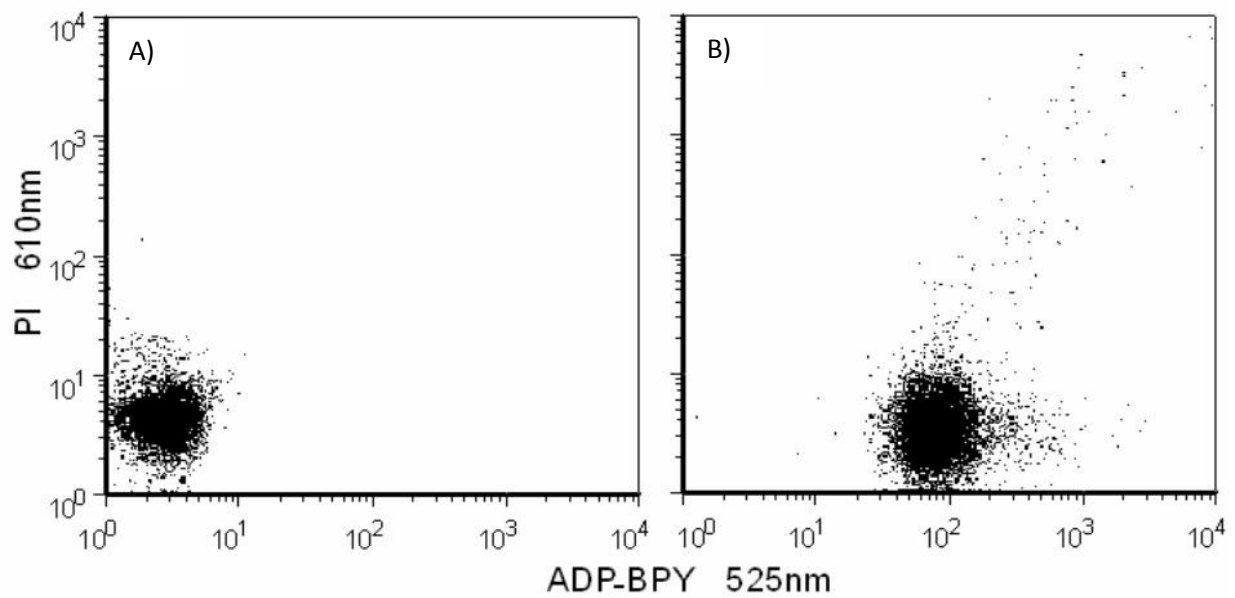


Figure 36. Fluorescence dot plots expressing results of monitoring fluorescence at 525 nm (BODIPY) and 610 nm (PI) on the flow cytometer for human leukemic monocytes (U937,  $10^6$  cells/ml) treated with peptides (1 ~M) A) ADP2(BY) or B) ADP3(BY) and PI for 30 min at room temperature before treating cells with Trypan blue.

The test confirmed that monomeric labelled ADPs interact with the surface of host cells membrane at antimicrobial concentrations without expressing any cytotoxicity.

## 4. Discussion

Bacteria are increasingly developing resistance to antibiotics, justifying research towards finding new anti-infective agents acting with diverse mechanisms (Taubes 2008). One promising class of anti-infective agents are AMPs, essential components of innate immunity, produced by all higher organisms. Cationic AMPs have remained effective against bacteria throughout evolution (Zasloff 2002; Yeaman and Yount 2007), but cannot be directly used as anti-infective drugs, outside their physiological context used. Therefore, numerous attempts have been made to modify natural AMPs to improve essential properties, such as selectivity, expressed as the therapeutic index (TI), and bioavailability. The need for developing sophisticated methods capable of improving known natural or synthetic AMPs was the driving force behind the work described in this thesis. The theoretical research, which provided the foundation for experimental thesis research, can be described as the knowledge-based computational usage of amino acid hydrophobicity scales (Juretić et al., 2009; Juretić et al., 2011). All of five amino acid scales used to construct three best descriptors (producing correlation higher than 0.9 among experimental and theoretical TI values, Table 8) are hydrophobicity scales (Appendix 5).

Thousands of endogenous AMPs have been reported, extracted from or identified in many different types of living organisms, as listed in several different databases (Hammami and Fliss 2010). For our research also, the first step was to collect appropriate data and sort it in the AMPad database. Our choice fell on AMPs isolated from anuran species, as these were likely the most abundant and well characterized in the literature. Database construction is an essential requirement for subsequent work on computational tool construction, so that a significant effort was expended to manually assemble a functional database for this purpose. Briefly, AMPad consists of 73 peptides of anuran origin, characterized by an  $\alpha$ -helical active conformation, and with published  $HC_{50}$  and MIC (*E. coli*) data, allowing the definition of TI values. The creation of the AMPad database is described in section 2.1, while the results of the methods used to design novel AMPs based on this database are described in section 3.1. Briefly, the separation of sequences into three distinct “training”, “testing” and “set of best peptides” sets allowed statistical analysis and algorithm construction and creation of the software tools: *i*) “PredictorSelector” to select descriptors associated with correlation higher than 0.90 (positive or negative) among predicted TI values and experimentally determined TI values from “training” set; *ii*) “Predictor” to allow evaluation of an AMP in terms of a predicted TI, based on its sequence; *iii*) “Designer” to suggest a limited set of completely novel peptide sequences predicted to have a high TI, and *iv*) “Mutator” to suggest one or more point mutations that should increase the selectivity of a known peptide in terms of an increased predicted TI (Juretić et al., 2009; Juretić et al., 2011; Kamech et al., 2012).

The guided increase in the “therapeutic index” was the main interest when starting this research which resulted in the individuation of a one-parameter linear model that effectively correlates measured and predicted TI value. This parameter, termed the D-descriptor was selected using the Pearson’s correlation coefficient on a data set with experimental TI values of non-homologous peptides from the AMPad data base that were not normally distributed. Exactly this feature gave the greatest weight to peptides with high TI values. We had actually not expected one parameter model to be effective, as several interrelated structural and physicochemical parameters such as charge, secondary structure,



hydrophobicity and amphipathicity were known to be relevant for modulating activity and specificity (Tossi et al., 2000). It is for this reason that multi-linear models for predicting peptide activity have been used in most structure-activity studies based on the sets of homologous antimicrobial peptides (Langham et al., 2008), while still more complex models were used with limited success on data sets of non-homologous peptides only after the “Predictor” and “Designer” algorithm were constructed and published (Aoki et al., 2012; Hammami and Fliss, 2010; Fernandes et al., 2012; Pirogova et al., 2011; Fjell et al., 2012; Unal et al., 2010).

An essential aspect of predictive bioinformatics tools is the need for a robust experimental verification. Only experimental data can confirm the accuracy (closeness of predicted and measured effect) and efficacy (proportion of corrected predictions over total predictions) of an algorithm or help to further improve the same algorithm. We had decided to construct peptides 23 AA long, which is the minimal length of an  $\alpha$  helical peptide that can span a bacterial membrane. The “Designer” algorithm proposed a workable load of 7 peptides (Table 9) with the desired characteristics, out of which one was chosen to be characterized in a first series of assays (Juretić et al., 2009), and the further two in a subsequent series of similar assays (Ilić et al., 2013). ADP1 was chosen as the only peptide not having a Cys at the C-terminus, as the reactive sulphhydryl group can result in unwanted side-effects. ADP2 was the ADP1 analogue with Cys instead of Ser at the C-terminus. This needed to be acetamidated, to block the sulphhydryl, for testing, or the Cys residue was exploited for dimerization or linking the fluorescent probe BODIPY. ADP3 was instead chosen as being the most different in sequence to ADP1 and 2, and as it has a C-terminal Cys, ADP3 was treated in a similar manner as ADP2.

A high relative amphipathicity (Zelezetsky et al., 2005) in the ADPs primary structures suggested a high probability of membrane association, as well as the possibility of helix-helix interactions in the membrane, leading to channel formation (Senes et al., 2000). Both effects were confirmed using different types of assays. Membrane insertion as well as permeabilization of membranes were respectively shown using CD spectroscopy in the presence of model membranes, and appropriate membrane permeabilization tests on the *E. coli* ML-35 pYC strain. Conformational variations observed by CD in the presence of anionic LUVs suggested insertion of ADPs into this “bacterial-like” membrane (see in 2.4), while in the presence of neutral LUVs they seemed to remain surface-bound and not inserted into the membrane. Permeabilization was tested in different ways: a) flow cytometry in the presence of PI (see section 2.6.2 and Figure 32) indicated that rapid and efficient permeabilization of both outer and cytoplasmic membrane of *E. coli* occurred; b) another permeabilization assay using two chromogenic substrates, Gal-ONp and CENTA<sup>®</sup>, for a periplasmic lactamase and cytoplasmic galactosidase respectively, confirmed an efficient permeabilization first of the outer and then of the cytoplasmic membrane at quite low concentration (see section 2.6.1 and Figure 31). Dimeric ADPs permeabilized bacterial membranes with a significantly faster kinetics than monomeric ones, and this correlated with lower MIC and IC<sub>50</sub>, suggesting that dimerization can be related with increasing potency (see in 2.5 and 3.5).

The effect of adeptantins on host cells (see sections 2.7 and 3.6) was evaluated by determining haemolysis and capacity to permeabilize host cell membrane to PI, in order to confirm the selectivity of ADPs as defined by their measured TI values (ratio of HC<sub>50</sub> to MIC<sup>E</sup>).

*coli*). ADPs seemed to interact poorly with neutral LUVs (as observed by CD, see section 3.4) letting us hope that their haemolytic activity could be low. The haemolysis test (see section 2.7.1) in fact revealed that very high concentrations of ADPs monomers were necessary for a detectable haemolysis in the presence of adeptantins, with some difference between peptides: ADP2(AM) > ADP1 > ADP3(AM). Dimers, on the other hand, had much lower HC<sub>50</sub> values than monomers, with a significant toxicity already at antimicrobial concentrations. Considering the results of CD spectra representing dimer peptide behaviour in the presence of neutral LUVs, this effect was unexpected, as no structuring was observed, indicating little insertion into this type of membrane (Figure 24). The membranolytic activity of dimeric peptides on eukaryotic membranes may either be caused by interaction of surface-type, or by a slightly shifted equilibrium to a structured form that can insert and exert a lytic effect, but insufficiently abundant to be visible by CD. In any case, peptide aggregation, which is obligatory in the dimers, seems to favour lytic activities against both eukaryotic and prokaryotic membranes. With regard to this hypotheses, flow cytometric analysis of U937 cells treated with bodipy-labeled ADPs confirmed a significant interaction with these eukaryotic cells (fluorescence channel increase), but these were surface-bound as the fluorescence could be quenched by Trypan blue. This confirms a strong interaction with the surface, albeit likely without insertions (as indicated by CD).

An attempt to localize the targets and binding sites of the ADP2(BY) in mammalian cells is reported by Novković in his thesis (Novković 2010), although the assay he used still needs adjusting. In the experiment, live NIH 3T3 murine fibroblasts from established tissue culture were treated with different concentrations of ADP2(BY) with different time exposures. Cells were then examined with an epifluorescent microscope and binding of ADP2(BY) to the nuclei of the treated cells was observed, as well as a concentration and time dependent staining of the cytoplasm. These results appear to contradict the results gathered with the flow cytometric study on the U937 cells which indicate attachment of the peptides to the cell without damaging it (cells remained PI negative). However, some questions as to the integrity of cells membrane in cells studied with the epifluorescent microscope remain, as the preparation protocol may have damaged them. Further testing with membrane-specific fluorescent dye is strongly recommended.

After calculating the TI values for all peptides (see Table 20) it is evident that ADP2 was the most selective adeptantin of the three tested, although all three tested adeptantins were quite selective, with regard to the natural peptides from the AMPad database (Appendix 1). Considering the TI values predicted by the "Predictor" algorithm (Juretić et al., 2009) these match calculated values nicely, taking into account that predicted TI values can vary between 5.3 and 94.9. Also noticeable is that as the predicted value gets closer to the upper limit, the measured one is more likely to be high and very often well over this upper limit of the linear, one descriptor fit. The algorithm's result for two reference natural peptides ascaphin 1, as an example of a selective peptide, and pseudin 2, as an example of a mediocre peptide, also showed a good match between the predicted and the measured values. The extensive testing described in this thesis thus confirms the D-descriptor as a robust and useful tool for estimating peptide's selectivity in the high TI range or estimating the direction of the TI changes after point mutations.

Some testing has been performed on very short, 13 AA ADPs (Separovic, private communication), with the results that are yet to be published. These were however not that

encouraging as for the 23 AA ADPs. It is probable that there is a lower limit in length for highly active AMPs, and as this is approached, it may become more difficult to distinguish a highly selective peptide which is also quite active. There are however still numerous sequences that the “Designer” algorithm can propose, with just slight changes of the inbuilt conditions, and further testing of these can be of interest. Furthermore, the success in constructing an algorithm that predicts selective AMPs against *E. coli*, suggests as a next step in the construction of similar types of algorithms predicting AMPs against other kind of microbes, such as Gram-positive bacteria or fungi. Some references to attempts at peptide construction can be found in (Hammami and Fliss 2010). The future construction of algorithm that would propose peptides, with broader spectrum of activity is recommendable. A limitation that appeared for other types of organisms at the time of AMPad database construction was the lack of data for the creation of “training” and “testing” sets with a sufficient number of sequences to be statistically significant. *E. coli* is used as a universal test microorganism in the literature reports, and this allowed collecting sufficient sequences with measured MIC for defining the D-descriptor. *S. aureus* and *C. albicans* are used respectively as Gram-positive and fungal reference microorganism, but less frequently than *E. coli*. The use of other microorganisms, such as the Gram-negative *P. aeruginosa*, *K. pneumoniae* or *S. thyphimurium*, the Gram-positive *B. megaterium*, *S. epidermidis* or *E. faecalis*, or fungal organisms such as other *candidae*, *criptococci* or *aspergilli* is considerably more sporadic. A significant effort was made during work for this thesis to prepare an equivalent database to AMPad with MIC and HC<sub>50</sub> values for *S. aureus*, possibly the most used microorganisms after *E. coli*, but for *S. aureus* it is much more difficult to find highly active peptides that are not haemolytic, and we failed in our first attempt to construct a TI-predictor for that organism.

The research also goes in the direction of considering AMPs as cell penetrating peptides (CPPs) with possibility of cargo delivery into cells (Milletti 2012; Madani et al., 2011; Chugh et al., 2010). There are also attempts to use AMPs in fighting cancer cells since AMPs can have a very localized and specific action on this type of cells. Factors leading to selectivity for neoplastic cells could be the higher membrane potential or division rates, as well as somewhat different membrane compositions to normal cells.

Peptides used in the research described here were of amphibian origin, but there are many other similar peptides also found in other kinds of organisms (Tossi et al., 2000). Genomics and proteomics approaches are oriented at deciphering the genomes and proteomes of as many species as possible, some of which are endangered. There are, for example, almost 6000 species of anurans, but only two genomes have been decoded until now (Li et al., 2007; Yang et al., 2012). This has led us to explore other less direct methods for finding possible novel AMPs, presently hidden in the proteomes, genomes or data listed in protein, DNA or cDNA databases. Some of the results have been published in Juretić et al., 2011 and Tessera et al., 2012. In the end, we can conclude that the field of AMPs offers many possibilities to explore.

## 5. Conclusion

The “Designer” algorithm is capable of proposing selective, amphipathic  $\alpha$  helical antimicrobial peptides, that we have named adepantins (ADPs). Tests performed on ADPs confirmed the efficacy and robustness of the algorithm, and in particular of the D-descriptor parameter, to help identify or propose selective AMP sequences, as well as give some insight into the mode of action of this large and important class of antimicrobial peptides (AMPs). ADPs are highly selective and quite potent against Gram-negative bacteria, especially *E. coli*, as the algorithm was trained on activity data for this type of bacterium. On the other hand, it is at the moment lacking the necessary features for Gram-positive bacteria. These characteristics combined with the fact that ADPs express low cytotoxicity against host cells, make ADPs potential tools for exploring selectivity mechanisms in AMPs.

ADPs are short, linear, 23 AA residue long peptides rich in Gly and Lys. In contact with anionic membranes ADPs structure into  $\alpha$  helical active forms which can insert into and then permeabilize these membranes. On the other hand, when in the contact with neutral membranes ADPs remain in random coil conformation, and it appears that they only interact with the surface of this kind of membranes. Covalently dimerised versions of ADPs showed that dimerization significantly impacts on both antimicrobial activity and cytotoxicity towards host cells. Taken together, experiments described in this thesis have confirmed that the “Designer” algorithm is a valid AMP design method, and suggest possible improvements in order to design optimized variants that may be developed as useful anti-infective agents.



## 6. References (alphabetical order)

- M. I. Aguilar, HPLC of Peptides and Proteins: Methods and Protocols, *Methods Mol. Biol.* 251 (2003) 191-209; 242(227-244).
- W. Aoki, K. Kuroda, M. Ueda, Next generation of antimicrobial peptides as molecular targeted medicines, *J Biosci Bioeng.* 114(4) (2012) 365-70.
- C. Auvynet, Y. Rosenstein, Multifunctional host defense peptides: antimicrobial peptides, the small yet big players in innate and adaptive immunity, *FEBS J.* 276(22) (2009) 6497-508.
- R. Bals, Epithelial antimicrobial peptides in host defense against infection, *Respir. Res.* 1 (2000) 141-150.
- M. Benincasa, M. Scocchi, E. Podda, B. Skerlavaj, L. Dolzani, R. Gennaro, Antimicrobial activity of Bac7 fragments against drug-resistant clinical isolates, *Peptides* 25 (2004) 2055-2061.
- B. Bommarius, D. Kalman, Antimicrobial and host defense peptides for therapeutic use against multidrug-resistant pathogens: new hope on the horizon, *IDrugs* 12 (2009) 376-380.
- K. A. Brogden, Antimicrobial peptides: pore formers or metabolic inhibitors in bacteria?, *Nat. Rev. Microbiol.* 3 (2005) 238-250.
- P. Bulet, R. Söcklin, L. Menin, Anti-microbial peptides: from invertebrates to vertebrates, *Immunol. Rev.* 198 (2004) 169–184.
- Y.H. Chen, J.T. Yang, K.H. Chau, Determination of the helix and beta form of proteins in aqueous solution by circular dichroism, *Biochemistry* 13 (1974) 3350-3359.
- A. Chugh, F. Eudes, Y. S. Shim, Cell-penetrating peptides: Nanocarrier for macromolecule delivery in living cells, *IUBMB Life*, 62(3) (2010) 183-93.
- J. M. Conlon, A. Sonnevend, C. Davidson, D. D. Smith, P. F. Nielsen, The ascaphins: a family of antimicrobial peptides from the skin secretions of the most primitive extant frog, *Ascaphus truei*, *Biochem. Biophys. Res. Commun.* 320 (2004) 170–175.
- T. E. Creighton, Disulfide bonds between cysteine residues, in: W. R. Gray (Ed.), *Protein Structure: A Practical Approach*, Oxford University Press, New York, 2002, pp. 165-186.
- M. Dathe, T. Wieprecht, Structural features of helical antimicrobial peptides: their potential to modulate activity on model membranes and biological cells, *BBA Biomembranes* 1462(1-2) (1999) 71-87.
- D. Eisenberg, R. M. Weiss, C. T. Terwilliger, W. Wilcox, Hydrophobic moments and protein structure, *Faraday Symp. Chem. Soc.* 17 (1982) 109-120.
- D. Eisenberg, E. Schwarz, M. Komaromy, R. Wall R, Analysis of membrane and surface protein sequences with the hydrophobic moment plot, *J Mol Biol.* 179(1) (1984) 125-42.

- D. Eisenberg, Three-Dimensional Structure of Membrane and Surface, Proteins, *Annu Rev Biochem.* 53 (1984) 595-623.
- R. M. Epand, H. J. Vogel, Diversity of antimicrobial peptides and their mechanisms of action, *BBA* 1462 (1999) 11-28.
- F. C. Fernandes, D. J. Rigden, O. L. Franco, Prediction of antimicrobial peptides based on the adaptive neuro-fuzzy inference system application, *Biopolymers*, 98(4) (2012) 280-7.
- C. D. Fjell, R. E. Hancock, A. Cherkasov, AMPPer: a database and an automated discovery tool for antimicrobial peptides, *Bioinformatics*, 23(9) (2007) 1148-55.
- C. D. Fjell, J. A. Hiss, R. E. W. Hancock, G. Sneider, Designing antimicrobial peptides: form follows function, *Nature reviews Drug discovery* 11 (2012) 37-51.
- E. Gasteiger, C. Hoogland, A. Gattiker, S. Duvaud, M. R. Wilkins, R. D. Appel, A. Bairoch, Protein Identification and Analysis Tools on the ExPASy Server, (In) John M. Walker (ed): *The Proteomics Protocols Handbook*, Humana Press (2005) 571-607.
- E. Glukhov, M. Stark, L. L. Burrows, C. M. Deber, Basis for selectivity of cationic antimicrobial peptides for bacterial versus mammalian membranes, *J. Biol. Chem.* 280 (2005) 33960-33967.
- M. M. Gromiha, A statistical model for predicting protein folding rates from amino acid sequence with structural class information, *J. Chem. Inf. Model.*, 45 (2005) 494-501.
- H. R. Guy, Amino acid side-chain partition energies and distribution of residues in soluble proteins, *Biophys. J.* 47 (1985) 61-70.
- R. Hammami, I. Fliss, Current trends in antimicrobial agent research: chemo- and bioinformatics approaches, *Drug Discov. Today* 15 (2010) 540-546.
- R. E. Hancock, R. Lehrer, Cationic peptides: a new source of antibiotics, *Trends Biotechnol.* 16(2) (1998) 82-8.
- R. E. W. Hancock, H. G. Sahl, Antimicrobial and host defense peptides as new anti-infective therapeutic strategies, *Nat. Biotechnol.* 24 (2006) 1551-1557.
- D. G. Higgins, A. J. Bleasby, R. Fuchs, CLUSTAL V: improved software for multiple sequence alignment, *Comput. Appl. Biosci.* 8(2) (1992) 189-91.
- N. Hirota, K. Mizuno, Y. Goto, Cooperative alpha-helix formation of beta-lactoglobulin and melittin induced by hexafluoroisopropanol, *Protein Sci.* 6(2) (1997) 416-421.
- N. Ilić, M. Novković, F. Guida, D. Xhindoli, M. Benincasa, A. Tossi, D. Juretić, Selective antimicrobial activity and mode of action of adepantins, glycine-rich peptide antibiotics based on anuran antimicrobial peptide sequences, *BBA Biomembranes* 1828(3) (2013) 1004-1012.
- J. Janin, Surface and inside volumes in globular proteins, *Nature* 277 (1979) 491-492.

- R. N. Jones, H. W. Wilson, W. J. Novick, Jr., A. L. Barry, C. Thornsberry, In vitro evaluation of CENTA, a new beta-lactamase-susceptible chromogenic cephalosporin reagent, *J. Clin. Microbiol.* 15 (1982) 954-958.
- D. Juretic, A. Lucin, The preference functions method for predicting protein helical turns with membrane propensity. *J. Chem. Inf. Comput. Sci.* 38, (1998) 575-585.
- D. Juretić, B. Lučić, D. Zucić, N. Trinajstić, Protein transmembrane structure: recognition and prediction by using hydrophobicity scales through preference functions, In *Theoretical and Computational Chemistry*; Párkányi, C., Ed.; Elsevier: Amsterdam, The Netherlands, 5 (1998) 405-445. (b)
- D. Juretic, D. Vukicevic, N. Ilic, N. Antcheva, A. Tossi, Computational design of highly selective antimicrobial peptides, *J. Chem. Inf. Model.* 49 (2009) 2873-2882.
- D. Juretic, D. Vukicevic, D. Petrov, M. Novkovic, V. Bojovic, B. Lucic, N. Ilic, A. Tossi, Knowledge-based computational methods for identifying or designing novel, non-homologous antimicrobial peptides, *Eur. Biophys. J.* 40 (2011) 371-385.
- E. Kaiser, R. L. Colescott, C. D. Bossinger, P. I. Cook, Color test for detection of free terminal amino groups in the solid-phase synthesis of peptides, *Anal. Biochem.* 34 (1970) 595-598.
- N. Kamech, D. Vukičević, A. Ladram, C. Piesse, J. Vasseur, V. Bojović, J. Simunić, D. Juretić, Improving the selectivity of antimicrobial peptides from anuran skin, *J. Chem. Inf. Model.* 52 (2012) 3341-51.
- S. M. Kelly, T. J. Jess, N. C. Price, How to study proteins by circular dichroism, *Biochim. Biophys. Acta* 1751 (2005) 119-139.
- S. B. H. Kent, Chemical Synthesis of Peptides and Proteins, *Ann. Rev. Biochem.* 57 (1988) 957-989; DOI: 10.1146/annurev.bi.57.070188.004521.
- K. Koch, S. Afonin, M. Ieronimo, M. Berditsch, A. S. Ulrich, Solid-State <sup>19</sup>F-NMR of Peptides in Native Membranes, *Top Curr. Chem.* 306 (2012) 89-118.
- B.J. Kuipers, H. Gruppen, Prediction of molar extinction coefficients of proteins and peptides using UV absorption of the constituent amino acids at 214 nm to enable quantitative reverse phase high-performance liquid chromatography-mass spectrometry analysis, *J. Agric. Food Chem.* 55 (2007) 5445-5451.
- J. Kyte, R. F. Doolittle, A simple method for displaying the hydrophobic character of a protein, *J. Mol. Biol.* 157 (1982) 105-132.
- A. A. Langham, H. Khandelia, B. Schuster, A. J. Waring, R. I. Lehrer, Y. N. Kaznessis, Correlation between simulated physicochemical properties and hemolysis of protegrin-like antimicrobial peptides: predicting experimental toxicity, *Peptides* 29(7) (2008) 1085-93.
- J. Li, X. Xu, C. Xu, W. Zhou, K. Zhang, H. Yu, Y. Zhang, Y. Zheng, H. H. Rees, R. Lai, D. Yang, J. Wu, Anti-infection peptidomics of amphibian skin, *Mol. Cell. Proteomics.* 6(5) (2007) 882-94.



- F. Madani, S. Lindberg, U. Langel, S. Futaki, A. Gräslund, Mechanisms of cellular uptake of cell-penetrating peptides, *J Biophys*, 2011 (2011) 414729.
- A. Mahamoud, J. Chevalier, S. Alibert-Franco, W.V. Kern, J.-M. Pages, Antibiotic efflux pumps in Gram-negative bacteria: the inhibitor response strategy, *J. Antimicrob. Chemother.* 59 (2007) 1223-1229.
- A. K. Marr, W. J. Gooderham, R. E. W. Hancock, Antimicrobial peptides for therapeutic use: obstacles and realistic outlook. *Curr. Opin. Pharmacol.* 6 (2006) 468–472.
- K. Matsuzaki, K. Sugishita, N. Fujii, K. Miyajima, Molecular basis for membrane selectivity of an antimicrobial peptide, magainin 2, *Biochemistry*, 34(10) (1995) 3423-9.
- M. Mattiuzzo, A. Bandiera, R. Gennaro, M. Benincasa, S. Pacor, N. Antcheva, M. Scocchi, Role of the Escherichia coli SbmA in the antimicrobial activity of proline-rich peptides, *Mol. Microbiol.* 66 (2007) 151-163.
- M. McKenna, The Enemy Within, *ScientificAmerican* 304(4) (2011) 46-53.
- R. B. Merrifield, Solid phase peptide synthesis. I. The synthesis of a tetrapeptide, *J. Am. Chem. Soc.* 85 (14)(1963) 2149-2154.
- F. Milletti, Cell-penetrating peptides: classes, origin, and current landscape, *Drug Discov Today*, 17(15-16) (2012) 850-60.
- F. Morgera, L. Vaccari, N. Antcheva, D. Scaini, S. Pacor, A. Tossi, Primate cathelicidin orthologues display different structures and membrane interactions, *Biochem. J.* 417 (2009) 727-735.
- L. T. Nguyen, E. F. Haney, H. J. Vogel, The expanding scope of antimicrobial peptide structures and their modes of action, *Trends Biotechnol.* 29(9) (2011) 464-72.
- M. Novković, Adepantini, nova klasa dizajniranih antimikrobskih peptida, *Diplomski rad*, Prirodoslovno-matematički fakultet, Sveučilište u Splitu, (2010) 62-64, 87-88.
- M. Novković, J. Simunić, V. Bojović, A. Tossi, D. Juretić, DADP: the database of anuran defense peptides, *Bioinformatics*, 28(10) (2012) 1406-7.
- L. Olson, A. Soto, F. C. Knoop, J. M. Conlon, Pseudin-2: an antimicrobial peptide with low hemolytic activity from the skin of the paradoxical frog. *Biochem. Biophys. Res. Commun.* 288 (2001) 1001–1005.
- Z. Oren, Y. Shai, Mode of action of linear amphipathic  $\alpha$ -helical antimicrobial peptides, *Biopolymers* 47(6) (1998) 451-463.
- E. Pirogova, T. Istivan, E. Gan, I. Cosic, Advances in methods for therapeutic peptide discovery, design and development, *Curr. Pharm. Biotechnol.*, 12(8) (2011) 1117-27.

- E. Podda, M. Benincasa, S. Pacor, F. Micali, M. Mattiuzzo, R. Gennaro, M. Scocchi, Dual mode of action of Bac7, a proline-rich antibacterial peptide, *Biochim. Biophys. Acta* 1760 (2006) 1732-1740.
- J. Reed, T.A. Reed, A set of constructed type spectra for the practical estimation of peptide secondary structure from circular dichroism, *Anal. Biochem.* 254 (1997) 36-40.
- M. Schiffer, A. B. Edmundson, Use of Helical Wheels to Represent the Structures of Proteins and to Identify Segments with Helical Potential, *Biophys. J.* 7(2) (1967) 121-135.
- M. Scocchi, M. Mattiuzzo, M. Benincasa, N. Antcheva, A. Tossi, R. Gennaro, Investigating the mode of action of proline-rich antimicrobial peptides using a genetic approach: a tool to identify new bacterial targets amenable to the design of novel antibiotics, *Methods Mol. Biol.* 494 (2008) 161-176.
- A. Senes, M. Gerstein, D. M. Engelman, Statistical analysis of amino acid patterns in transmembrane helices: the GxxxG motif occurs frequently and in association with beta-branched residues at neighboring positions, *J. Mol. Biol.* 296(3) (2000) 921-36.
- Y. Shai, Mechanism of the binding, insertion and destabilization of phospholipid bilayer membranes by  $\alpha$ -helical antimicrobial and cell non-selective membrane-lytic peptides, *BBA* 1462 (1999) 55-70.
- M. Simmaco, G. Mignogna, D. Barra, Antimicrobial peptides from amphibian skin: what do they tell us?, *Biopolymers.* 47 (1998) 435-450.
- B. Skerlavaj, M. Benincasa, A. Risso, M. Zanetti, R. Gennaro, SMAP-29: a potent antibacterial and antifungal peptide from sheep leukocytes, *FEBS Lett.* 463(1-2) (1999) 58-62.
- J. P. Tam, C. R. Wu., W. Liu, J. W. Zhang, Disulfide bond formation in peptides by dimethyl sulfoxide. Scope and applications, *J. Am. Chem. Soc.* 113 (1991) 6657-6662.
- J. P. Tam, C. Wu, J. L. Yang, Membranolytic selectivity of cystine-stabilized cyclic protegrins, *European Journal of Biochemistry.* 267(11) (2001) 3289-3300.
- G. Taubes, The Bacteria Fight Back, *Science* 321 (2008) 356-361.
- V. Tessera, F. Guida, D. Juretić, A. Tossi, Identification of antimicrobial peptides from teleosts and anurans in expressed sequence tag databases using conserved signal sequences, *FEBS J.* 279(5) (2012) 724-36.
- S. Thomas, S. Karnik, R. S. Barai, V. K. Jayaraman, S. Idicula-Thomas, CAMP: a useful resource for research on antimicrobial peptides, *Nucleic Acids Res.* 38 (2010) 774-780.
- E. Tiozzo, G. Rocco, A. Tossi, D. Romeo, Wide-spectrum antibiotic activity of synthetic, amphipathic peptides, *Biochem. Biophys. Res. Commun.* 249 (1998) 202-206.
- A. Tossi, M. Scocchi, B. Skerlavaj, R. Gennaro, Identification and characterization of a primary antibacterial domain in CAP1 8, a lipopolysaccharide binding protein from rabbit leukocytes, *FEBS Lett.* 339 (1994) 108-112.

- A. Tossi, C. Tarantino, D. Romeo, Design of synthetic antimicrobial peptides based on sequence analogy and amphipathicity, *Eur. J. Biochem.*, 250 (1997) 549-558.
- A. Tossi, L. Sandri, A. Giangaspero, Amphipathic, alpha-helical antimicrobial peptides, *Biopolymers* 55 (2000) 4-30.
- A. Tossi, L. Sandri, A. Giangaspero, New consensus hydrophobicity scale extended to non-proteinogenic amino acids, In *Peptides 2002, Proceedings of the 27<sup>th</sup> European Peptide Symposium, Sorrento, August 31 – September 6th, 2002*; E. Benedetti, C. Pedone, Eds., Edizioni Ziino: Napoli, Italy (2002) 416-417.
- A. Tossi, L. Sandri, Molecular diversity in gene-encoded, cationic antimicrobial polypeptides, *Curr. Pharm. Des.* 8(9) (2002) 743-61.
- M. Umeyama, A. Kira, K. Nishimura, A. Naito, Interactions of bovine lactoferricin with acidic phospholipid bilayers and its antimicrobial activity as studied by solid-state NMR, *Biochim. Biophys. Acta.* 1758(9) (2006) 1523-8.
- E. B. Unal, A. Gursoy, B. Erman, VitAL: Viterbi algorithm for de novo peptide design, *PLoS One*, 5(6) (2010) e10926, doi: 10.1371/journal.pone.0010926.
- T. Unger, Z. Oren, Y. Shai, The Effect of Cyclization of Magainin 2 and Melittin Analogs on Structure, Function, and Model Membrane Interactions: Implication to Their Mode of Action, *Biochemistry*, 40(21) (2001) 6388-6397.
- D. Vanhoye, F. Bruston, P. Nicolas, M. Amiche, Antimicrobial peptides from hylid and ranin frogs originated from a 150-million-year-old ancestral precursor with a conserved signal peptides but a hypermutable antimicrobial domain, *Eur. J. Biochem.* 270 (2003) 2068-2081.
- W.J. Waddell, A simple ultraviolet spectrophotometric method for the determination of protein, *J. Lab. Clin. Med.* 48 (1956) 311-314.
- G. Wang, X. Li, Z. Wang, APD2: the updated antimicrobial peptide database and its application in peptide design, *Nucleic. Acids. Res.* 37 (2009) D933-D937.
- T. Wieprecht, M. Dathe, M. Beyermann, E. Krause, W. L. Maloy, D. L. MacDonald, M. Bienert, Peptide Hydrophobicity Controls the Activity and Selectivity of Magainin 2 Amide in Interaction with Membranes, *Biochemistry* 36 (1997) 6124-6132.
- H.V. Westerhoff, D. Juretić, R.W. Hendler, M. Zasloff, Magainins and the disruption of membrane-linked free-energy transduction, *PNAS* 86 (1989) 6597-6601.
- X. Yang, W. H. Lee, Y. Zhang, Extremely abundant antimicrobial peptides existed in the skins of nine kinds of Chinese odorous frogs, *J. Proteome Res.*, 11(1) (2012) 306-19.
- M. R. Yeaman, N. Y. Yount, Mechanisms of Antimicrobial Peptide Action and Resistance, *Pharmacol. Rev.* 55 (2003) 27–55.
- M.R. Yeaman, N.Y. Yount, Unifying themes in host defence effector polypeptides, *Nat. Rev. Microbiol.* 5 (2007) 727-740.

J.A. Yethon, D.E. Heinrichs, M.A. Monteiro, M.B. Perry, C. Whitfield, Involvement of waaY, waaQ, and waaP in the Modification of Escherichia coli Lipopolysaccharide and Their Role in the Formation of a Stable Outer Membrane, *J. Biol. Chem.* 273 (1998) 26310-26316.

J.A. Yethon, C. Whitfield, Purification and characterization of WaaP from Escherichia coli, a lipopolysaccharide kinase essential for outer membrane stability, *J Biol Chem.* 276(8) (2001) 5498-504.

Z. Yuan, F. Zhang, M. J. Davis, M. Bodén, R. D. Teasdale, Predicting the solvent accessibility of transmembrane residues from protein sequence, *J. Proteome Res.* 5 (2006) 1063-1070.

M. Zasloff, Antimicrobial peptides of multicellular organisms, *Nature* 415 (2002) 389-395.

I. Zelezetsky, S. Pacor, U. Pag, N. Papo, Y. Shai, H.G. Sahl, A. Tossi, Controlled alteration of the shape and conformational stability of alpha-helical cell-lytic peptides: effect on mode of action and cell specificity, *Biochem. J.* 390 (2005) 177-188.

L. Zhang, T. J. Falla, Potential therapeutic application of host defense peptides, *Methods Mol. Biol.* 618 (2010) 303-327.

[79000 M<sup>-1</sup> cm<sup>-1</sup> at 504 nm in MeOH, *Molecular Probes Handbook*, Invitrogen, 10th Ed. p. 107].



### 6.1. Web link references (in order of appearance)

- [1] <http://cti.itc.virginia.edu/~cmg/Demo/wheel/wheelApp.html>
- [2] <http://split4.pmfst.hr/dadp/>
- [3] <http://www.bbcm.univ.trieste.it/~tossi/pag2.htm>
- [4] <http://aps.unmc.edu/AP/main.php>
- [5] <http://split4.pmfst.hr/mutator/>
- [6] <http://www.ncbi.nlm.nih.gov/pubmed/>
- [7] <http://split4.pmfst.hr/split>
- [8] <http://www.bbcm.univ.trieste.it/~tossi/HydroCalc/HydroMCalc.html>
- [9] <http://sites.google.com/site/adepantin1>
- [10] <http://split4.pmfst.hr/split/dserv1/>
- [11] <http://www.cem.com/page136.html>
- [12] <http://www.chempep.com/ChemPep-peptide-synthesis.htm>
- [13] [http://www.avantilipids.com/index.php?option=com\\_content&view=article&id=532&Itemid=296](http://www.avantilipids.com/index.php?option=com_content&view=article&id=532&Itemid=296).
- [14] [http://en.wikipedia.org/wiki/File:Propidium\\_iodide.png](http://en.wikipedia.org/wiki/File:Propidium_iodide.png)
- [15] <http://web.expasy.org/protparam/>



## CV and list of publications

Graduated from the Faculty of Science, University of Split at the department of Biology and Chemistry in 2002. Started doctoral study in biophysics at the Faculty of science, University of Spilt, in 2008. Has been working at the Faculty of Science, University of Spilt since 2007 as research assistant on project 177-1770495-0476 "Development and applications of maximal entropy production principle", leader Prof. Dr. Davor Juretić. Involved in bilateral project, 2009 – 2011, ZŽZ (SV1) "Design and synthesis of selective peptide antibiotics", leaders: Prof. Dr. Davor Juretić (Croatian coordinator), Prof. Dr. Alessandro Tossi (Italian coordinator). Leader of the scholarship project 2010, Alpe-Adria scholarship, University of Trieste: "Designing, synthesis and control of therapeutic activity of novel selective peptide antibiotics", mentors: Prof. Dr. Alessandro Tossi, Prof. Dr. Davor Juretić (5 months).

### Articles:

1. N. Ilić, M. Novković, F. Guida, D. Xhindoli, M. Benincasa, A. Tossi, D. Juretić, Selective antimicrobial activity and mode of action of adeptantins, glycine-rich peptide antibiotics based on anuran antimicrobial peptide sequences, *BBA Biomembranes* 1828(3) (2013) 1004-1012.
2. D. Juretic, D. Vukicevic, D. Petrov, M. Novkovic, V. Bojovic, B. Lucic, N. Ilic, A. Tossi, Knowledge-based computational methods for identifying or designing novel, non-homologous antimicrobial peptides, *Eur. Biophys. J.* 40 (2011) 371-385.
3. D. Juretic, D. Vukicevic, N. Ilic, N. Antcheva, A. Tossi, Computational design of highly selective antimicrobial peptides, *J. Chem. Inf. Model.* 49 (2009) 2873-2882.

### Posters:

1. Ilić, N., Novković, M., Guida, F., Xhindoli, D., Benincasa, M., Tossi, A., Juretić, D., Adeptantins, computationally designed, glycine-rich peptide antibiotics, with low toxicity and very high G-selectivity// 2<sup>nd</sup> NAM Workshop: New Antimicrobials Workshop in Trieste, Trieste, Itali, 2012. 37 (scientific poster).
2. Ilić, N., Novković, M., Guida, F., Antcheva, N., Tossi, A., Copic, T., Puizina, J., Juretić, D., Adeptantins, a new class of ab-initio designed antimicrobial peptides // Book of Abstracts AMP2010/ Juretić, Davor; Separovic, Frances (ur.). Split: University of Split, Faculty of science, 2010. 41-41 (scientific poster) – the best poster award.
3. Juretić, D., Vukičević, D., Ilić, N., Bojović, V., Tossi A., Design optimisation of novel peptide antibiotics predicted to have high selectivity against G-negative bacteria // The 3rd Adriatic Meeting on Computational Solutions in the Life Sciences/. Primošten, september 2009. Book of Abstracts, Tomić, Sanja; Smith, David (ur.). Zagreb: Centre for Computational Solutions in the Life Sciences, Ruđer Bošković Institute, 2009. 59-59 (scientific poster).
4. Juretić, D., Vukičević, D., Bojović, V., Lučić, B., Ilić, N., Design principles for peptide antibiotics // From solid state to biophysics, 4-th conference, Cavtat, Croatia, June 2008 (scientific poster).
5. Juretić, D., Bojović, V., Lučić, B., Ilić, N., Predicting the therapeutic index of peptide antibiotics, // Third Austrian-Croatian Science Days, Grac, Austrija, listopad 2007. (scientific poster).





## Abstracts

### Abstract

As an important part of the innate immune system of all organisms, antimicrobial peptides, are considered as a possible solution for fighting bacteria resistant to standard antibiotics. Crucial characteristic of peptide antibiotic, as drug candidate is its high selectivity, parameterized as the ratio of concentration causing 50% haemolysis ( $HC_{50}$ ) against erythrocytes and the minimal inhibitory concentration (MIC) against the reference bacterium *Escherichia coli*. Using the “Designer” algorithm adeptantins were designed - highly selective artificial glycine and lysine rich peptides in predominant  $\alpha$  helical conformation, having less than 50% homology of primary sequence to any known sequence of antimicrobial peptides. The algorithm used our database of anuran antimicrobial peptides with known selectivity index.

Structure and activity of adeptantins were experimentally and computationally tested in their monomeric, dimeric and fluorescently labelled form. Experimental investigations performed on different bacteria strains showed high selectivity of adeptantins for Gram-negative bacteria (MIC = 0.5 - 4  $\mu M$ ), especially *E. coli*. In membrane permeabilization measurements, different membrane models were used and adeptantins showed rapid permeabilization of both membranes of *E. coli*. These tests provided insight in their mode of action. All monomeric adeptantins have exceptionally low haemolytic activity, while dimers expressed certain toxicity against host cells. It is proven that adeptantins bind efficiently to the cell surface of the host cell membranes without subsequent membrane damage. Gathered results confirmed that adeptantins are indeed highly selective artificial peptide antibiotics.

### Sažetak

Kao važan dio urođenog imunološkog sustava svih živih bića, antimikrobni peptidi, smatraju se možebitnim rješenjem u brobi protiv bakterija otpornih na standardne antibiotike. Važna osobina dobrog kandidata za budući lijek njegova je selektivnost, koja se određuje kao omjer koncentracije pri kojoj se opaža 50%-tna hemolitična aktivnost prema eritrocitima i minimalne inhibitorne koncentracije pri kojoj se opaža 100%-tna inhibicija rasta bakterije *Escherichije coli*. Algoritmom „Designer“ dizajnirani su adeptantini – veoma selektivni umjetni peptidi u konformaciji  $\alpha$  uzvojnice, bogati glicinom i lizinom, a sličnost njihovih sekvenci s poznatim antimikrobnim peptidima manja je od 50%. Algoritam je koristio našu bazu podataka antimikrobnih peptida iz anura s poznatim indeksom selektivnosti.

Eksperimentalnim i računalnim metodama istražene su strukture i aktivnosti monomera, dimera i fluorescentno označenih oblika adeptantina. Eksperimentalna istraživanja provedena na različitim sojevima bakterija pokazala su visoku selektivnost adeptantina prema Gram-negativnim bakterijama (MIC = 0.5 - 4  $\mu M$ ), naročito prema *E. coli*. U mjerenju propusnosti membrana rabljeni su različiti modeli membrana, a pokazalo se da adeptantini vrlo brzo povećavaju propusnost obje membrane *E. coli*. Time je dobiven uvid u mehanizme djelovanja adeptantina. Svi monomeri adeptantina imaju izrazito malu hemolitičnost prema eritrocitima, dok su dimeri pokazali određenu toksičnost prema ljudskim stanicama. Dokazano je da se adeptantini vežu na staničnu površinu ljudskih stanica bez popratnog oštećenja membrane. Prikupljeni rezultati potvrdili su adeptantine kao jako selektivne umjetne peptidne antibiotike.



## Acknowledgements

My entrance into the world of antimicrobial peptides was fully opened thanks to my **mentor Prof. Dr. Davor Juretić**, Head of Biophysics graduate study and PhD study, Department of Physics, Faculty of Science University of Split, Croatia. In the years of working together I gained knowledge not only in the field of our research programme, but also in other topics connected to Biophysics, Bioinformatics and Bioenergetics and the research itself. Thanks to Profesor Juretić I was introduced to numerous other scientists in the field opening possible collaborations on the topics of interest. It was one of his connections that gave me the opportunity to do laboratory work in profesor Tossi's group in Trieste.

By welcoming me to his laboratory, my **co-mentor, Prof. Dr. Alessandro Tossi**, Department of Life sciences, University of Trieste, Italy, gave me the opportunity to experience genuine scientific laboratory work. Once again I worked with one of the leading scientists in the field who taught me how to critically "attack" the problem and even more critically the results I gathered in my findings.

I would also like to thank other members of my PhD defence committee, **Prof. Dr. Jasna Puizina, Dr. Bono Lučić**, and **Doc. Dr. Stjepan Orhanović** for critical editing and reading of my thesis and for all suggestions they had to improve it, as well as for fruitful discussions.

Another inspiring and a well-known scientist who collaborated with professor Juretić's group in which I was a part of, **Prof. Dr. Damir Vukičević**, helped me visualise how the living world can be transferred into numbers and computer code and back again.

**Mario Novković** was a challenging young student with billions of inspiring questions and endowed with physicist's precision entering the world of biology and chemistry. He challenged me to stay focused to provide explanations and answers during his work in Trieste. I am proud that I was able to help him completing his Diploma thesis.

I acknowledge all the help, advice, time and laboratory assistance of **Nikolinka Antcheva, Monika Benincasa, Daniela Xhindoli, Filomena Guida** and all other members of **Tossi-Genaro-Scocchi groups**. Special thanks to **Dr. Sabrina Pacor** for her assistance with cytotoxicity tests.

I thank **Mariana Mijaković** for being my "study buddy" during exam preparations in the PhD program, friend and the voice of reason as well. I thank **Larisa Zoranić** for being open to any type of discussion. **Viktor Bojović** was always a great help with little bioinformatical dilemmas and problems that somehow kept appearing.

Special thanks to all my **colleagues, friends and students** for their support, belief in me and their interest in the work I was doing. You kept me motivated.

Last but not least I have to thank my family: **husband, sister** and **parents** whose unconditional support on this long and turbulent journey of reaching the PhD title was priceless.

Many thanks to **Prof. Dr. sc. Ante Graovac**, the well known and esteemed scientist, but also my professor, mentor, the man who wrote many recommendation letters, challenged me with theoretical science, recommended me to professor Juretić, and finally simply a person who saw potential in another person.

Work on this thesis would not have been possible without the following funding:

Croatian Ministry of Science, Education and Sports, grant 177-1770495-0476; Friuli Venezia Giulia L26 project R<sup>3</sup>A<sup>2</sup>; Alpe Adria 2009 grant; Italy/Croatia scientific and technological cooperation programme 2009-2011, project SV1/ZŽ2.



## **Appendices**



## Appendix 1. “Set of AMPad peptides” (SAP) that forms AMPad database.

	Peptide name	Peptide sequence			
	„testing“ set		HC <sub>50</sub> (~M)	MIC(~M)	TI(exp)
1	Magainin 2 analogue F5W	GIGKWLHSAKFKGKAFVGEIMNS	1000,00	8,00	125,00
2	Pseudin 2 analogue K3, K10, K14	GLKALKKVFQGIHKAIKLINNHVQ	330,00	5,00	66,00
3	Magainin-analogue-12W-MG2	GIGKFLHSAKKGKAFVGEIMNS	550,00	12,50	44,00
4	Pseudin 2 analogue F19	GLNALKKVFQGIHEAIKLFNNHVQ	430,00	10,00	43,00
5	Brevinin-2PRc	GLMSVLKGVLTAGKHIFKNGGSLLDQA KCKISGQC	125,00	3,00	41,66
6	Temporin-1DRa-Lys-7	HFLGTLKNLAKKIL-NH <sub>2</sub>	330,00	8,00	41,25
7	Esculentin-1ARb	GLFPKFNKKVKTGIFDIIKTVGKEAGMD VLRTGIDVIGCKIKGEC	120,00	3,00	40,00
8	Ranatuerin-2CSa	GILSSFQGVAKGVAKDLAGKLETL KCKITGC	150,00	4,00	37,50
9	Brevinin-2TSa	GIMSLFKGVLTAGKHVAGSLVDQLKCKI TGCC	100,00	3,00	33,33
10	Brevinin-2PRd	GLMSVLKGVLTAGKHIFKNVGGSLLDQ AKCKITGQC	100,00	3,00	33,33
11	Brevinin-2PRE	GLLSVLKGVLTAGKHIFKNVGGSLLDQA KCKISGQC	80,00	3,00	26,67
12	Dermaseptin-L1	GLWSKIKEAAGAAGKAALNAVTVGLVNG GDQPS	200,00	8,00	25,00
13	Ranatuerin-2BYa	GILSTFKGLAKGVAKDLAGNLLDKFKCKIT GC	120,00	5,00	24,00
14	Ranatuerin 1 analogue K8	SMSVLKKGKVLGKLVACKINKQC	110,00	5,00	22,00
15	Brevinin-2PRb	GLMSLFRGVLTAGKHIFKNVGGSLLDQ AKCKITGEC	65,00	3,00	21,67
16	Dermaseptin-S4-N-term-derivative	ALWKTLKKVLA	50,00	4,50	11,11
17	Ascapin-8	GFKDLLGAALKVKTVLF	55,00	6,00	9,17
18	Magainin analog MG-H2	IICKFLHSIWKFGKAFVGEIMNI	16,00	2,00	8,00
19	Dybowski-4	VWPLGLVICKALKIC	60,40	9,10	6,64
20	Dermaseptin K4-S4(1-16)a	ALWKTLKKVLA	15,00	2,50	6,00
21	Temporin-1DRa-Lys-8	HFLGTLVLA	38,00	8,00	4,75
22	Ranatuerin 1 analogue A22	SMSVLKKNLKGKLVACKIAKQC	40,00	10,00	4,00
23	Temporin-1DRa	HFLGTLVLA	70,00	20,00	3,50
24	Temporin-1Va	FLSSIGKILGNLL	120,00	40,00	3,00
25	Brevinin-1BYa (Ser18, Ser24)	FLPILASLAAKFGPKLFLVTKKS	80,00	40,00	2,00
26	Temporin-1AR	FLPIVGRLLSGLL	210,00	125,00	1,68
27	Temporin-1CSd	NFLGTLVLA	50,00	64,00	0,78
28	Brevinin-Alb	FLPLAVSLAANFLPKLFLCKITKCC	1,88	2,44	0,77
29	Temporin-1CSb	FLPIIGKLLSGLL	95,00	128,00	0,74
30	Brevinin-1SPd	FFPIIAGMAAKVICAITKCC	8,00	13,00	0,62
31	Temporin-1CSa	FLPIVGKLLSGLL	75,00	128,00	0,59
32	Brevinin-1BYa	FLPILASLAAKFGPKLFLVTKCC	10,00	20,00	0,50
33	Brevinin-1AUa	FLPILAGLAAKLVKPVFCSITKCC	5,00	13,00	0,39
34	Brevinin-1AUb	FLPILAGLAANILPKVFCSITKCC	7,00	25,00	0,28
35	Brevinin-1BYb	FLPILASLAAKLGPVFLVTKCC	4,00	16,00	0,25
36	Magainin analogue MG-H1	GIKKFLHIIWKFIKAFVGEIMNS	2,90	16,00	0,18
37	Brevinin-1CSa	FLPILAGLAAKIVPKLFLCLATKCC	5,00	32,00	0,16



	„training“ set		HC <sub>50</sub> (~M)	MIC(~M)	TI(exp)
1	PGLA	GMASKAGAIAGKIAKVALKAL-NH <sub>2</sub>	900,00	8,60	104,65
2	ESCULENTIN-1ARa	GIFSKINKKKAKTGLFNIIKTVGKEAGMD VIRAGIDTISCKIKGEC	180,00	2,00	90,00
3	ASCAPHIN 1	GFRDVLKGAAGAFVKTAVAGHIAN-NH <sub>2</sub>	200,00	3,00	66,67
4	DERMASEPTIN 3	ALWKNMLKGIGKLAGKAALGAVKKLVG AES	50,00	0,80	62,50
5	RANATUERIN-2AUa	GILSSFQGVAKGVAKNLAGLLDELCKIT GC	290,00	5,00	58,00
6	XPF	GWASKIGQTLGKIAKVGLKELIQPK-NH <sub>2</sub>	375,40	8,80	42,66
7	ESCULENTIN-1GRA	GLFSKFAGKGIKNLIFKGVKHIGKEVGMD VIRTGIDVAGCKIKGEC	210,00	6,00	35,00
8	PEXIGANAN	GIGKFLKKAKKFGKAFVKILKK	45,00	1,50	30,00
9	BREVININ-2GRb	GVLGTVKNLLIGAGKSAQSVLKTLSCKL SNDC	180,00	6,00	30,00
10	DERMASEPTIN 1	ALWKTMLKKGTMALHAGKAALGAAA DTISQGTQ	40,00	1,50	26,67
11	MAGAININ 2	GIGKFLHSAKKFGKAFVGEIMNS	1000,00	50,00	20,00
12	PSEUDIN 2	GLNALKKVFQGIHEAIKLINNHVQ	360,00	20,00	18,00
13	PENTADACTYLIN	GLLDTLKGAANKVVGSLASKVMEKL	400,00	25,00	16,00
14	XT-1	GFLGPLLKLAAKGVAKVIPHLIPSRQQ	90,00	6,00	15,00
15	XT-7	GLLGPLLKIAAKVGSNLL	70,00	5,00	14,00
16	NIGROCIN-2GRb	GLFGKILGVGKVLCLGSLGMC	40,00	3,00	13,30
17	DRP-PBN2	GLVTSLIKAGKLLGGLFGSVTGGQS	75,00	6,25	12,00
18	NIGROCIN-2GRa	GLLSGILGAGKHIVCGLSGLC	295,00	25,00	11,80
19	RANATUERIN-2PRa	GLMDVFKGAANKLLASALDKIRCKVTKC	150,00	13,00	11,54
20	RANATUERIN-1	SMSVLKNLKGVLGFGVACKINKQC	150,00	13,00	11,54
21	BREVININ-2GRa	GLLDTFKNLALNAAKSAGVSVLNSLSCKL SKTC	140,00	12,50	11,20
22	GAEGURIN 4 D16W	GILDTLKQFAKGVGKWLKVGAAQGVLT VSCKLAKTC	26,00	2,60	10,00
23	BREVININ-2PRa	GLMSLFKGVLTAGKHIFKNVGGSLDQ AKCKITGEC	55,00	6,00	9,17
24	RANATUERIN-2ARb	GILDTIKNAAKTVAVGLEKIKCKMTGC	150,00	17,00	8,82
25	BREVININ-2GRc	GLFTLIKGAALKIGKTVAKEAGKTGLELM ACKITNQC	100,00	12,50	8,00
26	KASSINATUERIN-1	GFMKYIGPLIPHAVKAISDLI	30,00	4,00	7,50
27	TEMPORIN-1TGb	AVDLAKIANKVLSLF	250,00	37,50	6,67
28	RV-23	RIGVLLARLPKLFSLFKLMGKKV	35,00	6,00	5,83
29	BREVININ-2 RELATED PEPTIDE	GIWDTIKSMGKVFAGKILQNL	70,00	13,00	5,38
30	DERMASEPTIN 5	GLWSKIKTAGKSVAKAAAKAAVKAVTNA V	60,00	35,00	1,71
31	BREVININ-1SPA	FFPIIAGMAAKLIPSLFCKITKCC	7,00	13,00	0,54
32	BREVININ-1TSA	FLGSIVGALASALPSLISKIRN	12,00	25,00	0,48
33	MELITTIN RELATED PEPTIDE	AIGSILGALAKGLPTLISWIKNR	8,00	20,00	0,40
34	DERMASEPTIN 4	ALWMTLLKVKLAAAKAALNAVLVGAN A	1,40	4,30	0,33
35	BREVININ-1E	FLPLLAGLAANFLPKIFCKITRKC	0,41	2,33	0,18
36	BREVININ-1PRA	FLSLAALPKLFCLIFKCC	7,00	100,00	0,07

## Appendix 2. Contribution to the sequent moment of each AA for Janin and Guy scale - ADP1

### Adepatin 1 (GIGKHVKGALKGLKGLLKGLGES)

AA	x coordinate Janin scale	y coordinate Janin scale	x coordinate Guy scale	y coordinate Guy scale
G	0.00000	2.53415	0.00000	0.78423
I	0.06699	0.93669	-0.08031	-1.12279
G	0.01009	0.07018	-0.04679	-0.32540
K	0.30871	1.41910	0.11524	0.52976
H	0.15568	0.53020	-0.20187	-0.68752
V	-0.04115	-0.11033	-0.27407	-0.73482
G	0.05247	0.11490	-0.16110	-0.35275
K	0.16785	0.30739	-0.02426	-0.04442
A	-0.20257	-0.31520	-0.32048	-0.49867
L	-0.08964	-0.11975	-0.41354	-0.55243
K	0.42453	0.48993	0.10747	0.12402
G	0.13500	0.13500	-0.01819	-0.01819
L	-0.19776	-0.17136	-0.46636	-0.40410
K	0.40193	0.30088	0.15208	0.11384
G	0.25055	0.16102	0.23472	0.15085
L	0.07089	0.03871	-0.35020	-0.19122
L	0.10739	0.04904	-0.25473	-0.11633
K	0.30212	0.11268	0.17389	0.06486
G	0.12105	0.03554	0.03212	0.00943
L	-0.28645	-0.06231	-0.61433	-0.13364
G	-0.10058	-0.01446	-0.20656	-0.02970
E	-0.11491	-0.00822	-0.61610	-0.04406
S	-0.30647	0.00000	-0.63323	0.00000
sequent moment	1.23572	6.43379	-3.86658	-3.47905

### Appendix 3. Contribution to the sequent moment of each AA for Janin and Guy scale - ADP2

#### Adepatin 2 (GIGKHVKGKALKGLKGLLKGLGEC)

AA	x coordinate Janin scale	y coordinate Janin scale	x coordinate Guy scale	y coordinate Guy scale
G	0.00000	2.53415	0.00000	0.78423
I	0.06699	0.93669	-0.08031	-1.12279
G	0.01009	0.07018	-0.04679	-0.32540
K	0.30871	1.41910	0.11524	0.52976
H	0.15568	0.53020	-0.20187	-0.68752
V	-0.04115	-0.11033	-0.27407	-0.73482
G	0.05247	0.11490	-0.16110	-0.35275
K	0.16785	0.30739	-0.02426	-0.04442
A	-0.20257	-0.31520	-0.32048	-0.49867
L	-0.08964	-0.11975	-0.41354	-0.55243
K	0.42453	0.48993	0.10747	0.12402
G	0.13500	0.13500	-0.01819	-0.01819
L	-0.19776	-0.17136	-0.46636	-0.40410
K	0.40193	0.30088	0.15208	0.11384
G	0.25055	0.16102	0.23472	0.15085
L	0.07089	0.03871	-0.35020	-0.19122
L	0.10739	0.04904	-0.25473	-0.11633
K	0.85515	0.31896	0.48051	0.17922
G	0.78723	0.23115	0.40148	0.11788
L	0.55329	0.12036	-0.14874	-0.03236
G	1.05871	0.15222	0.43620	0.06272
E	1.92617	0.13776	0.51555	0.03687
C	-0.30647	0.00000	-0.63323	0.00000
sequent moment	6.49506	7.33101	-0.95061	-2.98160

### Appendix 4. Contribution to the sequent moment of each AA for Janin and Guy scale - ADP3

#### Adepatin 3 (GLKGLLGKALKGIGKHIGKAQGC)

AA	x coordinate Janin scale	y coordinate Janin scale	x coordinate Guy scale	y coordinate Guy scale
G	-0.00000	-0.44399	-0.00000	-0.18396
L	-0.08258	-1.15462	-0.17967	-2.51201
K	0.23250	1.61704	0.16977	1.18073
G	0.19775	0.90902	0.15388	0.70735
L	0.05941	0.20232	-0.15516	-0.52844
L	0.02930	0.07856	-0.16307	-0.43721
G	0.08908	0.19505	-0.01200	-0.02628
K	0.35364	0.64764	0.06866	0.12574
A	0.40164	0.62496	0.04721	0.07346
L	0.13257	0.17709	-0.30241	-0.40397
K	0.24039	0.27743	-0.05085	-0.05868
G	0.10727	0.10727	-0.26510	-0.26510
I	-0.07552	-0.06544	-0.50298	-0.43583
G	0.11428	0.08555	-0.28243	-0.21143
K	0.37782	0.24281	-0.11260	-0.07236
H	-0.04941	-0.02698	-0.81633	-0.44575
I	-0.13051	-0.05960	-0.73813	-0.33709
G	0.46940	0.17508	-0.21504	-0.08021
K	0.50685	0.14882	-0.16827	-0.04941
A	0.70787	0.15399	-0.25876	-0.05629
Q	0.76920	0.11059	-0.27217	-0.03913
G	1.11985	0.08009	0.15402	0.01102
C	-0.30647	0.00000	-0.68941	0.00000
sequent moment	5.26429	4.08268	-4.59085	-4.04486

### Appendix 5. Table of amino acid scales from Split 3.5 algorithm [7] used for finding D-descriptor

N <sup>o</sup>	ABBREVIATION	NAME OF THE SCALE	REFERENCE
1	KYTDO	Kyte and Doolittle	Kyte&Doolittle hydropathy values of amino acid residues. Selected (H) as published in: J. Kyte and R.F. Doolittle: "A Simple Method for Displaying the Hydrophathic Character of a Protein". J. Mol. Biol. 157(1982)105-132.
2	FAUPL	Fauchere and Pliska	Fauchere & Pliska scale of solution hydrophobicities for N-acetyl-amino-acid amides octanol/water distribution. Selected normalized (H) according to published values: J.-L. Fauchere and V. Pliska: "Hydrophobic parameters pi of amino-acid side chains from the partitioning of N-acetyl-amino-acid amides". Eur.J.Med.Chem. - Chim. Ther. 18(1983)369-375
3	PONNU	Ponnuswamy	Surrounding hydrophobicity scale. Selected normalized values (H) as published in the Cornette 1987 paper (reference from Cornette (27) scale) based on: P.K. Ponnuswamy, M. Prabhakaran and P. Manavalan Biochim. Biophys. Acta 623 (1980), 301-316.
4	ENGEL	Engelman	Engelman hydrophobicity values. Selected (H) with opposite sign from: D.M. Engelman, T.A. Steitz and A. Goldman: "Identifying Nonpolar Transbilayer Helices in Amino Acid Sequences of Membrane Proteins". Ann.Rev.Biophys.Biophys.Chem. 15(1986), 321-353.
5	JANIN	Janin	DeltaG-transfer from buried interior to solvent accessible surface. Selected normalized values (H) as published in the Cornette 1987 paper (reference from Cornette (27) scale) based on: J. Janin, Nature 277 (1979), 491-492.
6	JONES	Jones	Hydrophobicity scale (H)(NOZAKI-TANFORD-JONES). New version normalized differently and with slight difference in the His value is not taken here but can be found in: M. Mutter, F. Master & K.-H. Altman (1985) Biopolymers 24, 1057-1074. Normalized values in Cornette 1987 paper derived from: D.D. Jones: "Amino Acid Properties and Side-chain Orientation in Proteins: A Cross Correlation Approach". J.Theor.Biol. 50(1975)167-183.
7	GUY-M	Guy	Average of four hydrophobicity scales. Selected normalized values (H) as published in the Cornette 1987 paper (reference from Cornette (27) scale) based on: H.R. Guy: "Amino acid side-chain partition energies and distribution of residues in soluble proteins". Biophys.J. 47 (1985), 61-70.
8	KRIGK	Krigbaum and Komoriya	Ethanol to H2O interaction parameter (C). Selected normalized values from Cornette 1987 paper are derived from: W.R. Krigbaum and A. Komoriya Biochim. Biophys. Acta 576(1979)204-228.
9	VHEBL	von Heijne and Blomberg	Coil in water to helix in membrane values. Selected (H) as published in: G. von Heijne and C. Blomberg Eur.J.Biochem. 97(1979)175-181.
10	EIMCL	Eisenberg and McLachlan	Solvation energy (P). Normalized values from Cornette 1987 paper derived from: D. Eisenberg and A.D. McLachlan: "Solvation energy in protein folding and binding". Nature 319(1986)199-203. Table 1, third column.
11	LEVIT	Levitt	Hydrophobicity values (H) Statistical scale of hydrophobicity based on information theory of the observed solvent accessibility of residues in proteins of known structure. M. Levitt, J.Mol.Biol. 104(1976)59-107.
12	GIBRA	Gibrat	Distribution of residues toward protein interior. Scale (H) normalized as $ax+b$ with $a=0.02675$ , $b=2a$ so that glycine is associated with 0.0. For larger positive values residue is more often in the interior of a protein. J.F. Gibrat: "Modelization by Computers of the 3-D Structure of Proteins". Ph.D. thesis. Univ. of Paris VI, Paris, France. Scale collected from: G.D. Fasman: "Prediction of Protein Structure and the Principles of Protein Conformation", Plenum, New York 1989, page 457, Table XVII.
13	CIDAA	Cid	Hydrophobicity scale (H) for proteins of aa class, Ponnuswamy's 1980 procedure was used. Selected normalized values based on reported values in: H.Cid, M. Bunster, M. Canales and F. Gazitua: "Hydrophobicity and structural classes in proteins" Protein Engineering 5 (1992), 373-375.
14	CIDBB	Cid	Hydrophobicity scale (H) for proteins of bb class. Published values normalized to average=0, sigma=1. The same Cid reference as above.
15	CIDA+	Cid	Hydrophobicity scale (H) for proteins of a+b class. Published values normalized to average=0, sigma=1. The same Cid reference as above
16	CIDAB	Cid	Hydrophobicity scale (H) for proteins of a/b class. Published values normalized to average=0, sigma=1. The same Cid reference as above.
17	PONG1	Ponnuswamy and Gromiha	Globular protein surrounding hydrophobicity scale. Selected published values (H) from: P.K. Ponnuswamy and M.M. Gromiha: "Prediction of transmembrane helices from hydrophobic characteristics of proteins". Int. J. Peptide Protein Res. 42 (1993), 326-341.
18	PONG2	Ponnuswamy and Gromiha	Membrane protein surrounding hydrophobicity (H) scale from the Ponnuswamy and Gromiha 1993 reference (above).
19	PONG3	Ponnuswamy and	Membrane protein surrounding hydrophobicity (H) scale (combined membrane

		Gromiha	scale) from the Ponnuswamy and Gromiha 1993 reference (above).
20	KIDER	Kidera	Hydrophobicity-related scale (H). All published values multiplied with -1. A. Kidera, Y. Konishi, M. Oka, T. Ooi and A. Scheraga "Statistical Analysis of the Physical Properties of the 20 Naturally Occurring Amino Acids". J. Prot. Chem. 4 (1985), 23-55.
21	ROSEM	Roseman	Calculated values (H) for hydrophathy based on the transfer of solutes from water to alkalane solvents. Free energy changes are corrected for self-solvation. All published values are multiplied by -1 to associate positive numbers with Phe, Ile, Leu, Val. M.A. Roseman: "Hydrophilicity of Polar Amino Acid Side-chains is Markedly Reduced by Flanking Peptide Bonds". J. Mol. Biol. 200 (1988), 513-522.
22	WOLFE	Wolfenden	Wolfenden hydrophobicity scale (H) with proline. R.M. Sweet and D. Eisenberg: "Correlation of Sequence Hydrophobicities Measures Similarity in Three-Dimensional Protein Structure". J.Mol.Biol. 171(1983)479-488. R.V. Wolfenden, P.M. Cullis and C.C.F. Southgate Science, 206 (1979) 575-577.
23	CHOTA	Chothia	Chothia residue accessible surface area in tripeptide (H). Selected H as published but surface area in nm squared. C. Chothia: "The Nature of the Accessible and Buried Surfaces in Proteins". J. Mol. Biol. 105 (1976), 1-14.
24	ROSEB	Rose	Array (H) for Rose mean area buried on transfer from the standard state ( extended tripeptide ) to the folded protein ( proportional to the hydrophobic contribution to dG(conf)). All values expressed as nm squared. G.D. Rose, A.R. Geselowitz, G.J. Lesser, R.H. Lee and M.H. Zehfus: "Hydrophobicity of Amino Acid Residues in Globular Proteins". Science 229 (1985), 834-838.
25	ROSEA	Rose	Array for Rose standard state accessibility (H). Selected as published but area expressed in nm squared. G.D. Rose, A.R. Geselowitz, G.J. Lesser, R.H. Lee and M.H. Zehfus: "Hydrophobicity of Amino Acid Residues in Globular Proteins". Science 229(1985)834-838. (second column in Table 1.).
26	EISEN	Eisenberg	Eisenberg normalized consensus hydrophobicity values. Average of 5 other scales. Selected (H) normalized values as published in: D. Eisenberg, E. Schwarz, M. Komaromy and R. Wall: " Analysis of Membrane and Surface Protein Sequences with the Hydrophobic Moment Plot". J. Mol. Biol. 179 (1984), 125-142.
27	PRIFT	Cornette	Optimal amphipathic helices. Selected normalized values (S) as published in: J.L. Cornette, K.B. Cease, H. Margalit, J.L. Spouge, J.A. Berzofsky and C. DeLisi: "Hydrophobicity Scales and Computational Techniques for Detecting Amphipathic Structures in Proteins". J.Mol.Biol. 196 (1987), 659-685.
28	HOPPW	Hopp and Woods	Antigenic determinant scale (B). Normalized values from Cornette 1987 paper derived from: T.P. Hopp and K.R. Woods: "Prediction of protein antigenic determinants from amino acid sequences". Proc. Natl. Acad. Sci. USA 78 (1981), 3824-3828.
29	CHOTH	Chothia	Proportion of residues that are 95% buried. Selected normalized (H) according to the paper: C. Chothia: "The Nature of the Accessible and Buried Surfaces in Proteins". J. Mol. Biol. 105 (1976), 1-14.
30	ROSEF	Rose	Mean fractional area loss. Selected normalized values (H) as published in the Cornette 1987 paper (reference from Cornette (27) scale) based on: G.D. Rose, A.R. Geselowitz, G.J. Lesser, R.H. Lee and M.H. Zehfus: "Hydrophobicity of Amino Acid Residues in Globular Proteins". Science 229(1985)834-838.
31	GUYFE	Guy	Transfer free energy for 6 layers. Values for Trp, Tyr, Lys and Arg obtained by summing polar (positive) and apolar (negative) contribution. All values (H) normalized by Cornette (1987) and multiplied with -1. Original attributes published in the paper: H.R. Guy: "Amino acid side-chain partition energies and distribution of residues in soluble proteins". Biophys.J. 47(1985)61-70.
32	SWEET	Sweet and Eisenberg	Optimal matching hydrophobicity scale. Selected normalized values (H) as published in the Cornette 1987 paper (reference from Cornette (27) scale) based on: R.M. Sweet and D. Eisenberg: "Correlation of Sequence Hydrophobicities Measures Similarity in Three-Dimensional Protein Structure". J.Mol.Biol. 171(1983)479-488.
33	KUNTZ	Kuntz	Hydration (H <sub>2</sub> O that does not freeze) Selected normalized values (P) as published in the Cornette 1987 paper (reference from Cornette (27) scale) based on: Selected normalized values (P) as published in the Cornette 1987 paper (reference from Cornette (27) scale) based on: I.D. Kuntz, J.Am.Chem.Soc. 93(1971)514-516.
34	BULDG	Bull and Bresse	Surface tension of water (P). H.B. Bull and K. Bresse Arch.Biochem.Biophys. 161(1973)665-670.
35	NNEIG	Cornette	Eigenvalues of nearest neighbor matrix. Selected normalized values (H) as published in the Cornette 1987 paper (reference from Cornette (27) scale).
36	COHEN	Cohen and Kuntz	Nonpolar area for residues in isolated beta sheets. Selected values (H) are published values/100. Published values are from Fasman's 1989 book (see above) page 669, Table IX, column IV. F.E. Cohen and I.D. Kuntz: "Tertiary Structure Prediction", p 647-705 from Fasman's 1989 book.
37	KIMBE	Kim and Berg	Thermodynamic beta-sheet propensities (S) All published values were multiplied with -1 in order to associate larger positive values with beta forming residues. The value for Pro was taken to be 0.23 according to: C.K. Smith, J.M. Withka and L. Regan: "A thermodynamic Scale for the beta-Sheet Forming Tendencies of the Amino Acids". Biochemistry 33 (1994), 5510-5517. C.A. Kim and J.M. Berg, Nature:

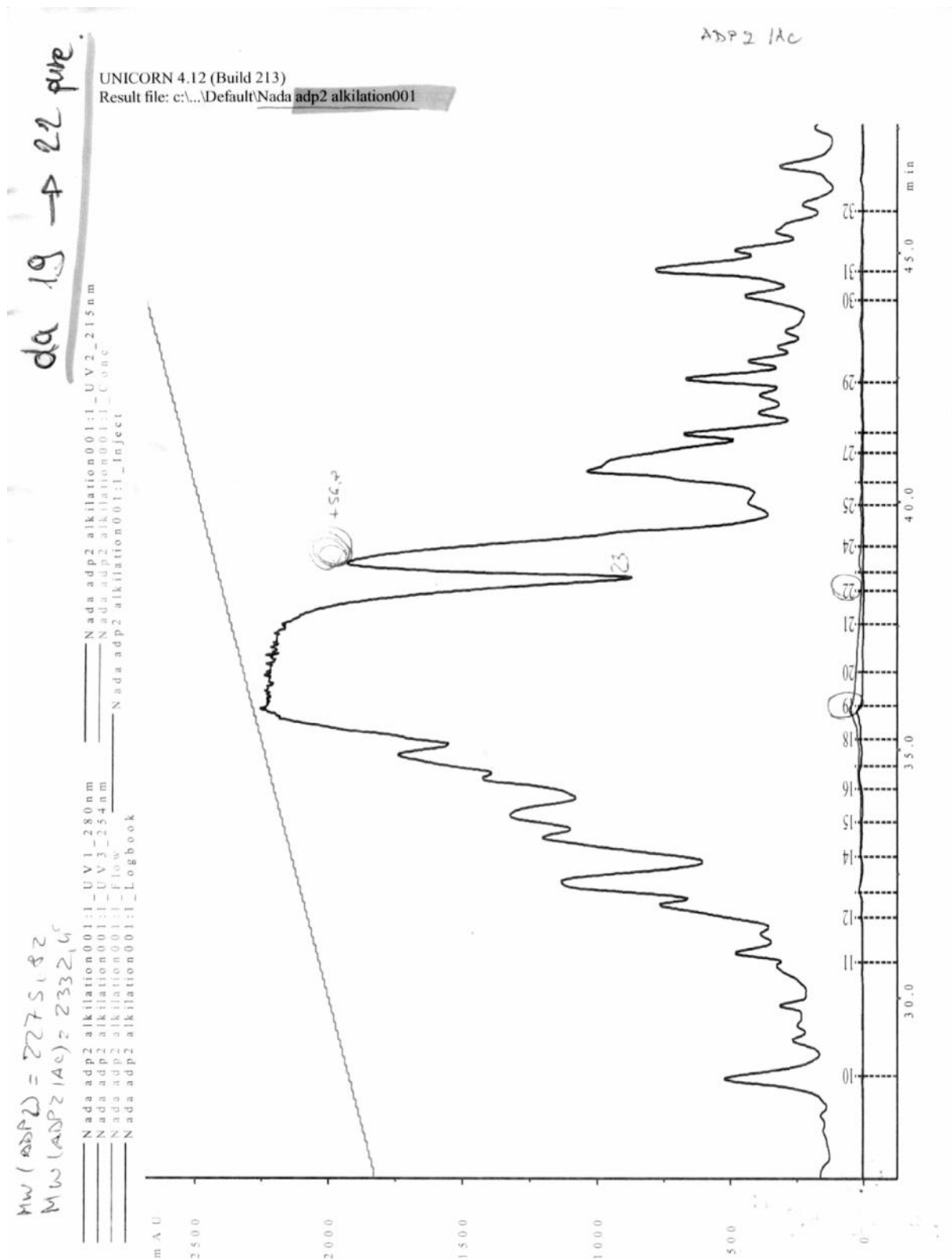
			"Thermodynamic beta-sheet propensities measured using a zinc-finger host peptide". Nature 362 (1993) 267-270.
38	MINKI	Minor and Kim	Beta-sheet propensities (S) D.L.Minor jr.,P.S.Kim, Nature, vol.367,no.6464 (1994) 660-665.
39	MEIRO	Meirovitch	Average normalized distance of the alpha-carbon of amino acid X from the center of the protein. Normalization by the radius of gyration. Normalized values (H) in Cornette 1987 paper derived from: H. Meirovitch, S. Rackovsky and H.A. Scheraga, Macromolecules 13 (1980), 1398-1405.
40	JACWH	Jacobs and White	Jacobs & White weights from their IFH scale (H): R. Jacobs and S.H. White: " The nature of the hydrophobic bonding of small peptides at the bilayer interface: implications for the insertion of transbilayer helices." Biochemistry 28 (1989), 3421-3437.
41	ZAMYA	Zamyatin	Partial specific volume = increase in volume of water after adding one gram of residue expressed in cubic centimeters per gram. This physical property scale (P) can be found in: T.E. Creighton: "Proteins. Structural and Molecular Properties". Freeman, New York 1992, p. 143, Table 4.3 A.A. Zamyatin, Ann. Rev. Biophys. Bioeng. 13 (1984), 145-165.
42	MIJER	Miyazava and Jernigan	An average contact energy scale (P). Selected normalized values from Cornette 1987 reference are derived from: S. Miyazava and R.L. Jernigan, Macromolecules 18(1985)534-552.
43	KUHLE	Kuhn and Leigh	Membrane propensity scale. Selected (S) as published in: L.A. Kuhn and J.S. Leigh: "A statistical technique for predicting membrane protein structure". Biochim. Biophys. Acta 828(1985)351-361.
44	DEBER	Deber	M/A ratio in membrane transport proteins. Selected (S) as published with 1.0 subtracted from each value. C.M. Deber, C.J. Brandl, R.B. Deber, L.C. Hsu and X.K. Young: " Amino Acid Composition of the Membrane and Aqueous Domains of Integral Membrane Proteins". Archives of Biochem. and Biophys. 251(1986) 68-76.
45	WERSC	Wertz and Scheraga	Scheraga ratio of in/out residues. Selected normalized values from Cornette 1987 reference are derived from: D.H. Wertz and H.A. Scheraga Macromolecules 11(1978)9-15.
46	NEILD	O'Neil and DeGrado	Helix formation parameters (C) - the differences in the free energies of helix stabilization for each amino acid relative to Gly (in kcal/mol). More negative values are more helix favoring. Ala is the most helix favoring residue ! One should multiply each value with -1 and try such scale for the prediction of transmembrane alpha helices. K.T. O'Neil and W.F. DeGrado: "A Thermodynamic Scale for the Helix-Forming Tendencies of the Commonly Occurring Amino Acids", Science 250 (1990), 646-651.
47	SCHER	Scheraga	Scheraga s values (P). From: J. Wojcik, K.-H. Altmann and H.A. Scheraga, Biopolymers 30 (1990) 12. We took these s values from: K.T. O'Neil and W.F. DeGrado: "A Thermodynamic Scale for the Helix-Forming Tendencies of the Commonly Occurring Amino Acids", Science 250(1990), 646-651.
48	JURPE	Juretic and Pesic	Statistical (S) scale of beta preferences derived from 8 membrane porins. D. Juretic and R. Pesic: " A scale of beta- preferences for structure-activity predictions in membrane proteins". Croatica Chemica Acta 68 (1995) 215-232.
49	HEIJN	von Heijne	Scale for transmembrane segments derived with the help of Engelman's scale (4) for bacterial inner membrane proteins: $h = \ln(fM/fA)$ . Selected (S) as published in: G. von Heijne: "Membrane Protein Structure Prediction. Hydrophobicity Analysis and the Positive-inside Rule. J.Mol.Biol. 225 (1992),487-494.
50	EDEWH	Edelman and White	Linear optimization weights. Optimal predictor scale (O) from: J. Edelman and S.H. White: "Linear Optimization of Predictors for Secondary Structure. Application to Transbilayer Segments of Membrane Proteins". J. Mol. Biol. 210 (1989), 195-209.
51	EDE31	Edelman-31	Optimal predictors (width 31). Selected (O) as published in Edelman 1993 paper.
52	EDE25	Edelman-25	Optimal predictors (width 25). Selected (O) values are the same as published values except for the Val value of 0.859 instead of 0.559 as in: J.Edelman: "Quadratic Minimization of Predictors for Protein Secondary Structure. Application to Transmembrane alpha-Helices". J.Mol.Biol. 232 (1993), 165-191.
53	EDE21	Edelman-21	Selected (O) as published in Edelman 1993 paper.
54	EDE15	Edelman-15	Optimal predictors (width 15). Selected (O) as published in Edelman 1993 paper.
55	FASMA	Chou and Fasman	Statistical preferences (S) for the alpha helix conformation in soluble proteins. Identical values reported in: P.Y. Chou and G.D. Fasman "Prediction of protein secondary structure" Adv. Enzymol. 47 (1978) 45-148. M. Charton and B.I. Charton: "The dependence of the Chou-Fasman parameters on amino acid side chain structure". J. theor. Biol. 102(1983), 121-134.
56	FASMB	Chou and Fasman	Beta preferences (S). Reported in the Chou & Fasman review (see above) from Adv. Enzymol. 47 (1978) 45-148.
57	FASMT	Chou and Fasman	Statistical turn preferences (S). Values reported in: P.Y. Chou and G.D. Fasman "Prediction of protein secondary structure" Adv. Enzymol. 47 (1978) 45-148. M. Charton and B.I. Charton: "The dependence of the Chou-Fasman parameters on amino acid side chain structure". J. theor. Biol. 102(1983), 121-134.
58	RICRI	Richardson and	Middle alpha helix preferences (S): 5-point averages of values N4, N5, Mid, C5 and C4

		Richardson	in the Table I from: Richardson & Richardson: Science 240(1988)1648. For full reference look at scale 60 comment.
59	JURET	Juretic	Statistical preferences (S) for alpha and beta conformation averaged for each amino acid residue. D. Juretic, N. Trinajstić and B. Lucić, "Protein secondary structure conformations and associated hydrophobicity scales". J. Math. Chem. 14 (1993), 35-45. Calculated from: G. Deleage and B. Roux: "An algorithm for protein secondary structure prediction based on class prediction". Protein Engineering 1 (1987), 289-294. Table I second and fourth column; values from each row averaged. Preference for alpha and beta conformation reported in: P.Y. Chou and G.D. Fasman "Prediction of protein secondary structure" Adv. Enzymol. 47 (1978) 45-148.
60	RICH1	Richardson and Richardson	Mid-alpha preference values (S) from: J.S. Richardson and D.C. Richardson: "Amino Acid Preferences for Specific Locations at the Ends of alpha Helices. Science 240 (1988), 1648-1652. Same P-mid values are used in the O'Neil & DeGrado 1990 reference.
61	CHOU1	Chou	Statistical preferences (S) for the alpha helix conformation in alpha class soluble protein. Values from Fasman's 1989 book: G.D. Fasman: "Prediction of Protein Structure and the Principles of Protein Conformation", Plenum, New York 1989. Page 568 from the chapter: P.Y. Chou: "Prediction of Protein Structural Classes from Amino Acid Compositions". p 549-586.
62	CHOU2	Chou	Statistical preferences (S) for beta conformation in beta class proteins. Values taken from the Fasman's 1989 book as for the Chou 66 scale (above).
63	CHOU3	Chou	Statistical (S) preferences for alpha conformation in alpha+beta class proteins. Values taken from: P.Y. Chou: "Prediction of Protein Structural Classes from Amino Acid Compositions". p 549-586 in the Fasman's 1989 book: G.D. Fasman: "Prediction of Protein Structure and the Principles of Protein Conformation", Plenum, New York 1989.
64	CHOU4	Chou	Statistical preferences (S) for the alpha helix conformation in alpha/beta class soluble proteins Fasman's book (see above), page 568.
65	CHOU5	Chou	Statistical (S) preferences for beta conformation in alpha+beta class proteins. Values taken from: P.Y. Chou: "Prediction of Protein Structural Classes from Amino Acid Compositions". p 549-586 in the Fasman's 1989 book: G.D. Fasman: "Prediction of Protein Structure and the Principles of Protein Conformation", Plenum, New York 1989.
66	CHOU6	Chou	Statistical preferences (S) for the alpha helix conformation in soluble alpha/beta class proteins. class proteins. Values taken from: P.Y. Chou: "Prediction of Protein Structural Classes from Amino Acid Compositions". p 549-586 in the Fasman's 1989 book: G.D. Fasman: "Prediction of Protein Structure and the Principles of Protein Conformation", Plenum, New York 1989.
67	MEEKR	Meek	Retention times at HPLC (C). J.L. Meek, Proc. Natl. Acad. Sci., USA 77 (1980), 1632-1636. J.L. Meek
68	KARPL	Karplus and Schulz	Karplus flexibility scale (P) from his FIGURE 1a in: P.A. Karplus and G.E. Schulz: "Prediction of Chain Flexibility in Proteins". Naturwissenschaften 72 (1985), 212-213.
69	MATPO	Mathusamy and Ponnuswamy	Mean rms fluctuational displacements F1 (P). R. Mathusamy and P.K. Ponnuswamy: "Variation of amino properties in protein secondary structures, alpha- helices and beta-strands." Int. J.Peptide Protein Res. 35 (1990), 378-395.
70	WOESE	Woese	Polarity values (P). All reported values subtracted from number 8 in order to obtain positive values for less polar residues. M. Di Giulio, M.R. Capobianco and M, Medugno: "On the Optimization of the Physicochemical Distances between Amino Acids in the Evolution of Genetic Code". J. theor. Biol. 168 (1994), 43-51 C.R. Woese, D.H. Dugre, S.A. Dugre, M. Kondo and W.C. Saxinger: "On the fundamental nature and evolution of the genetic code". Cold Spring Harbor Symp. Quant. Biol. 31 (1966) 723-736.
71	GRANT	Grantham	Polarity values (P). Normalized values derived from: R.Grantham: "Amino Acid Difference Formula to Help Explain Protein Evolution", Science, 185 (1974) 862-864.
72	ZIMMP	Zimmerman	Polarity values (P). Published values are divided with 10. D.D. Jones: "Amino Acid Properties and Side-chain Orientation in Proteins". J. Theor. Biol. 50 (1975), 167-183. Collected by: J.M. Zimmerman, N. Eliezer and R. Simha: "The Characterization of Amino Acid Sequences in Proteins by Statistical Methods". J. Theor. Biol. 21 (1968) 170-201. Table 3 third column.
73	MCMER	McMeekin	Refractivity values (P). All values from Jones paper divided with 10. D.D. Jones: "Amino Acid Properties and Side-chain Orientation in Proteins". J. Theor. Biol. 50 (1975), 167-183. Collected by: T.L. McMeekin, M.L. Groves and N.J. Hipp (1964) In "Amino Acids and Serum Proteins" (J.A. Stekol, ed) p. 54, Washington, D.C.: American Chemical Society.
74	FAUCH	Fauchere	Graph shape index (M). J.-L. Fauchere, M. Charton, L.B. Kier, A. Verloop and V. Pliska: "Amino acid side chain parameters for correlation studies in biology and pharmacology". Int. J. Peptide Protein Res. 32 (1988), 269-278.
75	KUBOT	Kubota	Relative mutability factor (B). Reported values divided with 100. Y. Kubota, H. Takahashi, K. Nishikawa and T. Ooi, J. Theor. Biol. 91 (1981), 347.
76	URRY1	Urry	The temperature T1 of inverse temperature transition (P). Selected values are 1-



			T1/100. Reported T1 values in: D.W. Urry: "Free energy transduction in polypeptides and proteins based on inverse temperature transitions" <i>Progress Bioph. &amp; Mol. Biol.</i> 57 (1992), 23-57. Table 1., column 2.
77	URRY2	Urry	The temperature T1 of inverse temperature transition (P). Selected values are T1/100. Reported T1 values from the reference cited above.
78	CASSI	Casari and Sippl	Structure-derived hydrophobicity scale (H) G. Casari and M. Sippl: "Structure-derived Hydrophobic Potential. Hydrophobic Potential Derived from X-ray Structures of Globular Proteins is able to Identify Native Folds". <i>J. Mol. Biol.</i> 224 (1992), 725-732.
79	MARTI	Landolt-Marticorena	Positional preferences for occurrence of residues in the middle segment of single helix transmembrane spanning segments. Selected (S) as published in: C. Landolt-Marticorena, K.A. Williams, C.M. Deber, and R.A.F. Reithmeier: 'Non-random distribution of amino acids in the transmembrane segments of human type I single span membrane proteins'. <i>J. Mol. Biol.</i> 229 (1993), 602-608.
80	MDK0	Juretic	Scale (H) derived from # 1 (Kyte-Doolittle) in an iterative procedure as described for Juretic (86).
81	MDK1	Juretic	Scale (H) derived from # 1 (Kyte-Doolittle) in an iterative procedure as described for Juretic (86).
82	MKD2	Juretic	Scale (H) derived from # 1 (Kyte-Doolittle) in an iterative procedure as described for Juretic (86).
83	MODKD	Juretic	Modified Kyte-Doolittle scale in an iterative procedure. Selected (H) as published in reference 1. Iterative procedure described in: D. Juretic, B. Lucic and N. Trinajstic, "Predicting membrane protein secondary structure. Preference functions method for finding optimal conformational preferences" <i>Croatica Chemica Acta</i> 66 (1993), 201-208.
84	MKD4	Juretic	Scale (H) derived from # 1 (Kyte-Doolittle) in an iterative procedure as described for Juretic (86).
85	OSMP1	Juretic	Optimal scale for memb. proteins with one transmembrane helix. Obtained in an iterative procedure described in: D. Juretic, B. Lucic and N. Trinajstic, "Predicting membrane protein secondary structure. Preference functions method for finding optimal conformational preferences" <i>Croatica Chemica Acta</i> 66 (1993), 201-208.
86	OSMP	Juretic	Optimal scale (S) for memb. proteins with more than one transmembrane helical segment. Obtained in an iterative procedure described in: D. Juretic, B. Lucic and N. Trinajstic, "Predicting membrane protein secondary structure. Preference functions method for finding optimal conformational preferences" <i>Croatica Chemica Acta</i> 66 (1993), 201-208.
87	JACWH2	Jacobs and White	Jacobs & White IFH(0.5) scale (H). Table V in the above reference.
88	CPREF	Juretic	Scale of constant preference values extracted from the reference data set of 168 integral membrane proteins. Selected (S) as published in the Juretic et al. reference 1 (see above), but the code number 88 instead of 100 is used by the server.

**Appendix 6. Preparative RP-HPLC spectra for ADP2(AC) (both synthesis), [ADP2]<sub>2</sub> (both synthesis), ADP2(BY), ADP3(AC), [ADP3]<sub>2</sub>, ADP3(BY)**



UNICORN 4.12 (Build 213)  
Result file: c:\...\Default\Nada2010\ADP2alkilation2cndreaction 160311

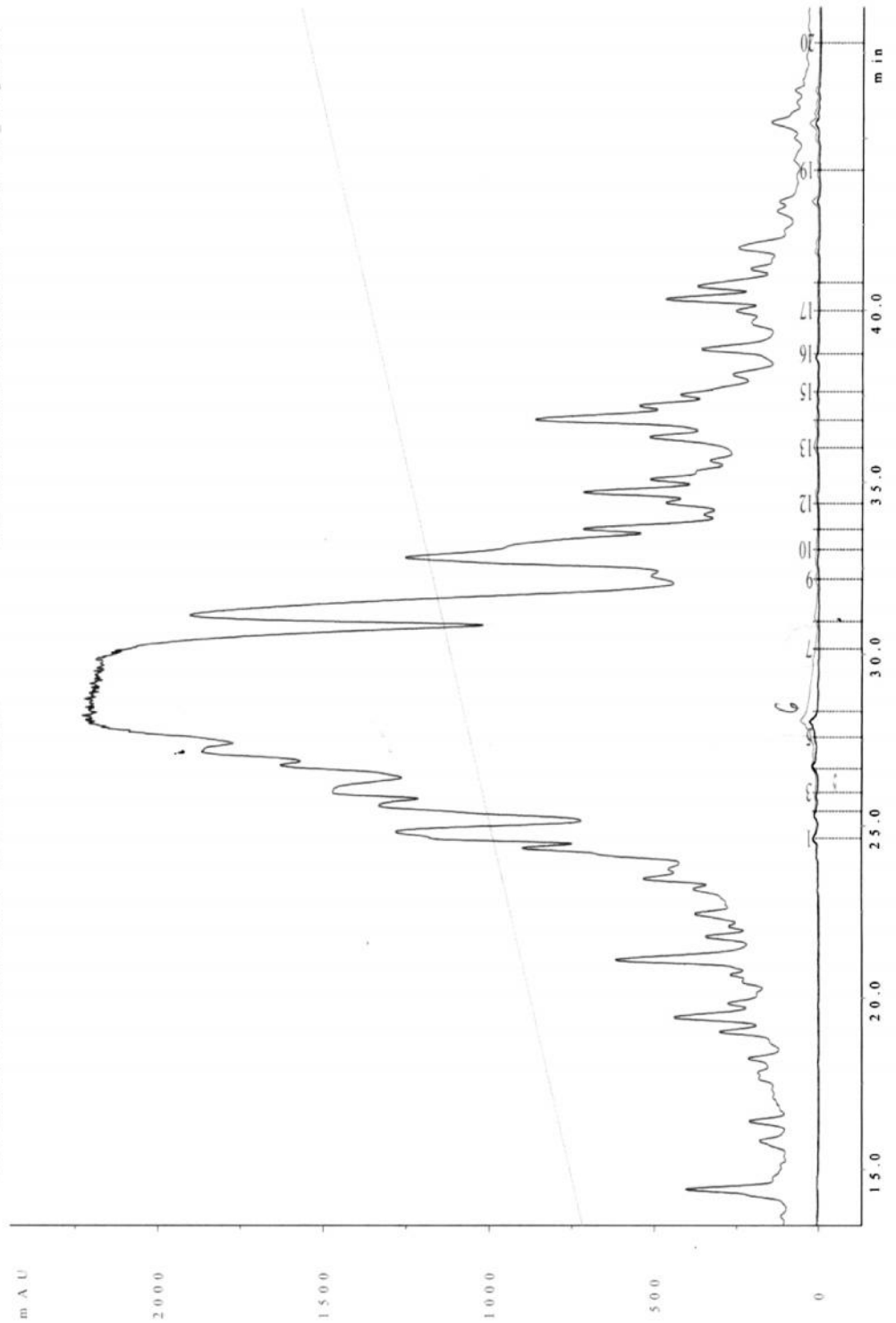
ADP2 IAC

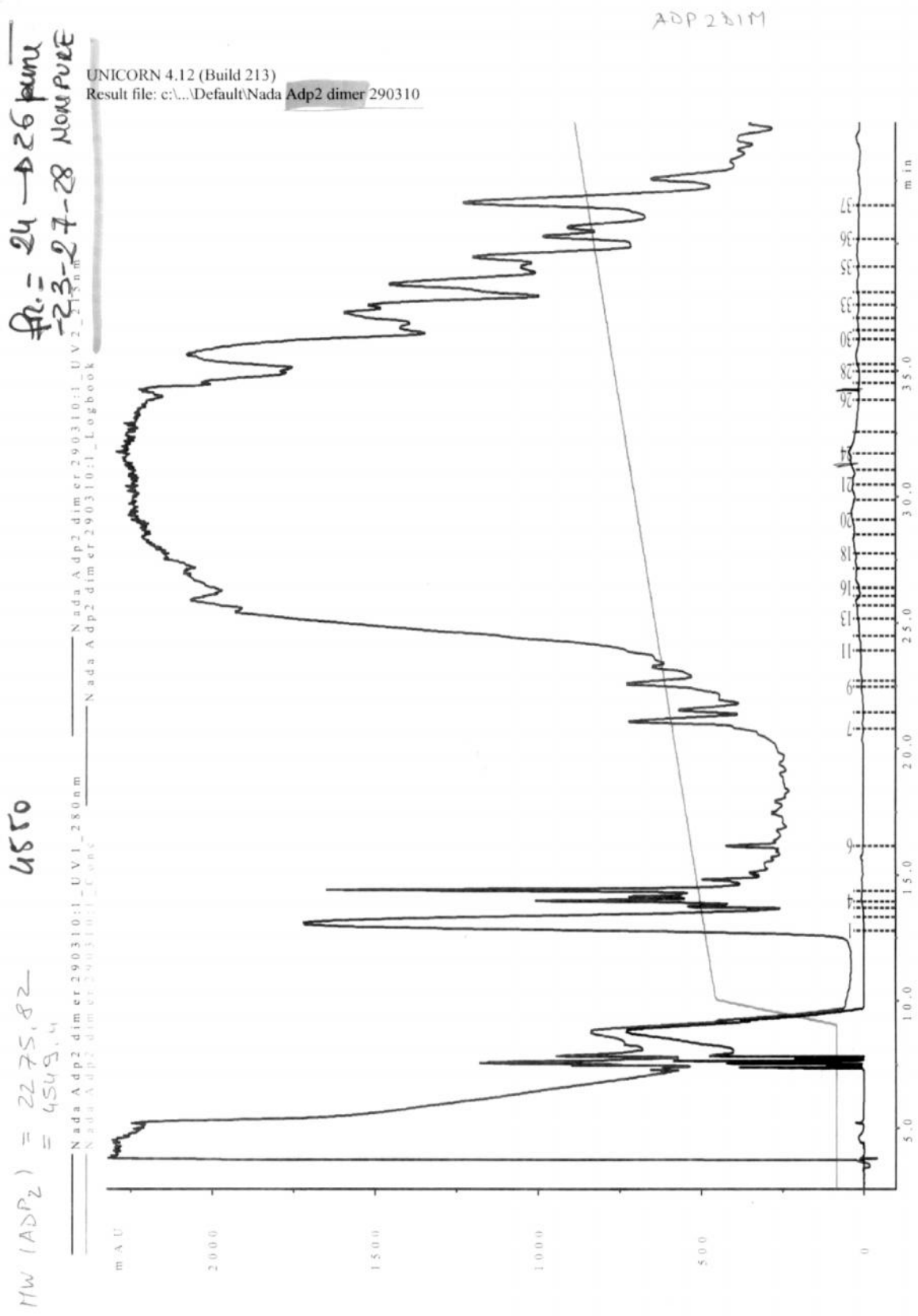
2nd time

bl. 5, 6, 7 pure

MW (ADP2) = 2275,82  
MW (ADP2 IAC) = 2332,48

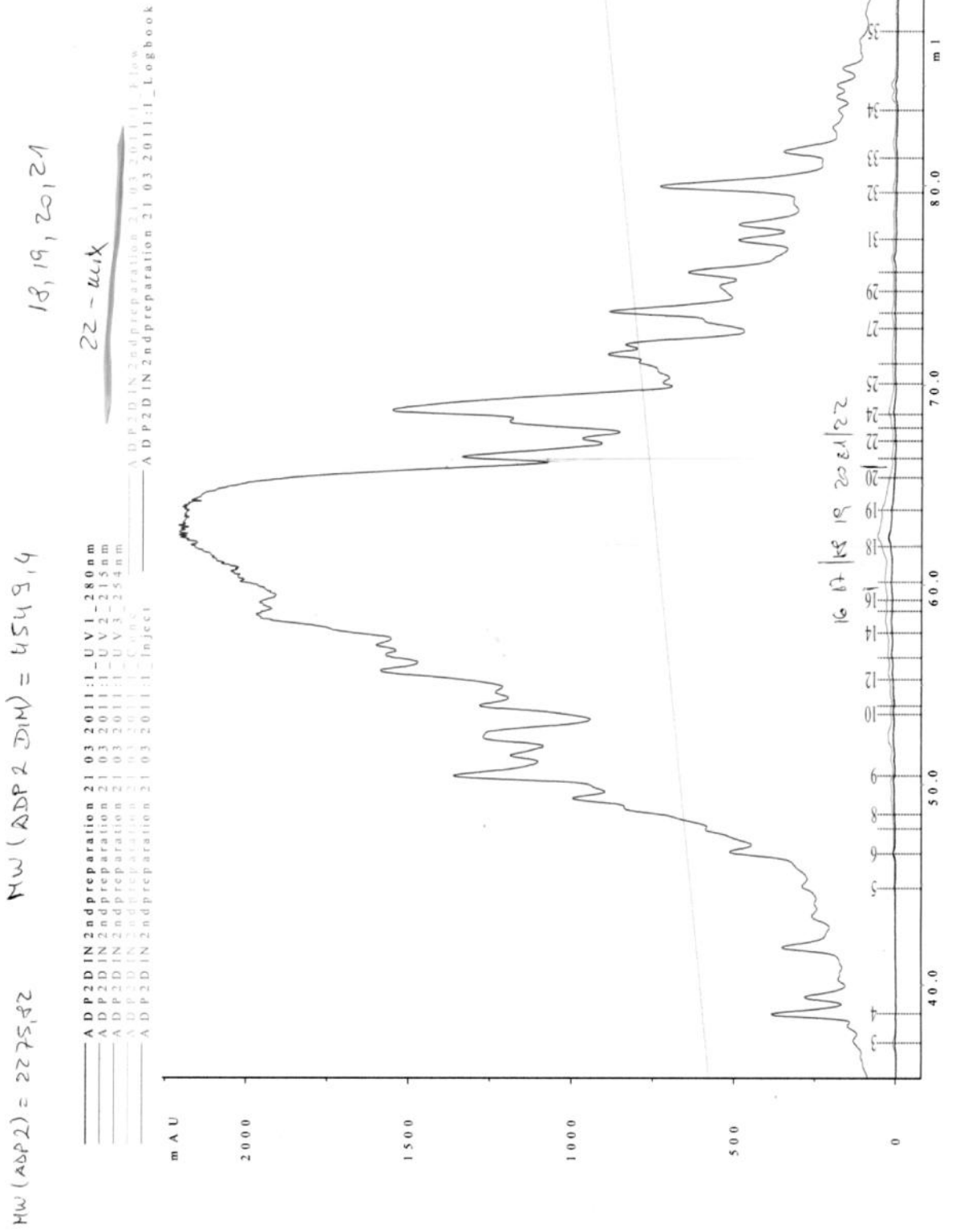
ADP2alkilation2cndreaction 160311:1 UV1\_280nm  
ADP2alkilation2cndreaction 160311:1 UV2\_215nm  
ADP2alkilation2cndreaction 160311:1 UV3\_234nm  
ADP2alkilation2cndreaction 160311:1 UV4\_250nm  
ADP2alkilation2cndreaction 160311:1 Inject  
ADP2alkilation2cndreaction 160311:1 Logbook

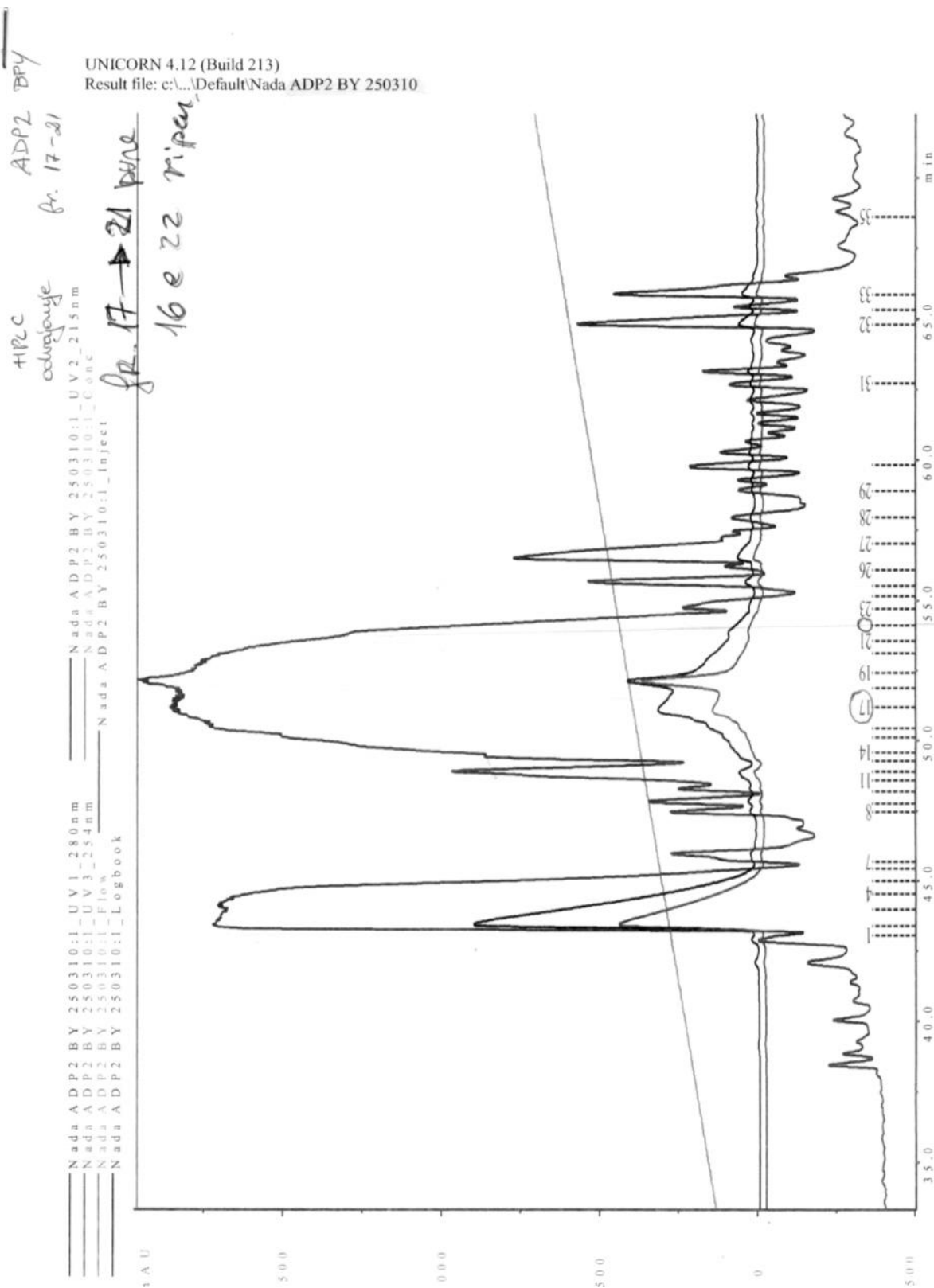


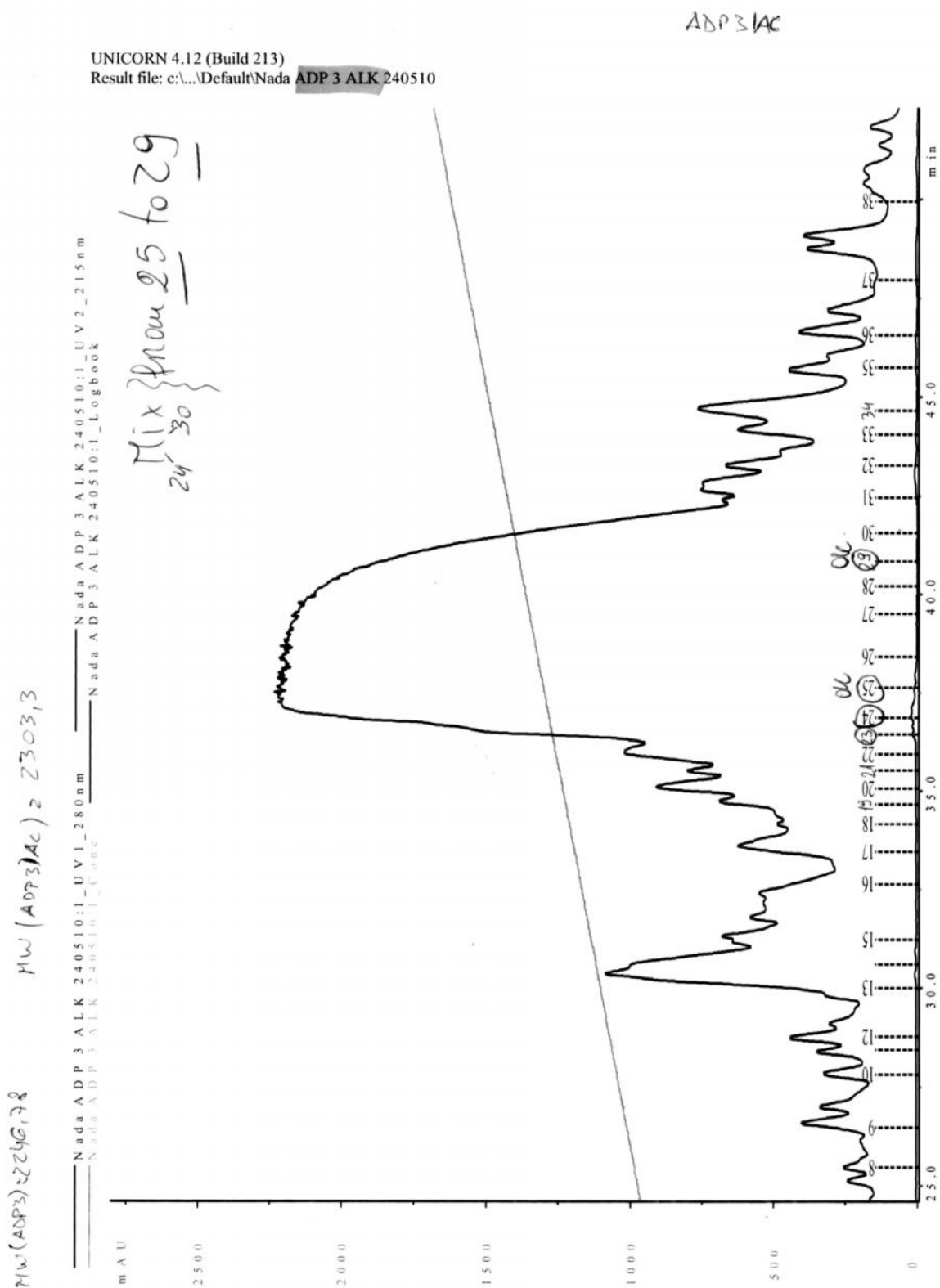


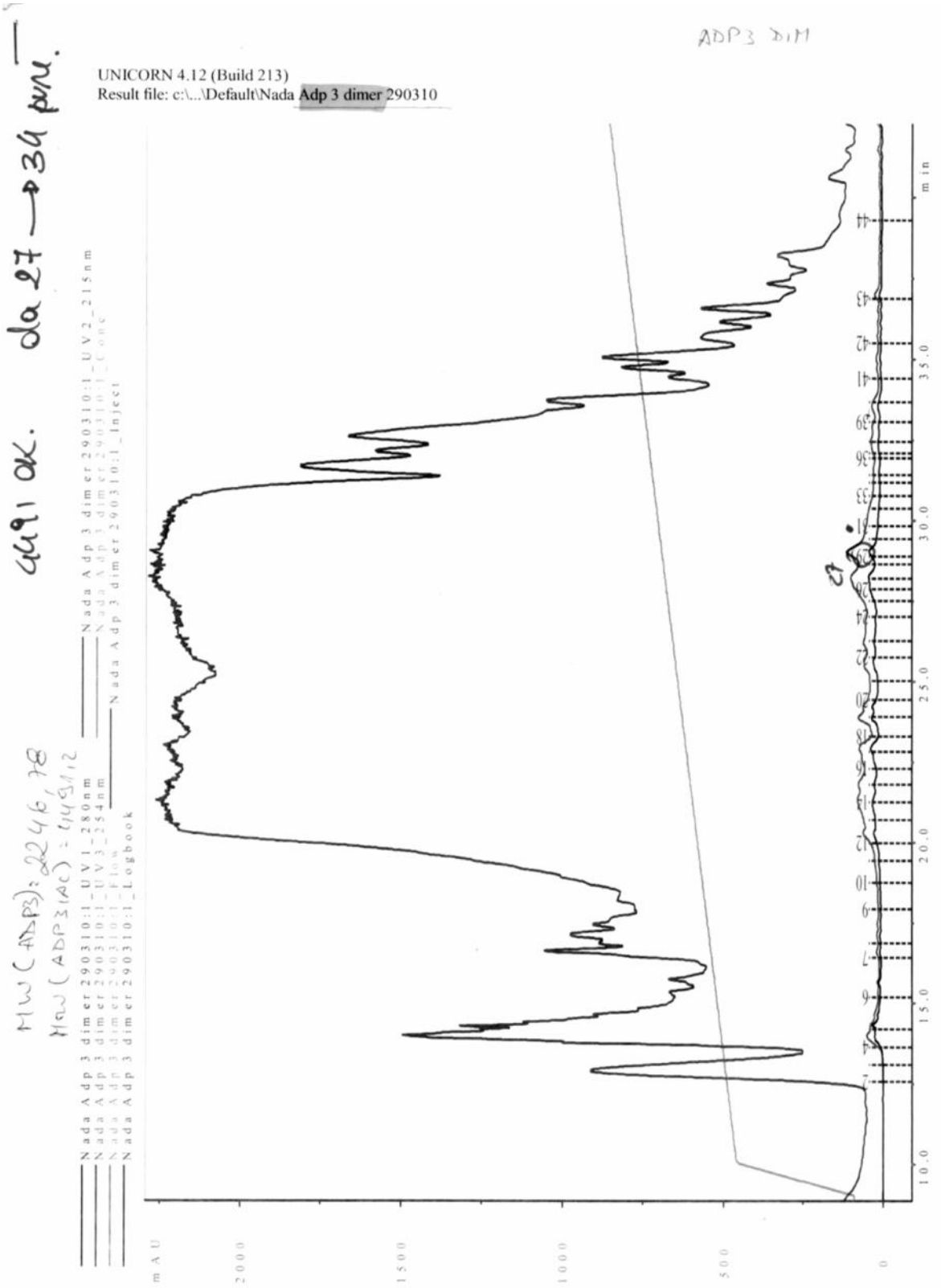
ADP2DIM 2nd time

UNICORN 4.12 (Build 213)  
Result file: c:\...\Default\Nada2010\ADP2DIM2ndpreparation 21 03 2011

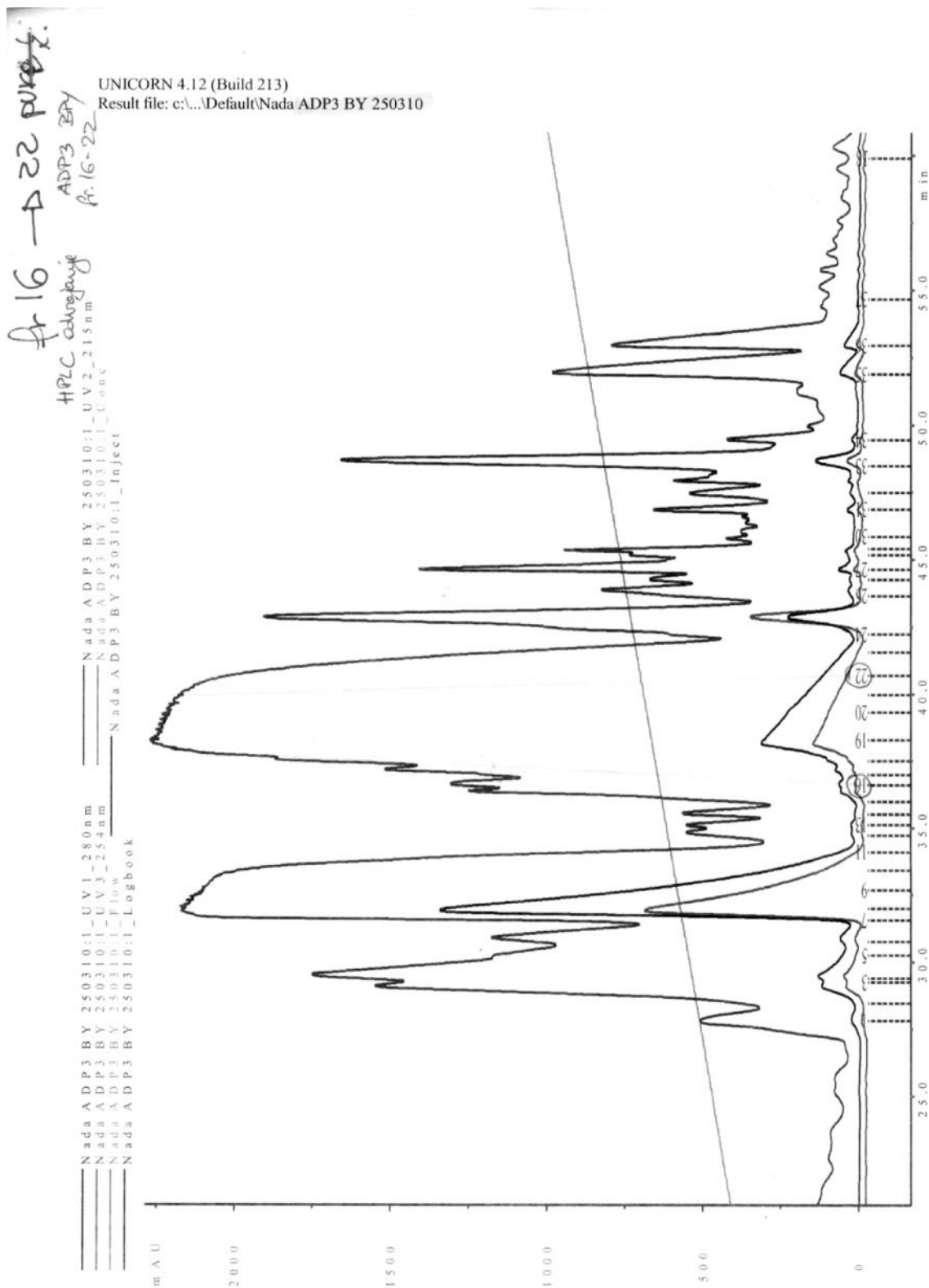








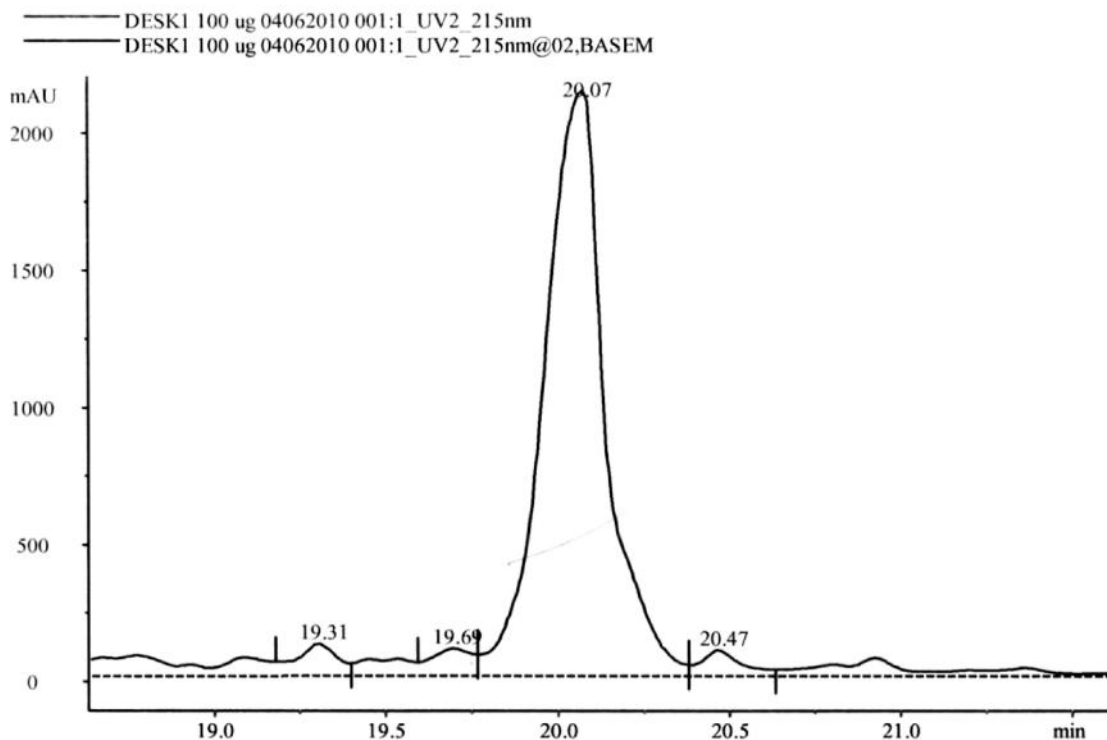




**Appendix 7. Analytical RP-HPLC for ADP1 (first testing name was DESC1) ADP2(AC), [ADP2]<sub>2</sub>, ADP2(BY), ADP3(AC), [ADP3]<sub>2</sub>, ADP3(BY), all graphs overlapped for comparison.**

UNICORN 4.12 (Build 213)

Result file: c:\...\Default\Nada2010\DESK1 100 ug 04062010 001



No	Ret min	Area mAU*min	Height mAU
1	-4.89	29.5865	143.319
2	-4.10	28.0094	135.084
3	-3.80	26.1808	133.859
4	-3.61	19.4317	131.089
5	-3.32	44.3260	176.935
6	-3.19	244.4073	1781.206
7	0.07	72.7233	80.654
8	1.23	24.5925	77.515
9	1.44	18.4544	82.877
10	1.67	17.1245	121.977
11	1.93	151.6429	1777.286
12	2.45	19.6492	64.131
13	2.88	38.2260	51.059
14	4.21	33.0787	34.858
15	18.36	18.4813	102.837
16	19.31	16.5201	116.908
17	19.69	13.8872	99.944
18	20.07	439.9089	2131.278
19	20.47	13.1395	93.985
20	46.83	287.0435	114.480

Total number of detected peaks = 103

Total area = 1724.9778 mAU\*min

Area in evaluated peaks = 1556.4137 mAU\*min

Ratio peak area / total area = 0.902280

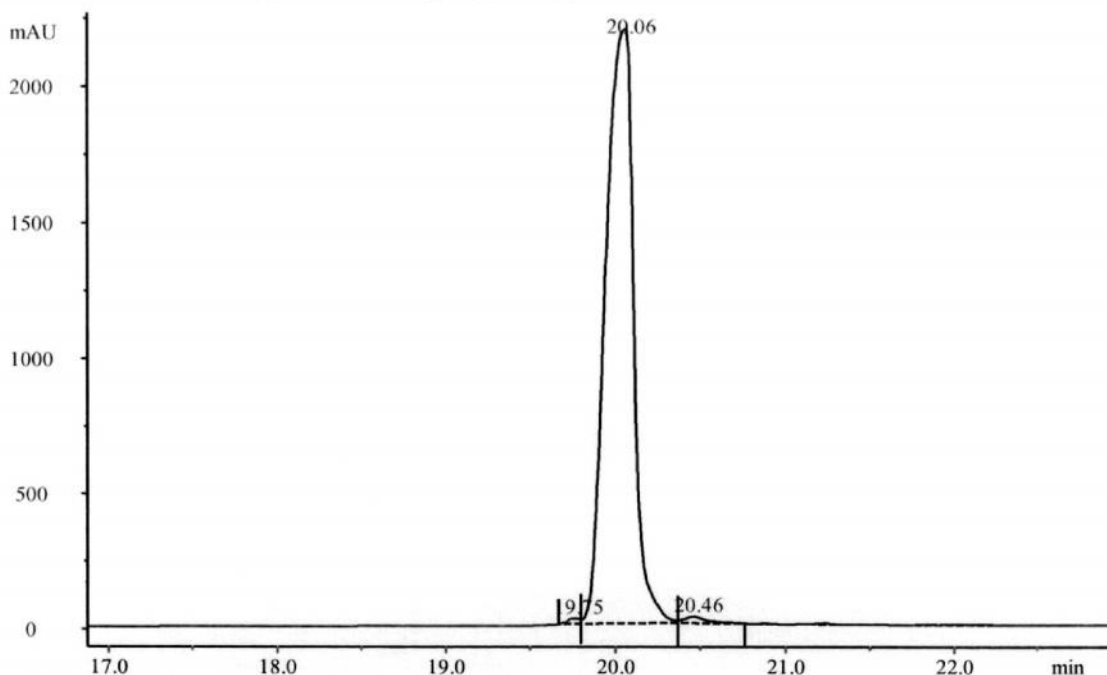
Total peak width = 18.13 min

Calculated from : DESK1 100 ug 04062010 001:1\_UV2 215nm

Baseline : DESK1 100 ug 04062010 001:1\_UV2\_215nm@02, BASEM

UNICORN 4.12 (Build 213)  
 Result file: c:\...\Default\Nada2010\ADP2 IAC 64 ug 07062010 001

ADP2 IAC 64 ug 07062010 001:1\_UV2\_215nm  
 ADP2 IAC 64 ug 07062010 001:1\_UV2\_215nm@02,BASEM



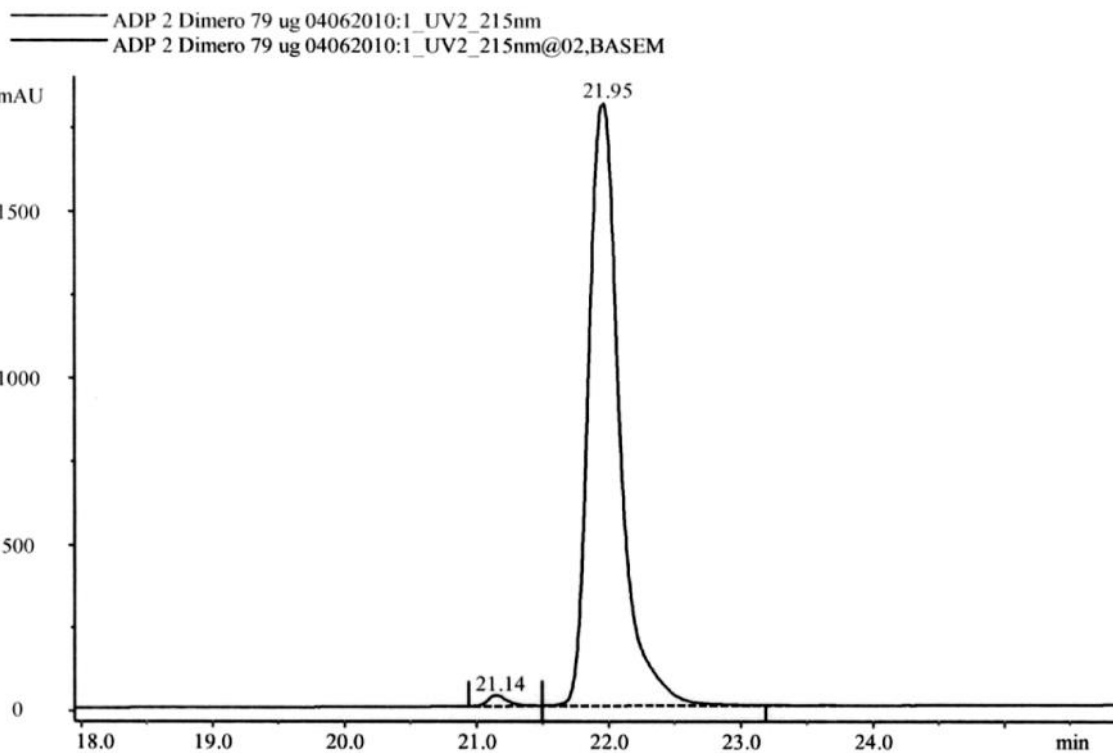
ADP2 IAC 64 ug 07062010 001:1\_UV2\_215nm@02, PEAK

No	Ret min	Area mAU*min	Height mAU
1	-4.90	4.7894	104.153
2	-4.72	16.0386	104.494
3	-3.13	2.0941	14.381
4	-3.02	0.5250	12.798
5	-0.01	11.0750	28.129
6	1.19	0.4578	2.704
7	1.47	2.3415	18.790
8	1.55	2.1008	23.338
9	1.64	0.9410	14.524
10	1.95	8.4186	99.158
11	2.47	0.8954	7.459
12	5.06	0.9970	3.315
13	19.75	1.6732	20.106
14	20.06	415.4260	2189.943
15	20.46	3.8407	24.465
16	37.95	3.7189	6.422
17	40.87	0.4761	6.715
18	41.56	2.0180	15.932
19	41.71	0.4408	4.949
20	42.51	0.4968	2.718

Total number of detected peaks = 301  
 Total area = 491.1670 mAU\*min  
 Area in evaluated peaks = 478.7649 mAU\*min  
 Ratio peak area / total area = 0.974750  
 Total peak width = 6.76 min  
 Calculated from : ADP2 IAC 64 ug 07062010 001:1\_UV2\_215nm  
 Baseline : ADP2 IAC 64 ug 07062010 001:1\_UV2\_215nm@02,BASEM

UNICORN 4.12 (Build 213)

Result file: c:\...\Default\Nada2010\ADP 2 Dimero 79 ug 04062010



ADP 2 Dimero 79 ug 04062010:1\_UV2\_215nm@02, PEAK

No	Ret min	Area mAU*min	Height mAU
1	-4.89	2.1309	16.580
2	-2.37	3.0287	7.273
3	-1.97	3.9283	6.264
4	-1.04	0.7434	3.177
5	-0.81	0.6701	3.020
6	0.10	2.4302	6.667
7	0.81	2.7997	7.067
8	1.09	2.9293	8.263
9	1.42	3.3306	15.840
10	1.93	12.4544	124.162
11	2.45	3.2875	7.657
12	3.19	0.5754	3.008
13	3.40	1.0461	2.976
14	21.14	5.9021	33.235
15	21.95	493.4998	1809.974
16	38.11	0.9097	3.839
17	38.15	1.0435	3.914
18	41.58	1.3094	10.522
19	42.52	0.5987	3.026
20	44.35	0.5464	3.122

Total number of detected peaks = 264

Total area = 560.2563 mAU\*min

Area in evaluated peaks = 543.1644 mAU\*min

Ratio peak area / total area = 0.969493

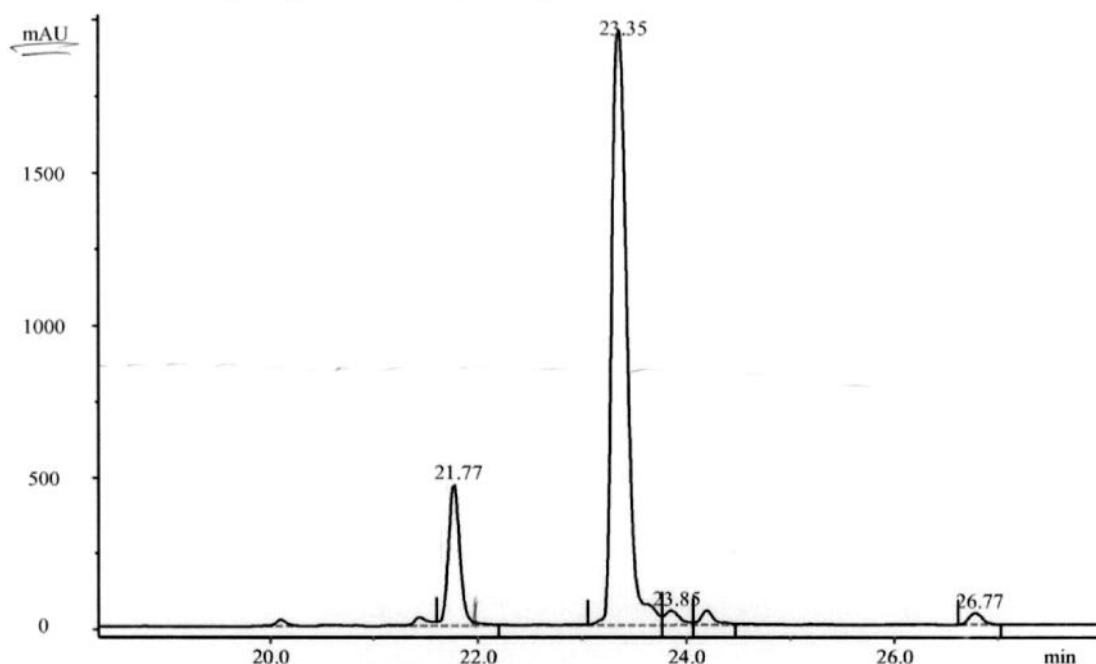
Total peak width = 9.51 min

Calculated from : ADP 2 Dimero 79 ug 04062010:1\_UV2\_215nm

Baseline : ADP 2 Dimero 79 ug 04062010:1\_UV2\_215nm@02, BASEM

UNICORN 4.12 (Build 213)  
 Result file: c:\...\Default\Nada2010\ADP2 BodyP 44 ug 08062010

ADP2 BodyP 44 ug 08062010:1\_UV2\_215nm      ADP2 BodyP 44 ug 08062010:1\_Logbook  
 ADP2 BodyP 44 ug 08062010:1\_UV2\_215nm@02.BASEM



ADP2 BodyP 44 ug 08062010:1\_UV2\_215nm@02, PEAK

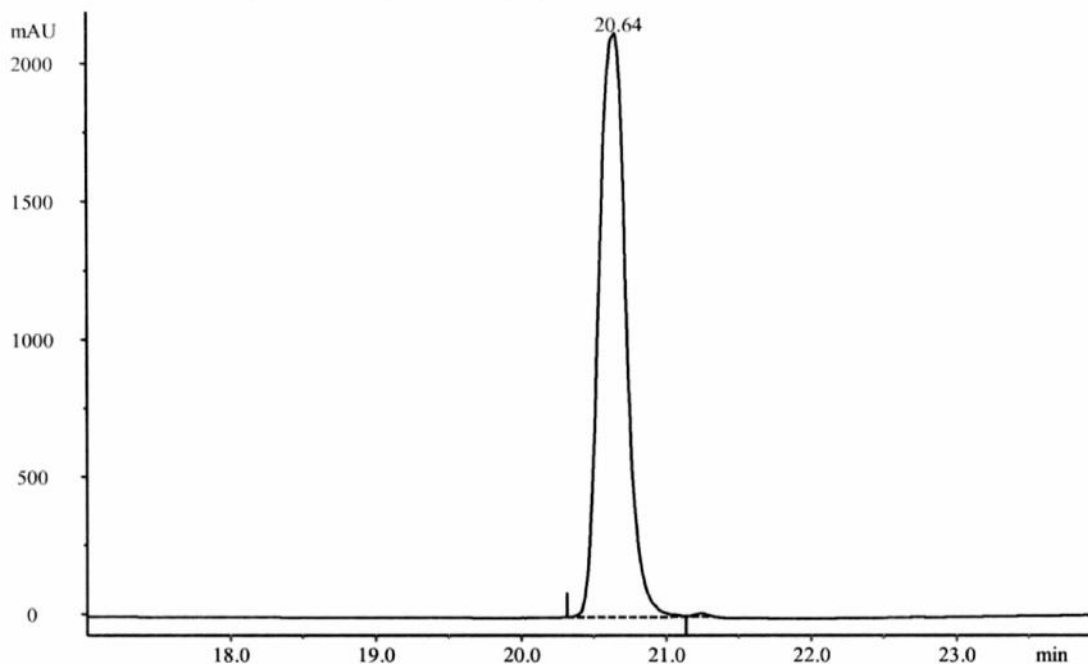
No	Ret min	Area mAU*min	Height mAU
1	-4.04	11.7978	14.758
2	-3.51	5.8136	14.598
3	-3.12	7.3317	36.064
4	-2.16	11.4894	15.162
5	-1.37	13.2798	15.988
6	-0.47	14.2176	16.949
7	1.18	5.4633	12.843
8	1.41	6.2139	37.186
9	1.93	8.1741	71.634
10	2.06	8.6165	46.154
11	2.43	8.9985	14.195
12	3.53	7.2411	8.965
13	5.13	7.0830	9.509
14	21.77	59.9904	468.037
15	23.35	330.3880	1956.841
16	23.85	8.1316	49.259
17	24.19	7.4413	49.459
18	26.77	5.8599	39.776
19	37.97	8.7015	14.376
20	46.81	132.1672	90.164

Total number of detected peaks = 134  
 Total area = 735.9254 mAU\*min  
 Area in evaluated peaks = 668.4004 mAU\*min  
 Ratio peak area / total area = 0.908245  
 Total peak width = 16.23 min  
 Calculated from : ADP2 BodyP 44 ug 08062010:1\_UV2\_215nm  
 Baseline : ADP2 BodyP 44 ug 08062010:1\_UV2\_215nm@02, BASEM

UNICORN 4.12 (Build 213)

Result file: c:\...\Default\Nada2010\ADP3 IAC 66ug 08062010

ADP3 IAC 66ug 08062010:1\_UV2\_215nm      ADP3 IAC 66ug 08062010:1\_Logbook  
 ADP3 IAC 66ug 08062010:1\_UV2\_215nm@02,BASEM



ADP3 IAC 66ug 08062010:1\_UV2\_215nm@02, PEAK

No	Ret min	Area mAU*min	Height mAU
1	-4.89	4.9559	24.968
2	-4.08	3.7652	6.483
3	-3.09	3.0348	14.215
4	0.12	10.9480	14.144
5	1.18	4.8818	14.354
6	1.41	7.1608	35.765
7	1.55	1.9643	21.839
8	1.95	11.0269	48.576
9	2.48	2.2147	12.559
10	2.73	5.1933	7.737
11	3.63	3.9715	5.265
12	4.57	2.3508	3.557
13	20.64	457.4390	2119.490
14	37.91	12.1167	17.065
15	41.54	3.3896	23.948
16	42.47	3.5453	8.892
17	42.83	2.6527	9.555
18	43.93	10.7714	13.188
19	44.57	9.6283	16.350
20	46.84	135.5438	89.280

Total number of detected peaks = 124

Total area = 740.0459 mAU\*min

Area in evaluated peaks = 696.5547 mAU\*min

Ratio peak area / total area = 0.941232

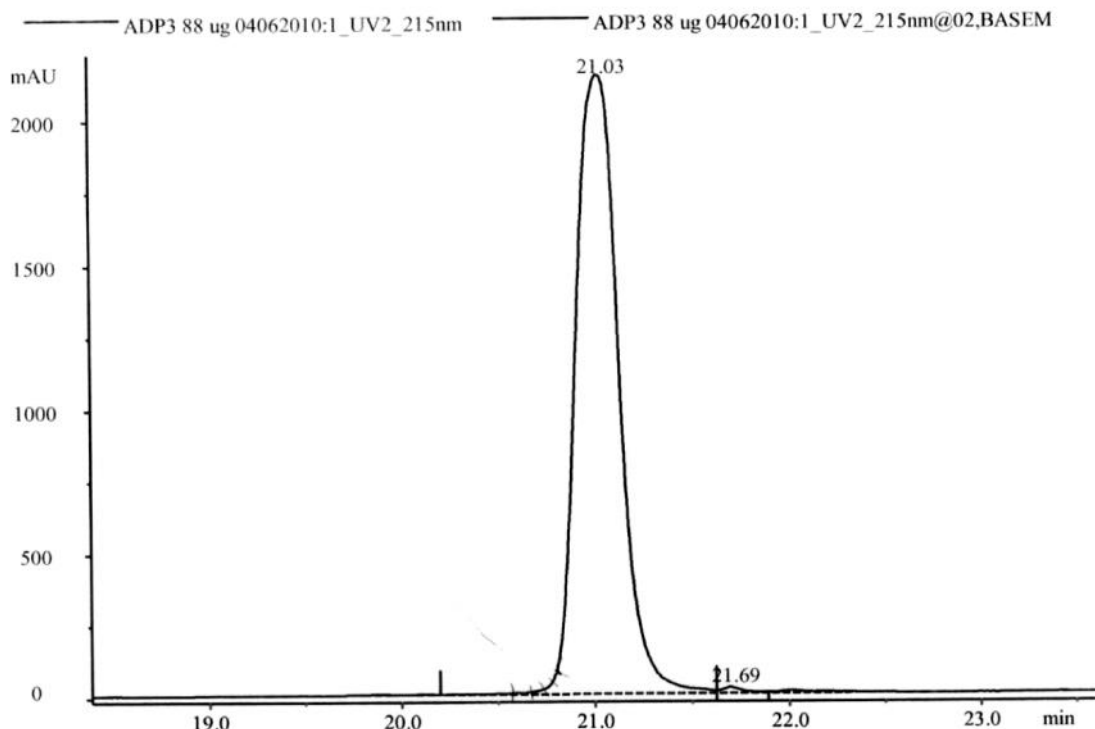
Total peak width = 14.89 min

Calculated from : ADP3 IAC 66ug 08062010:1\_UV2\_215nm

Baseline : ADP3 IAC 66ug 08062010:1\_UV2\_215nm@02, BASEM

UNICORN 4.12 (Build 213)

Result file: c:\...\Default\Nada2010\ADP3 Dimero 88 ug 04062010.



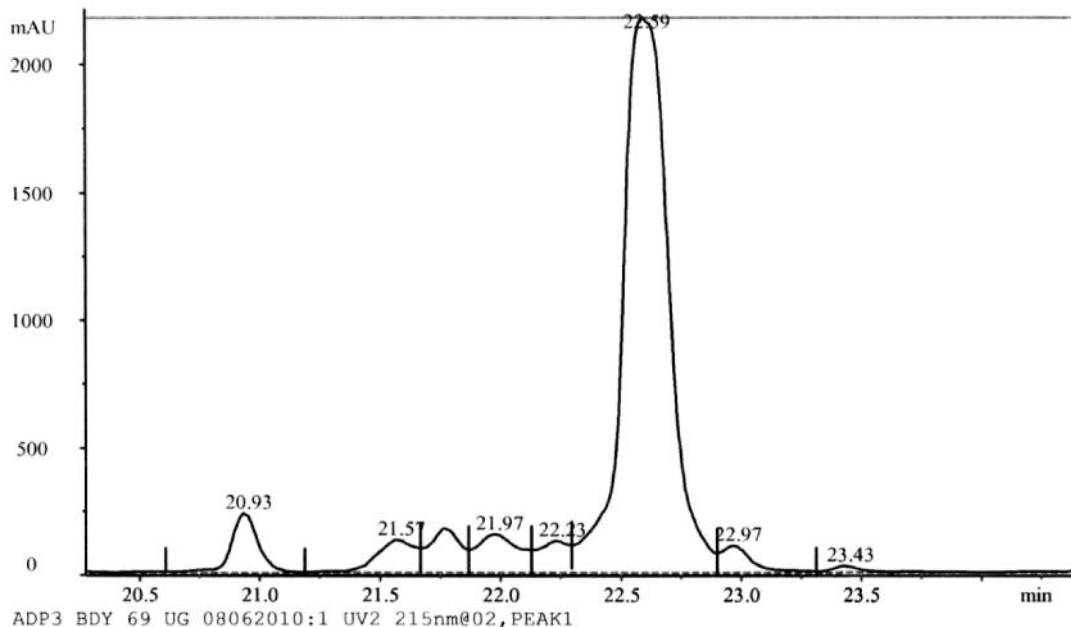
ADP3 88 ug 04062010:1\_UV2\_215nm@02, PEAK

No	Ret min	Area mAU*min	Height mAU
1	-4.65	3.7887	49.635
2	-2.33	6.5973	14.924
3	-1.99	11.1183	15.151
4	-1.04	9.1027	12.262
5	-0.21	8.5708	10.435
6	0.71	4.7368	9.463
7	1.10	3.1476	10.854
8	1.41	5.5986	19.937
9	1.94	16.1121	158.444
10	2.48	4.7388	10.022
11	3.23	5.7820	7.342
12	4.16	3.0184	6.173
13	21.03	547.3446	2142.823
14	21.69	2.6148	20.562
15	41.57	2.7570	15.194
16	42.52	5.4053	12.543
17	42.86	3.0728	14.342
18	43.45	8.3469	16.503
19	44.01	10.1830	19.535
20	46.81	169.8274	95.740

Total number of detected peaks = 131  
 Total area = 865.5743 mAU\*min  
 Area in evaluated peaks = 831.8642 mAU\*min  
 Ratio peak area / total area = 0.961055  
 Total peak width = 15.88 min  
 Calculated from : ADP3 88 ug 04062010:1\_UV2\_215nm  
 Baseline : ADP3 88 ug 04062010:1\_UV2\_215nm@02, BASEM

UNICORN 4.12 (Build 213)  
 Result file: c:\...\Default\Nada2010\ADP3 BDY 69 UG 08062010

ADP3 BDY 69 UG 08062010:1\_UV2\_215nm      ADP3 BDY 69 UG 08062010:1\_Flow  
 ADP3 BDY 69 UG 08062010:1\_Logbook  
 ADP3 BDY 69 UG 08062010:1\_UV2\_215nm@02,BASEM  
 ADP3 BDY 69 UG 08062010:1\_UV2\_215nm@02,BASEM1



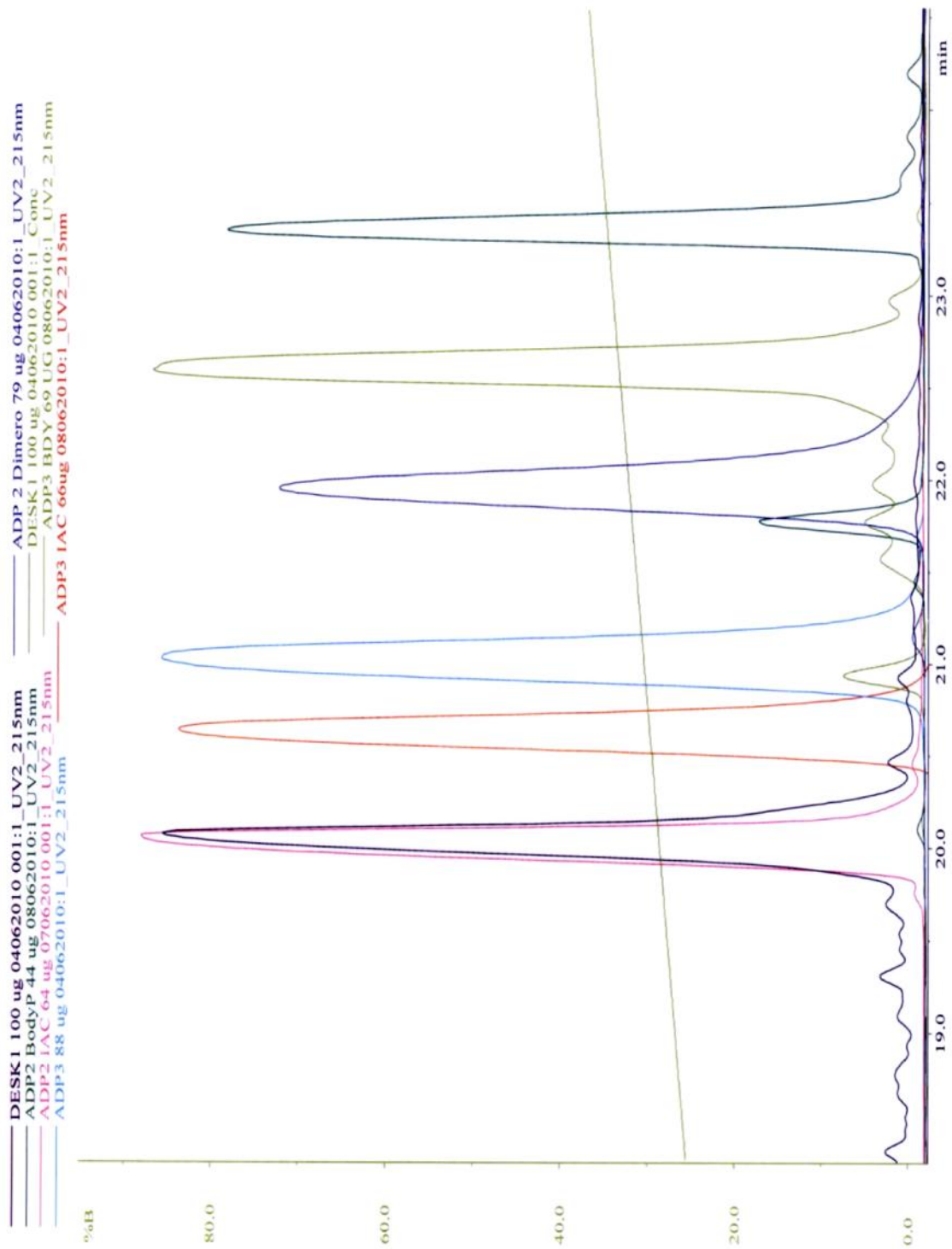
ADP3 BDY 69 UG 08062010:1\_UV2\_215nm@02, PEAK1

No	Ret min	Area mAU*min	Height mAU
1	-2.93	3.5763	13.354
2	-2.25	13.4216	21.778
3	-1.78	13.7389	18.650
4	-0.97	12.0565	14.877
5	-0.01	3.9428	13.482
6	1.93	6.6851	46.392
7	20.93	31.4439	235.014
8	21.57	24.5396	130.548
9	21.77	26.1176	173.992
10	21.97	30.6537	152.066
11	22.23	18.2087	125.321
12	22.59	488.1013	2171.975
13	22.97	16.2257	106.496
14	23.43	3.7775	25.837
15	24.66	4.1750	27.070
16	37.95	7.6499	12.664
17	43.70	4.5529	7.551
18	44.67	6.5611	12.046
19	45.30	9.3157	16.894
20	46.83	119.3849	89.533

Total number of detected peaks = 140  
 Total area = 894.4706 mAU\*min  
 Area in evaluated peaks = 844.1288 mAU\*min  
 Ratio peak area / total area = 0.943719  
 Total peak width = 13.45 min  
 Calculated from : ADP3 BDY 69 UG 08062010:1\_UV2\_215nm  
 Baseline : ADP3 BDY 69 UG 08062010:1\_UV2\_215nm@02, BASEM1



UNICORN 4.12 (Build 213)  
Result file: c:\...\Default\Nada2010\DESK1 100 ug 04062010 001



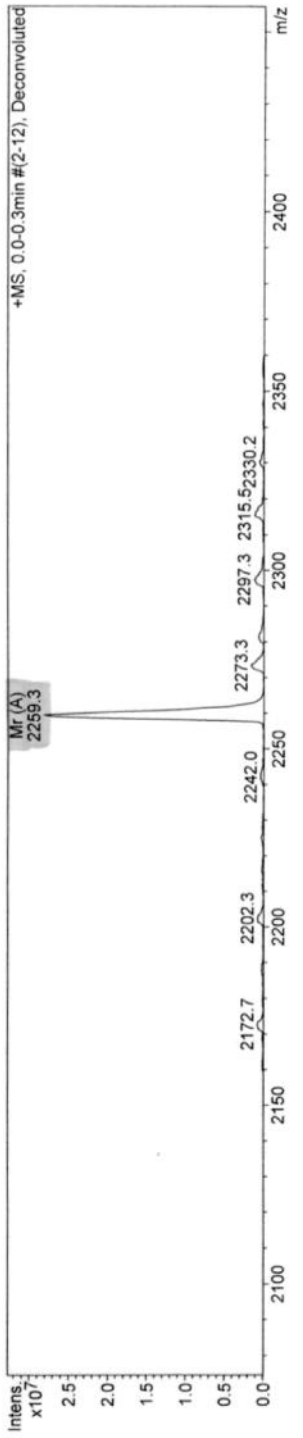
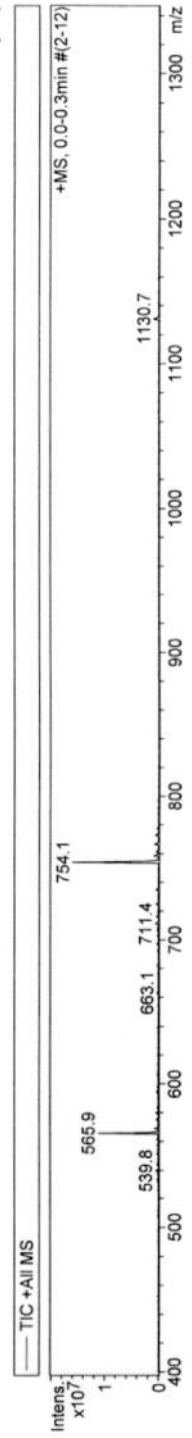
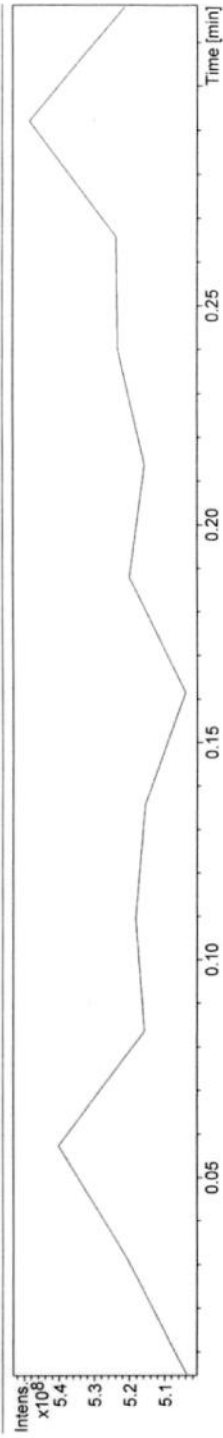
**Appendix 8. ESI - MS and Analytical RP-HPLC for ADP1 (first testing name was DESC1), PSEU2 (first testing name was PSEU2B), PSEU2 A9 (first testing name was PSEU2A), ASC1 (first testing name was ASC1B), ASC1 I2 (first testing name was ASC1A).**

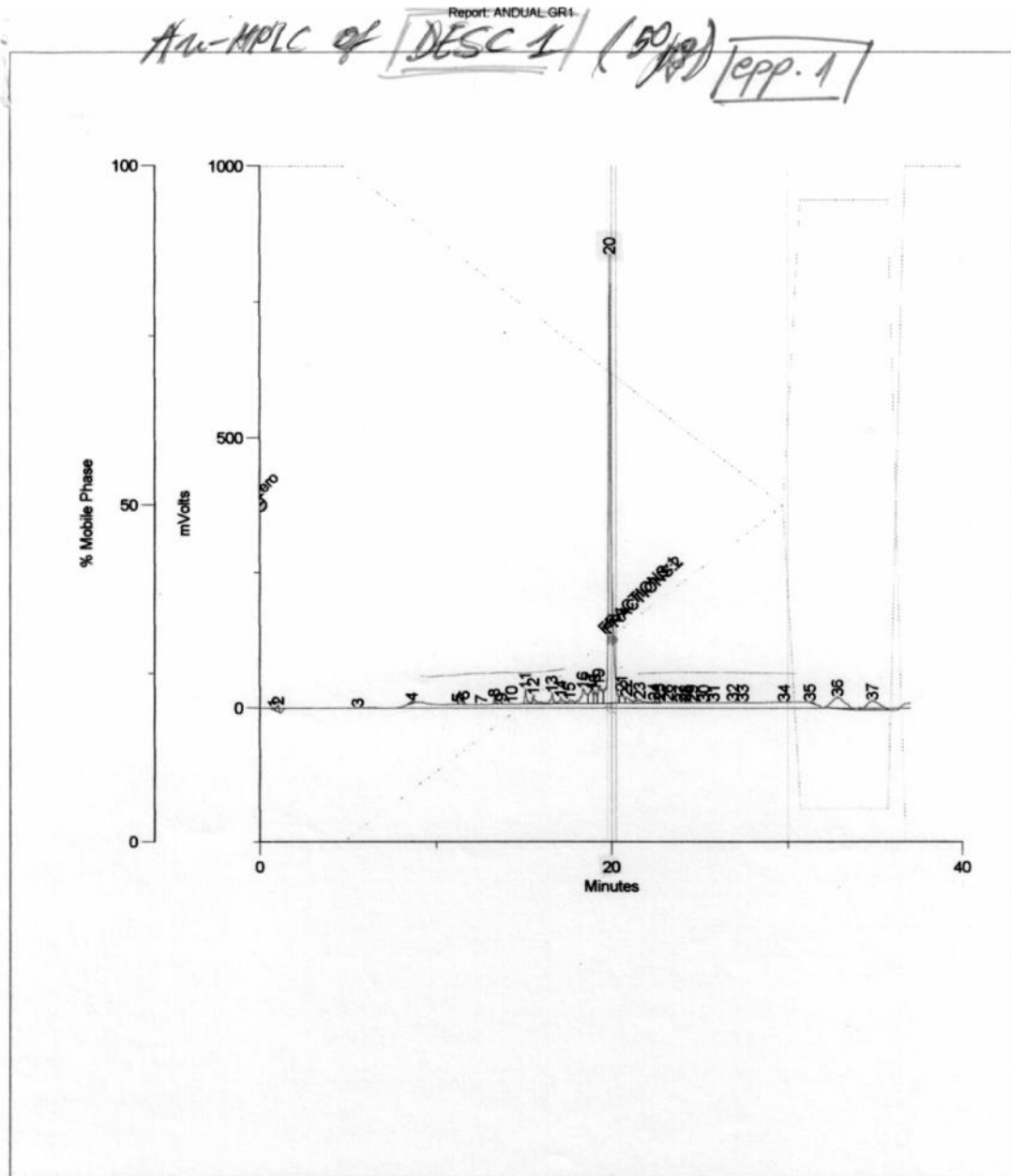
**Display Report**

**Analysis Info**  
 Analysis Name: D:\Data\3-GENNARO-TOSSID\DESC1 crude\_190908.d  
 Method: peptidi Nina\_default.m  
 Sample Name: DESC1 crude\_190908  
 Comment: 10x  
 Acquisition Date: 9/19/2008 12:43:59 PM  
 Operator: bruker  
 Instrument: esquire4000

**Acquisition Parameter**

Ion Source Type	ESI	Ion Polarity	Positive	Alternating Ion Polarity	off
Mass Range Mode	Std/Normal	Scan Begin	400 m/z	Scan End	1500 m/z
Capillary Exit	113.0 Volt	Skim 1	38.3 Volt	Trap Drive	44.0
Accumulation Time	109 µs	Averages	10 Spectra	Auto MS/MS	off

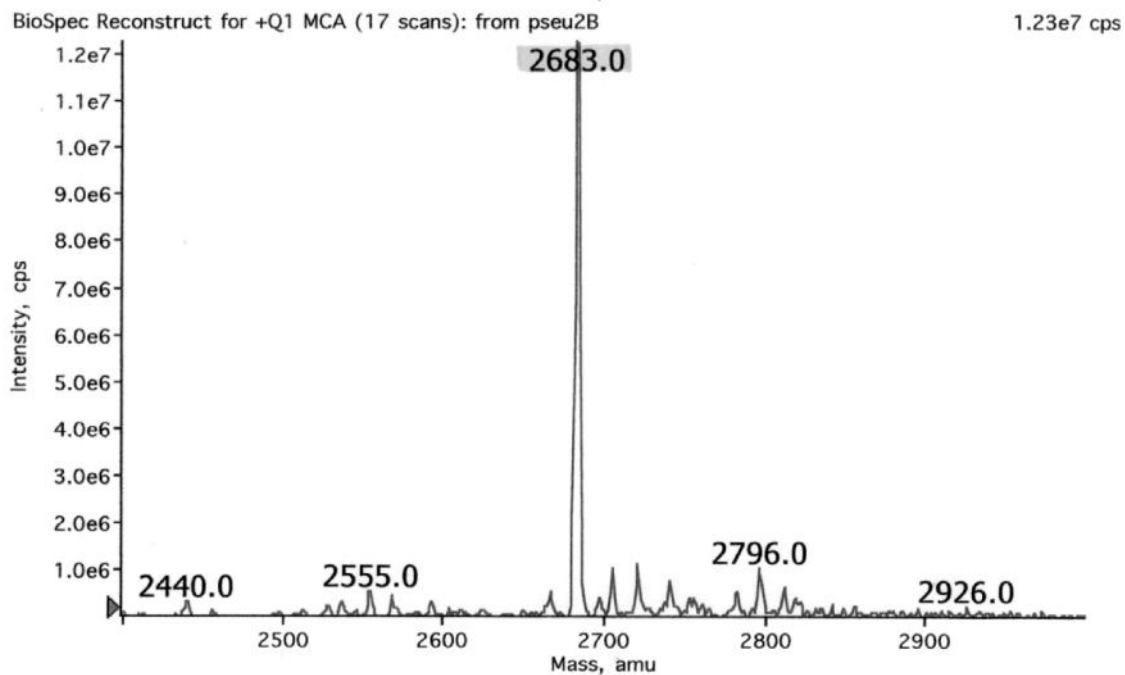
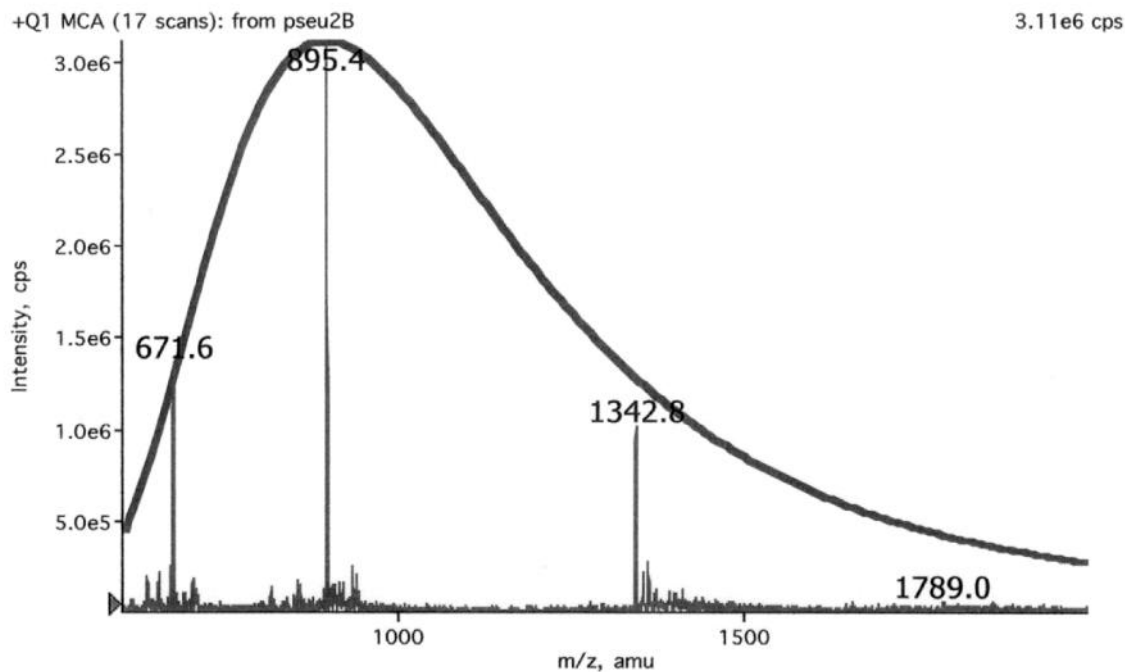


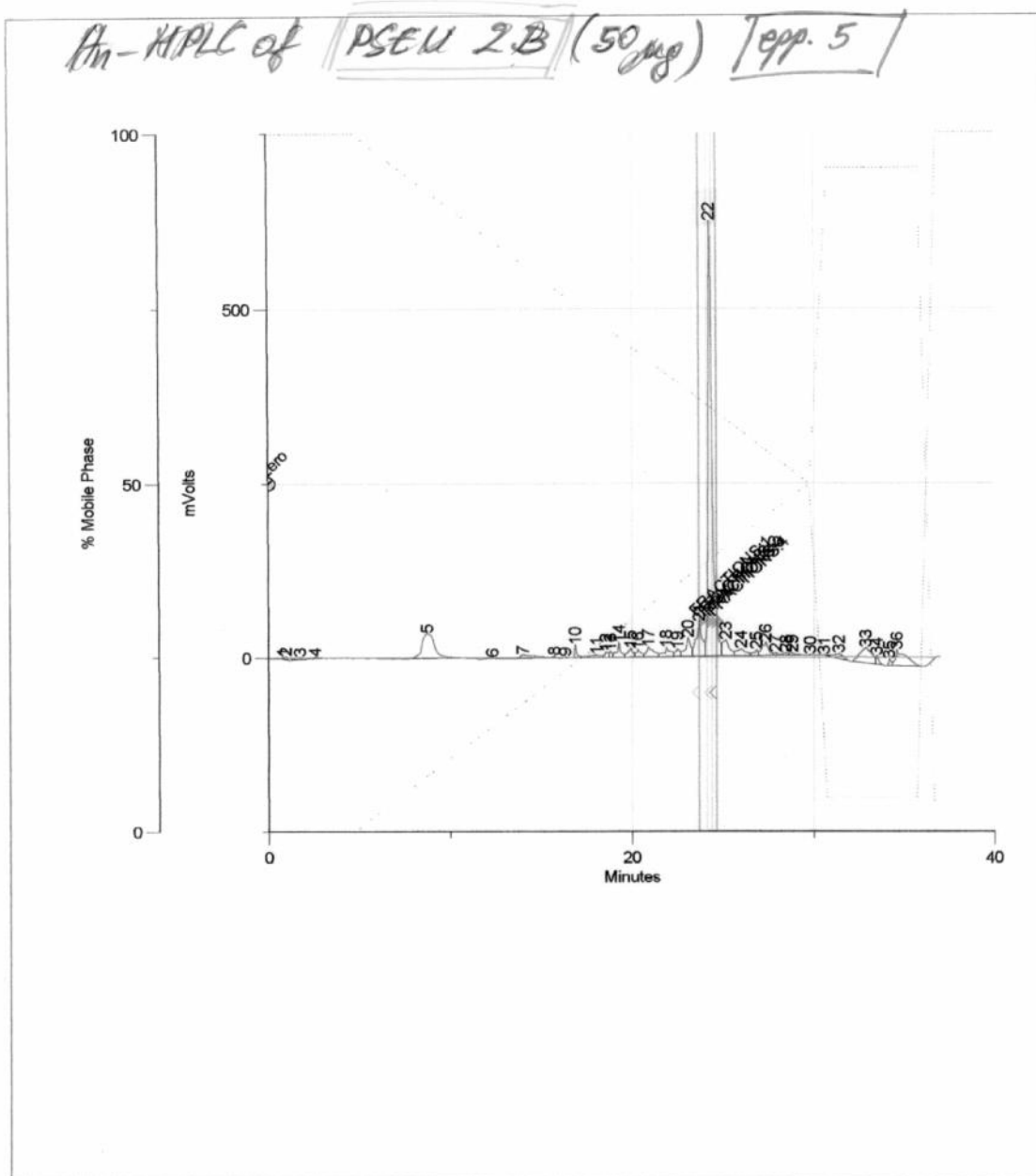


Inj. Number	Peak Name	R. Time	Area	Sample Descrip.					
1	1.00	1	0.82	100406.62	1, 0-50%B in :				
2	1.00	2	1.07	214878.39	1, 0-50%B in :				
3	1.00	3	5.53	11401.25	1, 0-50%B in :				
4	1.00	4	8.62	131352.66	1, 0-50%B in :				
5	1.00	5	11.26	44507.59	1, 0-50%B in :				
6	1.00	6	11.58	92852.35	1, 0-50%B in :				

	Inj. Number	Peak Name	R. Time	Area	Sample Descrip.					
7	1.00	7	12.59	9232.06	0, 0-50%B in 2					
8	1.00	8	13.35	187129.64	0, 0-50%B in 2					
9	1.00	9	13.73	42202.07	0, 0-50%B in 2					
10	1.00	10	14.33	11660.84	0, 0-50%B in 2					
11	1.00	11	15.11	414424.50	0, 0-50%B in 2					
12	1.00	12	15.55	420526.53	0, 0-50%B in 2					
13	1.00	13	16.63	372575.59	0, 0-50%B in 2					
14	1.00	14	17.12	294584.03	0, 0-50%B in 2					
15	1.00	15	17.64	245317.09	0, 0-50%B in 2					
16	1.00	16	18.41	979428.06	0, 0-50%B in 2					
17	1.00	17	18.88	676123.00	0, 0-50%B in 2					
18	1.00	18	19.08	383815.59	0, 0-50%B in 2					
19	1.00	19	19.31	840397.31	0, 0-50%B in 2					
20	1.00	20	19.92	14603451.00	0, 0-50%B in 2					
21	1.00	21	20.59	503798.38	0, 0-50%B in 2					
22	1.00	22	20.86	342624.16	0, 0-50%B in 2					
23	1.00	23	21.63	398795.59	0, 0-50%B in 2					
24	1.00	24	22.45	84247.41	0, 0-50%B in 2					
25	1.00	25	22.73	70207.54	0, 0-50%B in 2					
26	1.00	26	23.22	50095.48	0, 0-50%B in 2					
27	1.00	27	23.91	18203.15	0, 0-50%B in 2					
28	1.00	28	24.19	12365.59	0, 0-50%B in 2					
29	1.00	29	24.59	11596.64	0, 0-50%B in 2					
30	1.00	30	25.25	4197.50	0, 0-50%B in 2					
31	1.00	31	25.80	11028.32	0, 0-50%B in 2					
32	1.00	32	26.89	25727.21	0, 0-50%B in 2					
33	1.00	33	27.46	12207.41	0, 0-50%B in 2					
34	1.00	34	29.80	3426.66	0, 0-50%B in 2					
35	1.00	35	31.45	113130.07	0, 0-50%B in 2					
36	1.00	36	32.88	1959429.75	0, 0-50%B in 2					
37	1.00	37	34.88	1660652.50	0, 0-50%B in 2					

BioMultiView 1.3.1      Lunedì, 29 settembre 2008 5:55 PM      page 1 of 1  
 Info for pane 2: pseu2B\_(No Title)  
 Period 1, Expt. 1; Mass range: 600.0 to 2000.0 by 0.2 amu; Dwell: 0.3 ms; Pause: 5.0 ms  
 Acq. Time: Lun, 29 set 2008 at 5:53:35 PM





	Inj. Number	Peak Name	R. Time	Area	Sample Descrip.					
1	1.00	1	0.80	38591.87	0-50%B in 2!					
2	1.00	2	0.97	69483.55	0-50%B in 2!					
3	1.00	3	1.70	255212.80	0-50%B in 2!					
4	1.00	4	2.55	76633.83	0-50%B in 2!					
5	1.00	5	8.78	3018139.75	0-50%B in 2!					
6	1.00	6	12.36	9730.00	0-50%B in 2!					

	Inj. Number	Peak Name	R. Time	Area	Sample Descrip.					
7	1.00	7	14.01	534462.25	0-50%B in 2!					
8	1.00	8	15.75	84872.84	0-50%B in 2!					
9	1.00	9	16.36	39132.56	0-50%B in 2!					
10	1.00	10	16.90	278760.75	0-50%B in 2!					
11	1.00	11	17.94	301603.44	0-50%B in 2!					
12	1.00	12	18.59	185016.03	0-50%B in 2!					
13	1.00	13	18.83	147760.41	0-50%B in 2!					
14	1.00	14	19.29	540049.62	0-50%B in 2!					
15	1.00	15	19.93	430101.69	0-50%B in 2!					
16	1.00	16	20.33	349868.91	0-50%B in 2!					
17	1.00	17	20.93	664582.19	0-50%B in 2!					
18	1.00	18	21.90	574076.69	0-50%B in 2!					
19	1.00	19	22.51	337779.03	0-50%B in 2!					
20	1.00	20	23.10	889530.75	0-50%B in 2!					
21	1.00	21	23.69	1837171.50	0-50%B in 2!					
22	1.00	22	24.29	15091165.00	0-50%B in 2!					
23	1.00	23	25.16	1039500.88	0-50%B in 2!					
24	1.00	24	25.99	623609.00	0-50%B in 2!					
25	1.00	25	26.84	244983.70	0-50%B in 2!					
26	1.00	26	27.35	810763.06	0-50%B in 2!					
27	1.00	27	27.90	113742.27	0-50%B in 2!					
28	1.00	28	28.45	127679.77	0-50%B in 2!					
29	1.00	29	28.81	144130.06	0-50%B in 2!					
30	1.00	30	29.80	20556.69	0-50%B in 2!					
31	1.00	31	30.86	44405.75	0-50%B in 2!					
32	1.00	32	31.43	461933.81	0-50%B in 2!					
33	1.00	33	32.89	1739628.50	0-50%B in 2!					
34	1.00	34	33.50	261016.52	0-50%B in 2!					
35	1.00	35	34.19	158560.58	0-50%B in 2!					
36	1.00	36	34.61	1693211.12	0-50%B in 2!					

BioMultiView 1.3.1

Lunedì, 29 settembre 2008 5:44 PM

page 1 of 1

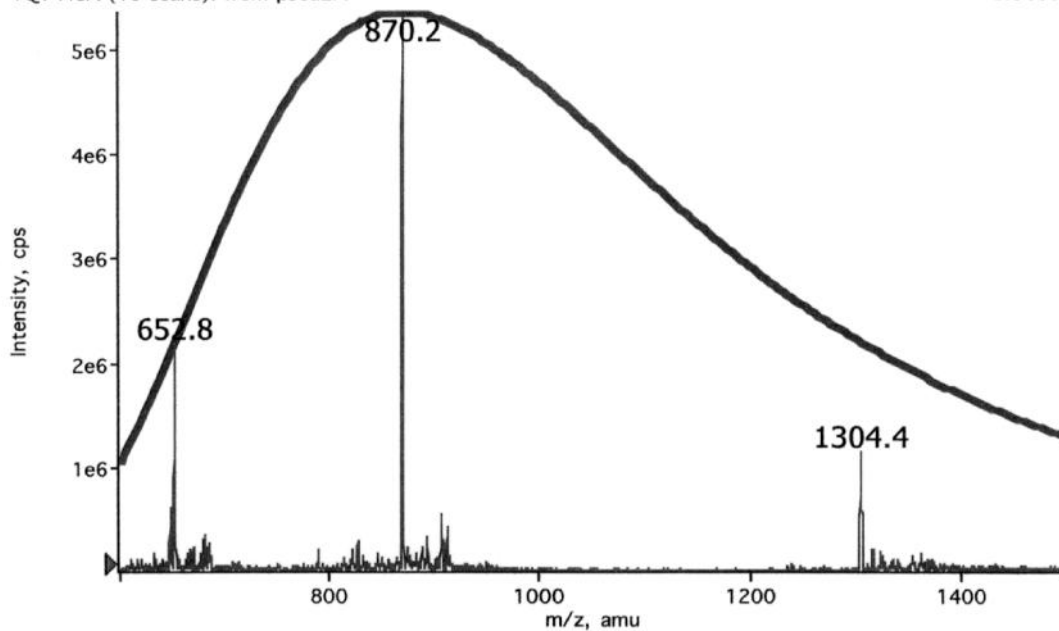
Info for pane 2: pseu2A (No Title)

Period 1, Expt. 1; Mass range: 600.0 to 1500.0 by 0.2 amu; Dwell: 0.3 ms; Pause: 5.0 ms

Acq. Time: Lun, 29 set 2008 at 5:42:15 PM

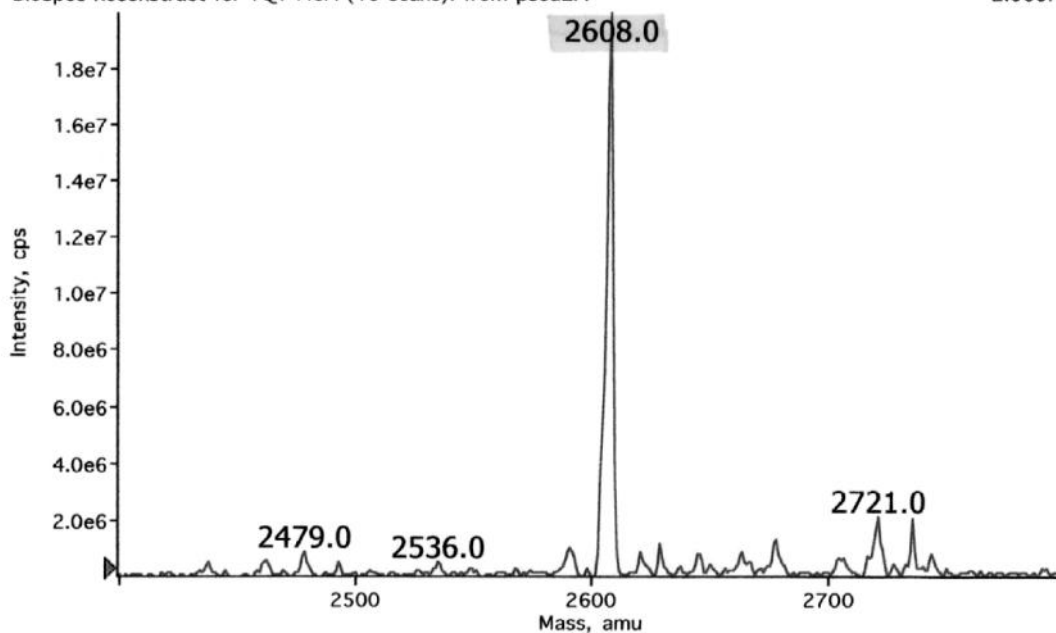
+Q1 MCA (15 scans): from pseu2A

5.36e6 cps

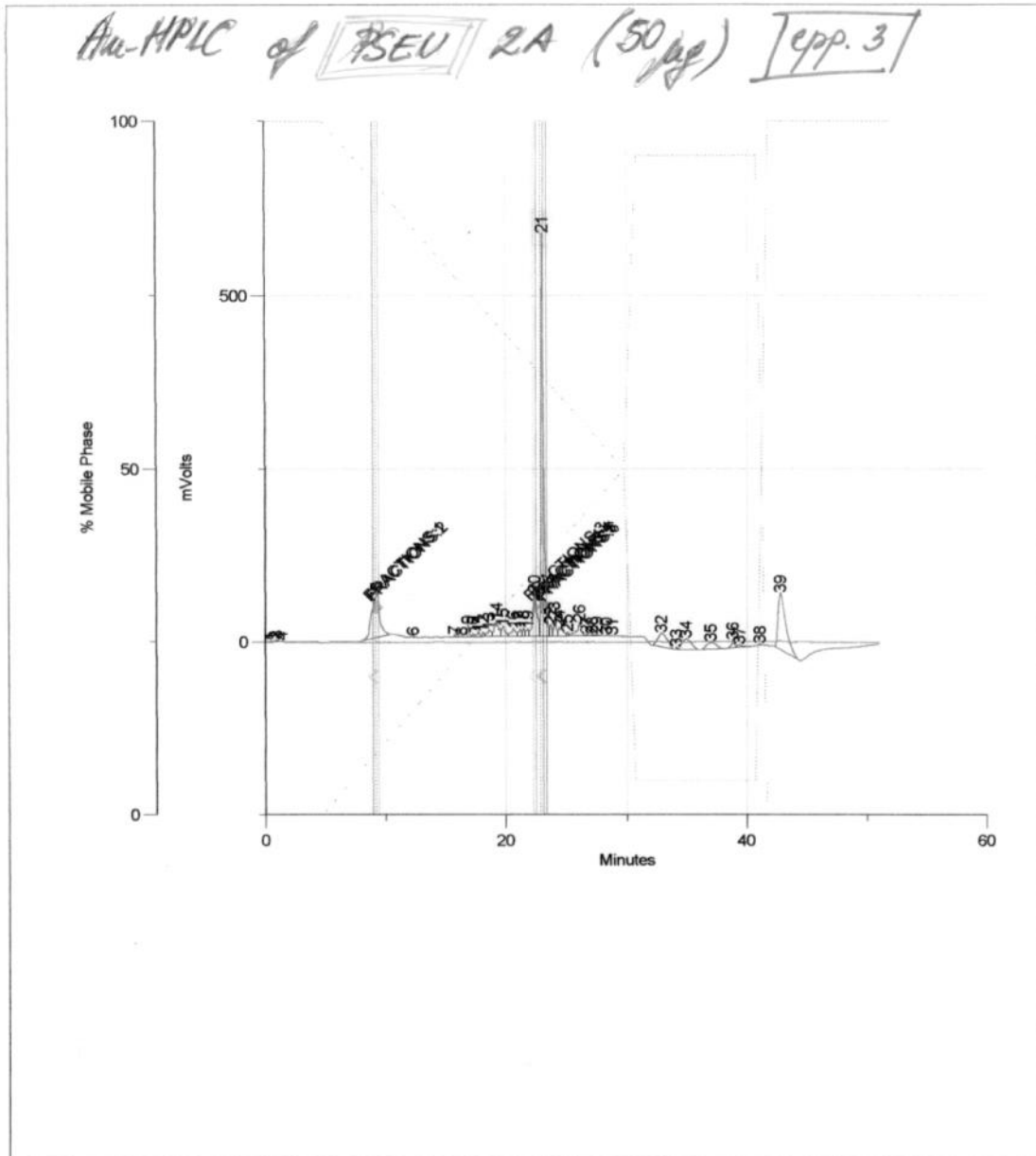


BioSpec Reconstruct for +Q1 MCA (15 scans): from pseu2A

2.00e7 cps







	Inj. Number	Peak Name	R. Time	Area	Sample Descrip.				
1	1.00	1	0.46	21202.51	0-50%B in 2'				
2	1.00	2	0.79	21670.31	0-50%B in 2'				
3	1.00	3	0.97	59888.85	0-50%B in 2'				
4	1.00	4	1.37	57341.26	0-50%B in 2'				
5	1.00	5	9.30	5107335.50	0-50%B in 2'				
6	1.00	6	12.32	79268.73	0-50%B in 2'				

	Inj. Number	Peak Name	R. Time	Area	Sample Descrip.					
7	1.00	7	15.80	86000.95	0-50%B in 2!					
8	1.00	8	16.38	27602.74	0-50%B in 2!					
9	1.00	9	16.92	243950.58	0-50%B in 2!					
10	1.00	10	17.36	67891.70	0-50%B in 2!					
11	1.00	11	17.78	219792.22	0-50%B in 2!					
12	1.00	12	18.15	127941.52	0-50%B in 2!					
13	1.00	13	18.65	413214.25	0-50%B in 2!					
14	1.00	14	19.24	949049.38	0-50%B in 2!					
15	1.00	15	19.81	521248.25	0-50%B in 2!					
16	1.00	16	20.62	538380.94	0-50%B in 2!					
17	1.00	17	21.21	296239.53	0-50%B in 2!					
18	1.00	18	21.49	239228.20	0-50%B in 2!					
19	1.00	19	21.81	301123.97	0-50%B in 2!					
20	1.00	20	22.39	2648059.75	0-50%B in 2!					
21	1.00	21	23.02	13299874.00	0-50%B in 2!					
22	1.00	22	23.69	395316.66	0-50%B in 2!					
23	1.00	23	24.03	604767.44	0-50%B in 2!					
24	1.00	24	24.41	588047.31	0-50%B in 2!					
25	1.00	25	25.10	85512.77	0-50%B in 2!					
26	1.00	26	26.08	954590.25	0-50%B in 2!					
27	1.00	27	26.68	57604.24	0-50%B in 2!					
28	1.00	28	27.12	57397.55	0-50%B in 2!					
29	1.00	29	27.52	127882.49	0-50%B in 2!					
30	1.00	30	28.30	23220.31	0-50%B in 2!					
31	1.00	31	28.78	5092.72	0-50%B in 2!					
32	1.00	32	32.91	1915349.38	0-50%B in 2!					
33	1.00	33	34.15	55026.11	0-50%B in 2!					
34	1.00	34	34.95	1498508.00	0-50%B in 2!					
35	1.00	35	37.00	1024043.69	0-50%B in 2!					
36	1.00	36	38.84	368067.47	0-50%B in 2!					
37	1.00	37	39.37	224608.36	0-50%B in 2!					
38	1.00	38	41.08	59721.34	0-50%B in 2!					
39	1.00	39	42.83	6191274.00	0-50%B in 2!					

### Display Report

**Analysis Info**

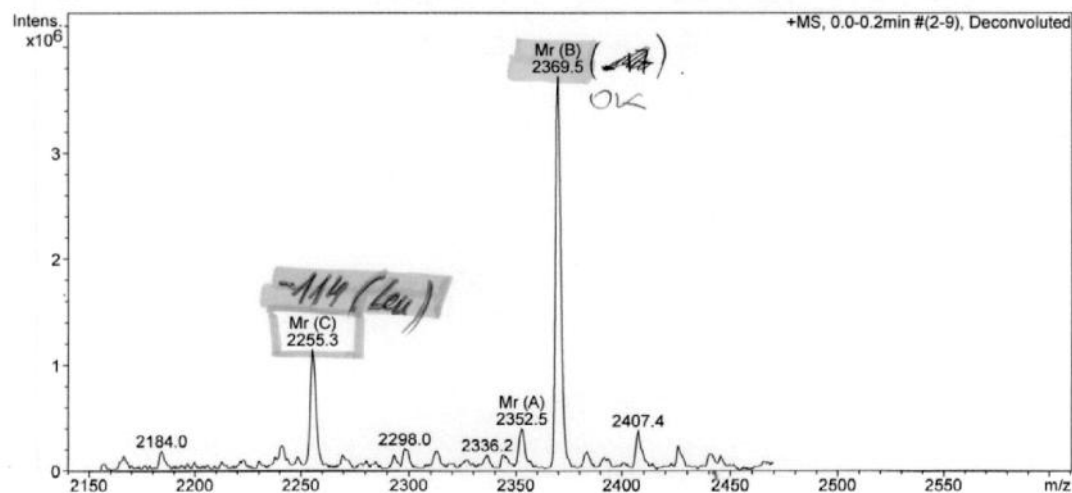
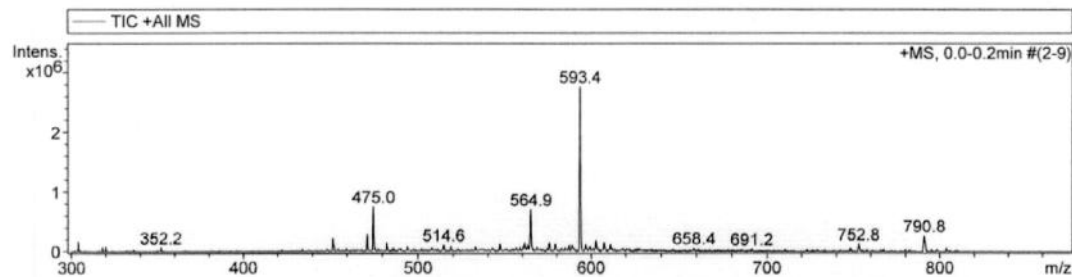
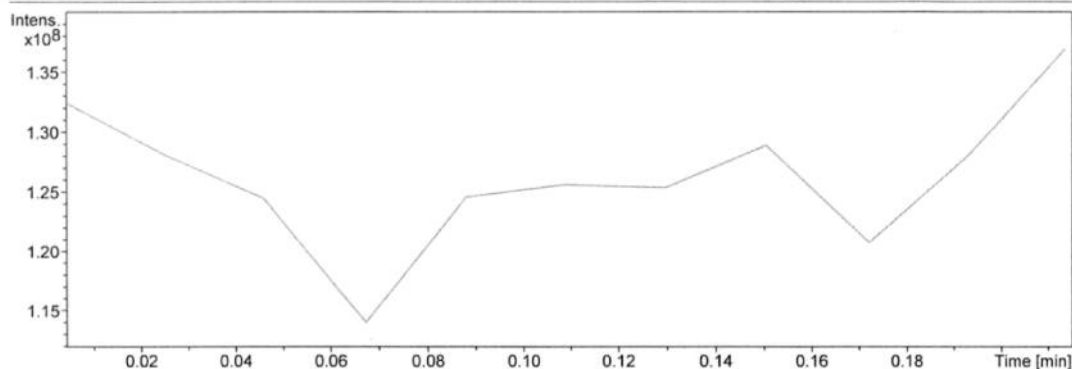
Analysis Name D:\Data3-GENNARO-TOSSIAAsc 1B crude.d  
 Method peptidi Nina\_default.m  
 Sample Name Asc 1B crude  
 Comment 10x

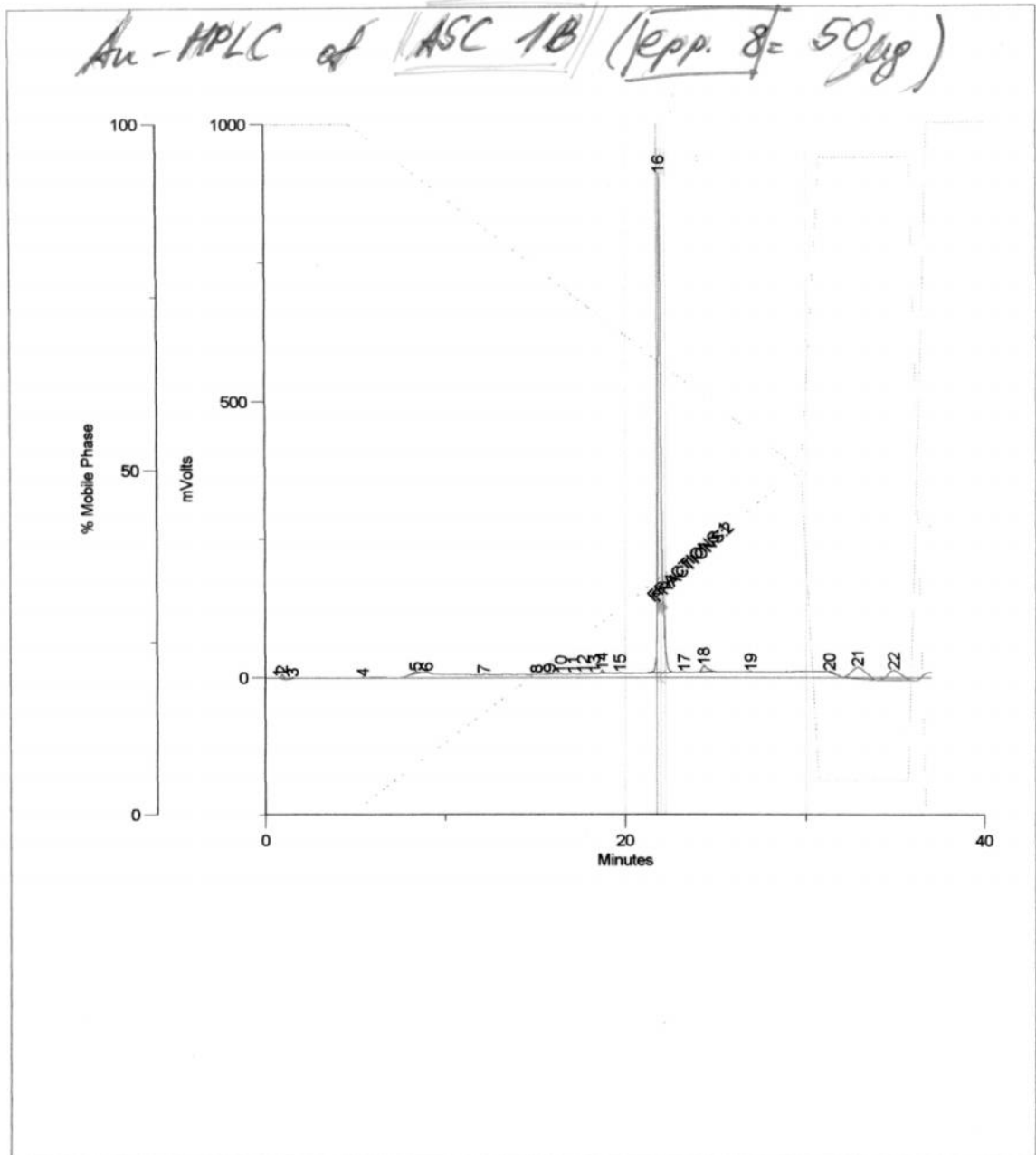
Acquisition Date 9/25/2008 6:02:27 PM

Operator bruker  
 Instrument esquire4000

**Acquisition Parameter**

Ion Source Type	ESI	Ion Polarity	Positive	Alternating Ion Polarity	off
Mass Range Mode	Std/Normal	Scan Begin	300 m/z	Scan End	1000 m/z
Capillary Exit	105.0 Volt	Skim 1	32.7 Volt	Trap Drive	37.6
Accumulation Time	404 µs	Averages	10 Spectra	Auto MS/MS	off





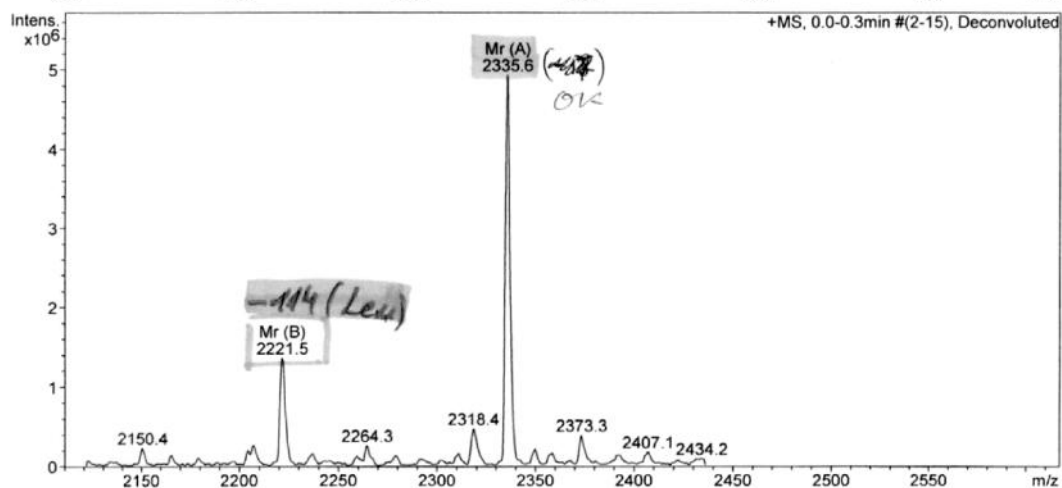
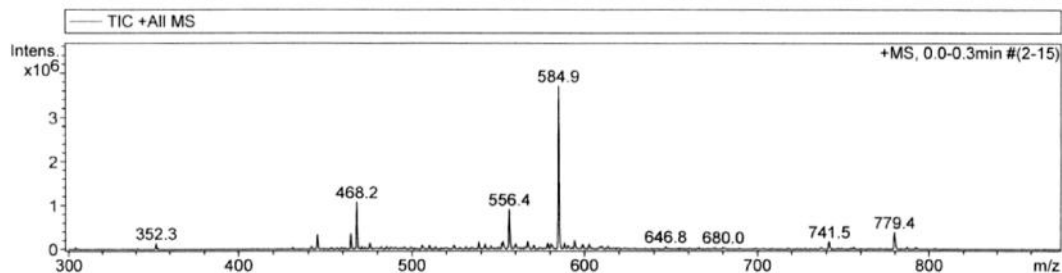
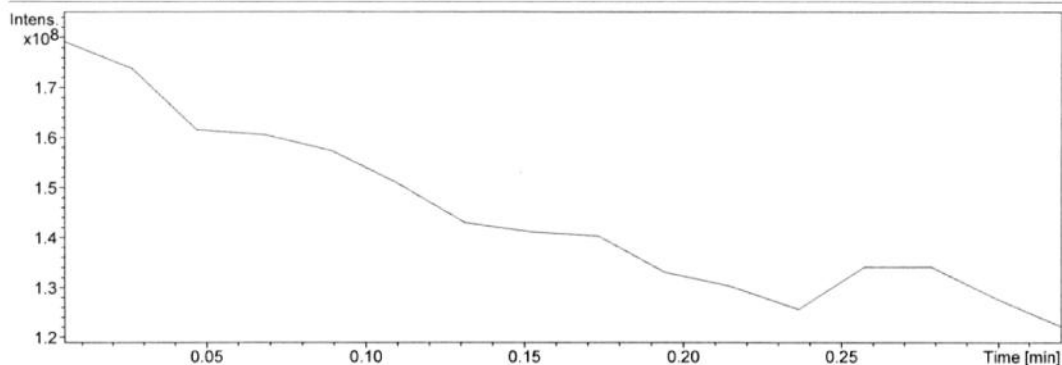
	Inj. Number	Peak Name	R. Time	Area	Sample Descrip.					
1	1.00	1	0.78	18058.66	j), 0-50%B in					
2	1.00	2	0.95	135137.58	j), 0-50%B in					
3	1.00	3	1.40	94567.06	j), 0-50%B in					
4	1.00	4	5.41	6255.84	j), 0-50%B in					
5	1.00	5	8.36	183553.11	j), 0-50%B in					
6	1.00	6	9.05	18013.41	j), 0-50%B in					

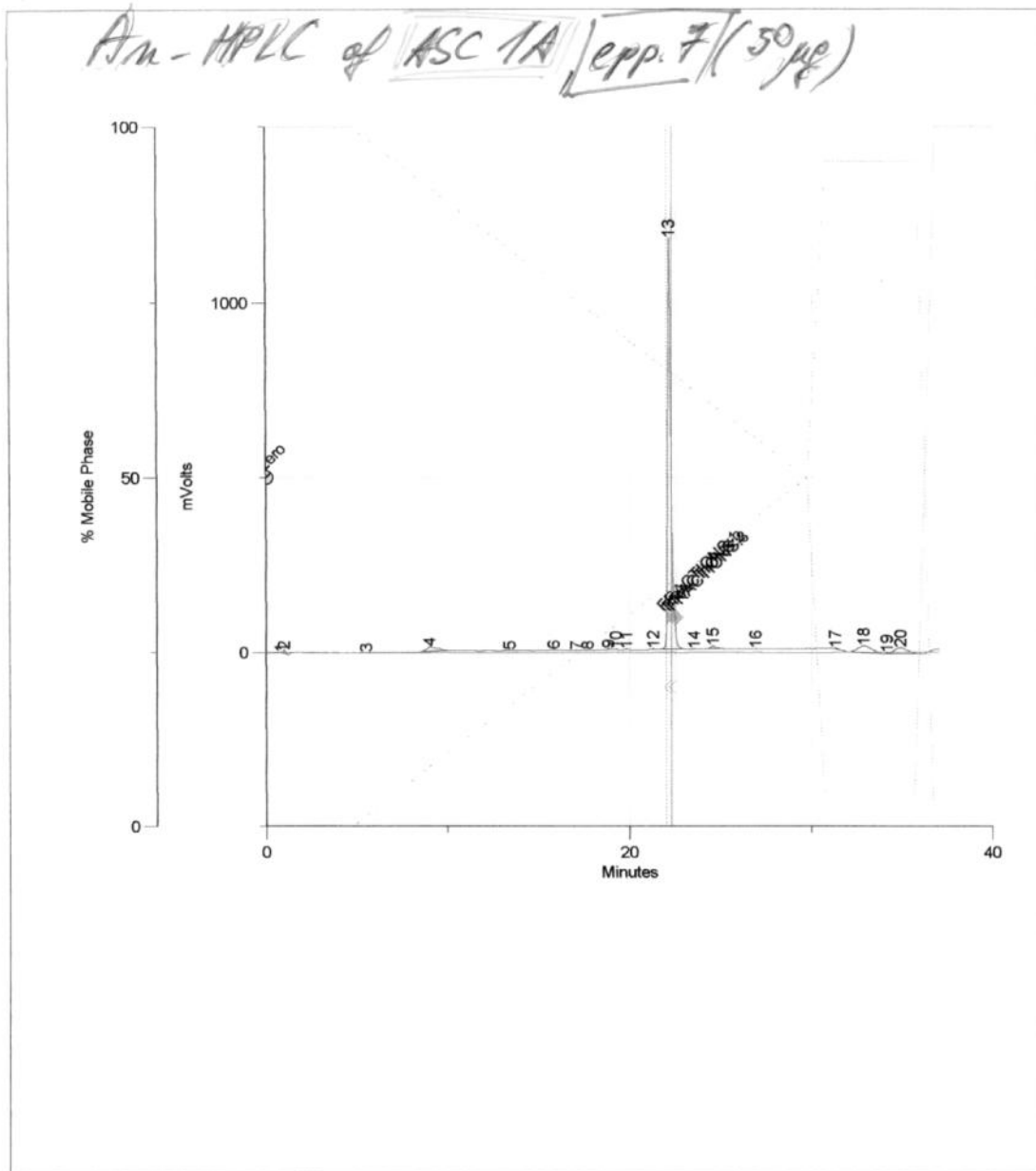
	Inj. Number	Peak Name	R. Time	Area	Sample Descrip.					
7	1.00	7	12.18	57737.50	j), 0-50%B in					
8	1.00	8	15.05	40390.73	j), 0-50%B in					
9	1.00	9	15.78	112922.91	j), 0-50%B in					
10	1.00	10	16.40	34157.81	j), 0-50%B in					
11	1.00	11	17.06	21094.17	j), 0-50%B in					
12	1.00	12	17.66	15375.00	j), 0-50%B in					
13	1.00	13	18.26	15285.84	j), 0-50%B in					
14	1.00	14	18.72	78951.74	j), 0-50%B in					
15	1.00	15	19.72	41312.50	j), 0-50%B in					
16	1.00	16	21.90	18021598.00	j), 0-50%B in					
17	1.00	17	23.27	2052.49	j), 0-50%B in					
18	1.00	18	24.37	496522.44	j), 0-50%B in					
19	1.00	19	26.93	9851.67	j), 0-50%B in					
20	1.00	20	31.44	146724.56	j), 0-50%B in					
21	1.00	21	32.90	1930752.88	j), 0-50%B in					
22	1.00	22	34.92	1699288.25	j), 0-50%B in					

### Display Report

<b>Analysis Info</b>		Acquisition Date	9/25/2008 5:55:50 PM
Analysis Name	D:\Data\3-GENNARO-TOSSI\Asc 1A crude.d	Operator	bruker
Method	peptidi Nina_default.m	Instrument	esquire4000
Sample Name	Asc 1A crude		
Comment	10x		

<b>Acquisition Parameter</b>					
Ion Source Type	ESI	Ion Polarity	Positive	Alternating Ion Polarity	off
Mass Range Mode	Std/Normal	Scan Begin	300 m/z	Scan End	1000 m/z
Capillary Exit	105.0 Volt	Skim 1	32.7 Volt	Trap Drive	37.6
Accumulation Time	311 µs	Averages	10 Spectra	Auto MS/MS	off





	Inj. Number	Peak Name	R. Time	Area	Sample Descrip.					
1	1.00	1	0.81	29797.12	j), 0-50%B in					
2	1.00	2	0.99	181194.58	j), 0-50%B in					
3	1.00	3	5.49	13442.51	j), 0-50%B in					
4	1.00	4	9.05	1145403.38	j), 0-50%B in					
5	1.00	5	13.35	51905.01	j), 0-50%B in					
6	1.00	6	15.82	141107.50	j), 0-50%B in					

	Inj. Number	Peak Name	R. Time	Area	Sample Descrip.					
7	1.00	7	17.06	19706.25	), 0-50%B in					
8	1.00	8	17.67	13011.25	), 0-50%B in					
9	1.00	9	18.84	71541.40	), 0-50%B in					
10	1.00	10	19.26	42969.42	), 0-50%B in					
11	1.00	11	19.81	43714.18	), 0-50%B in					
12	1.00	12	21.32	35478.71	), 0-50%B in					
13	1.00	13	22.17	23937200.00	), 0-50%B in					
14	1.00	14	23.54	10854.16	), 0-50%B in					
15	1.00	15	24.59	392372.47	), 0-50%B in					
16	1.00	16	26.94	14649.18	), 0-50%B in					
17	1.00	17	31.44	157933.84	), 0-50%B in					
18	1.00	18	32.90	1943118.12	), 0-50%B in					
19	1.00	19	34.17	56507.36	), 0-50%B in					
20	1.00	20	34.91	1659888.25	), 0-50%B in					